BIRD FOSSILS FROM THE TAKATIKA GRIT, CHATHAM ISLAND, NEW ZEALAND

A thesis submitted in partial fulfilment of the requirements for the

Degree of Master of Science in Geology

At the University of Canterbury

By Jacob Christopher Blokland

University of Canterbury

2017

Figure I: An interpretation of *Archaeodyptes stilwelli*. Original artwork by Jacob Blokland.

ACKNOWLEDGEMENTS

The last couple years have been exciting and challenging. It has been a pleasure to work with great people, and be involved with new research that will hopefully be of contribution to science.

First of all, I would like to thank my two supervisors, Dr Catherine Reid and Dr Paul Scofield, for tirelessly reviewing my work and providing feedback. I literally could not have done it without you, and your time, patience and efforts are very much appreciated. Thank you for providing me with the opportunity to do a vertebrate palaeontology based thesis. I would like to extend my deepest gratitude to Catherine for encouragement regarding my interest in palaeontology since before I was an undergraduate, and providing great information regarding thesis and scientific format. I am also extremely grateful to Paul for welcoming me to use specimens from Canterbury Museum, and providing useful information and recommendations for this project through your expertise in this particular discipline.

I would also like to thank Associate Professor Jeffrey Stilwell for collecting the fossil specimens used in this thesis, and for the information you passed on regarding the details of the fossils. Thank you to Geoffrey Guinard for allowing me to use your data from your published research in this study. The contribution was significantly useful, and is much appreciated. Also thank you to Vanesa De Pietri for your helpful additions to discussions surrounding the nature of the elements in this study. I am also extremely appreciative of St. George's hospital for their time and willingness to use their CT scanner and the "fossil" setting. Ben Griffin I also extend a big thanks to you for sharing this journey with me as a fellow palaeontology student with a huge passion for the subject. The time we spent together figuring out how to use *Materialise Mimics*, and the exchange of ideas in our respective projects has been invaluable. I look forward to working with you in the future.

I'd also like to thank all my family and friends for their love, support and putting up with my frequent unavailability. To my parents, Geoff and Mandy, I cannot thank you enough for the support you've given me throughout this thesis. I am extremely appreciative of your continued understanding, guidance, and for leaving dinner out for me when I regularly arrived back home at 4 am. I'd like to additionally thankJemima for your constant encouragement, and Liv for your valued technological expertise and putting up with my ramblings. I'd also especially like to thank my late grandparents for their love, wisdom, and for inspiring me to achieve the very best I can. Cheers!

ABSTRACT

The origin and radiation of crown group birds during the Late Cretaceous and Early Cenozoic is a subject of ongoing debate in palaeontology and molecular biology. This study involves the identification, formal description, and interpretation of two partial bird skeletons recovered from the Takatika Grit, Chatham Island. These fossils were deposited *in situ* during the late early-middle Paleocene, and are thus within the time-frame relevant to this crown group bird evolution. The two fossil specimens were subject to X-ray computed tomography and subsequently virtually manipulated using *Materialise Mimics* software. The resultant three-dimensional models of fossils were then measured, and their morphology was compared to that of extinct and extant bird relatives, by means of Principle Component Analysis. Morphological character scoring of the fossil elements was conducted, and were added to two phylogenetic matrices of two different previously published studies on Sphenisciformes, to consider the bird specimens in the context of an evolutionary framework. Phylogenetic testing was performed using parsimony-based heuristic analyses and Bayesian analyses, of both genetic and morphological characters, as well as solely osteological characters in separate datasets of each phylogenetic matrix, to produce a robust phylogenetic placement of the bird specimens. This study reports the description of the novel taxon *Archaeodyptes stilwelli* from these bird fossils, a species representative of the most basal of Sphenisciformes currently known to science. While there is no overlap between skeletal elements of the studied specimens, anatomical measurements, phylogenetic analyses, and shared locality that these fossils were recovered from, are compatible with them sharing the same taxon. As such, both specimens are described here as referred specimens of *Archaeodyptes stilwelli*, but further material may provide a more accurate revision of this assignment. Phylogenetic analyses and morphological comparisons consistently recovered *Archaeodyptes stilwelli* in a close association with *Waimanu*, however plesiomorphic features in the ulna and coracoid of *Archaeodyptes stilwelli* particularly validate it as a separate, more primitive penguin taxon. Based on plesiomorphic features reminiscent of aerial birds, and synapomorphies shared with solely aquatic penguins, *Archaeodyptes stilwelli* is interpreted as the most primitive known diver amongst Sphenisciformes. Morphologies observed in this novel taxon are consistent with a model of penguin evolution whereby early penguins diverged from volant ancestors

and specialised for the aquatic environment. Adaptations for swimming efficiency may have been coupled with a loss of aerial flight efficiency, and may have represented a biomechanical trade-off that culminated in the transition to a solely aquatic niche. This transition may have been influenced by competitive biotic interactions with other volant fauna during the Late Cretaceous. Furthermore, aerial flightlessness may have been facilitated by the absence of large marine predators and Hesperornithiformes in the wake of the K/Pg mass extinction, which allowed archaic penguins to diversify and specialised into the Early Cenozoic. The discovery of *Archaeodyptes stilwelli* not only contributes to the global understanding of early crown group bird evolution, but also significantly adds to the fossil record of Zealandia, as it gradually sank following its rifting from the eastern Gondwana margin. The study of this taxon, in conjunction with other fossils and marine sediments can provide important information on the life that inhabited the relatively greenhouse world that existed before the development of the Circum-Antarctic Current, and thus holds particular global significance in relation to the climatic changes that are observed today.

TABLE OF CONTEXTS

LIST OF FIGURES

LIST OF TABLES

CHAPTER I: INTRODUCTION

1.1 Introduction and Research Objectives

This research thesis covers two fossil bird specimens that were recovered from the Takatika Grit, Chatham Islands, New Zealand; a deposit that spans from the Late Cretaceous to the Early Paleocene (Consoli and Stilwell, 2009; Consoli and Stilwell, 2011; Hollis, in press). These fossils were discovered and excavated by Jeffrey Stilwell and his team, and later prepared by Mr. Al Mannering at Canterbury Museum. In this thesis, both prepared specimens are studied to describe and identify them in detail, to consider them in the context of the evolutionary phylogenetic framework, the New Zealand bird palaeontological record, and their global relevance.

When considering fossil birds of this age, how they fit into the evolutionary framework should be considered. It should be noted that the phylogeny and evolution of modern-day birds (class: Aves) has been a controversial topic for many years (Chiappe and Dyke, 2002; Xu et al., 2014; Zhou, 2004), and is the subject of ongoing debate (Brocklehurst et al., 2012; Burleigh et al., 2015; Chiappe and Dyke, 2002; Clarke, 2004; Ericson et al., 2006; Hackett et al., 2008; Jarvis et al., 2014; Lee et al., 2014; Prum et al., 2015). From the discovery of the first Mesozoic avian fossils such *Archaeopteryx* in the 1800s, to the rapid discovery of avian fossils in China through the 1990s, the avian fossil record continues to grow (Bell, 2014; Chiappe and Dyke, 2002; Zhou, 2004). The increasing quantity of such fossils has made it possible to research their evolution and ecology, using phylogenetic as well as morphometric methods.

Controversy surrounds the subject of the timing of origin and diversification of modern bird groups (also referred to as the Neornithes or crown group birds). Almost all neoavian modern bird groups have been shown to have diverged into distinct lineages by 50 million years ago (Ma) (Jarvis et al., 2014). Many molecular studies suggest a Cretaceous radiation, while fossil evidence points towards a rapid diversification in the wake of the Cretaceous/Palaeogene (K/Pg) mass extinction. For these reasons, the exact evolution surrounding Neornithes is an ongoing subject of debate (Brocklehurst et al., 2012; Burleigh et al., 2015; Chiappe and Dyke, 2002; Clarke, 2004; Ericson et al.,

2006; Hackett et al., 2008; Jarvis et al., 2014; Lee et al., 2014; Prum et al., 2015). It is through understanding of these ancient birds and their early radiations that allow for insight into the origin of living avian clades (Zhou, 2004). Hence the Late Cretaceous and Early Paleocene are very significant time-frames through which to study avian evolution and diversification of the clades we are familiar with today.

The oldest Palaeogene strata on the Chatham Islands, the Takatika Grit is highly relevant to the timing of diversification in Neornithes. The Takatika Grit, from which the bird fossils in this study were recovered, is a distinctive marine rock unit, initially formed through the flooding of the continental crust of Zealandia (Campbell et al., 1993), and was deposited very close to the K/Pg boundary (Wilson, 1982), around 62.5 – 60 Ma (Hollis, in press). This rock unit is reflective of both nearshore (Consoli and Stilwell, 2011) and deep marine, pelagic conditions (Hollis, in press), compatible with mid-outer shelf environments (Campbell et al., 1993; Consoli and Stilwell, 2005), and is also associated with the infilling of grabens and half-grabens during Zealandia's final fragmentation from Gondwana (Consoli and Stilwell, 2005; Stilwell et al., 2006). The resultant sedimentary unit preserves a diverse range of reworked fossils from the latest Cretaceous, as well as *in situ* earliest Paleocene assemblages (Campbell et al., 1993; Stilwell et al., 2006). While not only providing information on the understanding of avian dinosaur evolution, the Takatika Grit and these bird fossils additionally provide an invaluable resource for understanding the palaeobiology of Zealandia and the southern hemisphere during this time.

Most Palaeogene avian fossils from New Zealand are part of the Sphenisciformes (penguin) clade (Mayr and Scofield, 2014). Bird fossils are relatively rare in New Zealand before the Pleistocene, with the exception of Sphenisciformes, which first appear in the late Early Paleocene (Ksepka and Cracraft, 2008; Slack et al., 2006). The oldest penguin fossils (in New Zealand and worldwide) are *Waimanu manneringi* (~ 60.5 Ma) (Ksepka and Clarke, 2015; Prum et al., 2015) and the slightly younger *W. tuatahi* (~58 – 60 Ma) (Ksepka and Clarke, 2015), from the Waipara Greensand; representing Paleocene fossils from a well described sequence that includes an important K/Pg boundary site in North Canterbury, New Zealand (Slack et al., 2006). A tarsometatarsus that bears similarities to other waterbird clades such as Procellariiformes (albatrosses, shearwaters and petrels), Podicipediformes (grebes) and Gaviiformes (loons) has also been described from the Waimakariri River Gorge, near the K/Pg boundary, but it is too incompletely preserved to be phylogenetically

assigned (Ksepka and Cracraft, 2008). Since the birds of this study are potentially even older than both *Waimanu* species, these fossils possibly represent some of the oldest known bird fauna known to inhabit the continental block associated with New Zealand, and may also further the known understanding of the relationship among modern bird lineages.

Examination, description, and a comparison of anatomical and palaebiological information is therefore essential to be performed on these Paleocene bird fossils. Such information will aid in the progression of the understanding of the ecology of early Zealandia, as well as the early radiations of birds and Neornithes, effectively shedding light on the origin and phylogeny of living avian groups.

1.2 Aims of study

This research aims to:

- Formally identify and describe the two each specimens from the Takatika Grit;
- Analyse and discuss the biomechanical nature of each specimen and their palaeobiology;
- To infer estimated phylogenetic positions of each specimen in the context of comparing and contrasting with both extinct and extant bird relatives.

1.3 Setting the Global Stage—the Latest Cretaceous and Early Paleocene

Evolution during the Cretaceous was pivotal in the rise of important aspects of modern fauna, flora and ecosystems (Benson et al., 2013). The latest Cretaceous (Campanian–Maastrichtian, 83.6–65.5 Ma) was an interval of major global change (Brusatte et al., 2015), as was the transition to the Early Cenozoic, which saw dramatic ecosystem changes throughout the world (Hao et al., 2010). A better understanding of Earth system tectonic and subsequent climatic changes through this time can illuminate the affects it had on the evolution of taxa.

1.3.1 The Palaeogeographical and Palaeoclimatological Setting

Tectonic activity over the Cretaceous Period saw the progression of the two supercontinents Laurasia and Gondwana straddling the equatorial Tethys Ocean into terrestrial landmasses stretched over several continents that extended into higher latitudes, separated by shallow seas and oceans (Seton et al., 2012; Skelton, 2003) (Figure 1.1). Many modern landmass configurations formed over the tectonically active Cretaceous (Carvalho et al., 2010), with mountains forming predominately as a result of subduction, but also continental collision (Skelton, 2003). Orogenic activity also strongly affected atmospheric circulation, which determined changes in climate patterns such as precipitation and albedo (Carvalho et al., 2010; Skelton, 2003).

Figure 1.1 (next page): Global palaeogeographical reconstructions showing the extent of continental separation over the Cretaceous Period. The top image (**A**) shows a palaeographic map at the end of the Jurassic (Tithonian). The northern continents are part of Laurasia, while the equatorial and southern continents are part of Gondwana. The bottom image (**B**) shows a reconstruction from the very latest Cretaceous (Maastrichtian). From Skelton (2003).

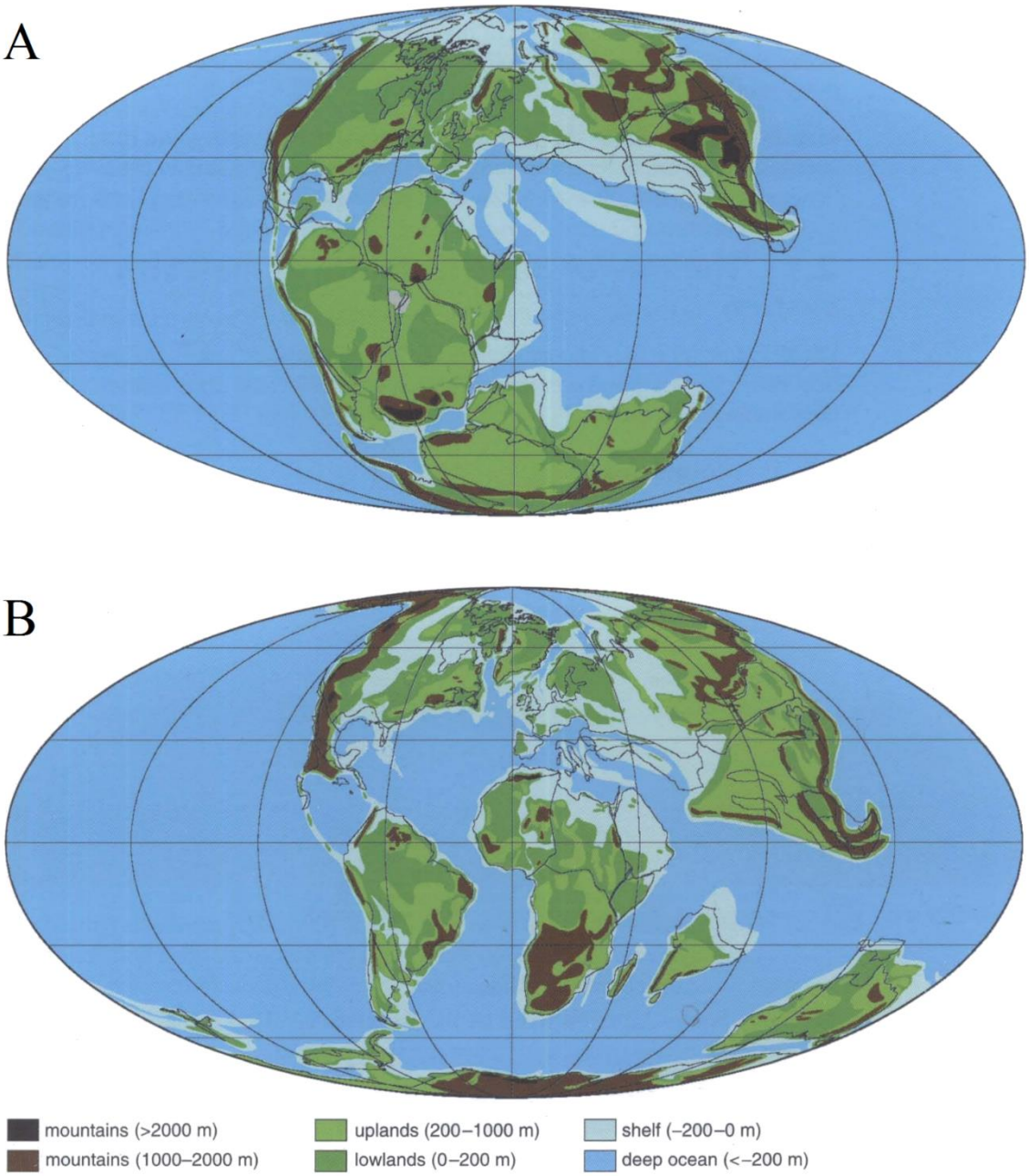

The Cretaceous Period was one of the warmest intervals in Earth's history and is considered to have had extreme "greenhouse" conditions (Barron et al., 1993; Barron and Peterson, 1989; Carvalho et al., 2010; Spicer and Corfield, 1992; Tajika, 1999) compared to today's relatively "icehouse" world (Skelton, 2003). The latest Cretaceous Earth was uniformly warm with iceless poles (Brusatte et al., 2015; Carvalho et al., 2010; Wolfe and Upchurch, 1987) and higher latitude areas supported what are now considered temperate forest ecosystems (Skelton, 2003). Recent work suggests that a detailed cooling trend is apparent in the latest Cretaceous, and that the Maastrichtian was globally significantly cooler compared to earlier in the Cretaceous (Adatte et al., 2002). Cretaceous

atmospheric temperatures have been coupled with higher carbon dioxide levels (Wang et al., 2014b). While carbon dioxide levels were high throughout the Cretaceous, the late Cretaceous experienced a slight decline in carbon dioxide concentrations (Brusatte et al., 2015; Wang et al., 2014b), which corresponded with a long-term cooling trend through the Campanian and Maastrichtian (Brusatte et al., 2015; Skelton, 2003). Resultantly, the last 5 million years of the Cretaceous represent the coldest climate experienced over the entire period (Keller et al., 2016).The latest Cretaceous also saw short-lived warming during the middle Maastrichtian, and also the last few hundred thousand years of the same stage, which correlate with the increase of carbon dioxide from the first and second of the Deccan Traps eruption phases in India respectively (Brusatte et al., 2015). Fluctuations in intermediate water and sea surface temperatures, representative of cooling and warming are also observed throughout this time-frame (Adatte et al., 2002). Major sea level fluctuations are also observed (Adatte et al., 2002), that varied more intensely over shorter time-frames during the Maastrichtian especially (Barrera, 1994; Brusatte et al., 2015). Predominately however, the latest Cretaceous saw a long-term sea level drop after a peak of 50-70m above existing levels, around 80 Ma (Brusatte et al., 2015). Consequently, the late Maastrichtian was a time of major climatic extremes (Keller et al., 2016) and instability (Thibault and Husson, 2016) associated with Deccan volcanism (Keller et al., 2016; Thibault and Husson, 2016).

The K/Pg transition is marked by the bolide impact in the Yucatán Peninsula that had profound ramifications on global climate; over a short time-frame (Brugger et al., 2016; Schulte et al., 2010), and also contributed to the long-term climate alterations induced by Deccan Traps volcanism (Arostegi et al., 2011). In general, because of diagenic alteration of carbonates over the K/Pg boundary, oxygen isotope records are obscured, meaning the exact record of how long-term climate changed across the K/Pg boundary into the Cenozoic is difficult to verify (Adatte et al., 2002; Corfield, 1994). However, from the late Campanian to the early Danian a global change in weathering and climate is observed through terrigenous detrital influx that culminated at the K/Pg transition—which is evidenced through a global sea-level rise, maximum flooding and associated sediment starvation, condensed to this interval (Adatte et al., 2002). Concurrently, a long-term trend of increasing humidity is observed, also culminating at the K/Pg boundary in the Tethys region (Adatte et al., 2002). The earliest Danian in the Tethys region is marked by warm humid climates, alternating with

seasonal temperate climates (Adatte et al., 2002). This interval is also characterised by sea-level rise and associated drier climates in the Tethys region of the early Danian (Adatte et al., 2002).

Middle and high southern latitudes in contrast show long-term climate cooling, suggesting that while low latitudes witnessed a long-term increase in humidity, high latitudes cooled, into the early Paleocene (Adatte et al., 2002). High latitude climates such as in New Zealand and Antarctica during the latest Cretaceous were characterised by temperate climates, with flora indicative of warm growing seasons and relatively cold polar winters (Consoli and Stilwell, 2011). In the transition to the Cenozoic however, cooler climates were observed in the early Paleocene of New Zealand (Vajda et al., 2004), and a cooling trend at high latitudes is observed in Seymour Island, Antarctica, where an absence of angiosperms typical of warm climates are noted in Danian strata (Askin, 1990).

Humidity was not only restricted to the Tethys region and similar latitudes however, as indicated by perennially wet climates that occurred across the K/Pg boundary in middle latitudes (Adatte et al., 2002). Mid-latitudes are evidenced to have experienced a shift from perennial subhumid temperate climate in the latest Cretaceous to warm seasonal climate during the Danian, early Paleocene (Figure 1.2) (Arostegi et al., 2011). From the late Danian to the Selandian (Figure 1.2) this climate at mid-latitudes changed to predominately warm and semi-arid to arid conditions (Arostegi et al., 2011).

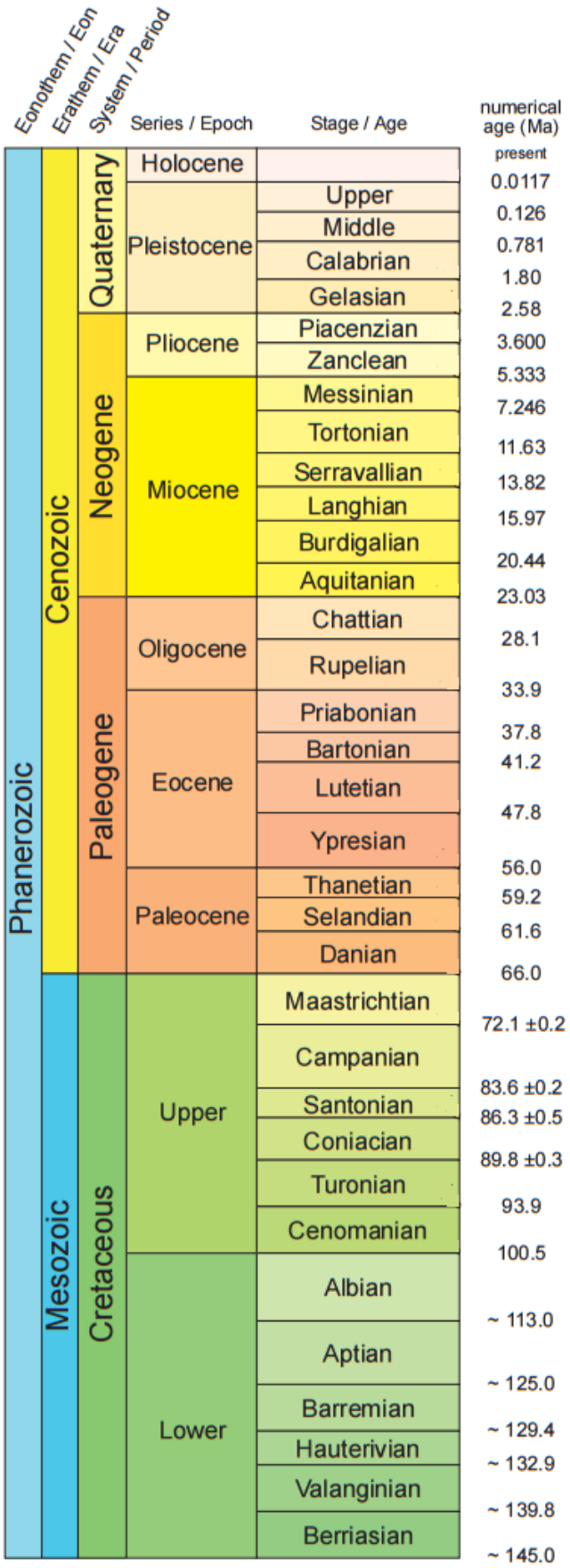

Figure 1.2: A chronostratigraphic chart displaying names and ages of the stages of the Cretaceous Period, and the Paleocene Epoch. Image taken from the International Commission of Stratigraphy, 2015 (Cohen et al., 2015)

While much hotter than today, the Paleocene overall was cooler relative to the preceding Cretaceous. Generally, compared to the latest Cretaceous, the early Cenozoic is characterised by a

decrease in surface water temperatures (Corfield, 1994). The Paleocene also experienced a general decline in deep water temperatures in observed from around 65 Ma to 62 Ma, before they dramatically increased again from the early Late Paleocene into the early Eocene (Corfield, 1994). The transition to cooler, more temperate waters, as well as the evolution of the Southern Ocean and related modern circulation patterns from active tectonics, is correlated with the rise of numerous species groups, during the Early Cenozoic (Fordyce and Jones, 1990). Notably, these conditions paralleled with the evolution of early representatives of modern avian groups, such as penguins (Fordyce and Jones, 1990).

1.3.2 The Palaeoecological Setting

The direct and indirect relationship that climate had with tectonics during the Cretaceous, has been associated with uplift, atmospheric circulation, volcanism, and also the hydrologic cycle (Skelton, 2003). Orogeny and resultant precipitation, for example, affected associated palaeogeographic distribution of deserts globally (Carvalho et al., 2010), and contributed to ecological change witnessed over the Cretaceous and into the Palaeogene. Inevitably, such changes induced a significant effect on the biosphere (Carvalho et al., 2010). Extensive variation in the fossil record can be explained by global climate patterns through the influencing of rates of extinction, and also speciation, not only on the species level but also in terms of genera and families (Carvalho et al., 2010) as continents moved towards their current configuration.

Cretaceous conditions saw a transitional period in the evolution of life, where the origination and diversification of many components of major and extant clades resulted (Benson et al., 2013). The sustained global ecological changes that occurred over this period, and the Maastrichtian stage particularly, are part of a longer biotic transition, that also includes the K/Pg mass extinction event (Macleod et al., 1997). Perhaps one of the most significant clades to develop during the Cretaceous were true angiosperms (Skelton, 2003), that replaced gymnosperms as the predominant terrestrial vegetation (Hao et al., 2010). Angiosperms rose from an ecologically unimportant and small percentage of terrestrial biomass before the mid-Cretaceous, to dominate the Late-Cretaceous and transform global vegetation (Skelton, 2003) into the Cenozoic. Pollinating insects also evolved and thus co-radiated with the angiosperm plants during this interval (Benson et al., 2013). Pollinating birds are also thought to have evolved in parallel several times during the evolution of angiosperms,

with bird pollination reported in 65 families of angiosperms today (Pansarin and Pedro, 2016), and first recorded in fossils from the Eocene (Mayr and Wilde, 2014). Many ancient lineages of tetrapod clades in terrestrial and marine environments crossed the Jurassic into the Cretaceous Period (Benson et al., 2013). Avian dinosaurs (birds) represent one of these groups to cross this boundary, and are characterised by a high ecological diversity through the Cretaceous (Benson et al., 2013; Zhou, 2004). Importantly, the Cretaceous saw the evolution of ornithurine (Ornithurae) birds, from which modern birds are descended (Benson et al., 2013; Zhou, 2004). Avian faunas of the Late Cretaceous were dominated by enantiornithine birds, which existed alongside ornithurines, and possibly also coexisted with more primitive long-tailed birds (Benson et al., 2013). Radiations of aquatic ornithurine birds, notably Hesperornithiformes, are also observed during this interval (Benson et al., 2013). During the early Late Cretaceous, many archaic tetrapod lineages such as lepidosaurs, dinosaurs, mammals, crocodylomorphs (Benson et al., 2013; Carvalho et al., 2010), pterosaurs, and ichthyosaurs witnessed temporally and geographically staggered declines and extinctions (Benson et al., 2013). These archaic tetrapod lineages were progressively replaced with clades more representative of modern fauna, like snakes, iguanians, gekkotans squamates, metatherian and eutherian mammals, cryptodiran turtles, and eusuchian crocodylomorphs (Benson et al., 2013). Though uncommon before this time, these clades would eventually reach levels of higher diversity in the Campanian and Maastrichtian (Benson et al., 2013). Differences between Gondwanan and Laurasian faunas became progressively greater as fragmentation of these supercontinents continued, and a substantial increase in continental-scale endemism over the latest Cretaceous resulted (Benson et al., 2013). In effect, the latest Cretaceous world before the terminal Cretaceous mass extinction was populated by species groups of exotic-looking biota, now extinct, along with taxa that are more representative of extant groups in the present day (Skelton, 2003).

Throughout the Cretaceous there was a steady increase in marine microfossil biodiversity, which corresponded with further increased relatively cooler temperatures of the Late Cretaceous, especially from the late Campanian, to reach maximum Cretaceous biodiversity during the middle Maastrichtian (Keller, 2008). Biodiversity also fluctuated as a product of climate variability over this time from (Li and Keller, 1998; Macleod et al., 1997), greenhouse effects and Deccan volcanism (Keller, 2008; Keller et al., 2016). As a product of rapid warming in marine and terrestrial environments from Deccan volcanism (Keller et al., 2016), and possibly ocean acidification (Thibault and Husson, 2016),

biota were subject to high-stress environments at the end of the Cretaceous (Keller et al., 2016). Overall, the last 500 ky of the Cretaceous witnessed a decrease the diversity of Late Cretaceous biota (Keller, 2008), and eventually cumulated in the end Cretaceous mass extinction (Keller et al., 2016).

The Mesozoic Era is perhaps most well known as the time the dinosaurs dominated the Earth, and their extinction that marked the end of the Cretaceous 66 million years ago (Ma) (Benson et al., 2013). This mass extinction event, which has been profusely researched, saw massive biotic turnover, and included the end of all non-avian dinosaurs, pterosaurs, most marine reptiles, and many marine invertebrate clades such as rudist bivalves and ammonoid cephalopods (Benson et al., 2013; Macleod et al., 1997; Schulte et al., 2010). Avian faunas were also heavily affected, and suffered widespread extinction, as many basal bird groups, including enantiornithes, and many ornithurine birds such as Hesperornithiformes, did not cross into the Cenozoic (Benson et al., 2013; Chiappe and Dyke, 2002; Zhou, 2004). In fact, no birds from lineages outside of neornithine (crown group) birds have ever been recovered in post-Cretaceous deposits (Chiappe and Dyke, 2002). Taxonomic groups such as land plants, planktic foraminifera, and calcareous nanofossils, for example suffered considerably during this extinction event also, and even taxa that were relatively minimally affected showed substantial changes in assemblage composition (Schulte et al., 2010). Irrespective however, the surviving taxa of this mass extinction were all common in that they shared morphological, physiological, and ecological characteristics that were biased by the selectivity of the extinction event (Hull, 2015).

In the aftermath of the K/Pg extinction event, the ecosystems of the Early Cenozoic were subject to extreme global change compared to the preceding Cretaceous, and represented the dawn of a "brave new world" (Stilwell et al., 2006). With the K/Pg mass extinction came an interval of global darkness and cooling (Brugger et al., 2016; Corfield, 1994), and associated decreased solar flux to the Earth's surface (Corfield, 1994) as a product of the K/Pg event resulted in relatively cut-off levels of photosynthesis, for a relatively short time-frame (Vajda et al., 2004). Carbon isotope data indicates that sea-surface productivity decreased globally during the earliest Paleocene (Adatte et al., 2002), related to extinctions of marine plankton from the K/Pg mass extinction (Corfield, 1994). This in turn is suggested to have negatively affected watermass stratification and nutrient balance, contributing to the low diversity and rate of recovery following the mass extinction (Adatte et al., 2002). Due to the devastation of the terrestrial environment, unfavourable conditions for growing

seed plants continued for a considerable amount of time (c. 8,000-20,000 years) following the K/Pg mass extinction event, which resulted in the relative dominance of low insolation-adapted understory plants such as ferns, over this interval, before forests re-established (Vajda et al., 2004). The interval of low insolation was eventually followed by the broadly simultaneous recovery of calcareous plankton radiolarians, diatoms, with the succession of land plants, during the early Paleocene (Vajda et al., 2004). An increase in carbon isotope values is observed during this time and onwards, before reaching maximum values in the late Paleocene, as a result of increasing surface water productivity and the accelerated burial of organic carbon (Corfield, 1994). The transition into the Paleocene also saw many ecological niches become vacant in the wake of the extinctions and associated environmental destruction that occurred globally, which allowed rapid radiation and proliferation of most surviving clades (Macleod et al., 1997). As such, the availability of vacant ecospace allowed taxa that were in either low abundance or diversity before the K/Pg boundary to radiate and/or increase their numbers during the early Paleocene (Hull, 2015). This especially included the successful spiny-rayed fishes, which increased in both occupations of ecospace and abundance relative to cartilaginous fishes (Hull, 2015). Similarly, surviving groups of mammals, in the absence of non-avian dinosaurs, radiated explosively, with a rapid increase in diversity over a relatively short amount of time (Kemp, 2005). Another vertebrate lineage, that actively diversified during the Cretaceous (Chiappe and Dyke, 2002; Zhou, 2004), but also paralleled the explosive radiation of mammals through the Paleocene and the rest of the Cenozoic, was the birds (Feduccia, 1995).

1.4 Avian Evolution and Lineages

The birds (class: Aves) (Linnaeus, 1758), are a clade which can be considered as including the last common ancestor all living birds and *Archaeopteryx* (Chiappe and Dyke, 2002). The evolution of this clade especially has been a subject of debate for many years—almost since the advent of evolutionary thought (Chiappe and Dyke, 2002; Xu et al., 2014; Zhou, 2004), and involved a variety of proposals. With the discovery of Mesozoic avian fossils however (Bell, 2014; Zhou, 2004), evidence has shed light on the nature of their divergence. Beginning with the discovery of *Archaeopteryx lithographica* in the 1800s (Owen, 1863), the discovery of many Early Cretaceous avian fossils in China through the 1990s (Bell, 2014; Chiappe and Dyke, 2002), the abundance and diversity of Mesozoic avian fossils have become increasingly apparent. In fact, the recent decades have seen more Mesozoic

birds discovered and described than had been discovered in total from the 1860s to the 1970s (Chiappe and Dyke, 2002; Zhou, 2004). The forever increasing quantity of such fossils has provided the means for the research into the evolution and ecology of these ancient bird predecessors, using phylogenetic (Jarvis et al., 2014; Prum et al., 2015) as well as morphometric means (Bell, 2014).

While considered by most to form a monophyletic clade, the position within Archosauromorpha and the consequent closest relatives of birds has been heavily argued (Feduccia, 1999; Xu et al., 2014; Zhou, 2004). Over the last four decades, the most widely accepted hypothesis is that birds have evolved from dinosaurian ancestors (Chiappe and Dyke, 2002). Similarities between birds and theropod dinosaurs were recognised as long ago as the nineteenth century (Brown and Van Tuinen, 2011; Chiappe and Dyke, 2002; Huxley, 1868; Zhou, 2004). However, the hypothesis of a small, terrestrial coelurosaurian theropod ancestor (Ostrom, 1976) has since gained an abundance of evidence (Chiappe and Dyke, 2002; Xu et al., 2014) that supports a maniraptorian origin of birds, thought to be most closely related to troodontids and dromaeosaurs (Figure 1.3A) (Xu et al., 2014).

Figure 1.3: Diagrams showing the evolution of birds towards Neornithes (modern bird groups). **A** displays the phylogenetic interrelationships of the closest theropod relatives to Aves (boxed). From Mayr (2016). **B** shows the interrelationships between different avian faunas in the Mesozoic, with the Late Jurassic *Archaeopteryx* in a basal position. The Cretaceous radiation of enantiornithes is shown, in coexistence with ornithurine birds. Neornithes (boxed) are displayed as radiating in the Late Cretaceous, and the Cenozoic especially. From Mayr (2016). **C** shows simplified phylogenetic interrelationships of major neornithine lineages from two recent studies Prum et al. (2015), and Jarvis et al. (2014). Several differences are revealed in comparison of the two phylogenetic trees, attesting to the nature of the hotly debated subject. Modified from Thomas (2015).

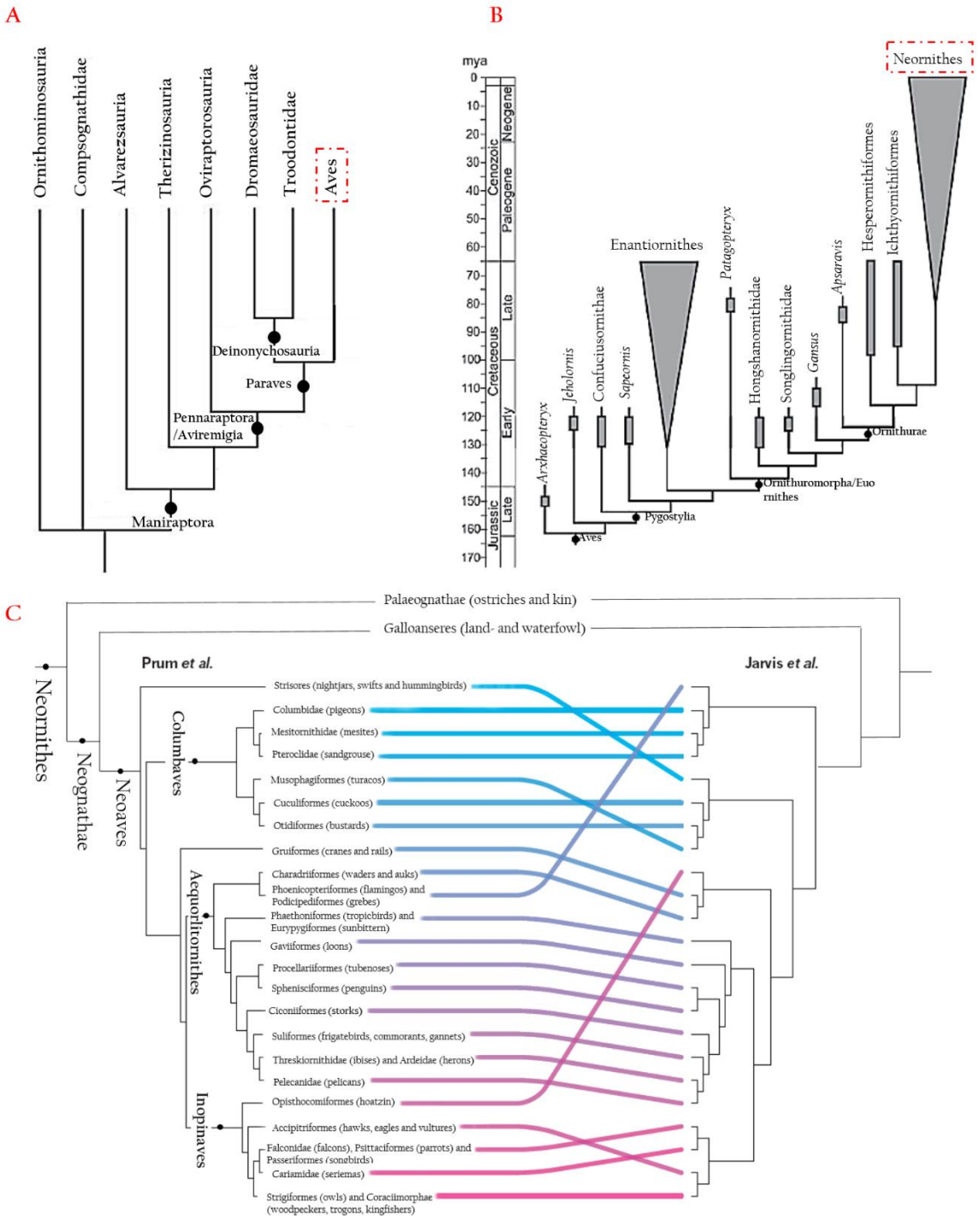

Though controversial (Xu et al., 2014), the Late Jurassic *Archaeopteryx* node is considered by most to be basal in the avian tree (Figure 1.3B) (Zhou, 2004), and has stood unchallenged as the oldest known bird for most of the history of palaeoornithology (Chiappe and Dyke, 2002). However, others such as the likely volant *Rahonavis* (Chiappe and Dyke, 2002), relatives of the four-winged and primitive *Anchiornis*, scansoriopterygids, and unenlagiid theropods are also suggested as occupying a basal position in the bird lineage (Xu et al., 2014). In general, birds evolved and diversified from

archaic forms such as these, during the Mesozoic, before subsequent extinctions and bottlenecks that lead to the existence of modern birds, as we know them (Feduccia, 1995).

During the Cretaceous, birds diversified into a wide variety of forms. The most diverse form of birds (Chiappe and Dyke, 2002) were the enantiornithines, which dominated the Cretaceous (Figure 1.3B) (Chiappe and Dyke, 2002; Zhou, 2004), and are considered the most important lineage of early birds due to their diversity, the abundance of species identified, and also their ecological variation (Chiappe and Dyke, 2002; Chiappe and Walker, 2002; Zhou, 2004). Enantiornithines are characterised by the developmental fusion of the three tarsal elements from proximal to distal; opposite to that of modern birds (Feduccia, 1995; see Chiappe, 1996 for review). Additionally, in enantiornithines the triosseal canal—which is involved in the upstroke of the bird's wing—is formed by a distinct bony formation (Feduccia, 1995). Enantiornithines possessed a long pygostyle with fused caudal vertebrae, rather than a long tail of the more primitive birds such as *Archaeopteryx*, yet retained primitive features associated with the pelvic region (Feduccia, 1995), as well as a toothed skull (Chiappe and Dyke, 2002; Feduccia, 1995). The fully flighted apparatus of enantiornithines is considered much more advanced compared to *Archaeopteryx* (Feduccia, 1995), however, and shares similarities with modern birds (Chiappe and Dyke, 2002), including the presence of a narrow interclavicular, a mobile scapulocoracoid articulation (Chiappe and Dyke, 2002), and also an alula on the forewing (Chiappe and Dyke, 2002; Zhou, 2004). Additionally, these birds such as *Longipteryx* (Zhang et al., 2001), also showed well-developed pedal morphology indicating they were capable of perching (Zhang et al., 2001; Zhou, 2004). By the Early Cretaceous enantiornithine birds had rapidly evolved to become ecologically diverse (Zhou, 2004), and while they have predominately been recovered from inland deposits, enantiornithines have also been recorded from littoral, marine, and even polar environments, resulting in an almost global distribution during the Cretaceous (Chiappe and Walker, 2002; Zhou, 2004). These birds also varied significantly in terms of diet (Zhou, 2004). *Longipteryx* for example possessed an elongated snout and densely distributed teeth, typical of fish-feeding (Zhang et al., 2001), and others such as *Longirostravis* had a long, slender and pointed bill, indicative of mud-probing behaviours (Hou et al., 2004; Zhou, 2004). While predominately small forms are known from the Early Cretaceous, by the Late Cretaceous enantiornithines occupied a diverse range of body sizes (Chiappe and Dyke, 2002); some with up to a 1 m wingspan (Chiappe,

1996; Chiappe and Dyke, 2002), while others such as *Parvavis* retained comparably smaller sizes (Wang et al., 2014a).

The Cretaceous also witnessed the divergence of another major avian monophyletic clade that co-existed alongside the enantiornithines, the ornithurines (Ornithurae) (Figure 1.3B) (Haeckel, 1866; Zhou, 2004). This lineage includes all extant bird taxa as well as their basal relatives (Chiappe and Dyke, 2002; Zhou, 2004), and in comparison to enantiornithines, ornithurines possessed a flying apparatus almost identical to their modern birds (Zhou, 2004; Zhou and Zhang, 2001). Specifically, ornithurines possessed a tail shorter than the femur, where the pygostyle is characterised by an upturned ploughshare-shaped compressed element of fused bone, consisting of less than six segments, and is shorter than the free up-curving tail part—which is composed of less than eight caudal vertebrae (Gauthier and De Queiroz, 2001). A coracoid with a well-developed procoracoidal process and a round fossa for scapular articulation, a completely fused carpometacarpal, as well as a deep keel that extends the full length of a longitudinally elongated sternum, are also among the synapomorphies that ornithurines share with their living descendants (Zhou, 2004). While enantiornithines dominated the Mesozoic terrestrial bird niches, one North American Maastrichtian fossil assemblage shows an abundance of advanced ornithurines relative to enantiornithine birds, suggesting a major radiation of advanced ornithurines before the end of the Cretaceous (Longrich et al., 2011). In addition, this fossil assemblage consisted of a very diverse range of avifauna, of both small and larger flying forms, accentuating the degree to which such avians had diversified before the end of the Cretaceous (Feduccia, 2014; Longrich et al., 2011). The large forms in this assemblage of around 3-5kg represent some the largest of flying avifauna of the Mesozoic, however birds of greater sizes (~10kg) did not exist, suggesting that perhaps the size of birds during the Mesozoic was constrained by large pterosaurs which occupied those ecological niches (Feduccia, 2014).

1.4.1 Diving Seabirds before Penguins

An important and highly specialised clade of ornithurines (Figure 1.3B) is the extinct lineage of the Hesperornithiformes, representing one of the most taxonomic, stratigraphic and geographically diverse groups of Mesozoic birds (Bell, 2014). Hesperornithiforms are a highly specialised clade, and were characteristically toothed, foot-propelled diving birds (Bell and Chiappe, 2015)—the first bird group to develop adaptations for a fully aquatic lifestyle (Bell, 2014). While highly specialised, the extensive fossil record of hesperornithiforms shows that they were also morphologically diverse (Bell

and Chiappe, 2015; Bell, 2014), and ranged in size up to 1.5 m in length (Bell, 2014). Predominately known from the Late Cretaceous before going extinct (Bell and Chiappe, 2015; Bell, 2014; Hills et al., 1999), these birds are consistently acknowledged phylogenetically as one of the sister groups closest to modern birds within Ornithurae (Bell and Chiappe, 2015). The Hesperornithiformes demonstrate a gradual, step-wise evolution of specialised diving adaptations, from more basal birds that may have been flighted with limited diving capabilities in the Early Cretaceous, to flightless birds, with highly specialised adaptations for diving behaviour in the Late Cretaceous (Bell and Chiappe, 2015). For example, in more basal Hesperornithiformes such as *Enaliornis* the spacing of the trochlea of the tarsometatarsus was close together, however in more derived Late Cretaceous forms such as *Hesperornis* there is almost no gap in the spacing of the trochlea to the point they are almost overlapping (Bell and Chiappe, 2015). In modern birds such as grebes, who have trochlea spacing similar to that of *Enaliornis*, closely spaced trochlea permits close overlapping of the toes in the recovery stroke while swimming, which allows for a more streamlined shape and preserves energy through reducing drag (Bell and Chiappe, 2015; Johansson and Norberg, 2001). Hesperornithiforms also underwent substantial increases in body size within evolutionary lineages towards the Late Cretaceous. This occurred through multiple independent events, decoupled with the development of skeletal diving specialisations, as effectively shown through some species within a lineage expressing the same degree of adaptations towards diving and swimming behaviour, yet substantially differing in size (Bell and Chiappe, 2015).

Another independent lineage of Late Cretaceous ornithurine birds (Lee et al., 2014), representing another close outgroups to modern birds, are birds of the genus *Ichthyornis* (Ichthyornithiformes)(Figure 1.3B)(Clarke, 2004). While previously referring to several species, only one *Ichthyornis dispar* (Clarke, 2004), is now recognised from southern North American (Porras-Muzquiz et al., 2014) specimens described from the late Cenomanian to the lower Campanian, a period of around 15 million years during the Late Cretaceous (Clarke, 2004). *Ichthyornis* was a toothed seabird, and resembled a tern (Marsh, 1880; Porras-Muzquiz et al., 2014; Shimada and Fernandes, 2006) or pigeon in size (Marsh, 1873; Shimada and Fernandes, 2006). Despite being small, these birds had the capability for powerful flight (Clarke, 2004; Porras-Muzquiz et al., 2014; Shimada and Fernandes, 2006), and are described as having a large keel in the sternum, a flexible scapulocoracoid joint with a triosseal canal, as well as small legs and feet (Clarke, 2004; Marsh, 1880) yet with well-

developed tibiotarsus and tarsometatarsus contributing to robust hindlimbs (Porras-Muzquiz et al., 2014). *Ichthyornis* also had a highly kinetic skull (Clarke, 2004; Porras-Muzquiz et al., 2014) with an elongate rostrum (Clarke, 2004). Many features, such as these, expressed in *Ichthyornis* share morphological characteristics converging on modern birds, yet are still placed phylogenetically outside the crown-group birds (Clarke, 2004; Porras-Muzquiz et al., 2014). This is no coincidence considering that *Ichthyornis* has an internal indicus process and well-developed reverse articulations of the anterior caudal vertebrae, features that are present modern birds, especially Charadriiformes among neoavian lineages, but not present in other bird groups (Clarke, 2004). Considering the apomorphies that *Ichthyornis* shares with Charadriiformes, *Ichthyornis* has been considered convergent on Charadriiform features, and has been inferred to have had aquatic habits similar to that of a tern (e.g., *Sterna maxima*) (Clarke, 2004; Marsh, 1880; Porras-Muzquiz et al., 2014).

1.4.2 Neornithes

Research of Mesozoic ornithurines not only assists in our understanding of the evolution and early radiations of birds, but also progresses our understanding of modern bird groups (Zhou, 2004). The evolution of crown-group (modern) birds—also known as Neornithes, in terms of timing of their origin and diversification is deeply controversial (Figure 1.3C) (Brocklehurst et al., 2012; Burleigh et al., 2015; Chiappe and Dyke, 2002; Clarke, 2004; Ericson et al., 2006; Hackett et al., 2008; Jarvis et al., 2014; Lee et al., 2014; Prum et al., 2015; Thomas, 2015). Nuclear (Ericson et al., 2006; Haddrath and Baker, 2012; Jetz et al., 2012; Lee et al., 2014; Meredith et al., 2011) and mitochondrial (Brown et al., 2008; Pacheco et al., 2011) DNA research has suggested that Neornithes radiated gradually (Jarvis et al., 2014) around the Mid-Cretaceous period 80-125 Ma (Ericson et al., 2006; Jarvis et al., 2014). The oldest molecular dates suggest that modern birds appeared around 155 Ma, only 20 million years (myr) after the time of *Archaeopteryx* (Lee et al., 2014). This idea has been supported by biogeographic research, where neornithine evolution is thought to have been greatly influenced by vicariance, isolating bird lineages with the fragmentation of continents from Gondwana (Cracraft, 2001), hence meaning Neornithes diversified related to such tectonic activity during the Cretaceous (Upchurch, 2008). This however would imply that the K/Pg mass extinction would have had little effect on neornithine lineages, and can be considered unlikely since birds are very sensitive to such levels of environmental stress (Brocklehurst et al., 2012; Feduccia, 2003).

In contrast, their first appearance in the fossil record is in stark discrepancy with many molecular proposals (Brocklehurst et al., 2012; Feduccia, 2014), where an explosive post-K/Pg boundary radiation is largely observed, and substantial fossil evidence for a deep Cretaceous origin is scarce (Feduccia, 2014). In this way, fossil evidence suggests this explosive radiation occurred after a bottleneck of Late Cretaceous bird lineages through the K/Pg mass extinction (Feduccia, 1995; Feduccia, 1999; Feduccia, 2003; Feduccia, 2014), while other archaic and more basal bird lineages suffered catastrophic extinction at the K/Pg boundary (Brocklehurst et al., 2012). The palaeontological standpoint is largely centred on a view that Neornithes originated in the latest Cretaceous, consisting of a few basal lineages (Ericson et al., 2006), and radiated after the K/Pg mass extinction into modern extant lineages (Benton, 1999; Brocklehurst et al., 2012; Clarke et al., 2005; Cracraft, 2001; Feduccia, 1995). Ericson et al. (2006) produced molecular evidence which also backs this perspective, and has also gained further support from recent studies, that have suggested a similar pattern of evolution (Jarvis et al., 2014; Prum et al., 2015). Jarvis et al. (2014) concluded that while Neornithes first diverged within the Cretaceous into Palaeognathae and Neognathae, and subsequently into Galloanseres and Neoaves, the hypothesis that rapid radiation and diversification of 36 neoavian lineages occurred over the space of 10-15 myr during the transitional period between the Cretaceous and the Palaeogene was also supported, meaning that by 50 Ma almost all neoavian orders had diverged. Similarly, research carried out by Prum et al. (2015), considering phylogenetically and geologically well-constrained fossil calibrations, as well as targeted next-generation DNA sequencing, also supported a very rapid radiation of neoavian lineages immediately following the K/Pg mass extinction—a phylogeny that has long been difficult to resolve due to the diversification happening so rapidly and so long ago, meaning very short internodes between the divergence of taxa.

Neornithes are well documented in the fossil record from the late Paleocene and Eocene, but are badly represented in the later stages of the Cretaceous and the Danian (Fountaine et al., 2005). Such scarcity of Neornithes in the Cretaceous could imply that Neornithes were simply rare lineages during this interval, and is a product of their biology rather than insufficient sampling (Fountaine et al., 2005). This is indicated by a relatively smaller and poorer preservation quality of neornithine birds compared to other bird groups that co-existed in the Cretaceous, and is emphasised considering that there is no reason why both should not have the same preservation potential (see

Fountaine et al., 2005). Brocklehurst (2012) suggests that such rarity is due to small, delicate vertebrate skeletons being more easily destroyed by taphonomic processes, yet easily preserved whole, which combined with patchy regional sample, explains the poor quality of Late Cretaceous neornithine birds. Therefore, it was proposed that neornithine bird lineages were present in the Late Cretaceous, but fossils are difficult to identify due to their fragmentary nature, or simply have not been sampled (Brocklehurst et al., 2012). It should be noted however, that research on terrestrial vertebrates from the Cretaceous shows that the preservation potential is independent of body size (Benton, 1999; Fara and Benton, 2000), and that taxa from both Neornithes and other bird groups show a similar range of body sizes with similar modes of life (Fountaine et al., 2005) and bone structure (Fountaine et al., 2005; Zhou, 2004), yet non-neornithine birds still have a higher abundance in the Late Cretaceous fossil record (Fountaine et al., 2005). It can therefore be argued that while poorly preserved, the ecological habitat of Cretaceous neornithine species may be of significant concern (Fountaine et al., 2005; Slack et al., 2006), and that neornithines were simply relatively rare in the Cretaceous (Fountaine et al., 2005). Regardless, even though the fossil bone material in the Late Cretaceous may be fragmentary (Fountaine et al., 2005; Hope, 2002), there is still a Cretaceous record of fossilised footprints belonging to web-footed birds that coexisted with pterosaurs 96-80 Ma (Hwang et al., 2002; Kim et al., 2003), and even bird tracks from the Cretaceous that show features convergent on Neornithes (Lockley et al., 2007). Slack et al. (2006) also suggested that the radiation of Neornithes can be witnessed in the fossil record through the displacement of taxa that would have shared a similar ecological niche to modern birds prior to the K/Pg mass extinction, considering pterosaurs, as well as archaic (such as enantiornithines, hesperornithiforms, and *Ichthyornis*-type ornithurines) and modern birds overlapped for millions of years, and may have had a degree of. competitive interaction (Slack et al., 2006). Despite their relative abundance, modern bird representatives existed in the Late Cretaceous and would have had ecological requirements and implications (Slack et al., 2006).

1.4.2.1 The Water Bird Clade

One clade of neoavian Neornithes that has been consistently recovered in phylogenetic analyses, based on morphological (Fürbringer, 1888; Livezey and Zusi, 2007; Mayr and Clarke, 2003) as well as molecular datasets, is that of the water birds (Ericson et al., 2006; Hackett et al., 2008; Jarvis et al., 2014; Kimball et al., 2013; Mayr, 2011; Prum et al., 2015; Yuri et al., 2013) such as diving

and wading birds (Prum et al., 2015) with various aquatic or semi-aquatic adaptations (Ericson et al., 2006; Mayr, 2014). This water bird clade consists of flightless birds such as penguins, volant birds like frigatebirds and albatrosses, storks and herons, as well as pelicans, and thus is one of the most morphologically diverse groups of crown group birds (Mayr, 2011; Mayr, 2014). Information and analyses of the specific relationships between water bird taxa is crucial for building an understanding of the morphological, behavioural and ecological evolution that has resulted in this clade (Mayr, 2011). Recent analyses by Prum et al., (2015) have revaluated and expanded this group to all shorebirds, diving birds and wading birds, emphasising the extent of the diversity that this clade shows. Specifically, this comprehensive clade is termed the Aequorlitornithes, (Prum et al., 2015), where flamingos and grebes (Ericson et al., 2006; Hackett et al., 2008; McCormack et al., 2013) are found to be the sister group to shorebirds (Prum et al., 2015), and sunbittern and tropicbirds (Ericson et al., 2006; Hackett et al., 2008; McCormack et al., 2013) are the sister group to wading and diving birds (Figure 1.3C) (Prum et al., 2015).

Early Aequorlitornithes have been recognised in the fossil record around the Late Mesozoic and Early Cenozoic with confidence, specifically fossils belonging to the clades of Sphenisciformes, Procellariiformes and possibly Gaviiformes (Mayr, 2014). Gaviiformes include extant species of foot-propelled diving birds called loons (Mayr, 2004), and while controversial, fossils of that may resemble modern loons have been found in the Mesozoic fossil record. *Neogaeornis wetzeli* is one of these controversial diving birds, from the Campanian-Maastrichtian of Chile, and is based on a single right tarsometatarus that bears resemblance to the highly derived bone of extant loons (Lambrecht, 1929; Mayr, 2004; Olson, 1992). Consequentially, due to the nature of the tarsometatarsus, which shows a laterally compressed shaft and retracted inner trochlea, distinctive of birds specialised for diving, *Neogaeornis wetzeli* has been compared to Aequorlitornithes such as loons and grebes (Podicipediformes), but also more archaic ornithurines such as hesperornithiforms (Lambrecht, 1929; Olson, 1992). However, research by Olson (1992) suggests that *Neogaeornis wetzeli* should be placed in the order Gaviiformes in the modern bird family Gaviidae. Chatterjee (1989) also discovered a partial skeleton from the of Seymour Island, Antarctica, dated to the latest Maastrichtian (Case et al., 2011) that resembles a loon, *Polarornis gregorii* (Chatterjee, 1989). While some consider that *Polarornis gregorii* was certainly a loon of the modern Gaviidae family (Chatterjee, 2002; Olson, 1992), this placement has been contested based on the fragmentary nature of the specimen and subsequent possible

inaccuracies in the specimen's reconstruction, as well as important features in *Polarornis gregorii* that differed from modern loons (Mayr, 2004). It is also possible however that both specimens could be referred to the genus *Neogaeornis*, if correctly assigned (Mayr, 2004; Olson, 1992).

The oldest fossils controversially associated with neornithine orders such as Procellariiformes (Mayr, 2014; Olson and Parris, 1987) and Pelecaniformes come from Maastrictian fossils from the Hornerstown Formation, New Jersey, North America (Olson and Parris, 1987). *Tytthostonyx glauconiticus* was proposed based on a right humerus that bears resemblance to both of these orders, for example the ectepicondylar spur appeared similar to both, yet was more developed than any modern Pelecaniformes, but also not as well developed as seen in extant Procellariiformes (Olson and Parris, 1987). While it bears similarities to both, *Tytthostonyx glauconiticus* does not appear to have the same distinctive morphology of modern clades, and thus it is considered that *Tytthostonyx glauconiticus* possibly possessed a humerus that was similar to that possessed by more ancestral birds that gave rise to the Procellariiformes (Olson and Parris, 1987). An ulna of a very small bird that has been compared to storm-petrels of the family Oceanitidae was also described along with *Tytthostonyx glauconiticus*, and may also be associated with Procellariiformes, yet due to differences between modern fauna and the fossil material this classification is uncertain (Olson and Parris, 1987). Therefore, while these specimens from the Hornerstown Formation appear to be Neornithes, and part of a neoavian radiation leading to extant bird lineages, they cannot be assigned to any modern clade of Aequorlitornithes (Olson and Parris, 1987). Conversely, Bourdon et al. (2008) considered that *Tytthostonyx glauconiticus* may rather represent a possible stem tropic bird (Prophaethontidae), instead of part of the Procellariiformes. In order to better assess the phylogenetic inference of such birds, more complete fossil material is required (Bourdon et al., 2008). Another fragmentary fossil that may represent early possible Procellariiformes is that of a tarsometatarsus described from the Waimakariri, Canterbury, of New Zealand, near the K/Pg Boundary (Ksepka and Cracraft, 2008). Numerous morphological characters of the bone are indicative of a semi-aquatic nature, and most are consistent with morphology shared by current Procellariiformes such as shearwaters (*Puffinus* spp.), yet because of its fragmentary nature it is only tentatively assigned (Ksepka and Cracraft, 2008). Because of asymmetry of the foot implied by the tarsometatarsus shape, the foot of the bird may have been related to foot-propelled diving or paddling, and may suggest an ecology similar to

Auquorlitornithes such as Gaviiformes and Podicippediformes, as well as Procellariiformes (Ksepka and Cracraft, 2008). The authors also considered the possibility that this bird may have belonged to an extinct ornithurine lineage, rather than certainly part of Neornithes (Ksepka and Cracraft, 2008).

Fossils attributed to the genus *Waimanu* from the Waipara Greensand, Canterbury, New Zealand are recognised as early members of the Sphenisciformes from the Paleocene, just above a well-known K/Pg boundary site (Slack et al., 2006), representing the oldest known definitive, uncontroversial crown group bird fossils (Prum et al., 2015) (minimum age ~ 60.5 Ma) (Ksepka and Clarke, 2015; Prum et al., 2015). These fossils represent two species of large, solely aquatic, wing-propelled diving birds. The oldest, *Waimanu manneringi*, is known only from the holotype specimen, is around the size of an Emperor penguin (*Aptenodytes forsteri*), with a minimum age of 60.5 Ma. *Waimanu tuatahi* which is represented by multiple specimens that together comprise almost a complete skeleton, is smaller (~80 cm tall), approximately the size of a yellow-eyed penguin (*Megadyptes antipodes*) (Slack et al., 2006), and are slightly younger (~58 – 60 Ma) (Ksepka and Clarke, 2015). Evidently, *Waimanu manneringi* has been recognised as the most basal penguin taxon based on morphological data (Slack et al., 2006), as well as molecular and morphological data combined (Clarke et al., 2010; Clarke et al., 2007; Ksepka et al., 2006; Ksepka and Clarke, 2010; Ksepka et al., 2012). As the earliest known genus in the waterbird clade, the *Waimanu* specimens are described as stem penguins, and are also considered to be closely related to the Procellariiformes, which are considered to have a sister group relationship with Sphenisciformes. However, it should be noted that the position of *Waimanu* does not hinge upon this interrelationship (Ksepka and Clarke, 2015). Bones from diving birds such as penguins, which have dense, thick-bones and occur in shallow marine environments, have a relatively higher preservation potential than other bird groups, contributing to the relatively more complete fossil record of penguins (Ksepka and Clarke, 2015; Ksepka and Ando, 2011). While birds from other Aequorlitornithes clades are scarce, fragmentary, controversial or completely absent during the Cretaceous and Early Paleocene, the appearance of penguins in the fossil record in the form of *Waimanu* likely corresponds to the timing of a shift to flightless marine ecology, and potential timing of a split from other bird groups (Ksepka and Clarke, 2015).

Slack et al. (2006) conservatively estimated, based on the *Waimanu* specimens, an origin for penguins as well as modern sea and shorebird lineages diverging from ancestral stock during the Late Cretaceous (74 ± 3 Ma, Campanian), as part of the radiation of Neornithes, consistent with records of fossil bones and footprints. Undescribed "penguin-like" fossils from the latest Cretaceous-Paleocene Takatika Grit of the Chatham Islands, in the same deposit as the specimens of this current research, also imply that the earliest penguins may have lived even earlier than *Waimanu* (Hansford, 2008), corresponding with the proposed evolutionary time-frame.

1.5 Geological Setting—The Chatham Rise Region

The fossils of this research were recovered from the Chatham Islands. The Chatham Islands, together with New Zealand, the Campbell Plateau, Lord Howe Rise, New Caledonia, and Norfolk Ridge form the continental landmass that is referred to as Zealandia (Campbell et al., 1993; Consoli and Stilwell, 2011). The Chatham Islands themselves consist of two large islands, Chatham and Pitt Island, and several smaller islands, and are the only non-submerged land areas of the Chatham Rise (Norris, 1964), located 860 km off the East Coast of New Zealand's mainland (Consoli and Stilwell, 2011). The Chatham Rise itself extends east of New Zealand from Banks Peninsula for over 1,000 km (Wood and Herzer, 1993), the crest of which on average is submerged 400 m below sea level, and also consists of numerous shallower banks (the Mernoo, Veryan and Matheson Banks) (Campbell et al., 1993; Norris, 1964).

The geological setting of Zealandia, and the Chatham Islands, during the Cretaceous/Paleocene time-frame is largely tied to the disintegration of the Gondwanan supercontinent—that became South America, South Africa, Australia, and Antarctica (Vaughan and Pankhurst, 2008)—and thus they are highly interrelated in terms of tectonic and magmatic history. Since the Permian, the tectonic and magmatic history of the south Pacific margin of Gondwana had been characterised by an active subduction zone (Bradshaw, 1989; Lawver et al., 1992), however, the Cretaceous Period witnessed a significant change in such persistent convergent tectonics (Adams et al., 2016; Storey et al., 1999), and a rapid change to an extensional and dispersal related regime (Adams et al., 2016; Laird and Bradshaw, 2004). This would see the end of New Zealand and associated Chatham Rise regions as part of the Gondwanan margin, as it separated to become own distinct entity—Zealandia (Figure 1.4) (Adams et al., 2016; Stilwell and Consoli, 2012). The mechanism behind the change in tectonic regime, whether it was from ridge subduction (Bradshaw,

1989), ridge stall (Luyendyk, 1995), or related to interaction with the Hikurangi Plateau (Davy et al., 2008), is a matter of debate. After the end of the Early Cretaceous and its subduction related tectonics (105 ± 5 Ma) (Bradshaw, 1989; Lawver et al., 1992; Luyendyk, 1995), a major angular unconformity marked the change in tectonic activity, where it separates the predominately very deformed subduction-related rocks, from the overlying less-deformed rocks (Laird and Bradshaw, 2004). Considering that both the younger extensional rocks, as well as the older subduction-related rocks contain fossils related to the Albian stage of the Cretaceous, and are both of similar age (100 Ma), this indicates a very rapid change in tectonic regimes occurred (Laird and Bradshaw, 2004). This meant that by 105-100 Ma subduction had ceased along the eastern Gondwana margin, from central New Zealand to the eastern tip of the Chatham Rise (Laird and Bradshaw, 2004), and is associated with the rifting of the Bounty Trough (Stilwell and Consoli, 2012). This process of continental breakup may have been related to secondary heating, and thermal expansion associated with convective upwelling—which may have resulted in a period of uplift, emergence and erosion immediately prior to sea-floor spreading (Laird and Bradshaw, 2004).

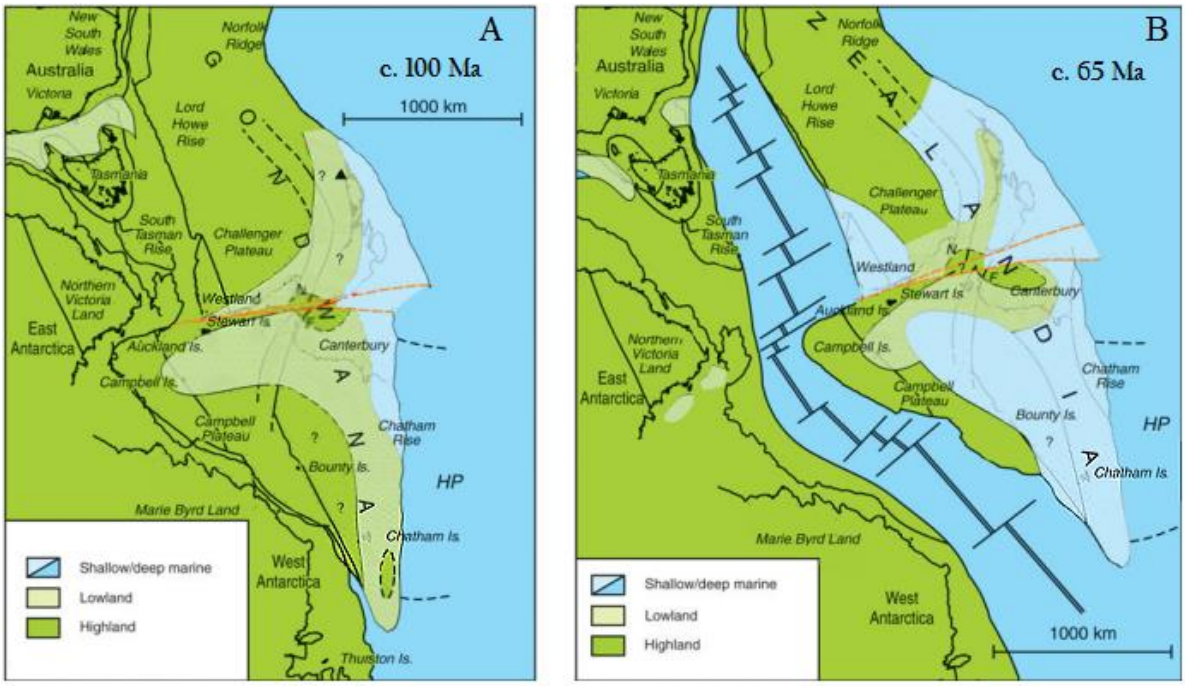

Figure 1.4: The palaeogeography of Gondwana and Zealandia during the initiation of rifting activity and the c. 100 Ma termination of the active Gondwanaland margin in southern Zealandia (**A**); and Zealandia as a product of continental break-up and rifting, during the Campanian – Maastrichtian, and into the Early Cenozoic (c. 65 Ma) (**B**). The orange dashed lines refer to the present approximate Alpine Fault region, and distinguish between north and south of Zealandia. It should be noted that areas denoted "Highland" refer to volcanic plateaux, mountains, and deserts; and "Lowland" signifies areas of fluvial, deltaic and/or semi-marine nature. Modified from Adams et al. (2016).

As Zealandia continued to rift from East Gondwana, by around 87 Ma (late Coniacian) most of Zealandia underwent a subsequent period of change as widespread transgression took place, and accelerated through the Santonian (86.3-83.6 Ma) (Laird and Bradshaw, 2004). The elongated landmass known as the Chatham Peninsula (Consoli and Stilwell, 2009), was subjected to this second-order transgressive phase (Consoli and Stilwell, 2011), and was progressively submerged as a product of thermal subsidence, crustal thinning, and sediment loading (Consoli and Stilwell, 2009). Marine transgression, associated with an extended time of passive margin subsidence would continue throughout most of Zealandia, reaching its peak in the Oligocene (Laird and Bradshaw, 2004), and has subsided to the current depth of 200-500 m below sea level since the Late Cretaceous (Wood and Herzer, 1993).

Coinciding with the extensive transgression across Zealandia (Laird and Bradshaw, 2004), the consequence of extensional activity and progressive rifting from Eastern Gondwana (Falvey, 1974) due to sea-floor spreading, culminated in the separation of Zealandia from West Antarctica, around 80-85 Ma (Laird and Bradshaw, 2004; Luyendyk, 1995; Tappenden, 2003)—more specifically 83.0-82.5 Ma (Campbell and Hutching, 2007; Stilwell, 2016). The seafloor spreading that took place between Marie Byrd Land (attached to West Antarctica) and the margin of Zealandia associated with the Campbell Plateau and the Chatham Rise, constrained by anomaly Chron 34 (Mayes et al., 1990; Royer et al., 1990; Storey et al., 1999), is coupled with the opening of the Tasman Sea, progressively separating the Gondwanan continental landmasses (Stilwell, 2016). Rifting of the continental fragment of Zealandia from eastern Australia, and the opening of the Tasman Sea, would continue from the Late Cretaceous to the Eocene, before the complete continental isolation of Zealandia (Bache et al., 2014). Widespread marine transgression of Zealandia continued concurrently, through post-rift thermal relaxation and subsidence between 85 and 56 Ma, as Zealandia drifted from eastern Australia (Rouillard et al., 2015). Since the early Eocene (Bache et al., 2014), the position of the Chatham Rise relative to New Zealand and the rest of the Pacific Plate has experienced minor change (Stilwell et al., 2006; Wood and Herzer, 1993).

Evidence of emergent and actual crustal extension is widely developed from 100 Ma onwards and continued until continental separation (Laird and Bradshaw, 2004). The 20 myr interval between the change to extensional tectonic regime and the continental separation from the West Antarctica

fragment of Eastern Gondwana (Laird and Bradshaw, 2004) witnessed widespread uplift and block faulting (Stilwell and Consoli, 2012), that resulted in the development of grabens and half-grabens over Zealandia (Laird and Bradshaw, 2004). Associated with uplift at the onset of rifting from Antarctica, grabens were accumulated with predominately rift-fill sediments that eroded from eastern highlands, and are widespread across both the Chatham Rise and Antarctica (Stilwell and Consoli, 2012). The extensional regime on the Chatham Rise saw the formation of a series of predominately latitudinal (Consoli and Stilwell, 2011) east-west trending half-grabens (20 – 50 km wide), hinged to the south, and extended to the Canterbury region of the South Island, New Zealand (Stilwell and Consoli, 2012). Rifting activity was also associated with intraplate volcanism (Cande and Kent, 1995; Stilwell et al., 2006), which occurred in correlation with structural events (Stilwell and Consoli, 2012). The Late Cretaceous Chatham Rise region was thus punctuated by localised episodes of basaltic volcanism (Campbell et al., 1993; Stilwell et al., 2006), which produced numerous basaltic provinces through terrigenous sequences (Stilwell and Consoli, 2012). Notably, this volcanic activity included the eruption of a 20-25 km wide alkaline basalt, low-angle, intraplate stratovolcano on the southern area of Chatham Island and Pitt Strait, from 82.3 - 85.5 Ma (Stilwell and Consoli, 2012; Stilwell et al., 2006). Volcanoclastics subsequently infilled the half-grabens on the Chatham Rise, accumulating in thick sequences (Stilwell et al., 2006). Another consequence of rifting was the crustal thinning and the emergence of extensional sedimentary basins over Zealandia (Laird and Bradshaw, 2004). Erosion from uplifted basement rock and aforementioned volcanics acted as sedimentary sources for the basin and graben sediments, which kept pace with subsidence, and produced sedimentary and volcanic successions between 7 and 12 km thick through the Cretaceous (Stilwell and Consoli, 2012), and continued to be filled towards its end (Stilwell et al., 2006). Consequently, a basin and basement range landscape existed over the Chatham Peninsula exposed above sea-level (Stilwell and Consoli, 2012). Broad floodplains and deltas also characterised this landscape, as a product of the basement range erosion, where horsts were eroded to hills of relatively low topographic relief (Stilwell, 2016; Stilwell et al., 2006).

During late Coniacian rifting from the eastern margin of Gondwana, Zealandia had been reduced to an exposed, low-relief landmass (Laird and Bradshaw, 2004), and the Chatham Rise was likely close to sea level for much of the Late Cretaceous (Stilwell et al., 2006). Land bridges would have also been present in the Late Cretaceous during the rifting of continental landmasses,

connecting Zealandia and Eastern Gondwana (Stilwell and Consoli, 2012). A shallow sea existed north of the Chatham landmass, associated with potential upwelling zones; restricted embayments adjacent to the Chatham landmass also existed (Stilwell and Consoli, 2012). Additionally, north of the Chatham Rise during this Late Cretaceous interval existed a broad continental shelf known as the Hikurangi Plateau (Stilwell and Consoli, 2012). To the south of the Chatham Rise was the Bounty Trough, which produced an increasingly deepening incision between the Chatham Rise and Antarctica (Stilwell and Consoli, 2012).

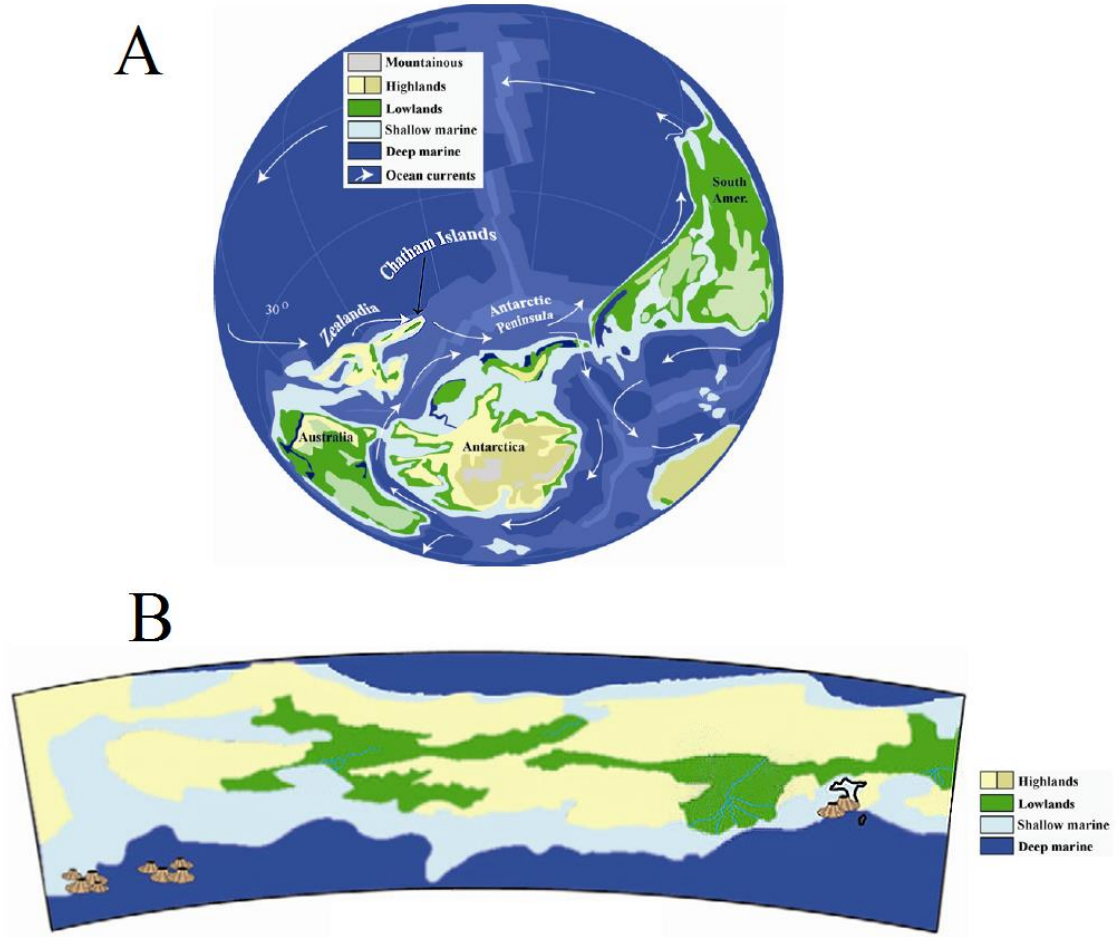

Figure 1.5: A Palaeographic map of the separating Gondwana supercontinent close to the K/Pg boundary (**A**), displaying the terrestrial and flooded areas of Zealandia, as well as information on topographic knowledge of the region. The position of the Chatham Islands is indicated. A close-up of a palaeogeographic reconstruction of the Chatham Islands is also illustrated (**B**). The black outlined area indicates the current location of the Chatham Islands. The positions of volcanoes are also illustrated. Modified from Stilwell and Consoli (2012).

Around the close of the Cretaceous and the dawn of the Cenozoic, the Chatham Rise existed as a peneplained landmass (Figure 1.5) (Stilwell and Consoli, 2012), comprised of low hills and coastal plains (Consoli and Stilwell, 2009), with a deep ocean to the north and south (Stilwell and Consoli, 2012). It has been suggested that oceanic inundation of the Chatham Rise region resulted in its total submergence by the time of the K/Pg boundary, however, the discovery of avian fossils in the region indicate that land was exposed to some extent during these times (Stilwell, 2016; Stilwell and Consoli, 2012). These terrigenous components likely existed as ephemeral oceanic islands into the Cenozoic (Consoli and Stilwell, 2011). This interval is characterised by a significant deepening event on the Chatham Rise, related to local tectonic response to eustatic sea-level fall, and is associated with an unconformity that represents an interval of erosion and non-deposition into the early Cenozoic (Stilwell and Consoli, 2012). Indications of sea-level fluctuations are also observed (Hollis, in press) in the late Campanian and Maastrichtian, from major unconformities over eastern New Zealand (Crampton et al., 2006).

Through the early Cenozoic, the Chatham Rise is characterised by marine sedimentation, deposited through the regional subsidence of the region (Stilwell and Consoli, 2012). Most of the Chatham Rise during this time accumulated greensands and deep-water limestones, however the western portion of the Chatham Rise in comparison experienced a thick terrigenous input from uplifted Zealandia landscape (Stilwell and Consoli, 2012). The western Chatham Rise additionally experienced sub-alkaline to tholeiitic basaltic volcanism (Stilwell and Consoli, 2012). Basaltic volcanism associated with the accumulation of tuffs, breccias, and bioclastic limestones (the Kekerione Group) (Stilwell and Consoli, 2012), occurred contemporaneously with marine sedimentation from the Late Cretaceous until the Eocene, related to the fragmentation of Gondwana (Consoli and Stilwell, 2011). Renewed volcanic activity also occurred from the late Eocene to the early Oligocene (Consoli and Stilwell, 2011), related to the movement on the Australian-Pacific plates, and the reactivation of some Cretaceous half-grabens in the north-west of the Chatham Rise (Stilwell and Consoli, 2012).

1.5.1 The Takatika Grit

Associated with the regional subsidence of the Chatham Rise and Zealandia, and coupled with aforementioned volcanism associated with the rifting of Zealandia from Gondwana (Stilwell and Consoli, 2012), widespread, fossiliferous marine deposits resulted (Stilwell, 2016). The Tioriori

Group—comprised of the Takatika Grit, Tutuiri Greensand and the Tumaio Limestone—in particular, was deposited between the Santonian and the early Eocene, and comprises of a series of condensed, deepening marine glauconitic sandstone successions (Stilwell and Consoli, 2012). Specifically, these successions are described as fossil-bearing, phosphatized conglomerate, grit, gritty sandstone, biogenic silica-rich sandstone and greensand (Hollis, in press). This accumulation of thin sandstones and greensands, related to oceanic inundation and the formation of the basin and basement range style landscape, was deposited within half-grabens on the Chatham Rise simultaneously with aforementioned intraplate volcanics (Campbell et al., 1993; Consoli and Stilwell, 2009; Consoli and Stilwell, 2011), and is associated with the divergent motion separating the Chatham Rise from Marie Byrd Land (Stilwell et al., 2006). Specifically, as the most basal sequence of the Tioriori Group, the Takatika Grit represents marine transgression and flooding over a subdued topography, that resulted in the preservation of a rich fossil assemblage (Consoli and Stilwell, 2009; Consoli and Stilwell, 2011) (Consoli and Stilwell, 2005), deposited within intervening grabens (Consoli and Stilwell, 2005) in the northwest and central area of Chatham Island (Consoli and Stilwell, 2011).

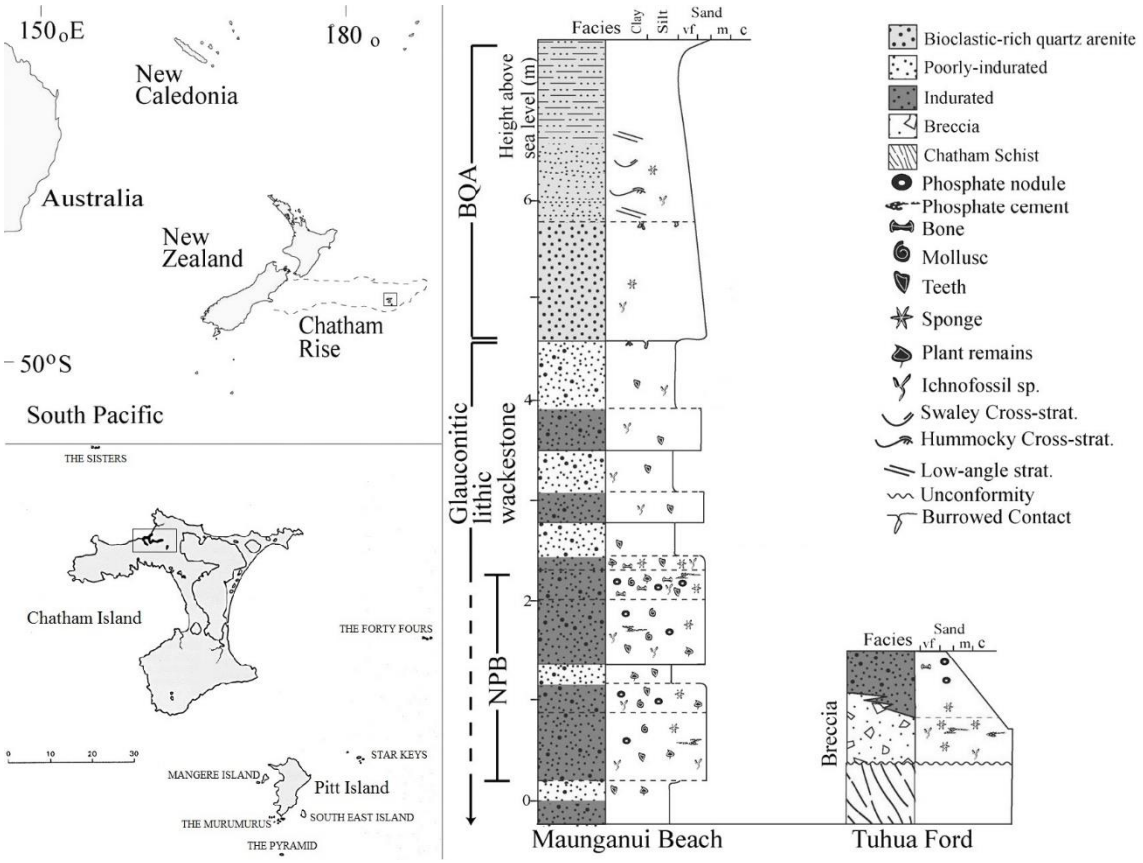

Figure 1.6 (previous page): The upper left panel of this figure depicts the current location of the Chatham Islands (boxed area), with respect to New Zealand. The dotted line indicates the extent of the Chatham Rise. The lower left panel shows the location of outcrops of the Tioriori Group on Chatham Island (distribution is shown in black within boxed area), which includes the Takatika Grit, Tutuiri Greensand and Tumaio Limestone. The location of other Chatham islands is also shown. Scale is measured in kilometres. The right panel illustrates a stratigraphic section of the Takatika Grit. The nodular-phosphate bone package (NPB) and the bioclastic-quartz arenite package (BQA) are shown. Figure modified from Consoli et al. (2009), and Campbell et al. (1993).

Today, the Takatika Grit (Figure 1.6) outcrops as steep, low-lying coastal cliffs (Consoli, 2008; Consoli and Stilwell, 2009) and a 2 km span of wave-cut platforms and float blocks (between 43.743°S, 176.683°W and 43.750°S, 176.667°W) along the length of Maunganui Beach (Consoli, 2008; Consoli et al., 2009; Consoli and Stilwell, 2009; Stilwell et al., 2006), and additionally inland along Tutuiri Creek as a series of creek cuttings (Consoli, 2008), of north-western Chatham Island (Campbell et al., 1993; Consoli and Stilwell, 2009). While the Takatika Grit does not occur *in situ* on Pitt Island, large blocks of the Takatika Grit exist at the mouths of several streams, in northern Pitt Island (Campbell et al., 1993). The Takatika Grit unconformably overlies the regional basement Chatham Schist, and is conformably succeeded by the Tutuiri Greensand (Campbell et al., 1993; Consoli and Stilwell, 2005). At a maximum of 10 m thick (Consoli et al., 2009; Consoli and Stilwell, 2009; Stilwell, 2007; Stilwell et al., 2006), this thin marine succession is defined as a distinctive, fossiliferous, dark green-grey, well-bedded, poorly-sorted, glauconitic lithic wackestone, with fine-grained glauconitic inclusions, abundant mono- and poly-crystalline quartz, and metamorphic lithic fragments amongst a clay matrix, often supported by siliceous cement (Consoli and Stilwell, 2009), in addition to a minor volcanogenic constituent (Stilwell, 2007; Stilwell et al., 2006), and basal breccia (Consoli et al., 2009). The Takatika Grit is characterised by beds that alternate from silicified cemented, to poorly indurated, non-silicified beds; predominately a product of preferential diagenetic cementation of the lower clay-poor section of normal graded beds (Consoli et al., 2009). The basal breccia of the Takatika Grit outcrops inland, and fines upwards into the glaucony lithic wackestone (Consoli et al., 2009). The basal breccia, however, is not observed along Maunganui Beach, which is instead dominated by glaucony lithic wackestone (Consoli et al., 2009). Notably, authigenic phosphorite nodules exist through the sequence in the lower section of the glaucony lithic wackestone (Consoli et al., 2009; Stilwell, 2007), of pebble to boulder size, occurring largely in the unit's mid-section as a succinct package of beds—known as the nodular-phosphate bone package

(NPB) (Consoli, 2008; Consoli and Stilwell, 2009; Stilwell et al., 2006). The NPB is notably fossiliferous, comprised of abundant macrofossils in addition to the phosphate nodules (Consoli, 2008). Three NPB horizons containing fossils are known from the Takatika Grit, increasing in fossil abundance up-section, representing mass fossil accumulations (Stilwell et al., 2006). Lower in this unit is characterised by poorly sorted, phosphatised grit among phosphate nodules and macrofossils, while the upper part is characterised by nodular bedded sandstone and grit (Hollis, in press). The bed that succeeds the NPB lacks nodules but is also fossiliferous (Consoli et al., 2009). This upper section of the Takatika Grit culminates in a bioclastic-quartz arenite package (BQA) (Consoli et al., 2009). The BQA is characterised by a lower heavily bioturbated section, while parallel laminations and sinusoidal ripples exist in the upper section (Hollis, in press).

The exact depositional nature of the Takatika Grit is complex (Stilwell and Consoli, 2012), and is reflective of terrigenous origin as well as an authigenic formation of glauconite (Stilwell et al., 2006). On the Chatham Rise, cool, nutrient-rich waters at depth are forced up onto shallow warmer waters on the southern shelf of the Chatham Rise, and allow for the precipitation of glauconite; originating from dissolved potassium in seawater (Campbell and Hutching, 2007; Consoli et al., 2009). The basal breccia and upwards fining of the glaucony lithic wackestone of the Takatika Grit is representative of initial marine transgression across the underlying Chatham Schist, followed by rapid deepening (Consoli et al., 2009). The glaucony lithic wackstone component of the Takatika Grit and the fossil-rich NPB is indicative of deposition during a predominately shallow-marine environment, with highly productive rich phosphatic bioproductive waters (Consoli et al., 2009). The NPB represents a period of extremely low sedimentation rates, as well as seafloor exposure and erosion from sea-level fluctuations (Consoli et al., 2009; Consoli and Stilwell, 2009). The NPB was produced in a lag-style accumulation, therefore, and was subsequently reworked in the early Paleocene (see below) (Consoli et al., 2009). As such, the NPB beds appear to be condensed with low energy reworking in the form of bioturbation and low current activity (Stilwell, 2007). In general, the Tioriori Group—including the Takatika Grit—had been thought to have been deposited in a shallow-marine environment (Consoli and Stilwell, 2011; Stilwell et al., 2006; Wilson, 1984b), however, the Takatika Grit has also been cited as representative of a mid-outer shelf depositional settings (Consoli and Stilwell, 2005). Indeed, the diversity of radiolarian assemblages within ripple-bedded sandstone associated with the Takatika Grit, are typical of deep marine and pelagic settings

(Hollis, in press). The unique combination of both dynamic sedimentary processes in oceanic conditions, that favoured the productivity and preservation of these radiolarians (Hollis, in press), further attests to the complex nature of the Takatika Grit. In contrast, the BQA unit of the Takatika Grit is indicative of being deposited in a nearshore environment, that may have been strongly influenced by storm activity (Consoli et al., 2009). It is possible that the BQA may be representative of a single depositional event (Consoli et al., 2009). The presence of masses of pollen microspores associated with *Azolla*, which occupied fresh, still-water bodies, are also suggestive of nearshore depositional settings for Paleocene Takatika Grit sediments (Consoli and Stilwell, 2011). The existence of basement highs and volcanic islands that allowed the existence of freshwater lakes in the Early Paleocene, local to the depositional setting of the Takatika Grit, have therefore been suggested (Consoli and Stilwell, 2011). It has been proposed that depositional settings indicative of both shallow and marine settings in the Takatika Grit may be representative of mass movements of sediments from shallow marine settings into the bathyal environment, which has preserved this apparent mixture, specifically in the BQA (Consoli, 2008). In general, however, the Takatika Grit records depositional settings and processes that are thought to be representative of what is occurring on the submerged crest of the Chatham Rise today (Consoli and Stilwell, 2005).

Previous research based on palynomorphic analyses proposed that the Takatika Grit began accumulating in the mid-Campanian, and ranged to the mid-Danian (Consoli and Stilwell, 2009). This age range was based predominately on the correlated zonation of dinoflagellate cyst assemblages from the Takatika Grit sediments, that were inferred to have represented mid-Campanian sediments, and also included a smaller constituent that related to the mid-Danian (Consoli and Stilwell, 2009; Wilson et al., 2005). However, based on an updated zonation for dinoflagellate cysts (Crouch et al., 2014), this biostratigraphy and age was revised by Hollis et al. (in press). Examined dinoflagellate cyst assemblages of this study found that the phosphatic unit of the Takatika Grit cannot be older than late early Paleocene (62.5 Ma), associated with the presence of *Deflandrea foveolata*, while also no younger than the middle Paleocene (60 Ma) from the presence of *Isabelidinium cingulatum*. No index species relating to the late Campanian and Maastrichtian were identified in the Takatika Grit samples—indicative of non-deposition and/or during this time. An early Campanian (82-80 Ma) age is inferred from reworked Cretaceous assemblages, due to the presence of *Satyrodinium haumuriense*. Species of the *Satyrodinium haumuriense* Zone had previously been identified with samples of the

Takatika Grit, and were representative of the mid-Campanian (Consoli and Stilwell, 2009; Wilson, 1982; Wilson et al., 2005), based on samples removed from the matrix on and around marine reptile fossils from the NPB (Consoli and Stilwell, 2009), using a previous version of dinoflagellate cyst zonation information. Diatom floras investigated by Hollis et al. (in press) inferred a middle Paleocene age for the Takatika Grit. Some are also indicative of reworking form the Late Cretaceous, however since some of the taxa originated in the Late Cretaceous and persisted through the Paleocene, the true extent of reworking compared to *in situ* deposition is unknown. The diverse radiolarian component of this study also suggests a Paleocene age, with an extent of reworking from middle Campanian to Maastrichtian age. Similar to diatom floras, because some radiolarian species persisted into the Paleocene, the reworking of Cretaceous specimens is less certain. It has also been proposed that New Zealand taxa characteristic of the K/Pg boundary have been recorded (Consoli and Stilwell, 2009; Wilson, 1982), however further research by Hollis (in press) indicates there is no biostratigraphic evidence for an intact K/Pg boundary succession.

As a result of sedimentary starvation and reworking, phosphate nodules and macrofossils from the Late Cretaceous have also been recorded amongst Paleocene microfossil assemblages in the NPB of the Takatika Grit (Consoli and Stilwell, 2009; Stilwell et al., 2006). The overlying Tutuiri Greensand, with a dated range of Paleocene-early Eocene (Wilson et al., 2005), hosts late Cretaceous fossils due to reworking (Consoli and Stilwell, 2011; Stilwell et al., 2006). Part of the Takatika Grit may therefore represent an accumulation of sediment and fossils that originated from elsewhere during the Late Cretaceous, deposited post-K/Pg boundary during the Danian (Stilwell et al., 2006). It is interpreted that macrofossils of Late Cretaceous age were transported into the shallow marine environment in which they were preserved, from adjacent terrestrial settings, and hence display wear and are preserved with microfossils of Danian age (Stilwell et al., 2006). Based analyses of diatom, dinoflagellate and radiolarian microfossils, Hollis et al. (in press) suggests that oceanic inundation began in the early Campanian and progressively continued, whereby erosion removed late Campanian and later sedimentary successions of the area. Effectively, the Takatika Grit preserves the initial marine transgression in the early Campanian (82-80 Ma), followed by an interval of non-deposition in the latest Cretaceous and earliest Paleocene (Hollis, in press). This was followed by renewed transgression and marine sedimentation in the late early to middle Paleocene (62.5-60 Ma) (Hollis, in press). Because sedimentation associated with the Takatika Grit would have been

occurring at the same time that Campanian marine sediments were being eroded, dinoflagellate assemblages and macrofossils of both Campanian and Paleocene age were preserved together (Hollis, in press). As such, Cretaceous macrofossils are proposed to have been partially exhumed and reburied *in situ* (Hollis, in press). In contrast, the upper section of the Takatika Grit, the BQA, does not show signs of reworking, and is thought to be representative of early Paleocene deposition (Consoli et al., 2009).

1.4 Palaeontology of the Takatika Grit

For a full review of the palaeontology of the Chatham Islands, please refer to Consoli and Stilwell (2011). After the isolation of the Chatham Rise region through the separation of Zealandia from Gondwana, the biota of the Chatham Rise became a biogeographically distinct entity (Consoli and Stilwell, 2011). The fossil record of the Chatham region is well represented through sequences such as the Takatika Grit (Consoli and Stilwell, 2011), which expands understanding of terrestrial and marine biota and climate over the Late Cretaceous-Early Paleocene period, in the progressive geological evolution of Zealandia from Gondwana.

Microfossils such as spores, pollen, dinoflagellates, foraminifera and acritarchs are well represented from the Chatham Islands, which are essential to the determination of depositional environments as well as age of sedimentary sequences (Consoli and Stilwell, 2011). The age of the Tiotiori Group (and thus the Takatika Grit) was determined through the documentation and analysis of dinoflagellate species (Wilson, 1984a; Wilson, 1984b), as well as radiolarians and diatoms (see above). Palynomorphic data from diverse spore and pollen assemblages, in addition to dinoflagellate species, has given important information about the floral component of the Chatham Rise region during the Late Cretaceous and into the Paleocene (Consoli and Stilwell, 2011). These indicate that Podocarpaceae and Cupressaceae conifers, proteacean angiosperms dominated the forests of the Late Cretaceous Chatham landscape, while ferns occupied the understory (Consoli and Stilwell, 2011), blanketed by clubmosses (Lycopodiopsida) (Stilwell et al., 2006). As the Chatham region progressed through to the Paleocene, relative abundances changed as ferns became less common, while *Podocarpus* were in high abundance, and *Nothofagus* abundance also increased, coupled with an overall decrease in diversity (Consoli and Stilwell, 2011). The palynological data is also supported through unidentified wood fragments (Campbell et al., 1993), and also plant fossils that include a species of *Araucaria* cone (Consoli and Stilwell, 2011; Stilwell et al., 2006). The combination

of both microfossil and macrofloral records over the Chatham Island geological record suggest that the latest Cretaceous Chatham region landscape was dominated by a community of conifers in low diversity, and also experienced a temperate climate with cold winters and warm growing seasons (Consoli and Stilwell, 2011; Pole and Philippe, 2010).

While many invertebrate taxa including corals, bryozoans, brachiopods, clitellate annelids, insects, barnacles and echinoids have been identified from the Chatham Islands, only molluscs and siliceous sponges have been described from the Takatika Grit (Consoli et al., 2009; Consoli and Stilwell, 2011; Consoli and Stilwell, 2005; Stilwell, 2007). Specifically, the molluscan taxa include an assemblage of gastropods of Neritopsidae, Naticidae and Ringiculidae families as well as a bivalve of the *Modiolus* sp. (Stilwell, 2007). Additionally, nautiloid *Procymatoceras* sp., and large ammonites of *Pachydiscus* sp. have also been described (Consoli and Stilwell, 2005), while new specimens of large ammonite tentatively assigned to *Eupachydiscus* await formal description (Consoli and Stilwell, 2011). The variety of siliceous sponges recovered from the Takatika Grit, including numerous taxa from both Hexactinellida and Demospongiae classes (Consoli et al., 2009). These sponges, rare in the Cretaceous-Palaeogene record, are representative of the first known sponges from the Late Creatceous/early Paleocene in the New Zealand and southwest Pacific regions (Consoli et al., 2009).

Overall, the vertebrate fossil record of the Takatika Grit is poor, similar to mainland New Zealand (Campbell et al., 1993; Consoli and Stilwell, 2011). However, vertebrates from both marine and terrestrial settings are known from the Takatika Grit, representing some of the oldest and most important fossiliferous successions of Zealandia (Consoli and Stilwell, 2011). Numerous marine reptile fossils have been identified from the NPB of the Takatika Grit, including incomplete mosasaurine mosasaur remains, comprising of post-cranial elements such as limb bones and vertebrae, in addition to numerous bones assigned to an individual elasmosaurid plesiosaur (Consoli and Stilwell, 2009). A chimaeroid fish *Edaphodon kawai* has also been described from the NPB (Campbell et al., 1993; Consoli, 2006). Terrigenous fossils from the NPB include theropod dinosaur remains, known from post-cranial material such as a centrum, a claw and limb bones, indicative of medium-sized theropod individuals, as well as one that may have been up to 10 m in length, and similar to *Carnotaurus* (Stilwell et al., 2006). Other dinosaur remains are also being researched (Consoli and Stilwell, 2011). Other large vertebrate elements, initially thought to be of non-avian dinosaurian origin, have more recently been associated with the bones of a large bird over 1.5 m tall

(Stilwell and Consoli, 2012). A pneumatic, proximal end of a radius thought to be from a large flighted bird of Early Paleocene age has also been documented from the Takatika Grit (Fordyce, 1991). Articulated avian remains (Consoli and Stilwell, 2011), including undescribed articulated penguin-like fossils (Consoli et al., 2009; Hansford, 2008), such as the fossils that are the subject of this research thesis, have been recovered from the BQA (Consoli et al., 2009). The presence of articulated avian remains in the BQA is indicative of non-reworking in this unit, in contrast to the underlying NPB. Fossils belonging to a deep-water frilled-shark *Chlamydoselachus tatere*, with characteristic three-pronged teeth (Consoli, 2008), have also been recovered from the BQA of the Takatika Grit (Consoli et al., 2009).

CHAPTER II: METHODS

2.1 Photostacking

Both specimens consist of fossils imbedded within a rock matrix. These had both been previously prepared and excavated as much as possible prior to examination by Al Mannering, and could not be prepared any further due to high risk of damage to individual fossils within each rock. Photostacking was done to produce high quality photographs of each, to display exposed fossils in detail. Multiple photographs were taken of each specimen at different focus distances, and then merged to produce an image with a greater depth of field than an ordinary photograph would have. The resultant image for both specimens shows the rock, as well each of the exposed fossils in focus throughout the object allowing for greater resolution and clarity when viewing the exposed fossils in photographic form, as well as potentially aiding in identification of fossil characteristics and diagnostic features.

Photographs for this procedure were taken at Canterbury Museum, Christchurch, March 2015. This was done using a Canon EOS 5D Mark II camera, with a 50 mm macro lens, and was carried out through vertically mounting the camera to a StackShot™ Focus Stacking Rail System, Cognisys, Inc. Using the Auto Step setting specifically, the StackShot™ Focus Stacking Rail System lowered the camera from a set start focus point to a set end focus point on each specimen. The number of photographs/steps to be taken as the camera was lowered in between the start and end focus points was also set, calculated by the StackShot™ Focus Stacking Rail System to take photographs at equal intervals over the distance. The specimens themselves were placed on a sheet of cream-coloured foam, upon a table underneath the StackShot™ Focus Stacking Rail System and camera, and were supported in a constant position by some black leather material (Figure 2.1). A 45 cm metal ruler was used as a scale, and a KODAK Colour Control Patch provided colour control. The placement of lamps in the room where the station was set-up was purposefully set up to provide optimum lighting for the specimens, and was kept constant throughout.

Images produced were transferred to a computer, and the images for each specimen were then "stacked" together to form a single completely in-focus image for each specimen using Adobe Photoshop CC 2015, at the University of Canterbury.

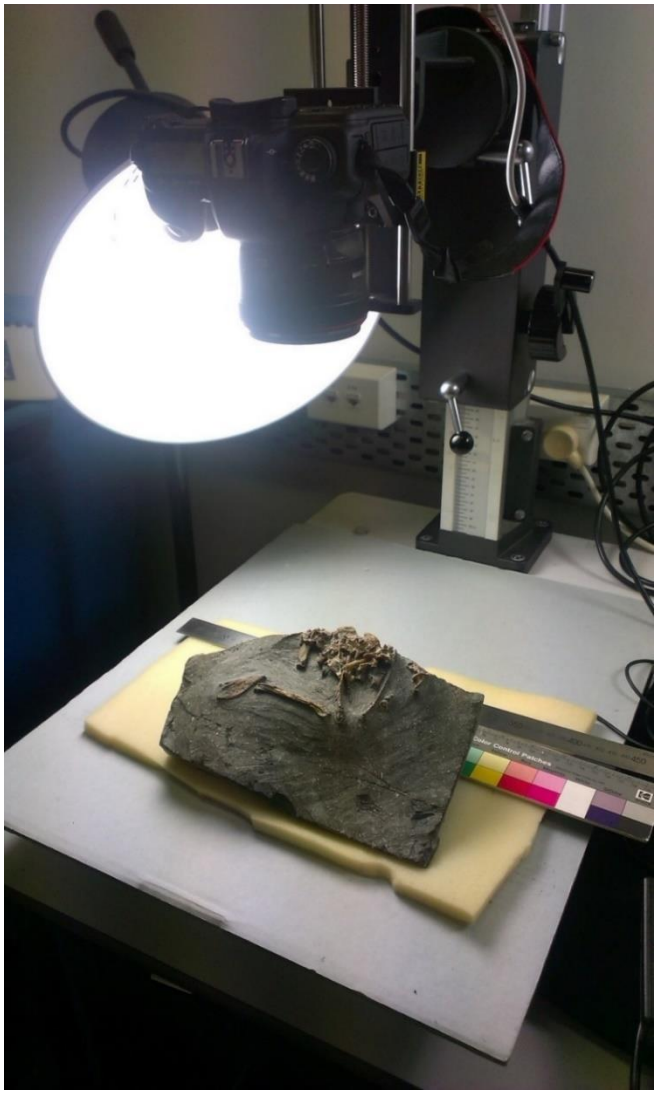

Figure 2.1: Specimen JDS8344, the StackShot™ and camera apparatus, used for photostacking.

2.2 CT Scanning (X-ray Computed Tomography)

In order to allow non-destructive taxonomic assessment of the specimens without damaging the fragile fossils, CT scanning, also known as X-ray computed tomography was used. CT scanning is a radiologic technique that permits detailed assessment of the objects within a surrounding material without actually cutting into it. It does this by producing many profiles of narrow-beam X-ray transmission from multiple angles, resulting in many virtual "slices" of the CT scanned subject. Subsequent reconstruction from these X-ray images can be used to produce a cross-sectional image (McCullough, 1975). Narrow-beam photon attenuation from such X-rays differ based on the material properties that are being CT scanned (McCullough, 1975), and is closely related to density of the

matter itself (Ketcham and Carlson, 2001). Hence, images from CT scans provide a cross-sectional map of the variation in X-ray attenuation in this way (Ketcham and Carlson, 2001).

This type of technique is typically applied in medical imaging, and is also successfully used in palaeontological research (Cnudde et al., 2006). As an example, it has been used to permit high-resolution assessment of Mid-Cretaceous lizard assemblages contained in amber (Daza et al., 2016), and can also be applied in a geological context (Ketcham and Carlson, 2001), including petrology, sedimentology, soil science, and fluid-flow research (Cnudde et al., 2006). Once recognised, the non-destructive application of CT scanning in palaeontology thus provided a valuable tool (Conroy and Vannier, 1984; Haubitz et al., 1988; Ketcham and Carlson, 2001). Vertebrate palaeontological analysis using CT scanning can permit separation of fossils from a lithological matrix through the previously described imaging of density variation in the material, in-turn producing virtual restorations of bones, teeth, cavities and other internal structures within rocks or material that has not or could not be fully prepared without damaging the fossilised contents (Iurino et al., 2013). Furthermore, this technique allows for information to be acquired that may not have been available using conventional palaeontological methods, such as knowledge of internal bone structure, bone density, as well as cavities that may represent the moulds of soft tissues (Iurino et al., 2013). Subsequent use of three-dimensional digital software can additionally produce reconstructions of such fossils in the form of three-dimensional models in a virtual space, transforming real fossils into virtual images and objects that can be further manipulated (Iurino et al., 2013; Wu and Schepartz, 2009). As a result, this non-destructive technique can potentially provide greater information on fossil elements, and enables greater definition of potentially diagnostic features (Iurino et al., 2013).

CT scans of the specimens of this research in particular were carried out at the radiology department of St Georges Hospital, Christchurch, New Zealand, on Tuesday April 14th 2015. This was carried out using a SIEMENS/SOMATOM definition CT scanner, with the radiation setting of scans at 140 KVP. For specimen JDS8344 821 slices were made, each slice taken 0.2 mm apart and 0.4 mm thick. Each slice corresponded to 512 pixels in height and width, where each pixel represents 0.351562 mm. For JDS8341.b 411 slices were made, in 0.2 mm increments and each with a thickness of 0.4 mm. Like JDS8344, each slice in JDS8341.b also corresponded to 512 pixels in height and also width, however each pixel represented 0.357422 mm. The data for each slice produced, was recorded in DICOM files for each specimen (1,504 for JDS8344, and 1,065 for JDS8341.b).

2.3 Generation of Digital Three-dimensional Models

In order to create three-dimensional digital models, the DICOM files produced from the CT scans of each specimen were compiled using the *Materialise Mimics* (Materialise's Interactive Medical Image Control System) Innovation Suite 17.0. Mimics was used to load and process the two-dimensional images stored in DICOM format from the CT scans, to be reconstructed, viewed and measured in a three-dimensional aspect.

To create three-dimensional models of the fossils in the digital space, once the uploaded DICOM files were compiled by Mimics, the orientation of the combined images was selected, so that the two-dimensional images of each profile from each angle CT scanned would line up correctly. From this point it was possible to create "masks" from the resultant reconstructed three-dimensional cross-section (Figure 2.2). Masks are generated by selecting certain parts of an individual slice, which when selected over multiple slices can be transformed into a three-dimensional image. The production of masks can be aided by the use of the 'Threshold' tool in Mimics that selects parts of the image of a certain brightness, where brightness of the image is predominately controlled by the density of the material CT scanned. The differences in densities throughout the rock therefore directly relate to the brightness observed in Mimics, allowing the Threshold tool to separate materials of like-densities, such as fossils (usually brighter) from the surrounding matrix. Selecting brighter pixels in each slice using the Threshold tool, the resultant three-dimensional image or mask can generally reflect the fossils, and other higher density objects (relative to the matrix) within each specimen. Masks created for each fossil can then be edited by selecting or deselecting pixels in each individual two-dimensional slice or by editing the mask in three-dimensions. Overall, both of these can be manipulated to create a more accurate representation of the fossil. In the case where brightness of pixels did not correctly represent the fossil itself, this may be due to the presence of other like-density objects interacting with fossils, or the presence of artifacts. While the brightness of pixels correlates with the density of fossils within each specimen, the representation of the scanned volume can be confounded by artifacts, such as reflective minerals on the surface of the specimen, or in the matrix such as pyrite, which scatter X-rays during the CT scan and produce distinctive flares in the subsequent images. Furthermore, it should be noted that while bright pixels can be generally associated with fossils, they may also be representative of individual rocks within the specimen of

different densities to the surrounding matrix. The effectiveness of the rendering of a three-dimensional model is also limited by resolution of the CT scan, and also by the number of slices made.

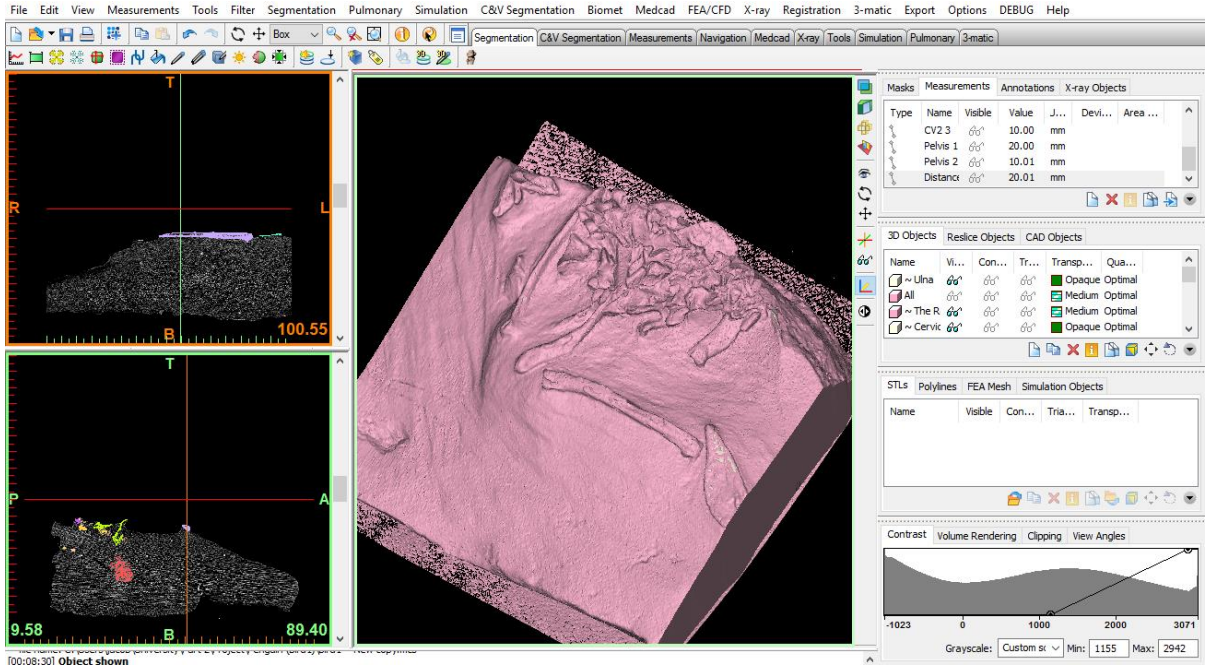

Figure 2.2: A screenshot in *Materialise Mimics* showing two-dimensional cross-sectional images of JDS8344, as well a three-dimensional mask created of the specimen's surface. Coloured pixels in cross-sectional images refer to masks of individual fossils, and letters T, B, R, L, P, A correspond to the orientations Top, Bottom, Right, Left, Posterior and Anterior respectively.

Using this methodology, accurate individual masks were created for each fossil in both specimens over the course of 2015 and early 2016. These were subsequently exported as .STL files from Mimics to allow for further manipulation of the three-dimensional digital fossils in a wide range of programs and 3D printing. Individual fossil masks were also measured using the measurement tool, provided by Mimics, in millimetres. Measurements were performed in Mimics by placing an initial marker point on a three-dimensional mask, and then placing a subsequent point at another place on the same mask, whereby a straight line of displacement is generated connecting the two points; giving the distance measurement between them.

2.4 Comparative Palaeontology

Comparative palaeontology was carried out at the Canterbury Museum, Christchurch by comparing the measurements of the fossils of JDS8344 and JDS8341.b with taxa within the museum's collections. Additionally, further measurement data was also added from published literature. General comparison of morphology of elements within JDS8344 and JDS8341.b were also compared with images of relevant bones of taxa using the Smithsonian National Museum of Natural History, Division of Birds Collections (http://collections.nmnh.si.edu/search/birds/).

All direct measurements of comparative material at Canterbury Museum were carried out using a Mitutoyo 500-196-30CAL Absolute Advanced Onsite Sensor (AOS) digital calliper, accurate to 0.01 mm.

2.4.1 JDS8341.b: Cervical Vertebra IV

For the comparison of the morphology of cervical vertebrae IV of JDS8341.b to other Aequorlitornithes bird groups, measurement of vertebrae was carried out as per the methodology in Guinard et al. (2010), which included the study of neck structure and cervical vertebrae morphology in extant penguins such as the King Penguin (*Apenodytes patagonicus*), Gentoo Penguin (*Pygoscelis papua*), Macaroni Penguin (*Eudyptes chrysolophus*) and Humboldt Penguin (*Spheniscus humboldti*). Importantly, the authors carried out biometric measurements taken directly from the material of each of these species at different life stages (Guinard et al., 2010), which measured the distance between certain points on the vertebrae (Figure 2.3), and could then be replicated and performed on the cervical vertebra IV of JDS8341.b, as well as other taxa. Hence, measurements of cervical vertebra IV following Guinard et al. (2010), were performed on numerous adult specimens of various species at Canterbury Museum including Emperor Penguin (*Aptendytes forsteri*), King Penguin, Macaroni Penguin, Gentoo Penguin, Adélie Penguin (*Pygoscelis adeliae*), Humboldt Penguin, Waimanu Penguin (*Waimanu tuatahi*), Wandering Albatross (*Diomedea exulans*), Shy Mollymawk (*Thalassarche cauta*), Southern Giant Petrel (*Macronectes giganteus*), Black Shag (*Phalacrocorax carbo*), Adjutant Stork (*Leptoptilos* sp.), Australian Pelican (*Pelecanus conspicilatus*), Red-throated Diver (*Gavia stellata*), Great Crested Grebe (*Podiceps crisatus*), Southern Screamer (*Chauna torquata*), and Mute Swan (*Cynus olor*). These measurements were carried out between December 2015 and January 2016, and were added to

those from cervical vertebra IV of JDS8341.b, and the data gratefully provided from Guinard et al. to produce a comparative dataset (see Appendix).

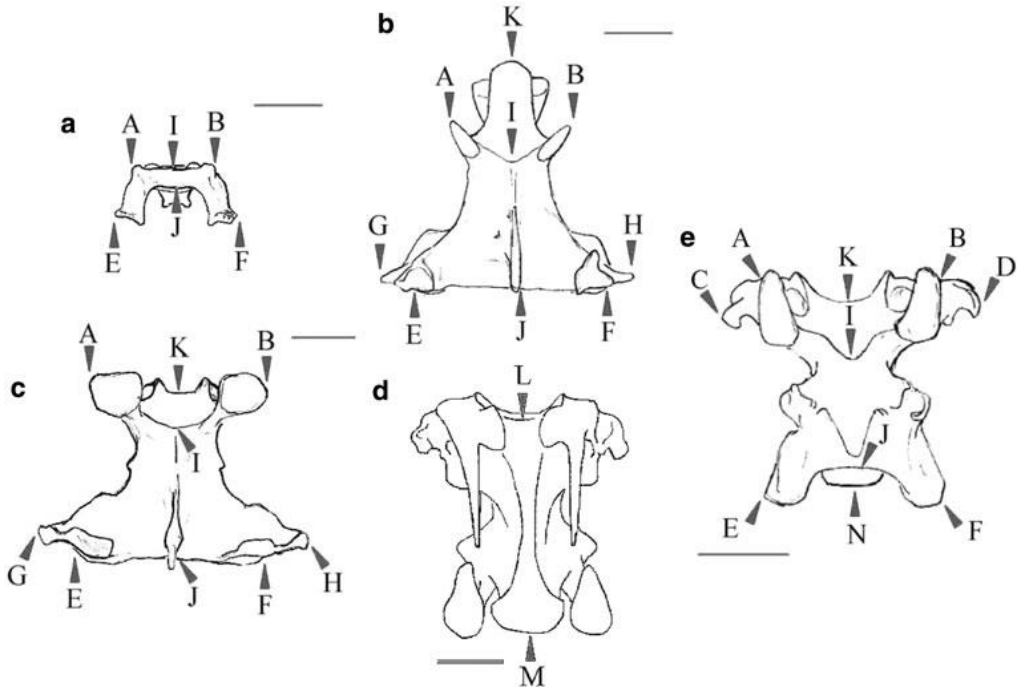

Figure 2.3: Direct measurements performed on cervical vertebrae, image taken from Guiard et al., (2010). **a**, atlas, **b**, axis, **c**, cervical IV, **d**, cervical VII, **e**, cervical VIII. **a**-**c** and **e** dorsal aspects; **d** ventral aspect. Distance between certain points notation: A-B Front width 1 (Fw1), C-D Front width 2 (Fw2), E-F Back width 1 (Bw1), G-H Back width 2 (Bw2), I-J Length 1 (L1), B-F Length 2 (L2), K-J Length 3 (L3), L-M Length 4 9(L4), K-N Length 5 (L5). Scale bars = 1cm.

This compiled dataset of cervical vertebrae measurements (see Appendix) was then used to produce a Principle Components Analysis (PCA), a commonly used method of analysis for studying patterns of variation for size and shape within a group (Cracraft, 1976), which finds hypothetical components that account for as much variance as possible in the multivariate dataset. Effectively, this was considered in order to compare the differences in cervical vertebrae IV morphology between taxa of the Auquorlitornithes clade, and also to give an estimated phylogenetic perspective of JDS8341.b compared to other Auquorlitornithes, both extant and extinct. This was performed using PAST (PAleontological STatistics) version 3.12 (Hammer, 2001), where the raw data was converted to log values prior to analysis. Considering that this analysis compared taxa with a variable size range, in this multivariate morphometric analysis it can be assumed that the first component is descriptive of size variability and will therefore account for a high percentage of the total explained variance

(Cracraft, 1976). Thus the subsequent components will likely explain other morphometric variables such as shape (Cracraft, 1976) which may also be considered when comparing the relatedness of different evolutionary lineages. The Mute Swan was used as an outgroup, as part of the more basal Galloanserae superorder, when compared to Auquorlitornithes, as per recent studies of avian higher phylogeny (Jarvis et al., 2014; Prum et al., 2015).

2.4.2 JDS8344: Ulna and Radius

In order to allow direct comparison of morphology between JDS8344 and extinct Aequorlitornithes, measurements of the ulna and radius of JDS8344 were compared with the morphology of the basal *Waimanu* penguin. Measurements of the ulna and radius of JDS8344 were performed using the measurement tool in *Materialise Mimics*. Direct measurements of the radius and ulna of *Waimanu* specimens OR2994, 2009.99.1, 2010.108.3 and 2010.108.1 were carried out at Canterbury Museum on the 28th April 2016, using a digital calliper. On each bone, measurements were taken of the total length, proximal width, mid-shaft width, proximal depth, proximal depth, mid-shaft depth, and the distance from the proximal end to the bend in the bone's shaft (distance to bend) (Figure2.4). The compiled measurements were then compared by producing a PCA, using the statistical program PAST. This was done as per the methodology used to compare the measurements of cervical vertebra IV.

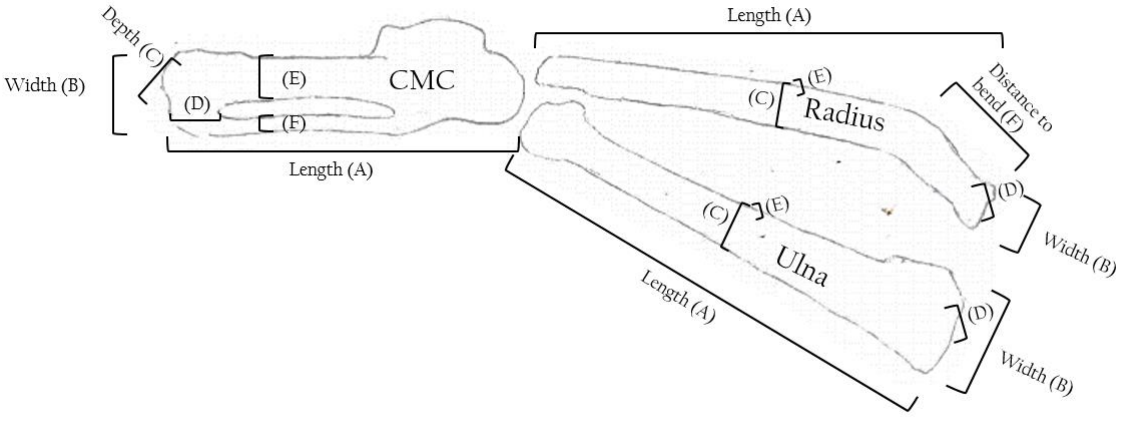

Figure 2.4: Locations of direct measurements taken from Carpometacarpus (CMC), radius, and ulna elements across *Waimanu* specimens and JDS8344. Reference for labels for the CMC is as follows: (A) length, (B) width, (C) depth, (D) distance from *sulcus interosseus* to distal facet, (E) width of metacarpal II, (F) width of metacarpal III. Labels for radius and ulna measurements: (A) length, (B) proximal width, (C) mid-shaft width, (D) proximal depth, (E) mid-shaft depth, (F) Distance from proximal facet to anterior bend (radius only). Shape of outlines are based on the forewing elements of *Waimanu tuatahi*.

2.6 Phylogenetic Analysis

2.6.1 Data Set

To permit the evaluation of the phylogenetic placement of both specimens JDS8344 and JDS8341.b when compared to living and extinct species, the most recent revisions of morphological character data matrixes were utilised, from both Ksepka and Clarke (2010) and Ksepka et al. (2012). Both matrixes were used, rather than a single matrix, as a means of testing the accurate placement of JDS8344 and JDS8341.b relative to other species, across studies.

The character matrix of both Ksepka and Clarke (2010) and Ksepka et al. (2012) are versions of previous work of multiple authors, consisting of combined morphological and molecular datasets for Sphenisciformes, formulated and used for comparative and phylogenetic research (Ando, 2007; Bertelli and Giannini, 2005; Clarke et al., 2010; Clarke et al., 2007; Giannini and Bertilli, 2004; Hospitaleche et al., 2007; Ksepka et al., 2006; Ksepka and Clarke, 2010; Ksepka et al., 2012; Ksepka and Thomas, 2012; O'Hara, 1989; Schreiweis, 1982; Zusi, 1975). The combined dataset presented in Ksepka and Clarke (2010) consists of 219 morphological characters and >6,000 base pairs of molecular genetic sequence data. Outgroup taxa are represented by 2 species of Gaviiformes as a distal outgroup taxon, and 13 species of Procellariiformes are also used as the extant sister taxon to Sphenisciformes. The ingroup taxa consists of 19 extant penguin species and 33 extinct penguin species (Ksepka and Clarke, 2010). The character matrix of Ksepka et al. (2012) is comprised of 245 morphological characters, combined with genetic sequence data from RAG-1, cytochrome b, 12SrDNA, 16SrDNA and COI. This combined dataset contains a total of 23 extant and 33 extinct penguin ingroup taxa, and two Gaviiformes and 13 Procellariiformes were used as outgroup species (Ksepka et al., 2012).

In the present study, both datasets of Ksepka and Clarke (2010) and Ksepka et al. (2012) were altered to include the anatomical information of JDS8344 and JDS8341.b. Constrained to the use of characters derived from the available known elements (for a list and description of each element see ***Chapter 3: Systematic Palaeontology***), morphological characters were initially scored for both JDS8344 and JDS8341.b, using the morphological character definitions presented in Ksepka and

Clarke (2010), and also the definitions available online from Dryad (dx.doi.org/10.5061/dryad.93j174jd) as part of the Supplementary Information for Ksepka et al. (2012).

A morphological character matrix was initially modified from the matrix presented in Ksepka and Clarke (2010) to include both JDS8344 and JDS8341.b as separate taxa. Both matrixes of Ksepka and Clarke (2010) and Ksepka et al. (2012) were also separately altered and tested with JDS8344 and JDS8341.b referred to as a single merged taxon. Additionally, the dataset from Ksepka and Clarke (2010) was modified to merge the morphological characters of *Waimanu manneringi* and *W. tuatahi* into a single taxon group using the genus name '*Waimanu*' to describe both species as a single taxon. This was done due to large variability in morphology of both *Waimanu* species, and also the consideration that both species do not have any conflicting morphological characters, and share the same characters that are presented within the matrix (P. Scofield, 2016, pers. commun). Taxon groups IB/P/B-0382 and "*Tonniornis*" were also omitted from the modified Ksepka and Clarke (2010) dataset, because of incomplete and contradictory data for these taxa. The molecular aspect of each respective dataset were not altered for this present study. To test both extinct and extant taxa under the same settings, with consideration that fossil specimens can only be scored for osteological morphological characters, each dataset was also separately modified to include only osteological characters, omitting all other morphological and genetic character data.

Analyses for the testing of phylogenetic placement were performed for each modified matrix, from Ksepka and Clarke (2010) and Ksepka et al. (2012), of both morphological and molecular data, as well as osteology-only data. Character matrixes modified from Ksepka and Clarke (2010) consist of 219 morphological characters, using 71 taxa where JDS8344 and JDS8341.b are included as separate taxa, and 70 taxa where JDS8344 and JDS8341.b are merged into a single taxon. The resultant dataset modified from Ksepka et al. (2012) is comprised of 245 morphological characters, and 72 taxa.

2.5.2 Primary Search Strategy

Heuristic searches were performed using PAUP* (Phylogenetic Analysis Using Parsimony, * and other methods) version 4.0a150 (Swofford, 2003) on both morphological and molecular character matrixes, as well as osteology-only character matrixes, where JDS8344 and JDS8341.b are referred to as a single merged taxon. Heuristic search strategy was conducted with 1,000 replicates of random taxon addition, saving 10 trees per replicate, where no more than 2 trees of score (length) greater than

or equal to 5 were saved in each replicate. TBR (Tree Bisection and Reconnection) branch swapping methodology was applied. No Parsimony optimality criterion was used, where all characters were equally weighted, and gaps in the matrix were treated as "missing". Additionally, multistate characters within the matrixes were used to represent polymorphism, and branches with a minimum length of zero were collapsed to create polytomies. All trees were rooted to *Gavia immer*.

Two heuristic searches were also performed on the character matrix modified form Ksepka and Clarke (2010); one that included JDS8344 and JDS8341.b as separate taxa, and another where the characters of JDS8344 and JDS8341.b were merged and included as a single taxon. This was carried out using TNT (Goloboff et al., 2008). Searches were performed using 1,000 random taxon addition replicates, where 10 trees were saved per replicate. TBR branch swapping was used; all characters were equally weighted; and zero-length branches were to collapsed to produce polytomies. Trees were also rooted to *Gavia immer* for this analysis.

2.5.3 Bayesian Analyses

To determine posterior probabilities for clades within the phylogenetic tree, including that relevant to JDS8344 and JDS8341.b, Bayesian analyses was carried out using MrBayes 3.1.2 (Ronquist and Huelsenbeck, 2003). An analysis was performed for the modified osteology-only dataset of both Ksepka and Clarke (2010), and also Ksepka et al. (2012). JDS8344 and JDS8341.b were merged into a single taxon for both of these analyses, and all other modifications regarding characters and ordering assumptions were tested as per the primary phylogenetic analyses. The outgroup similarly consisted of *Gavia immer*. Analysis of the output from each Bayesian analysis was performed using Tracer v1.6 (Rambaut and Drummond, 2004).

Characters were assumed to have rate variability distributed according to gamma parameter (rates = gamma) with flat prior distribution (0–200), and only variable characters were assumed to have been included (coding = variable). Two independent analyses were performed simultaneously to check for sufficient convergence—a combined total of 10,000,000 generations, which was sampled every 1,000 generations. To improve exploration of tree topology space, branch swapping was set to 3, the heating parameter was set to 0.20, and one cold and five incrementally heated chains were used per analysis (totalling 6 chains per analysis). Using relative burnin, the first 25% of sampled trees were discarded after the analysis of each dataset was completed, and a consensus tree was produced.

CHAPTER III: TAXONOMY

This chapter outlines and describes the elements of specimens JDS8344 and JDS8341.b, from which morphological character scores were drawn for subsequent phylogenetic analyses. The formal description and systematic palaeontology of the novel taxon *Archaeodyptes stilwelli*, is presented below and further discussed through the results of phylogenetic analyses, as addressed in ***Chapter IV: Analyses.*** Figures presented below are developed from *Materialise Mimics* software manipulation of CT scanning as described in ***Chapter II: Methods***, unless otherwise stated. All anatomical terminology follows Baumel and Witmer (1993).

3.1 Systematic Palaeontology

Class: Aves Linnaeus, 1758

Subclass: Ornithurae Haeckel, 1866

Infraclass: Carinatae Merrem, 1813

Order: Sphenisciformes Sharpe, 1891 (*sensu* Clarke et al., 2003)

Genus: *Archaeodyptes*, gen. nov.

3.1.1 Type species: *Archaeodyptes stilwelli* sp. nov.

3.1.2 Included species: Type species.

3.1.3 Etymology:

From Greek archae meaning "ancient" or "beginning", and dyptes meaning "diver". The implication of both words used in conjunction as "*Archaeodyptes*" produces the meaning "first diver" or "ancient diver".

3.1.4 Diagnosis:

The forelimb elements (*ossa alae*) such as the carpometacarpus, radius and ulna are flattened, and on the phalanx of the third digit (*ossa digitorum manus, phalanx digiti minoris*) the proximal tubercle is present. The position of the coronoid process (*mandibula, processus coronoideus*) on the dorsal margin of the mandible is on the rostral end of the caudal fenestra (*fenestra caudalis mandibulae*). The caudal fenestra on the mandible is also open, and can be seen through in both medial and lateral aspects. The mandible is also caudally projected in dorsal aspect, forming the retroarticular process (*mandibula, os angulare, processus retroarticularis*); in dorsal aspect the retroarticular process is moderately long and narrow relative to the articular area. The furcular process (*furcula, apophysis furculae*) is absent. Pronounced, deep concavity of the *facies articularis humeralis* on the coracoid is not observed. The acrocoracoid neck (*collum acrocoracodei*) of the omal end of the coracoid, particularly associated with the *facies articularis clavicularis* and *processus acrocoracoideus* is not bent significantly medially, and shows dorsoventral curvature.

3.1.5 Discussion:

Based on the osteological autapomorphies mentioned in the diagnosis, such as flattened long bones of the forewing, and the presence of the proximal tubercle on the phalanx of the third digit, *Archaeodyptes* is more closely related to penguins than any other bird order. An inability to fly can also be interpreted, based on the flattened long bones of the forewing/flipper— a commonly known synapomorphy of the penguin group. Unique to most other stem-group and modern crown-group penguins, *Archaeodyptes* has a proximally bent radius with a narrow shaft, and a carpometacarpus that is relatively straight and broad, and is not anteriorly bowed on metacarpal II. These features are apomorphic with *Waimanu tuatahi*, but not with other Sphenisciformes. A plesiomophy of *Archaeodyptes* is that the olecranon and posterior border of the ulna in *Archaeodyptes* arise as an acute rounded projection from the humeral facet, a feature more characteristic of flying birds, such as *Diomedea exulans*. Furthermore, in *Archaeodyptes* the acrocoroid neck of the omal coracoid is not bent significantly medially, and thus does not display a 'hooked' morphology in dorsal aspect; a morphology that is shaped more similarly to that of Procellariformes (i.e. the shy albatross *Thalassarche* cauta).

Clarke et al. (2003) applied the name Spheniscidae to all crown-group penguins, Sphenisciformes to all penguin forms that have lost the ability of aerial flight—homologous to that of

modern penguins, and Pansphenisciformes to all avian taxa more closely related to extant penguins of Spheniscidae than any other extant avian lineage (Clarke et al., 2003). Since there are no volant penguin taxa currently known to science, the clade names Pansphenisciformes and Sphenisciformes currently refer to the same taxa, until a more basal volant taxa of the penguin lineage is potentially discovered (Ksepka et al., 2008). Since *Archaeodyptes* was not capable of aerial flight, it is placed within Sphenisciformes.

Species: *Archaeodyptes stilwelli* sp. nov.

3.1.6 Etymology (Species):

The type species "*stilwelli*" honours palaeontologist Jeffrey Stilwell, who found and collected both the holotype and the referred specimen.

3.1.7 Holotype:

NMNZ (Te Papa Tongarewa The Museum of New Zealand) JDS8344 (Figure 3.1); associated part skeleton comprising of the distal half of a left carpometacarpus, a right ulna, the proximal half of a right radius, a right proximal phalanx of the second digit, a right phalanx of the third digit, an almost complete axis, four cervical vertebrae, a caudal vertebra, a left rib, and a partial worn ilium.

3.1.8 Type Locality and Horizon:

Both specimens JDS8344 and JDS8341.b were discovered and collected by Jeffrey Stilwell and party. JDS8344 was collected early 2008. JDS8341.b is one of four pieces (JDS8341a, b, c, and d), and was collected mid-February 2006. Both specimens were recovered from Maunganui Beach, east of Tahatika Creek, north western Chatham Island, near 43°45'10.1"S, 176°40'46.8"W; New Zealand. Fossil Record Number CH/f0651. Both specimens were recovered *in situ* from the relatively narrow "bird horizon", the outcrop of which was part of the upper horizon of nodular-phosphate and bone package, spanning approximately 0.5 km, on a wave cut platform; associated with other semi-articulated bird and dinosaur fossils, as well as teleost vertebrae and shark teeth. Upon recovery, both specimens were subsequently accessioned into the collections of Te Papa Tongarewa The Museum of New Zealand and subsequently loaned to Canterbury Museum on 30/09/2014, where they were prepared by Mr. Al Mannering. Part of the Tioriori Group (Cretaceous—Tertiary); attributed to the

Takatika Grit rock unit, constrained to mid-Campanian to mid-Danian stage in age (Late Cretaceous to early Paleocene) (Consoli and Stilwell, 2009; Hollis, in press).

Figure 3.1: Holotype specimen of *Archaeodyptes stilwelli* sp. nov JDS8344, as a product of photostacking, explained in Chapter II: Methods, section 2.2. Scales shown include a 45 cm metal ruler and a KODAK Colour Control Patch.

3.1.8.1 Carpometacarpus:

Description – From the left wing of the animal, the distal half of the carpometacarpus is well preserved (Figure 3.2). It appears that while incomplete, the *spatium intermetacarpale* is long and ovoid in shape between metacarpals II and III. Subtle flattened dorsal and ventral surfaces are observed, while an ovoid cross-section is present dorsoventrally. The shape of the carpometacarpus is relatively straight and broad, and metacarpal II (*os metacarpale majus*) does not show distinct anterior bowing. The distal articular surface also broadens anteriorly in a distal aspect. Metacarpals II and III (*os metacarpale minus*) appear to be sub-equal in distal extent—yet without certainty due to only the distal portion being available for study.

Discussion – What is preserved resembles a carpometacarpus generally similar to that of *Waimanu* taxa, only differing notably where the carpometacarpus of *Waimanu* have a more rounded distal end, whereas that of *Achaeodyptes stilwelli* is relatively flattened. Also characteristic of *Waimanu* (Slack et al., 2006), the presence of sub-equal metacarpals II and III is a feature of many birds, also including the basal mid Eocene penguin *Perudyptes devriesi*, and Late Eocene penguin *Pachydyptes ponderosus*. In contrast, metacarpal III extends significantly distal to metacarpal II in some more recent penguin species, including Early Miocene *Palaeospheniscus patagonicus*, latest Oligocene/earliest Miocene *Platydyptes marplesi*, and also penguins within the Spheniscidae family (Ksepka et al., 2008).

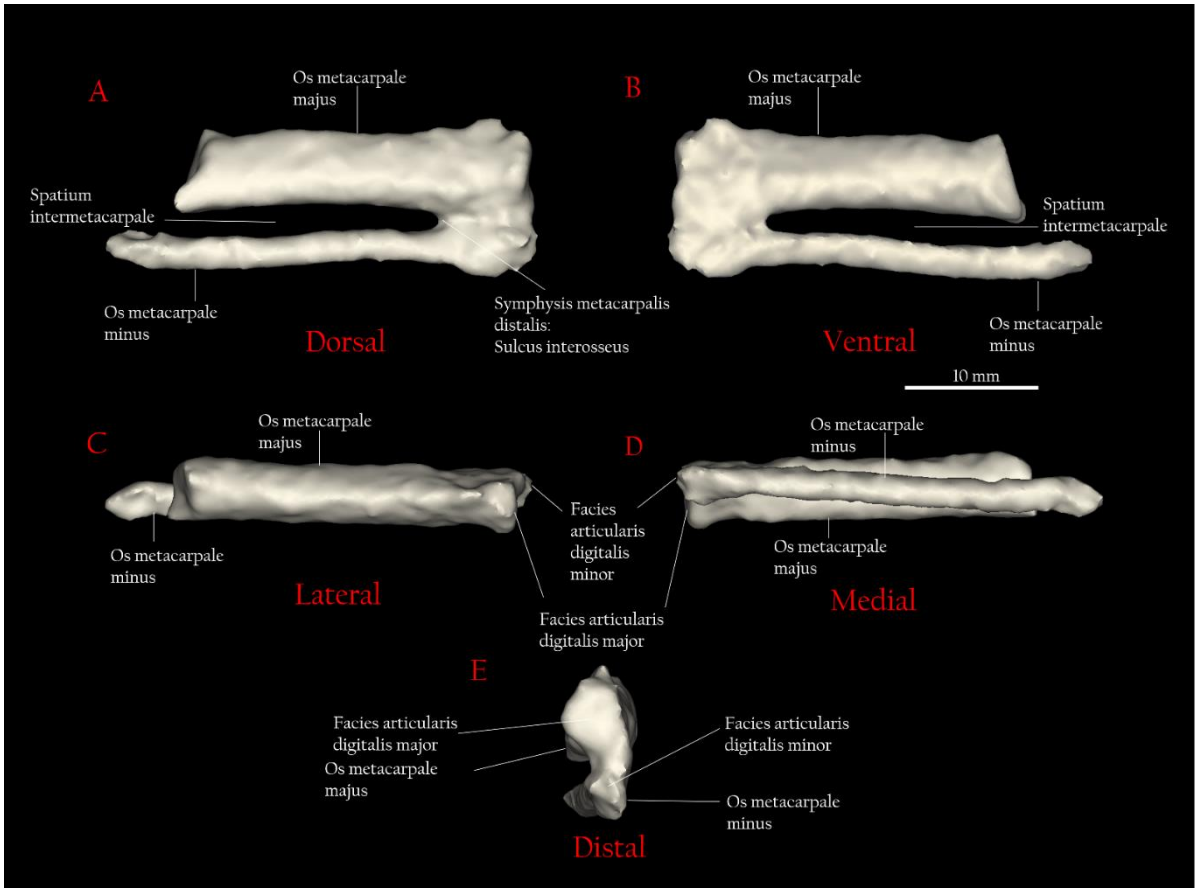

Figure 3.2: The left carpometacarpus of JDS8344. Shown in dorsal (A), ventral (B), lateral (C), medial (D), and distal (E) aspects.

3.1.8.2 Ulna

Description – The ulna of the right wing is preserved almost completely intact, only missing an eroded fragment from the posterior margin of the fossil, which can be viewed in the lateral aspect (Figure 3.3). Dorsal and ventral surfaces are flattened, and an ovoid dorsoventral cross-section

is observed. The olecranon arises proximally from the humeral facet as an acute projection, rounded in the lateral aspect of the posterior border. The posterior margin of the ulna is thin relative to the anterior margin. The ulnar shaft is thinnest proximally, after the humeral facet, and thickens distally. The ulna also presents a subtle bend around a third of the length of the shaft from the proximal end. At the distal end of the ulna, the ventral condyle (*condylus ventralis ulnaris*) is projected slightly more distally compared to the dorsal condyle (*condylus dorsalis ulnaris*).

Discussion – The ulna of JDS8344 represents the most distinctive feature in contrast other known penguin species. Particularly, the presence of a proximally projected olecranon from the humeral facet appears markedly different compared to other ulna morphologies of currently known penguin species. In more crownward penguins, the posterior border and olecranon morphology may form an acute projection distally displaced from the humeral facet, as can be seen in *Spheniscus* and *Eudyptes* genera. Earlier penguins have also shown well-developed tab-like projection arising proximally very close to the humeral facet, such as in *Waimanu* spp. and *Icadyptes salasi*, or as a smooth curve with the apex located one quarter of the length of the bone to the distal end, such as in *Archaeospheniscus lowei* and *Archaeospheniscus lopdelli*. This is in distinct While similar, the olecranon and posterior border morphology is also different compared to other closely related seabirds, such as Procellariiformes like *Diomedea exulans*, which display a completely rounded morphology. While a degree of flattened morphology is present, it is not to as great of an extent as the forms exhibited in known penguins. Attachment protuberances for feather quills, which are sometimes preserved in along the ulnar shaft of penguins (Mayr, 2005), are not visible and therefore were either not preserved, or may have been susceptible to erosion.

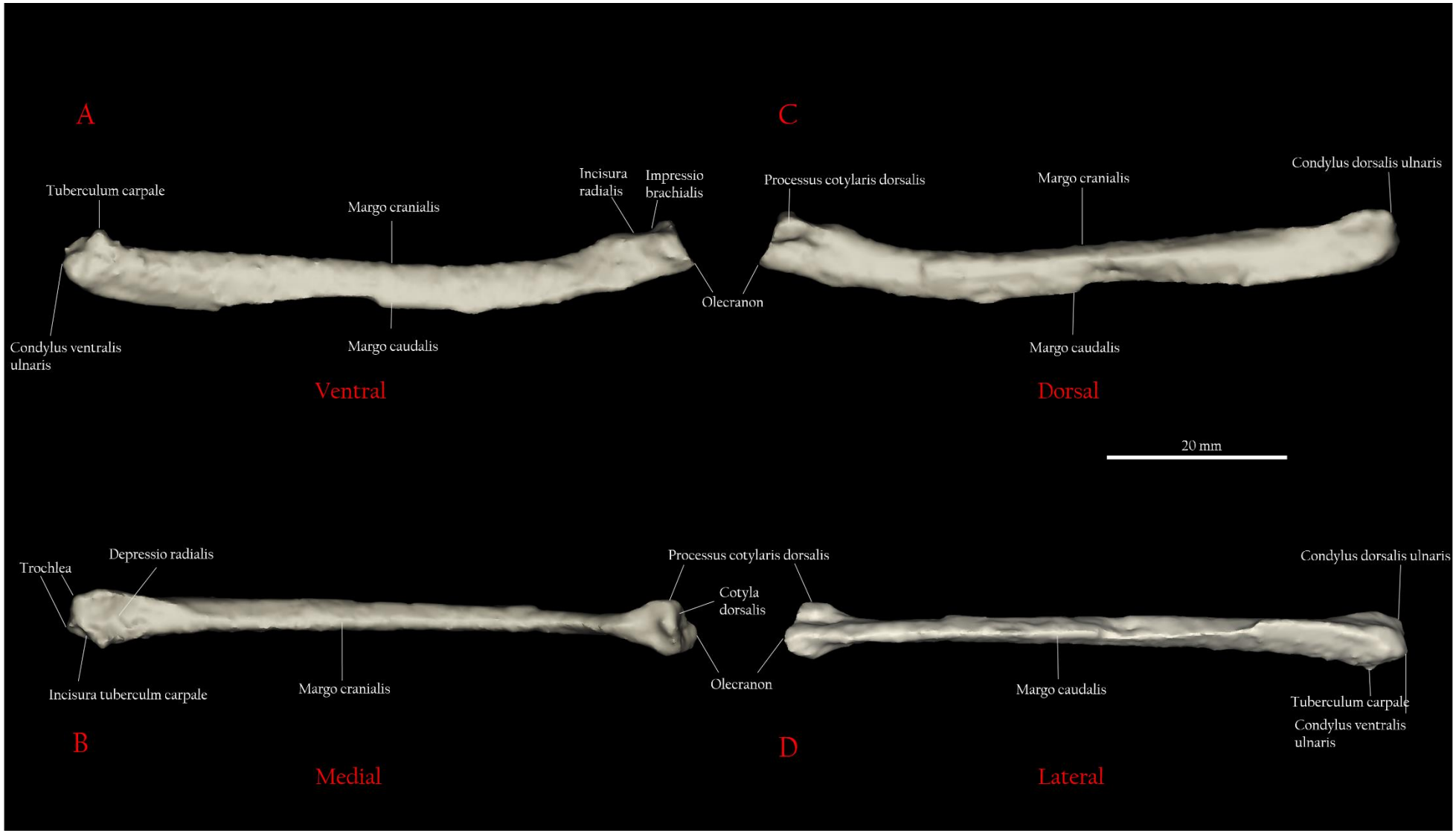
A
Tuberculum carpale
Margo cranialis
Incisura radialis
Impressio brachialis
Condylus ventralis ulnaris
Margo caudalis
Olecranon
Ventral
C
Processus cotylaris dorsalis
Margo cranialis
Condylus dorsalis ulnaris
Margo caudalis
Dorsal
20 mm
Trochlea
Depressio radialis
Incisura tuberculm carpale
Margo cranialis
B
Medial
Processus cotylaris dorsalis
Cotyla dorsalis
Olecranon
Margo caudalis
Condylus dorsalis ulnaris
Tuberculum carpale
Condylus ventralis ulnaris
D
Lateral

Figure 3.3 (previous page): The right ulna of JDS8344. Shown in ventral (A), medial (B), dorsal (C), and lateral (D) aspects.

3.1.8.3 Radius

Description – The radius is incompletely preserved due to recent erosion from the block it was preserved in. The specimen retains the proximal end of the bone and the humeral articulation, and almost half of the radial shaft. Despite a longitudinal fracture (Figure 3.4), the radius shows obvious medio-anterior bowing (however it is impossible to tell if this is morphological or due to *post-mortem* preservation) and is flattened dorsoventrally. Although flattened on both dorsal and ventral surfaces, the radius is not substantially widened, like the ulna. The radius is bent anterior-dorsally and is slightly more flat and widened near the proximal facet. The radius of *Archaeodyptes stilwelli* also lacks an anterior angulation and notch. A depression is additionally visible on the dorsal side of the radius, between the anterior border and the mid-line, created by the *musculus extensor metacarpi radialis* tendon.

Discussion – The flattened nature of the radius of JDS8344 facilitates diving behaviour, and is similar to all other known Spheniscifomes. The features of the proximal half of the radius, particularly the lack of widened shape, and the presence of an anterior-dorsal bend, differ from all other stem- and crown-group Spheniscifomes except *Waimanu* (i.e. are apomorphic of this clade). However, the posterior margin of the bicipital tubercle (*tuberculum bicipitale radii*) is more prominent on the radius of *Waimanu* than *Archaeodyptes stilwelli*. The furrow produced by the *musculus extensor metacarpi radialis* tendon on the radius of JDS8344 is a feature that is also visible in extant penguins, as well as extinct penguin fossils such as in *Icadyptes salasi*, where the *metacarpi radialis* crosses the radius and inserts to the anterior margin of the proximal articulation facies of the carpometacarpus (Ksepka et al., 2008).

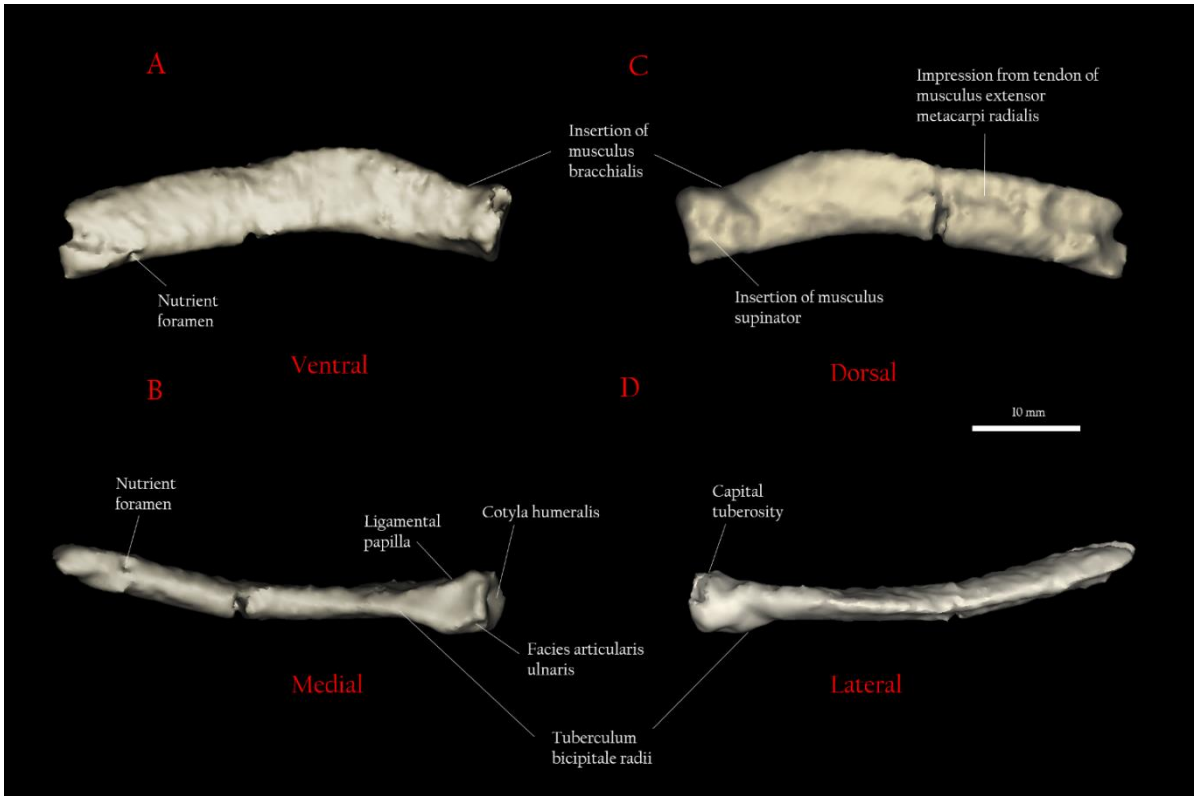

Figure 3.4: The right radius of JDS8344. Presented in ventral (A), medial (B), dorsal (C), and lateral (D) aspects.

3.1.8.4 Proximal manus phalanx of the second digit

Description – The right proximal manus phalanx of the second digit (phalanx II-1) is completely intact and is well preserved (Figure 3.5). The bone appears flattened, thickest at the proximal carpometacarpal articulation facet, and thins towards the articulation facet with the distal phalanx of the second digit (phalanx II-2)—which has not been recovered. The proximal facet is also wider and has greater depth compared to the distal facet. The anterior border from the mid-line of the phalanx is also particularly thin and flattened in contrast to the rest of the bone. The proximal phalanx of the second digit is widest around the mid-point of the length of the bone, where the anterior border is thinned most extensively.

Figure 3.5 (next page): The right proximal manus phalanx of second digit of JDS8344. Presented in dorsal (A), ventral (B), lateral (C), medial (D), proximal (E), and distal (F) aspects.

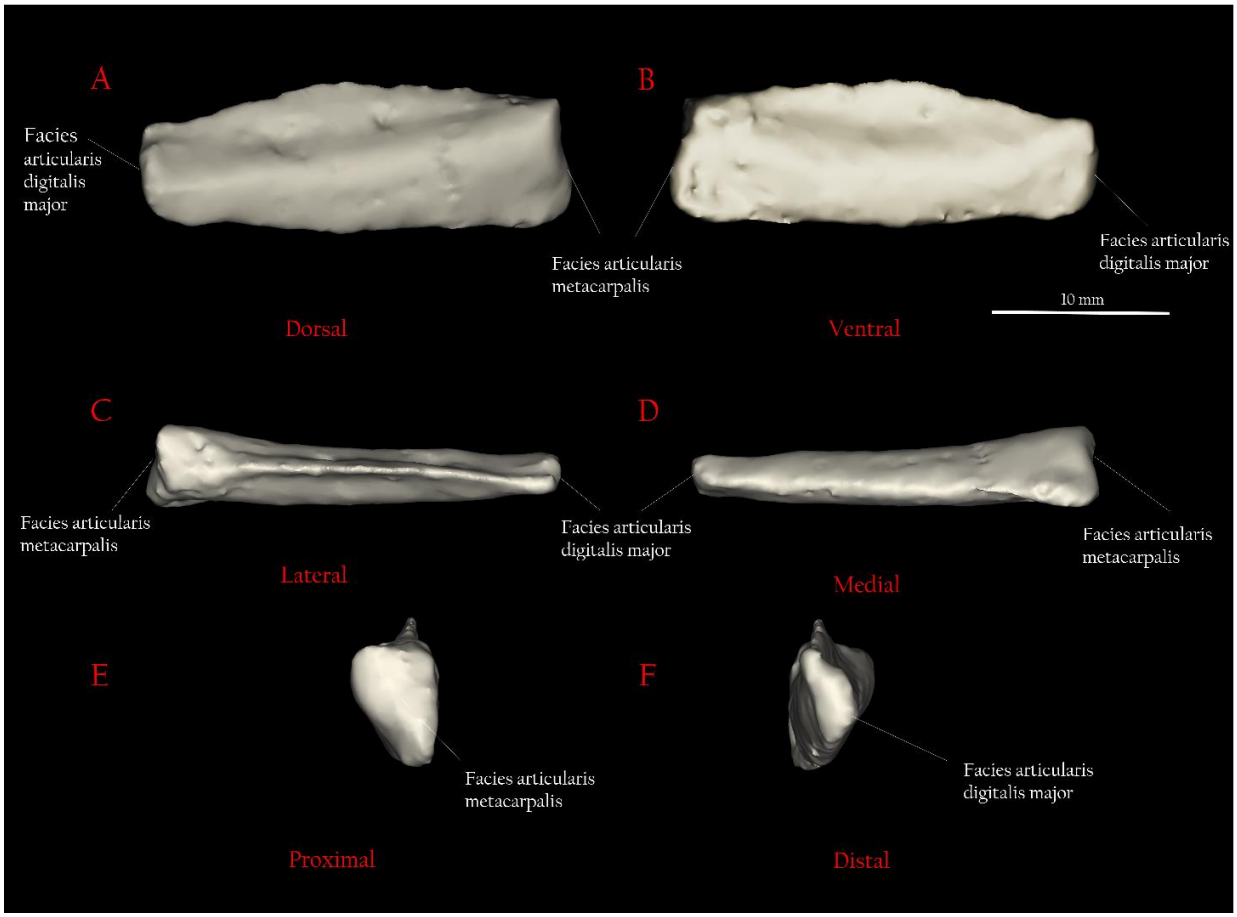

3.1.8.5 Manus phalanx of the third digit

Description – The manus phalanx of the third digit (phalanx III-1) of the right wing (Figure 3.6) is incompletely preserved, preserving the articulation facet with the carpometacarpus and most of the bone's body except for the tapered tip at the distal end. At the proximal end, separate from the carpometacarpal facet, the proximally projected tubercle is preserved. What is preserved of phalanx III-1 is shorter in length than the length of phalanx II-1, however the extent of this and the true length of the complete bone is unknown since the tip of the digit was not preserved.

Discussion – The presence of a proximal tubercle on phalanx III-1 is also observed in extant penguin species, but has not been recovered from any fossil stem penguins. While the true length of phalanx III-1 is not preserved in JDS8344, it is typical of avian morphology that phalanx III-1 is shorter than the length of phalanx II-1 (Ksepka et al., 2008).

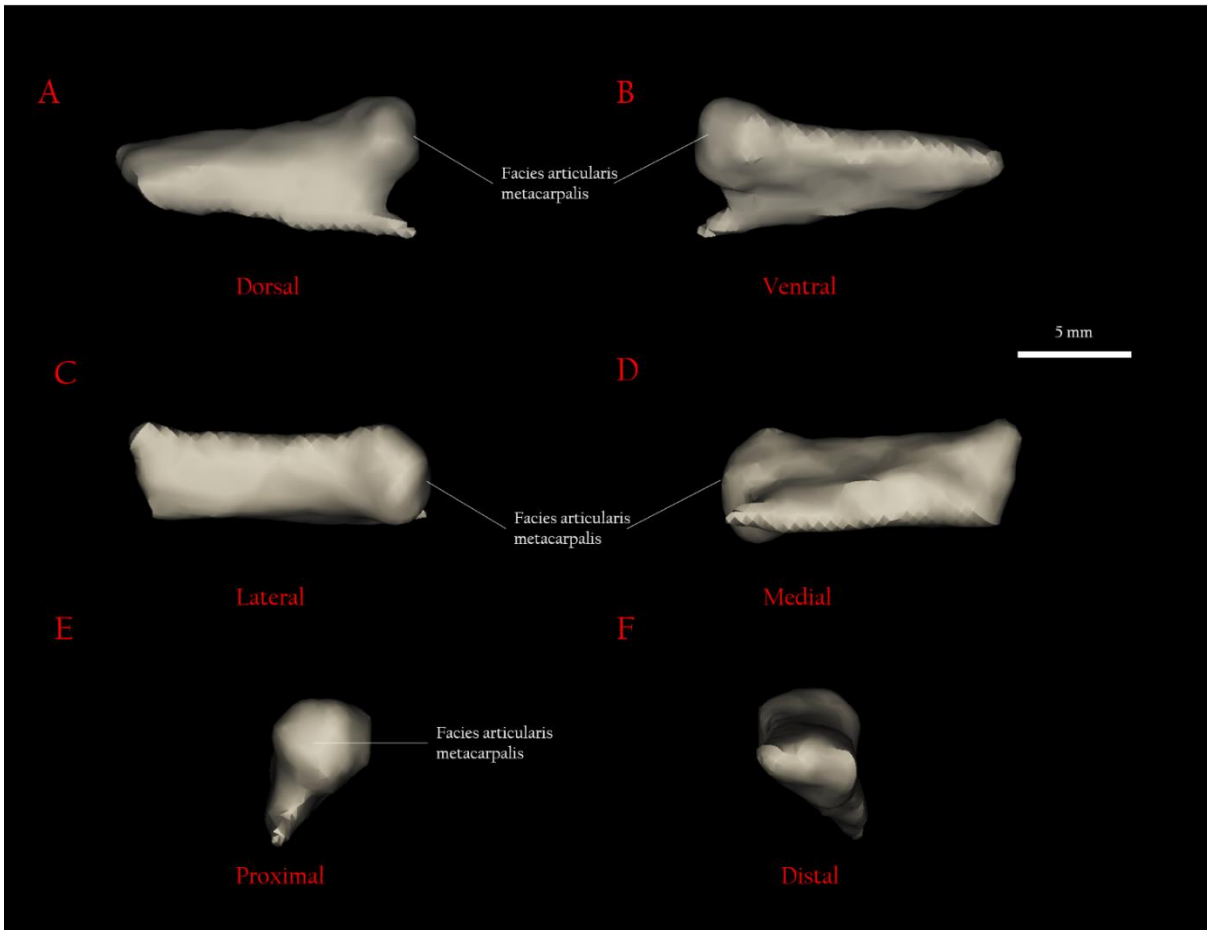

Figure 3.6: The right phalanx of the third digit of JDS8344. Presented in dorsal (A), ventral (B), lateral (C), medial (D), proximal (E), and distal (F) aspects.

3.1.8.6 Axis

Description – While there were other cervical vertebrae associated with this specimen, the axis (Figure 3.7) was not articulated or fused with any other vertebrae elements in the rock, and was exposed at the surface. In anterior and posterior aspects, the neural canal (*foramen vertebrale*) appears to be a rounded subtriangular shape, and is widest dorsally. The neural spine (*processus spinosus*) of the axis is blade-like in shape, rises dorsally, and is extended posteriorly. A fragment has been broken or eroded off the tip of the neural spine on the left side. The ventral process (*processus ventralis corporis*) is even more blade-like than the neural spine, extending further ventrally than the neural spine does

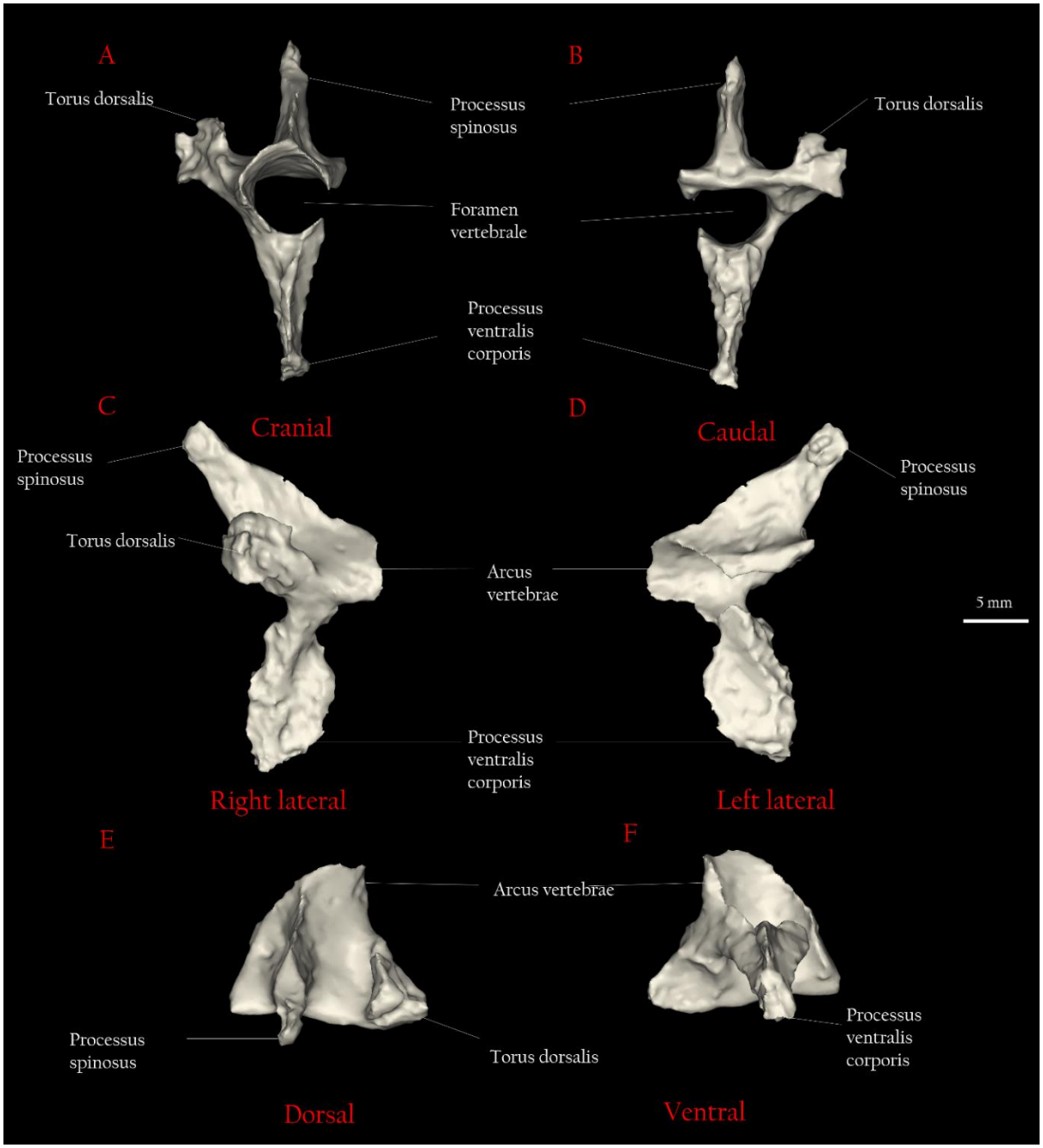

Figure 3.7: The axis of JDS8344. Presented in cranial (A), caudal (B), right lateral (C), left lateral (D), dorsal (E), and ventral (F) aspects.

dorsally, and is also posteriorly orientated. The extremity of the ventral process is bifurcated; however, the left projection has not been preserved. The left transverse process (*processus transversus*) is missing, including the left-most side of the neural arch (*arcus vertebrae*), leaving the neural canal exposed, and may have been broken off or eroded away. The right transverse process is well preserved, thick relative to the neural spine and ventral process, and is extended right laterally and

dorsally. The right transverse process is bifurcated at its extremity and also presents a dorsal tuberous process (*torus dorsalis*).

Discussion – The posterior orientated, blade-like nature of these structures of the axis and the subsequent cervical vertebrae linked as a cohesive structure, when articulated, contributes to allowing adult penguins the mechanical neck flexion to bring their head back towards their body to effectively shorten their neck—which is particularly used when swimming (Figure 3.8) (Guinard et al., 2010).

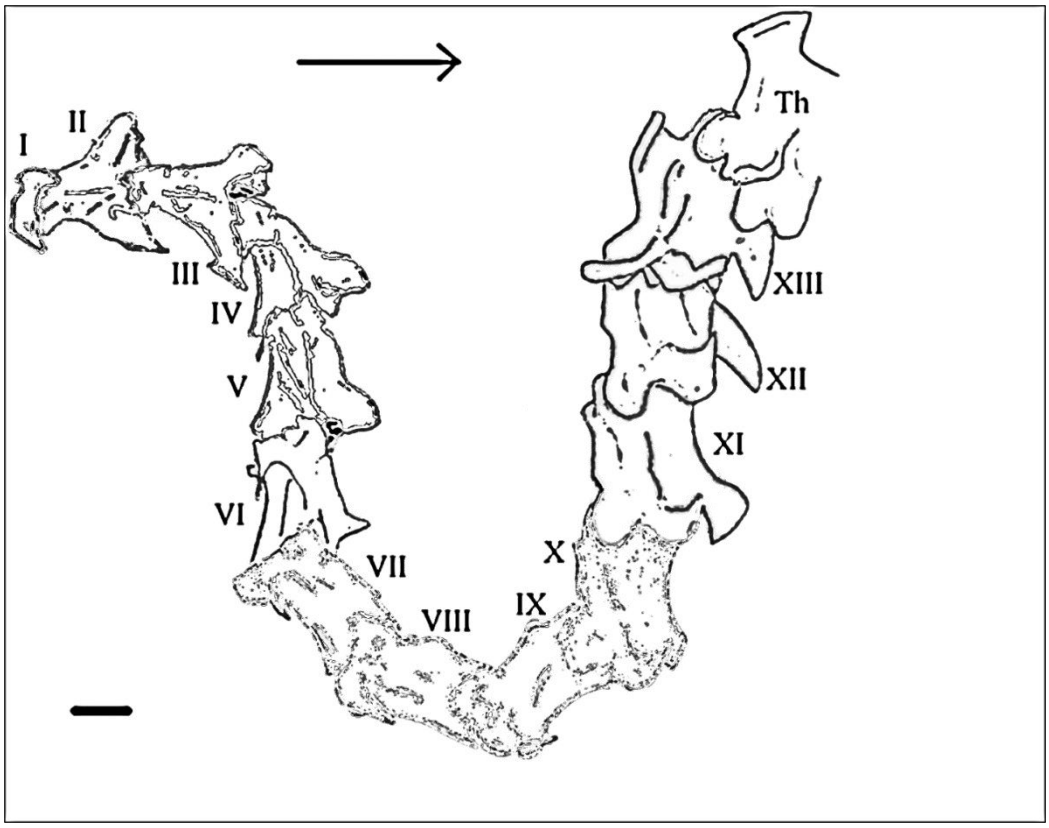

Figure 3.8: Diagram showing the mechanical flexion in an adult penguin neck, modified from Guinard et al., (2010). The neck is presented in a left-lateral aspect, in a flexed shape. Numerals **I** through to **XIII** represent cervical vertebra numbers in the vertebral column, while **Th** corresponds with the first of the thoracic vertebra. The arrow shows how the anterior section of the neck is able to move closer to the thoracic section, which effectively shortens the neck. Diagram is modelled after *Aptenodytes patagonicus*. Scale bar = 1 cm.

3.1.8.7 Cervical vertebrae

Description – While three of the four cervical vertebrae (excluding the axis) were preserved in partial articulation with one another, because they were not in contact with the axis the exact position of each vertebra along the vertebrae column are unknown. Each vertebra will thus be

described in order of articulation, beginning with the vertebra closest to the axis within the rock (Figure 3.1).

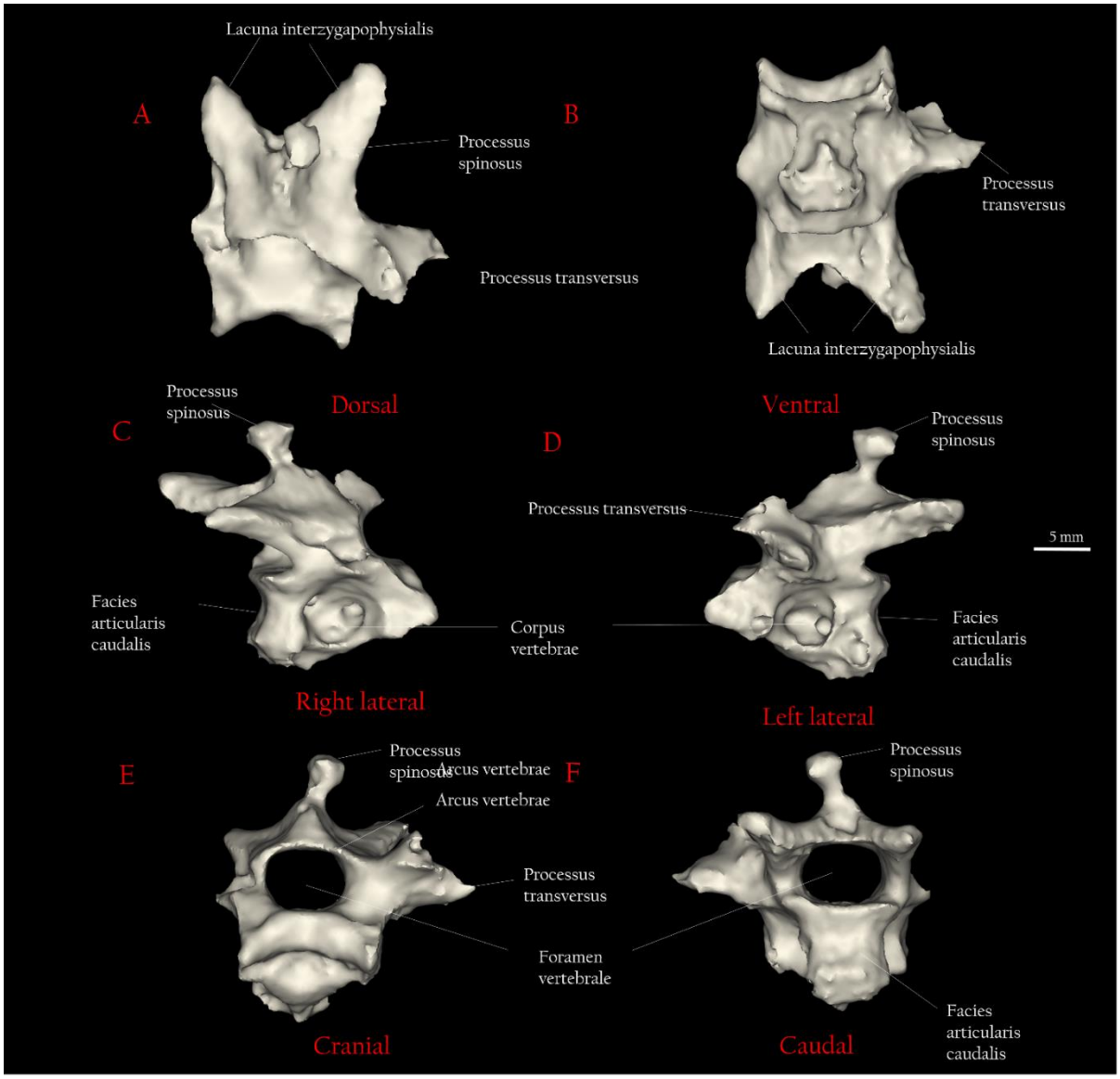

Figure 3.9: A cervical vertebra (a) of JDS8344. Presented in dorsal (A), ventral (B), right lateral (C), left lateral (D), cranial (E), and caudal (F) aspects.

The first cervical vertebra (a) (Figure 3.9) is partially exposed at the surface within the rock, is not in contact with any of the other cervical vertebrae, and appears heavily eroded. This cervical vertebra appears to be representative of an anterior position within the vertebral column, possibly cervical vertebrae III based on the position of the caudal articulation facies (*facies articularis caudalis*) relative to the rest of the body of the vertebra, and that it seems that the ventral process (*processus ventralis corporis*) may have extended further ventrally but has not been preserved. While it is heavily eroded, it is visible that the neural spine (*processus spinosus*) extends dorsally and posteriorly. While

the right transverse process (*processus transversus*) is missing, the left transverse process extends left laterally and is bifurcated and eroded at its extremity. The *lacuna interzygapophysialis* is preserved, presenting a "v"-shape at the caudal end of the vertebra, which allowed dorsal flexion between the vertebrae (Tambussi et al., 2012). In both posterior and anterior views, the neural canal (*foramen vertebrale*) appears to be well-preserved and is ovoid in shape, widest in the mid-section. The cranial facet (*facies articularis cranialis*) for articulation with the preceding anterior vertebra, appears well preserved and forms a concave shape in dorsal and ventral aspects. The caudal facet is also well preserved and is concave in right and left lateral aspects for articulation with the immediately subsequent vertebra.

The second cervical vertebra (b) (Figure 3.10) is partially in contact with another cervical vertebra, however this may be a result of post-mortem disturbance rather than life-position along the vertebral column. Like the preceding vertebra, this vertebra appears to have been anterior in the vertebral column, based on its structure. This vertebra seems to have been deformed through diagenesis and is also severely broken with multiple fractures over the vertebral body (*corpus vertebrae*). An especially large fracture is visible in ventral aspect running from the right to the left side of the vertebra body, and has resulted in twisting a posterior part of the vertebra body associated with the caudal facies (*facies articularis caudalis*) relative to the rest of the vertebra body. Another large fracture is present on the base of the right transverse process (*processus transversus*), and the entire right transverse process has been pushed into the neural canal (*foramen vertebrale*). Both transverse foramen (*foramen transversium*) and *ansa costotransversium* are present on each transverse process, though the right transverse process is pushed inwards to the neural canal as previously described, and left transverse process is broken, and as such the left transverse foramen is not completely enclosed. The *lacuna interzygapophysialis* are well preserved yet deformed as viewed in dorsal and ventral aspects, when each branch of the "v" shape is compared to each other. Widely expanded and ovoid *zygapophysis cranialis* and *zygapophysis caudalis* are also present on each transverse process and the *lacuna interzygapophysialis* respectively. The neural spine (*processus spinosus*) is not preserved on this vertebra.

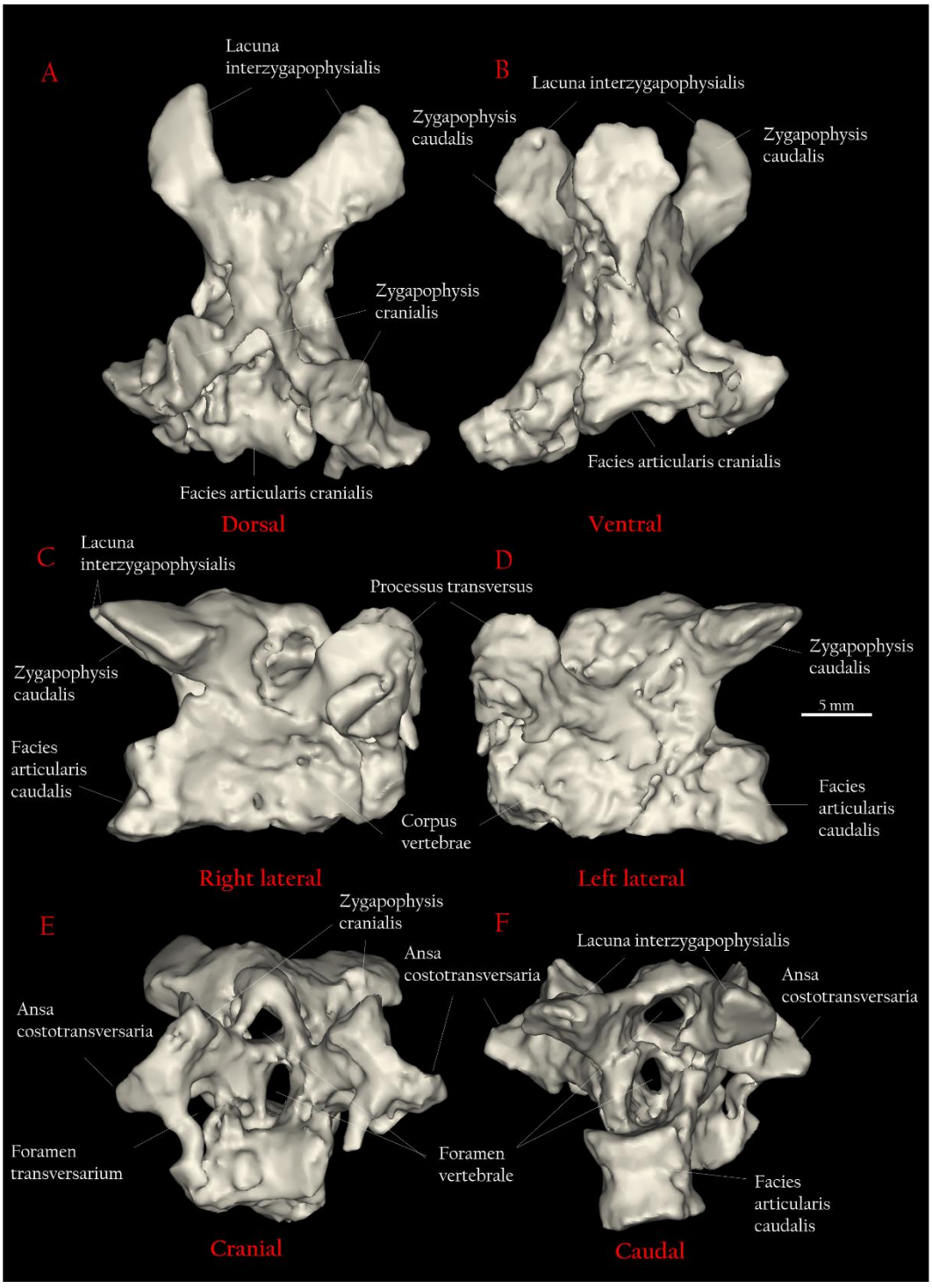

Figure 3.10: A broken cervical vertebra (b) of JDS8344. Presented in dorsal (A), ventral (B), right lateral (C), left lateral (D), cranial (E), and caudal (F) views.

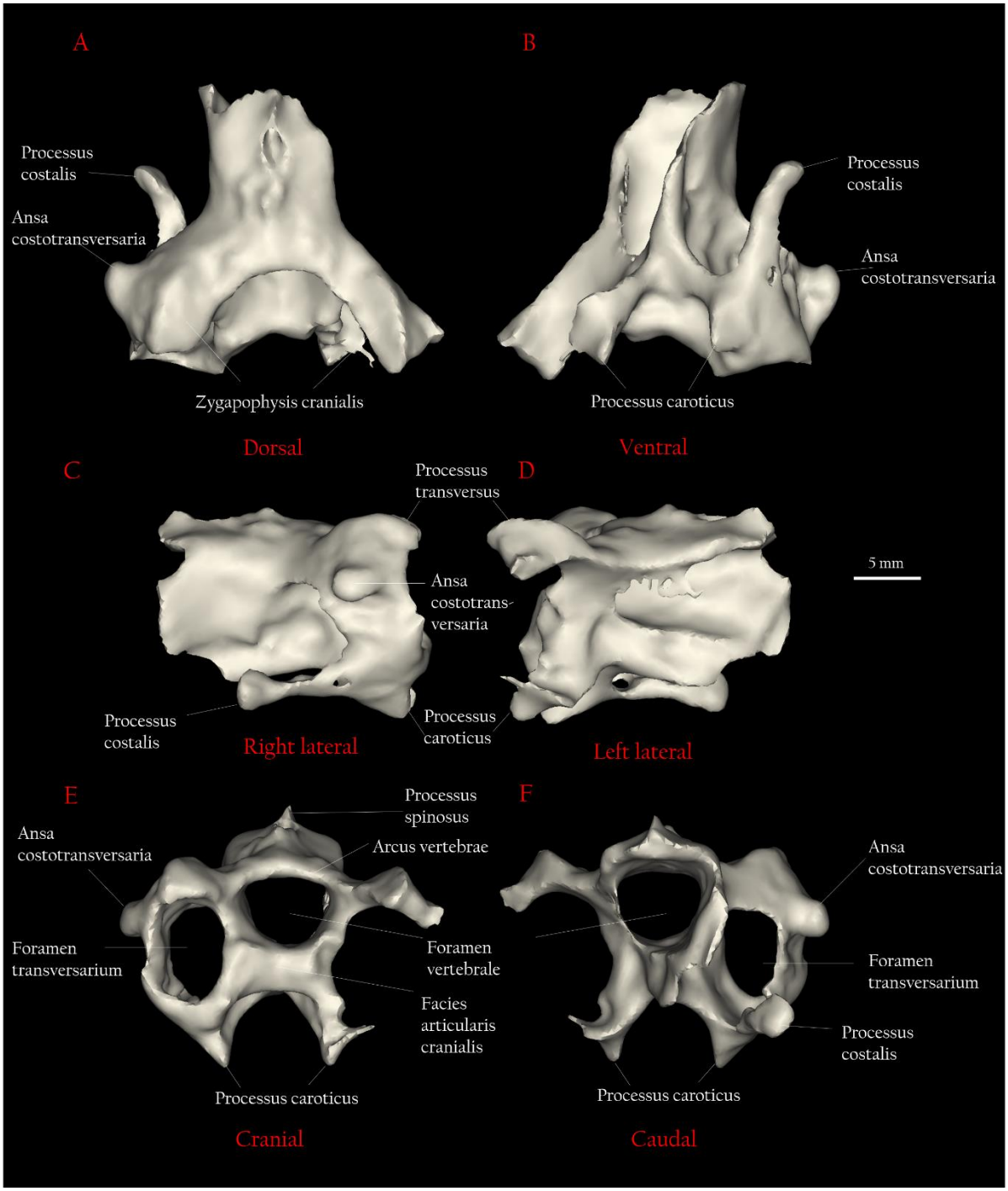

Figure 3.11: A partial cervical vertebra (c) of JDS8344. Presented in dorsal (A), ventral (B), right lateral (C), left lateral (D), cranial (E), and caudal (F) aspects.

The next cervical vertebra (c) (Figure 3.11) in succession appears to be nearly completely articulated with the subsequent cervical vertebra caudally (Figure 3.1). This vertebra is partially preserved, limited to mainly the cranial section of the vertebra, and appears to have perhaps existed mid-series in the vertebral column based on its structure, shape and features. The neural spine (*processus spinosus*) is missing, however it is clear from a depression on the dorsal surface of the hvertebra that it was present but has been eroded away. While the left side of the vertebra body

(*corpus vertebrae*) has been partially eroded away, the shape of the neural canal (*foramen vertebrale*) is still visible in anterior and posterior aspects, where it is sub-triangular in shape, and widest dorsally. The right transverse process (*processus transversus*) is completely intact, preserving the *ansa costotransversium* as well as the transverse foramen (*foramen transversium*)—which is ovoid in shape, narrowest between the right lateral and left sides, and is widest between the dorsal and ventral surfaces of the foramen. The right transverse process also has a long *processus costalis* extending posteriorly off the ventral part of the structure. The left transverse process is only partially complete, and the transverse foramen is not enclosed, however it appears similar in shape to that of the right side. Both transverse processes have preserved flat, oval *zygapophysis cranialis*. Two *processus caroticus* extend at an acute angle ventrally on the cranio-ventral surface of the vertebra.

The last cervical vertebra within the holotype specimen (d) (Figure 3.12) is severely damaged and appears to have been flattened on predominately the right lateral side, in a ventral-dorsal direction. Despite being crushed, the vertebra seems to be almost complete, and may have been part of the mid-series on the vertebral column. The neural canal (*foramen vertebrale*) is intact though is deformed through that flattening of the vertebra. While broken, the cranial facet (*facies articularis cranialis*) has been forced by ventral-dorsal compression through the neural canal, and presents a rough concave shape when viewed from dorsal and ventral aspects. The caudal facet (*facies articularis caudalis*) is in better condition and is almost whole, with relatively minor breakages on the right part of it, and is concave in shape in right and left lateral aspects. Both transverse processes (*processus transversus*) in the cranial section of the vertebra appear to have been broken also, yet both present compressed and entirely enclosed transverse foramen (*foramen transversium*). The left transverse process is in relatively better condition compared to the right transverse process, and is only broken at its base where it connects to the vertebra body (*corpus vertebrae*). Both *processus caroticus* and the left *processus costalis* are also intact. The left transverse process also presents an oval, flat *zygapophysis cranialis*. While the cranial section of the vertebra is crushed, the caudal section appears to be in better condition, and is partially separated from the cranial section by a large fracture that extends from the ventral surface dorsally through the vertebra body to the mid-section of the vertebra. Both limbs of the *lacuna interzygapophysialis* are preserved, which extend posteriorly and laterally, and a

large, flat, oval *zygapophysis caudalis* are present on each. No neural spine (*processes spinosus*) is present on this vertebra.

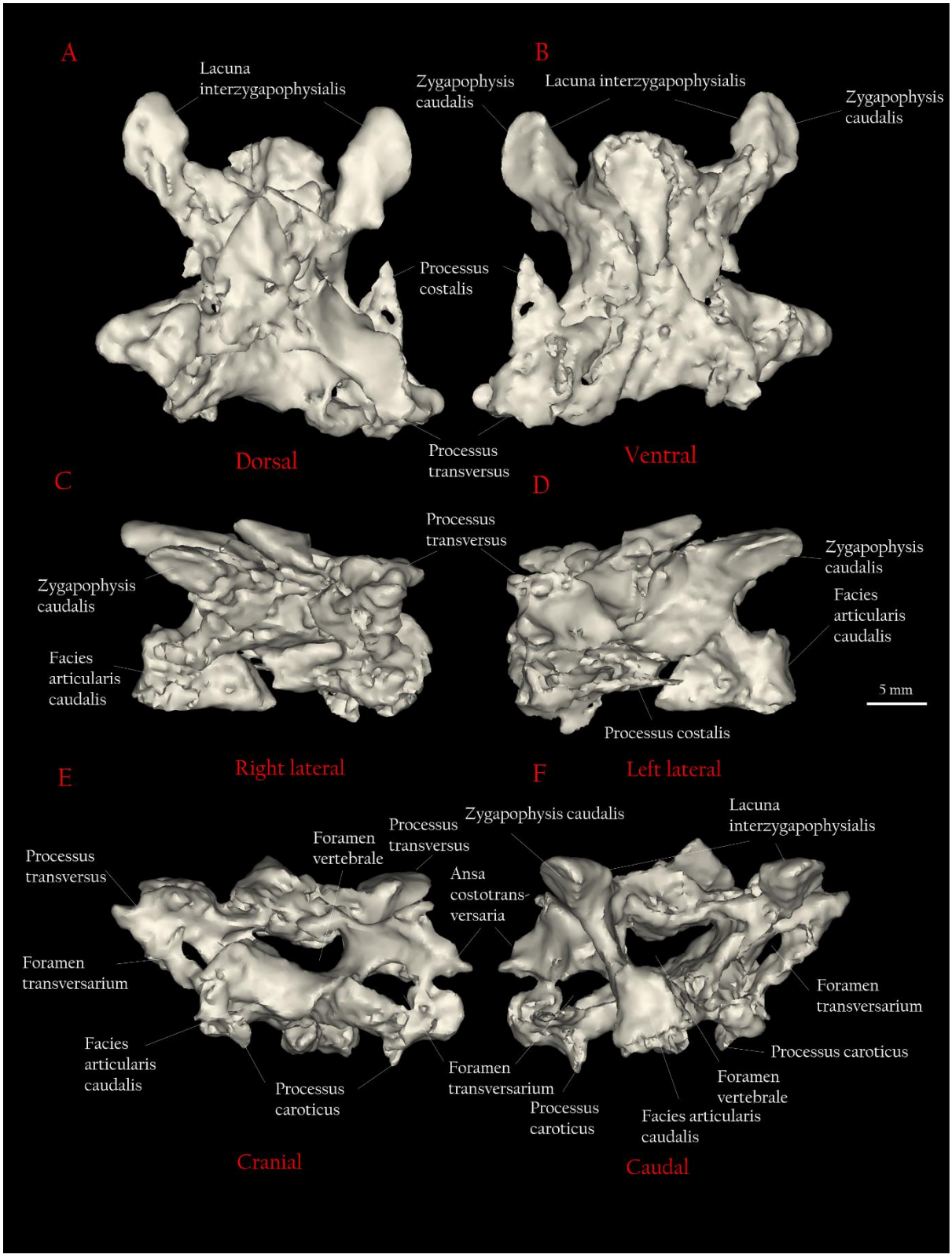

Figure 3.12: A crushed cervical vertebra (d) of JDS8344. Presented in dorsal (A), ventral (B), right lateral (C), left lateral (D), cranial (E), and caudal (F) aspects.

3.1.8.8 Caudal vertebra

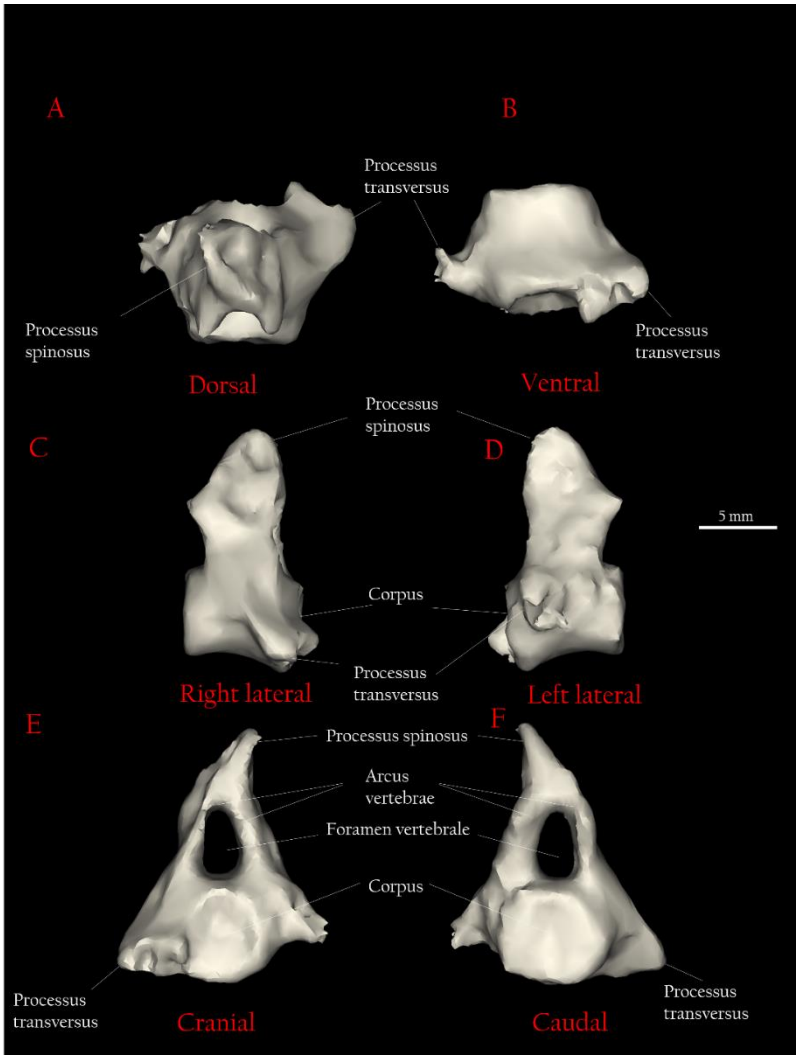

Figure 3.13 (left): A caudal vertebra present in JDS8344. Shown in dorsal (A), ventral (B), right lateral (C), left lateral (D), cranial (E), and caudal (F) aspects.

Description –

One largely intact caudal vertebra (Figure 3.13) is present in the holotype specimen, separate from the rest of the fossil elements. The vertebra has a prominent triangular-shaped neural spine (*processus spinosus*) that extends dorsally and appears to have been eroded and/or deformed on the right lateral side. The neural canal (*foramen vertebrale*) is completely enclosed by the *arcus vertebrae*, and oval in shape—greatest in diameter between its dorsal and ventral surfaces, and narrowest between right and left sides. Both transverse processes (*processus transversus*) are present, extending anteriorly, laterally and ventrally, yet both are eroded; the left transverse process to the most extent. The centrum (*corpus*) of the vertebra is well preserved, presenting a shallow concave nature on both anterior and posterior faces, with flattened surfaces in lateral, dorsal and ventral views to allow for attachment with intervertebral discs.

3.1.8.9 Rib

Description – A single rib is well preserved and almost completely intact (Figure 3.14). The rib appears to have come from the left side of the animal. Both the head (*capitulum*) and the tubercle (*tuberculum costae*) of the rib are bulbous at the facies that connect to the associated vertebra (*articulatio capitis costae* and *articulatio costo transversia* respectively), and are well preserved. The body or shaft (*corpus costae*) of the rib is widest and best preserved at the dorsal end. The shaft is less well preserved and shows erosion progressively ventrally, and is tapered at its ventral-most end. The uncinate process is not preserved.

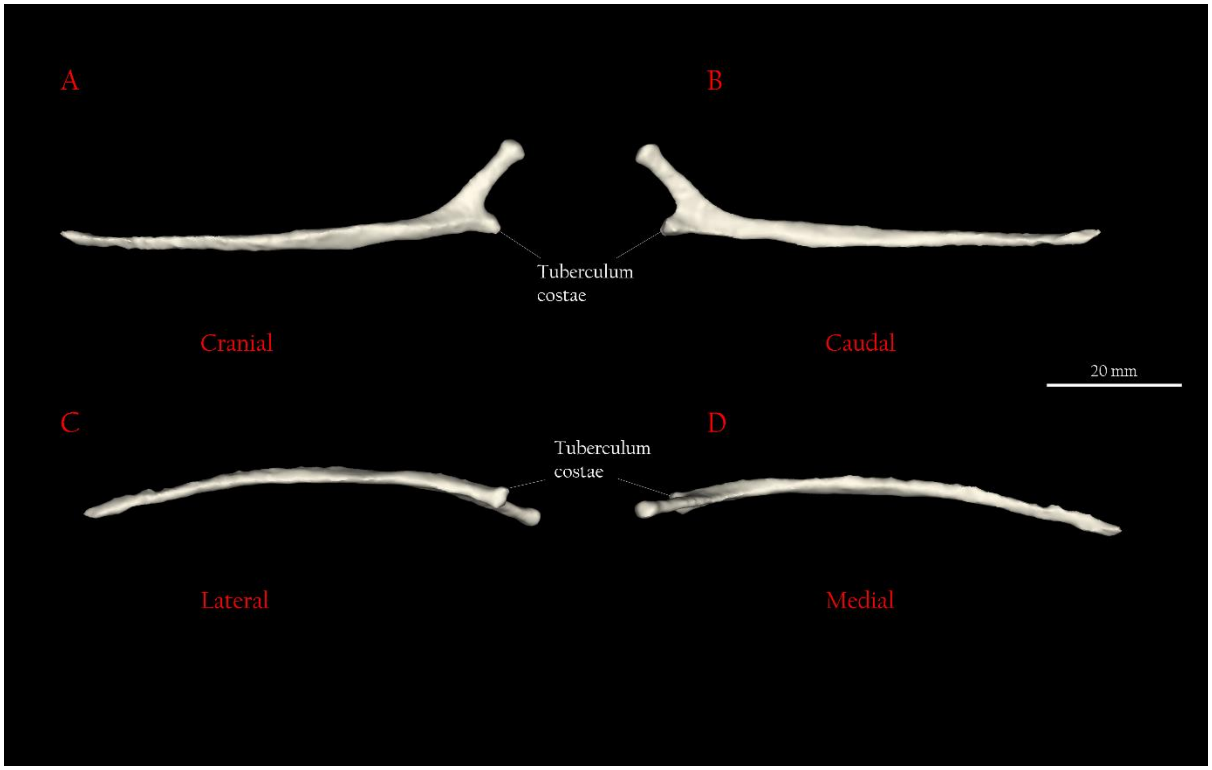

Figure 3.14: A left rib that was present in JDS8344. Shown in cranial (A), caudal (B), lateral (C), and medial (D) aspects.

3.1.8.10 Pelvis (ischium)

Description – A fragment of the right side of the pelvis is preserved (Figure 3.15) which is described here as the wing of the ischium (*ala ischii*) of the holotype specimen. The majority of the ischium is wide, flat and ovoid in shape, but is tapered to a point representing the bone's caudal-most extent. The caudal tip of the ischium is also curved medially towards the centre of the animal. The

shape is does not differ markedly from that of extant penguin species, and is especially synonymous to that of *Aptenodytes forsteri*.

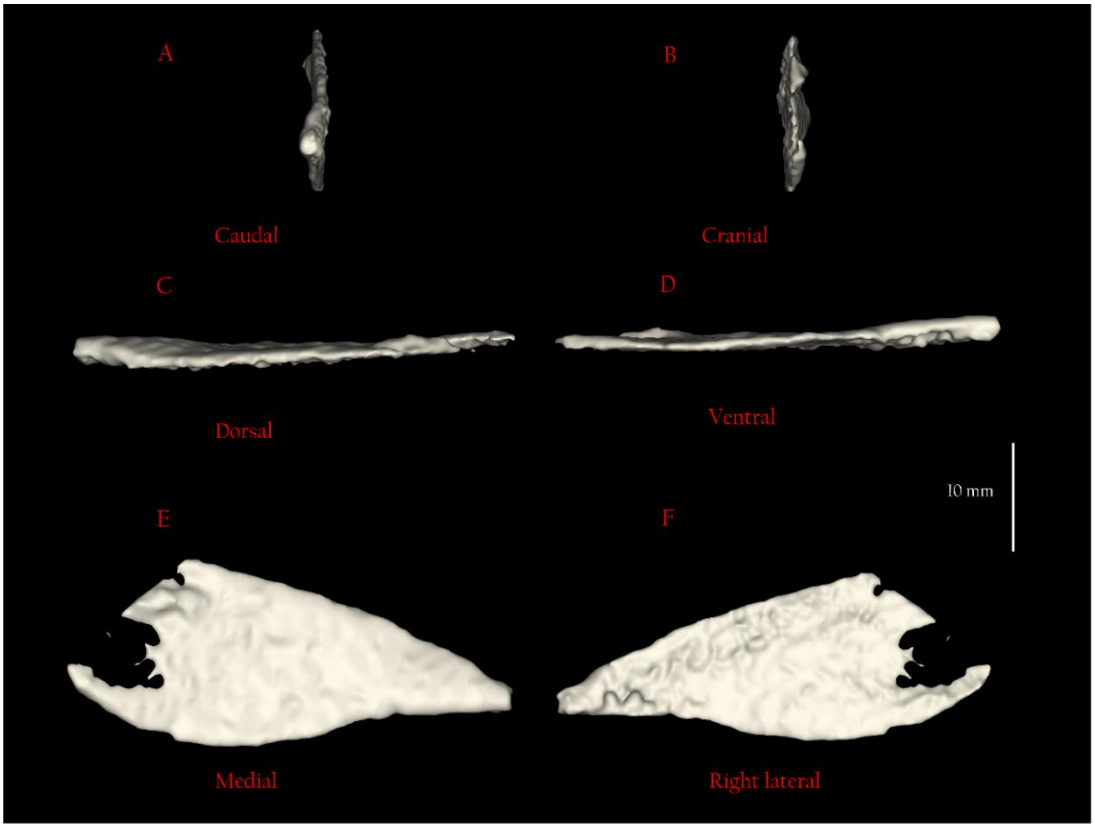

Figure 3.15: A fragment from the right side of the pelvis, the wing of the ischium, as preserved in JDS8344. Aspects shown include caudal (A), cranial (B), dorsal (C), ventral (D), medial (E), and right lateral (F).

Table 1: ***Table of Measurements (JDS8344):***

Element		Measurement (mm)
Carpometacarpus	Total length	31.9
	Distal width	11.73
	Distal depth	4.16
	Distance from distal facet to *sulcus interosseus*	7.04
	Width of metacarpal II (mid-shaft)	5.65
	Width of metacarpal III (mid-shaft)	2.34
Ulna	Total length	69.16
	Proximal width	7.33
	Mid-shaft width	6.38
	Proximal depth	4.61
	Mid-shaft depth	3.35
	Distance to bend	24.82
Radius	Total length	41.91
	Proximal width	7.06

	Mid-shaft width	7.58
	Proximal depth	5.75
	Mid-shaft depth	3.3
	Distance to bend	17.5
Phalanx II-1	Total length	24.14
	Proximal width	6.54
	Proximal depth	3.66
	Distal width	5.05
	Distal depth	1.85
	Maximum width	8.51
Phalanx III-1	Total length	13.17
	Proximal facet width	4.3
	Proximal facet depth	3.75
	Mid-shaft width	4.65
Axis	Length of neural canal[1]*	12.28
	Lateral diameter of neural canal	5.5
	Total distance between tips of ventral process and neural spine	25.9
Cervical (a)	Length of neural canal[1]**	13.9
	Lateral diameter of neural canal	7.14
	Total distance between tips of ventral process and neural spine	23.42
Cervical (b)	Length of neural canal[1]**	19.07
	Maximum cranial width	23.11
	Maximum width at caudal zygapophyses	17.99
	Maximum width at cranial zygapophyses	14.1
Cervical (c)	Length of neural canal[1]**	17.45
	Lateral diameter of neural canal	7.27
	Maximum cranial width	24.55
	Maximum width at cranial zygapophyses	18.15
Cervical (d)	Length of neural canal[1]**	16.8
	Lateral diameter of neural canal	7.95
	Maximum cranial width	30.7
	Maximum width at cranial zygapophyses	24.47
	Maximum width at caudal zygapophyses	24
Caudal vertebra	Diameter of centrum/corpus	7.34
	Maximum width	13.89
	Maximum height	15.57
	Maximum length/depth of centrum/corpus	7.45
Rib	Maximum length	70.42
Pelvis (ischium)	Maximum length	41.42
	Maximum width	14.99
	Maximum depth	2.36

[1] Due to the broken nature of these vertebrae, measurements of the neural canal had to be measured dorsally or ventral, depending on what was most accessible for measure on each vertebra.

* Length was recorded from the anterior-most dorsal edge of the neural canal to the posterior-most edge of the neural canal.

** Length was recorded from the anterior-most ventral edge of the neural canal to the posterior-most edge of the neural canal.

3.1.9 Referred Material:

Other referred specimen: JDS8341.b (Figure 3.16). JDS8341.b refers to an associated partial skeleton comprising of a caudal portion of the left mandible, a partially complete furcula, a fourth cervical vertebra (CVIV), a partial right coracoid, a fragmentary portion of the sternum, and a vertebra fragment. There are also several other bones that could not be accurately identified (see Appendix). While both specimens are tentatively referred to as the same taxon (*Archaeodyptes stilwelli*) here, in the case of further material becoming available this may be subject to change.

Figure 3.16: Referred specimen JDS8341.b. as a product of photostacking, as explained in Chapter II: Methods, section 2.2. Scales shown include a 45 cm metal ruler and a KODAK Colour Control Patch.

3.1.9.1 Mandible:

Description – An incomplete caudal portion of the left mandible (Figure 3.17) is preserved in JDS8341.b. What is interpreted as the articular element is well preserved, notably the lateral (*cotyla lateralis*), caudal (*cotyla caudalis*) and medial cotylae (*cotyla medialis*). The position of the lateral condyle is notably dorsal to both the medial and caudal condyles, and its anterior margin is also sharply

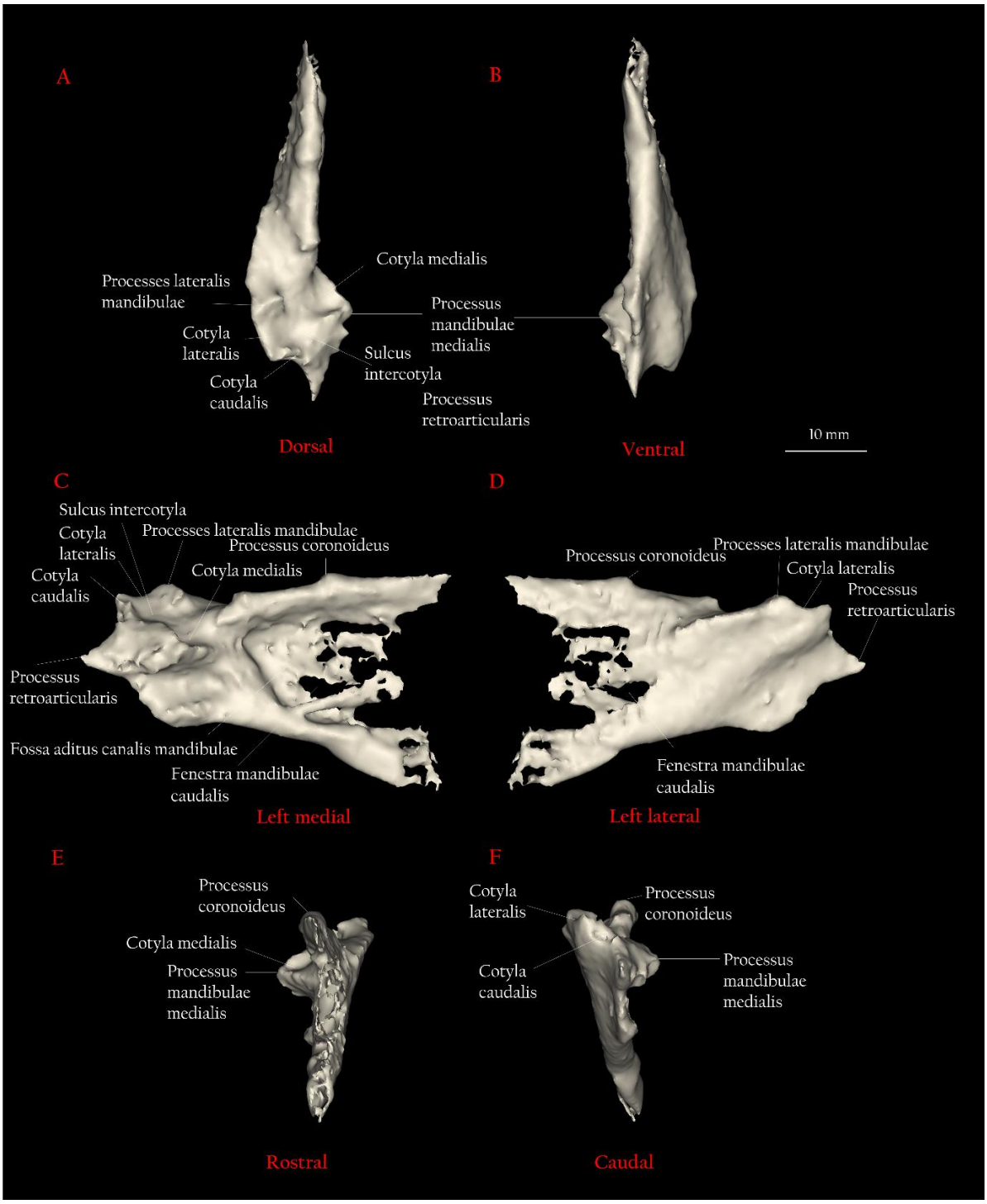

Figure 3.17: The caudal portion of the left mandible in JDS8341.b. The mandible is presented in dorsal (A), ventral (B), left medial (C), left lateral (D), rostral (E), and caudal perspectives.

projected. From the posterior margin with the lateral condyle, the caudal condyle is angled ventrally, and is markedly smaller compared to the other cotylae. The medial condyle is ventral-most relatively to the other cotylae and presents pronounced concavity for articulation with the quadrate. Separating the medial and lateral cotylae on the articular fossa, the *sulcus intercotylaris* is subtly projected and rounded, which can be viewed in Figure 3.18. The medial process (*processus mandibulae*

medialis) has been subject to erosion, yet is clearly projected. The retroarticular process (*processus retroarticularis*) is also preserved, as an acute, sharp caudal projection on the articular. Ventral to the medial process in the medial aspect is a deepened and wide depression that marks the fossa for insertion of the *musculus pterygoideus*. In medial aspect the mandible presents an extensive medial mandibular fossa (*fossa aditus canalis neurovascularis*), which deepens anteriorly, the extent of which is unknown due to lack of preservation. There are multiple perforations within the medial mandibular fossa, and are likely the result of the break-down and erosion of the lateral side of the mandible. A particular perforation, distinct from the others, can potentially be considered the caudal mandibular fenestra (*fenestra caudalis mandibulae*), and is small compared to the depth of the medial mandibular fossa itself. The true size of the caudal mandibular fenestra is tentative due to marks of breakage and erosion surrounding the perforation however, but regardless may be an indeterminate feature of classifying taxa considering the significant intraspecific variation observed in penguins (Ksepka and Bertelli, 2006). On the dorsal surface of the surangular element (*os supra-angulare*) the coronoid process (*processus coronoideus*) is preserved, as a slight rounded projection on the dorsal margin of the mandible. The coronoid process is approximately in-line with the potential caudal mandibular fenestra.

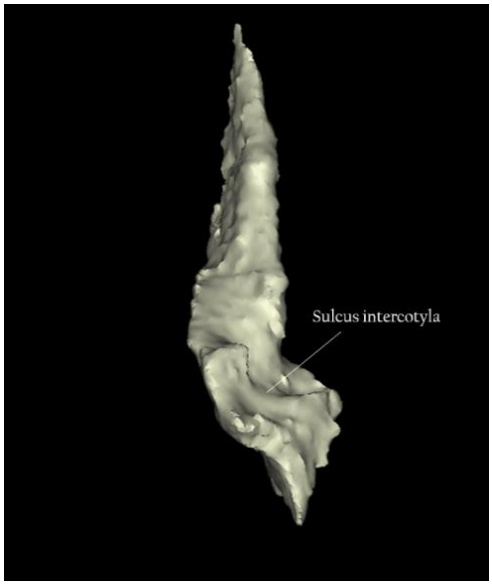

Figure 3.18: An oblique perspective of the caudal portion of the left mandible in JDS8341.b, in order to clearly see the *sulcus intercotyla*. For scale please see **Figure 3.17**.

Discussion – In dorsal aspect, the positions of the cotylae are broadly similar to that of extant penguin species. Extant penguins typically exhibit a "hook-like" medial process morphology, however, while projected, the medial process in JDS8341.b has been subject to erosion; and does not display this morphology. While it may have suffered some erosion, the shape of the retroarticular process present in *Archaeodyptes stilwelli* is most similar to that of modern *Spheniscus* species, yet it is less projected. Some other extant penguin species such as *Pygoscelis adeliae* and *Eudyptula* minor have wider, more rounded retroarticular processes, while the Miocene *Paraptenodytes antarcticus* presented a wider and less projected

morphology (Bertelli et al., 2006). In contrast, in the Paleocene *Waimanu* the retroarticular process has not been preserved and is effectively absent (Slack et al., 2006). In extant penguins a thin sheet of bone connects the medial process with the retroarticular process (Bertelli et al., 2006), however this characteristic is not visible on this left mandible, and instead is consistently thick from the medial to the retroarticular process, with no clear separation. However, considering there are marks of erosion of both of these elements of the articular, exact judgement on the true nature of this part of the mandible should be reserved and is uncertain.

3.1.9.2 Furcula:

Description – The furcula of the specimen (Figure 3.19) is incompletely preserved, presenting the majority of the left clavicle, and an eroded fragment of the right clavicle, while the articular omal regions of each clavicle are not preserved. Generally, the shape of the furcula can be described as a shallow, rounded 'U'-form, with a widened interclavicular width. The *extremitas sternalis claviculae* is also wide, and the *apophysis furculae* is absent.

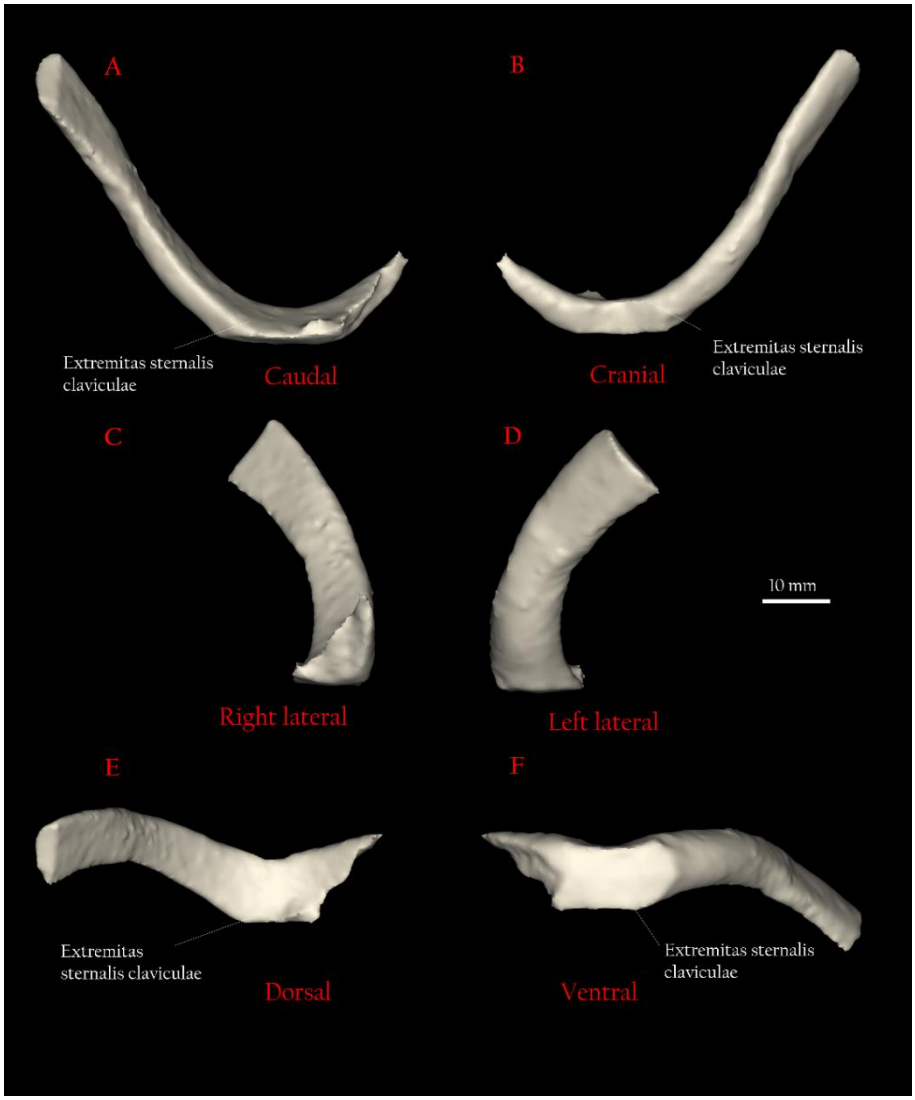

Figure 3.19 (previous page): The furcula of specimen JDS8341.b. The element is presented in caudal (A), cranial (B), right lateral (C), left lateral (D), dorsal (E), and ventral (F).

3.1.9.3 Cervical vertebra IV:

A single complete cervical vertebra is preserved in JDS8341.b, representing cervical vertebra IV (Figure 3.20). The vertebra has a blade-like neural spine (*processus spinosus*) that extends dorsally and posteriorly. The neural canal (*foramen vertebrale*) is sub-triangular in shape, widest dorsally, and also rounded ventrally. The neural canal appears to have been slightly misshapen, where the left dorsal lamina of the *arcus vertebrae* has been deformed. Ventral to the neural canal the *facies articularis cranialis* is complete and concave in shape from dorsal and ventral aspects. The anterior of the vertebra presents two transverse processes (*processus transversus*), each with a large, flat, ovoid *zygopophypsis cranialis*. The transverse processes also present entirely enclosed transverse foramen (*foramen transversium*), which are both oval in shape. The left transverse foramen appears slightly deformed, similar to the left side of the neural canal. A completely intact *processus caroticus* is present on the ventral surface of each transverse process, as a sharp projection, ventral to the transverse foramen. Blade-shaped *processus costali* are also extend posteriorly from each transverse process, the left of which appears to have the posterior-most tip broken or eroded off. On the ventral surface of the vertebra body (*corpus vertebrae*) the *processus ventralis corporis* is projected ventrally perpendicular to the vertebra body and posteriorly. The *processus ventralis corporis* is wide when viewed from lateral aspects relative to the vertebra body, while thin in caudal and cranial views, and is thus "keel"-like in shape. The *facies articularis caudalis* is present on the posterior of the *processus ventralis corporis*, is completely intact, and is concave in lateral views. A limb is present either side of and posterior to the neural spine, as a caudolateral extension of the dorsal surface of the vertebral arch. Each extend onto its caudal zygopophysis (*zygopophysis caudalis*), which are both ventrally flattened and oval in shape. On the dorsal side and tips of the caudal zygopophysis are *tori dorsalis*, both extending dorsally from the vertebral arch.

Figure 3.20 (next page): Cervical vertebra IV of specimen JDS8341.b. The element is presented in dorsal (A), ventral (B), right lateral (C), left lateral (D), cranial (E), and caudal (F) aspects.

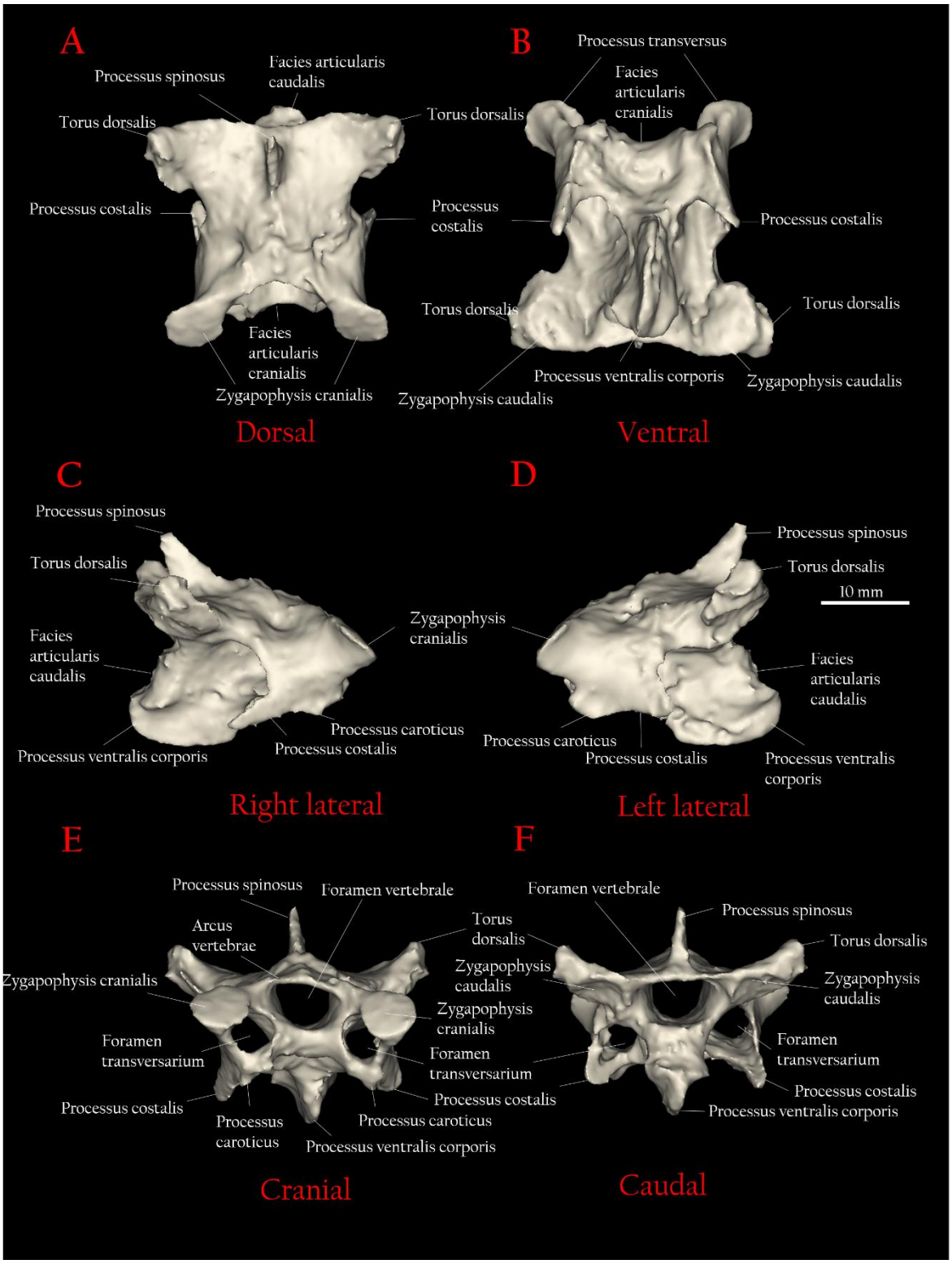

Discussion – In appearance this vertebra is almost identical to cervical vertebra IV of *Diomedea exulans*. As previously mentioned (see holotype JDS8344: Axis), the posterior extending blade-like shape of the neural spine in the cervical vertebrae is characteristic of penguins, allowing them the mechanical neck flexion to bring their head back towards their body and effectively shorten their neck (Guinard et al., 2010).

3.1.9.4 Coracoid:

Description – The anterior section of the right coracoid is preserved (Figure 3.21). The shaft of the coracoid is stout, and the omal end is concave, but not to the extent that the acrocoracoid neck (*collum acrocoracodei*) is hook-like. A large flattened surface as viewed from the medial aspect, the *facies articularis clavicularis* is on an oblique angle with respect to the alignment of the coracoid's axis. On the ventral side of the coracoid, the acrocoracoid process (*processus acrocoracoideus*) is present as a rounded projection, and is not hooked. Caudal to the tip of the projection of the acrocoracoid process is a shallow depression on the ventral face (see *fossa*, Figure 3.21). The *impressio ligamenti acrocoracohumeralis* is not crested, and runs between the acrocoracoid process and the *facies articularis clavicularis* as a shallow groove. The humeral facet (*facies articularis humeralis*) is vertically expanded on the dorsolateral plane of the coracoid. Caudal to the humeral facet on the dorsal side of the coracoid, the scapular cotyle (*cotyla scapulae*) is deep and rounded. The procoracoid process (*processus procoracoideus*) projects medially, ending on a broken edge. Therefore, the extent and true nature of the shape of the procoracoid process, nor the nature of the coracoidal fenestra cannot be ascertained from this fossil, yet it does give an indication on the level that the procoracoid process exists relative to the rest of the bone. The posterior edge of the coracoid is thinned and broken, concealing the true extent of the coracoid's length.

Discussion – The morphology of the coracoid of JDS8341.b is unlike the morphology of extant and extinct penguin species, which all have hooked omal sections of the coracoid associated with the *facies articularis clavicularis* and the *processus acrocoracoideus*. The basal stem penguin *Waimanu* also show hooked omal end morphology on each coracoid, and is thus unlike JDS8341.b, but otherwise the shape of the anterior section of the coracoid present is visually similar. The shape of the omal end present in JDS8341.b is unique among penguins, and more resembles that of albatrosses such as *Thalassarche cauta*. The shallow fossa present caudal to the acrocoracoid process on the coracoid of JDS8241.b may be analogous to a deeper ovoid depression is present on the ventral face of the acrocoracoid process in *Icadyptes salasi*, and a slight indentation is present on some extant penguin species. Otherwise, however, both living and extinct penguins tend to exhibit a flat surface on the ventral side of the acrocoracoid process.

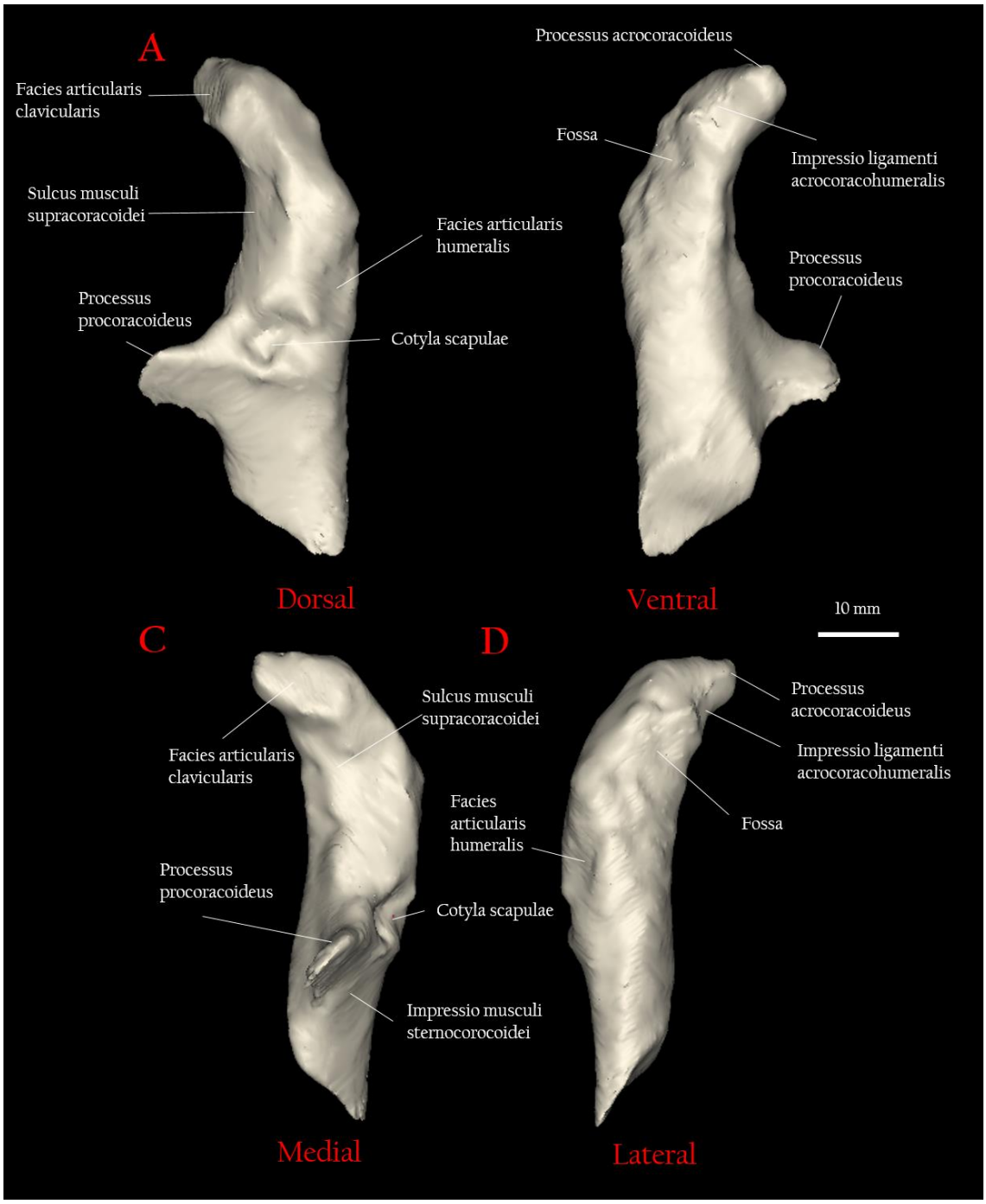

Figure 3.21: The anterior section of the right coracoid present in JDS8341.b. The element is presented in dorsal (A), ventral (B), medial (C) and lateral (D) perspectives.

3.1.9.5 Sternum:

Description – A fragment of the sternum is preserved (Figure 3.22), representing the cranial-most extent of the sternum. The bony point from the median anterior and ventral margin of the *rostrum sterni* is described as the *spina externa*, which shows evidence of breaking and deformation. The dorsal surface of the sternum fragment is concave, and a cavity which may be a single pneumatic

foramen (*foramen pneumaticum*) is observed. The ventral surface of the sternum is convex and there is evidence that it is also keeled. While the *carina sterni* is not complete, an evident projection along the length of midline of the ventral surface is representative of this structure, which grows in width and breadth and protrudes more ventrally perpendicular to the ventral surface, towards the sternum's caudal end. A lateral groove is also present on either side of this midline.

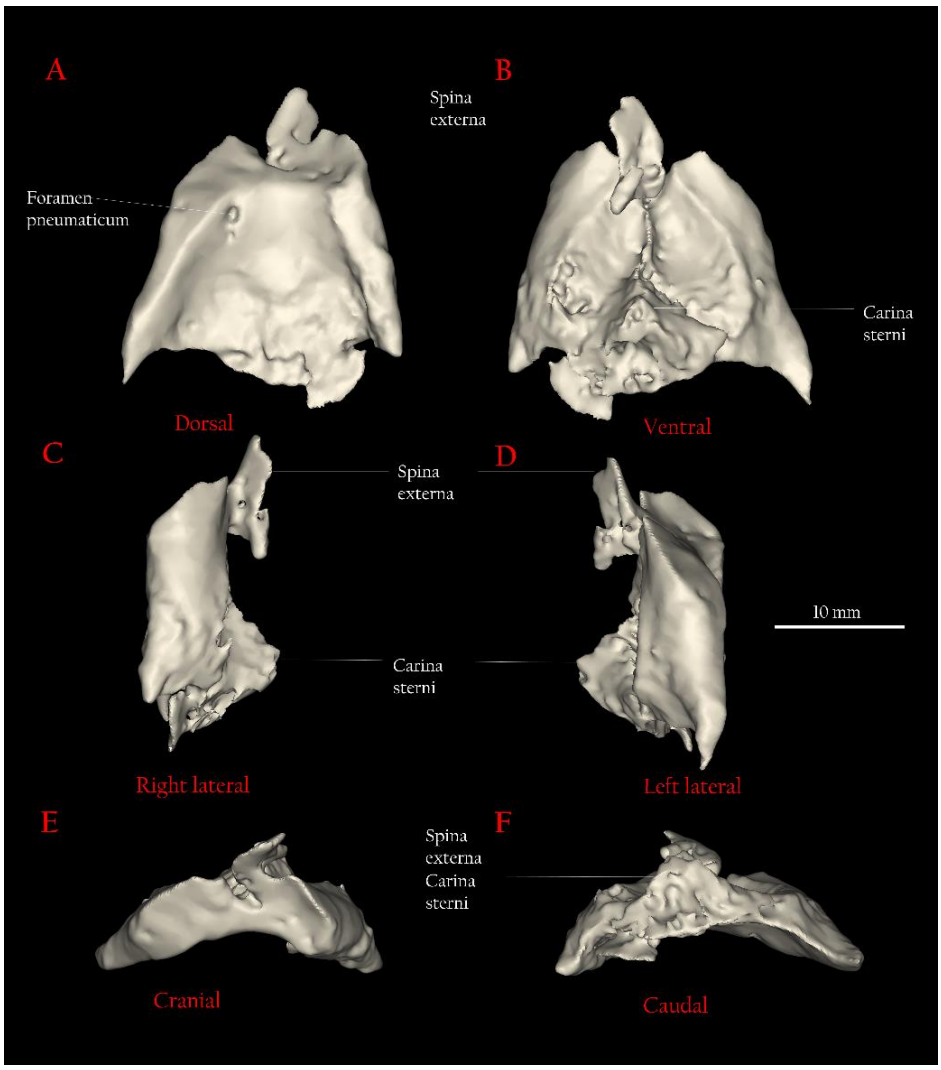

Figure 3.22 (above): The fragment of the sternum preserved in JDS8341.b. The element is presented in dorsal (A), ventral (B), right lateral (C) and left lateral (D), cranial (E), and caudal (F) perspectives.

Discussion – The presence of a pneumatic foramen may provide a degree of evidence that the sternum of JDS8341.b was pneumatic. Lightweight bones through some pneumatized skeletal elements is a characteristic adaptation of birds to reduce the metabolic cost of flight (Dumont, 2010), lowering the wing-load without losing strength (Soldaat, 2009). In contrast, in diving birds a decrease in pneumaticity is correlated with an increase in diving ability (Schorger, 1947). Hence true

diving birds like penguins preserve a relative lack of pneumatized bones to reduce buoyancy (Soldaat, 2009). While it cannot be said with certainty how pneumatized the complete sternum was, the presence of what may be a pneumatic foramen in the portion of the sternum of JDS8341.b preserved is therefore unlike that of modern penguins. The sternum of JDS8341.b may therefore be more comparable to albatrosses, which have very pneumatized sternums, or gulls and related taxa, which are pneumatized to a mid-extent between albatrosses and penguins (Soldaat, 2009). Shearwaters also show a range of pneumaticity depending on whether they are adapted to gliding or diving (Soldaat, 2009).

3.1.9.6 Vertebra:

Description – What is interpreted as a single vertebra fragment is preserved (Figure 3.23), however due to its incomplete nature it is difficult to describe it in further detail.

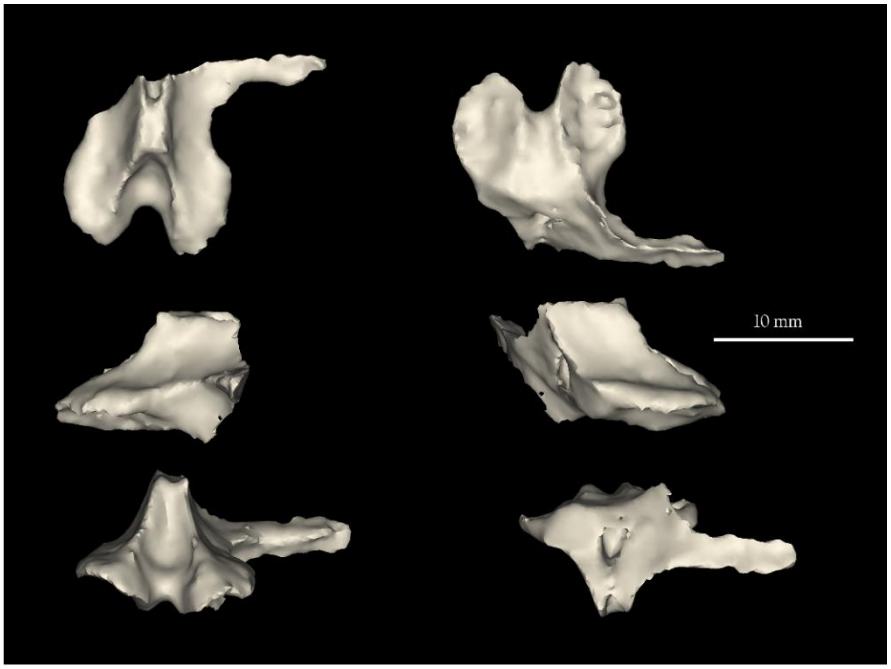

Figure 3.23: A fragment of a potential portion of a vertebra, present in specimen JDS8341.b. Six different perspectives are shown of the element, however their particular orientation cannot be specified with certainty because of the element's incomplete nature.

Table 2: Table of Measurements (JDS8341.b):

Element		Measurement (mm)
Mandible	Maximum length	45.65
	Maximum width	13.23
	Maximum depth	24.94
Furcula	Maximum length of left clavicle from omal end to *extremitas sternalis claviculae*	46.99
	Distance between omal ends of each clavicle	59.85
	Maximum width	5.45
	Maximum depth	11.32
Cervical vertebra IV	Length of neural canal*	19.28
	Lateral diameter of neural canal	6.09
	Maximum width at cranial zygapophyses	25.73
	Maximum width at caudal zygapophyses	26
	Maximum caudal width	30.32
	Total distance between tips of ventral process and neural spine	24.09
Coracoid	Diameter of scapular condyle	8.45
	Maximum length	62.02
	Maximum diameter of coracoidal fenestra	29.25
Sternum	Maximum length	24.48
	Maximum width	22.23
	Maximum depth of *carina sterni*	6.09

* Length was recorded from the anterior-most ventral edge of the neural canal to the posterior-most edge of the neural canal.
** Please note that due to the nature of the vertebra fragments, measurements have not been recorded.

CHAPTER IV: ANALYSES

This chapter addresses the reasoning for the classification of the novel taxon *Archaeodyptes stilwelli*, the morphology of which was previously described in ***Chapter III: Taxonomy***. Tests to determine the phylogenetic relationship(s) of *Archaeodyptes stilwelli* compared to other taxa were carried out using data from morphological character scores in the form of parsimony-based heuristic analyses, as well as Bayesian analyses. Morphological character scores (see Appendix) were determined through aforementioned morphological descriptions in ***Chapter III Taxonomy***. The results of comparative analyses are also detailed in this chapter, whereby elements from the specimens of this research thesis were compared to the same elements in other taxa.

4.1 Phylogenetic Analysis

4.1.1 Primary Analyses

The heuristic analysis conducted in TNT on the modified dataset of Ksepka and Clarke (2010), where JDS8344 and JDS8341.b were included in the matrix as separate taxa, revealed that while JDS8344 occupied a relatively basal position in in the resultant phylogenetic tree, JDS8341.b occupied a position within crown group penguins. Considering that modern or crown group penguins have a much shallower fossil record, sharing a basal divergence around 12.7 Ma (Gavryushkina et al., 2016), while JDS8341.b is Palaeocene in age, this placement must be incorrect. The position occupied by JDS8341.b in the analysis may be an artefact of the low number of morphological characters that could be scored. In contrast, the tree produced from the heuristic search where JDS8344 and JDS8341.b were included as a single merged taxon occupied the same basal position occupied by JDS8344 in the separate taxa analysis. Morphological characters scored in JDS8341.b that place it alongside crown group penguins therefore did not affect the basal placement of JDS8344 when merged, providing support for an overall basal position, and the treatment of JDS8344 and JDS8341.b as a single merged taxon in further phylogenetic analyses (please refer to ***Chapter V: Discussion*** for further validation based on preservation and comparative morphology).

Analysis of the modified character matrix from Ksepka and Clarke (2010) in PAUP* v 4.0a150 resulted in 504 Most Parsimonious Trees (MPTs) trees, with a score of 555 steps for tree length. The analysis of the modified dataset of Ksepka and Clarke (2010) where only osteological morphological characters were included produced 736 MPTs where the best score throughout the trees was 289. In the strict consensus trees produced for all characters included (Figure 4.1B), and osteology-only characters (Figure4.1B), both Procellariiformes and Sphenisciformes are recovered as monophyletic clades, and are identical in positions occupied for all stem penguin taxa. *Archaeodyptes stilwelli* is recovered in a most basal position to all other Sphenisciformes in both of these analyses, where is placed one node basal to that of *Waimanu*, as a sister-taxa position relative to the node leading to all Procellariiformes, and one node crownward relative to *Gavia stellata*. The placement of all contemporary stem penguin taxa included is identical in both analyses. Minor differences exist between these analyses in the pairings and placement of extant most-crownward species of both Procellariiformes and Sphenisciformes, yet do not affect the placement of *A. stilwelli*.

Figure 4.1 (next page): Comparison of strict consensus parsimony-based phylogenetic trees produced via heuristic search analyses, using PAUP*. A. shows the phylogenetic tree generated from the modified dataset of Ksepka and Clarke (2010) using both genetic and all morphological characters. B. is the result of the modified dataset from Ksepka and Clarke (2010) using only osteological morphological characters. Gaviiformes are presented in black; Procellariiformes are presented in blue; Sphenisciformes are presented in red; and the position of *Archaeodyptes stilwelli* is presented in green.

A.

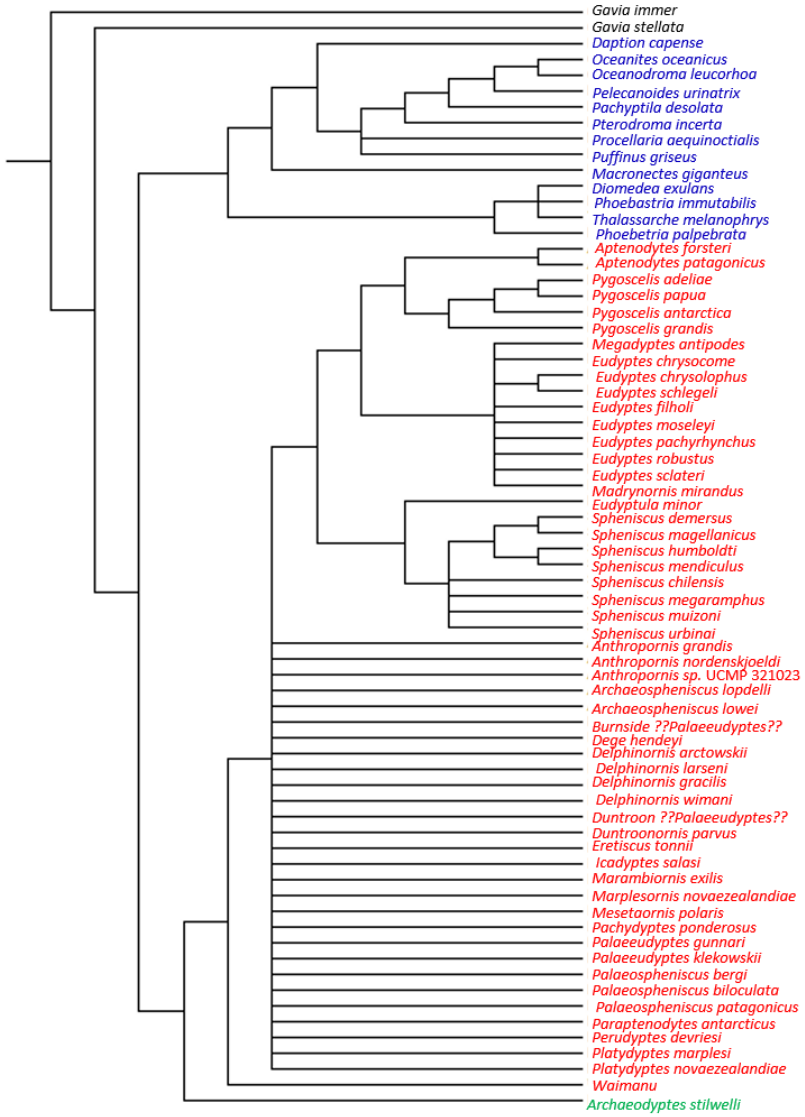
Gavia immer
Gavia stellata
Daption capense
Oceanites oceanicus
Oceanodroma leucorhoa
Pelecanoides urinatrix
Pachyptila desolata
Pterodroma incerta
Procellaria aequinoctialis
Puffinus griseus
Macronectes giganteus
Diomedea exulans
Phoebastria immutabilis
Thalassarche melanophrys
Phoebetria palpebrata
Aptenodytes forsteri
Aptenodytes patagonicus
Pygoscelis adeliae
Pygoscelis papua
Pygoscelis antarctica
Pygoscelis grandis
Megadyptes antipodes
Eudyptes chrysocome
Eudyptes chrysolophus
Eudyptes schlegeli
Eudyptes filholi
Eudyptes moseleyi
Eudyptes pachyrhynchus
Eudyptes robustus
Eudyptes sclateri
Madrynornis mirandus
Eudyptula minor
Spheniscus demersus
Spheniscus magellanicus
Spheniscus humboldti
Spheniscus mendiculus
Spheniscus chilensis
Spheniscus megaramphus
Spheniscus muizoni
Spheniscus urbinai
Anthropornis grandis
Anthropornis nordenskjoeldi
Anthropornis sp. UCMP 321023
Archaeospheniscus lopdelli
Archaeospheniscus lowei
Burnside ??Palaeeudyptes??
Dege hendeyi
Delphinornis arctowskii
Delphinornis larseni
Delphinornis gracilis
Delphinornis wimani
Duntroon ??Palaeeudyptes??
Duntroonornis parvus
Eretiscus tonnii
Icadyptes salasi
Marambiornis exilis
Marplesornis novaezealandiae
Mesetaornis polaris
Pachydyptes ponderosus
Palaeeudyptes gunnari
Palaeeudyptes klekowskii
Palaeospheniscus bergi
Palaeospheniscus biloculata
Palaeospheniscus patagonicus
Paraptenodytes antarcticus
Perudyptes devriesi
Platydyptes marplesi
Platydyptes novaezealandiae
Waimanu
Archaeodyptes stilwelli

B.

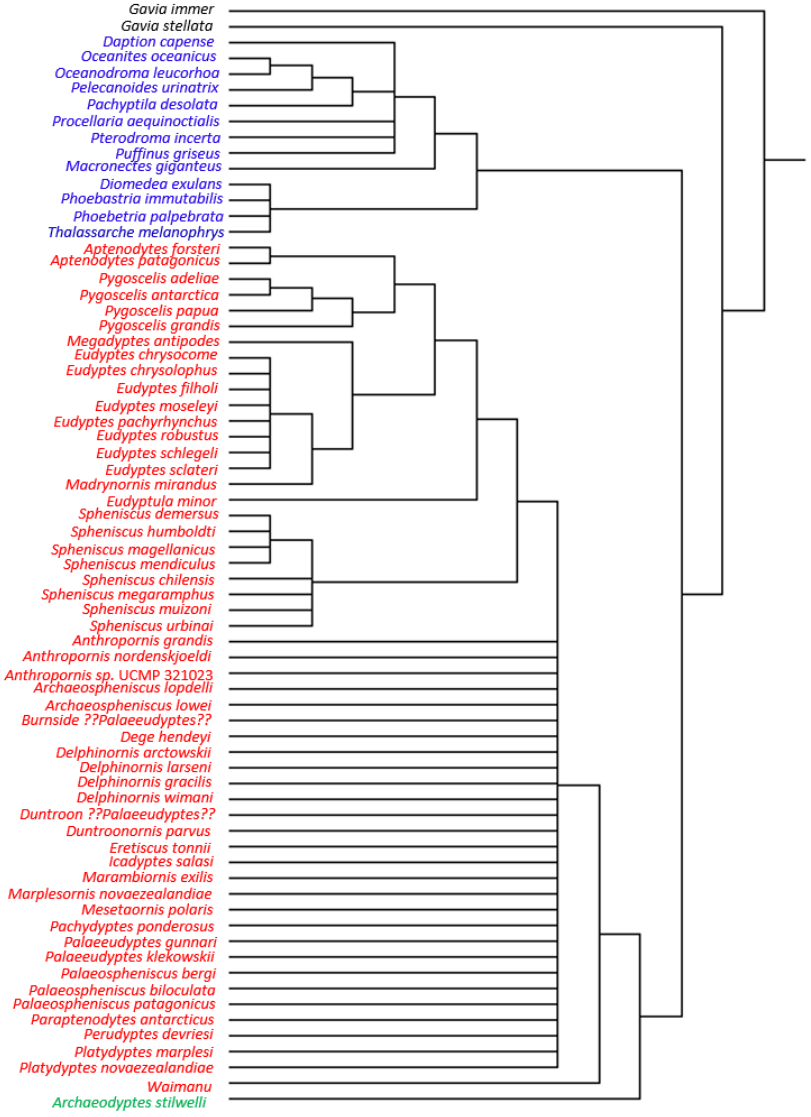
Gavia immer
Gavia stellata
Daption capense
Oceanites oceanicus
Oceanodroma leucorhoa
Pelecanoides urinatrix
Pachyptila desolata
Procellaria aequinoctialis
Pterodroma incerta
Puffinus griseus
Macronectes giganteus
Diomedea exulans
Phoebastria immutabilis
Phoebetria palpebrata
Thalassarche melanophrys
Aptenodytes forsteri
Aptenodytes patagonicus
Pygoscelis adeliae
Pygoscelis antarctica
Pygoscelis papua
Pygoscelis grandis
Megadyptes antipodes
Eudyptes chrysocome
Eudyptes chrysolophus
Eudyptes filholi
Eudyptes moseleyi
Eudyptes pachyrhynchus
Eudyptes robustus
Eudyptes schlegeli
Eudyptes sclateri
Madrynornis mirandus
Eudyptula minor
Spheniscus demersus
Spheniscus humboldti
Spheniscus magellanicus
Spheniscus mendiculus
Spheniscus chilensis
Spheniscus megaramphus
Spheniscus muizoni
Spheniscus urbinai
Anthropornis grandis
Anthropornis nordenskjoeldi
Anthropornis sp. UCMP 321023
Archaeospheniscus lopdelli
Archaeospheniscus lowei
Burnside ??Palaeeudyptes??
Dege hendeyi
Delphinornis arctowskii
Delphinornis larseni
Delphinornis gracilis
Delphinornis wimani
Duntroon ??Palaeeudyptes??
Duntroonornis parvus
Eretiscus tonnii
Icadyptes salasi
Marambiornis exilis
Marplesornis novaezealandiae
Mesetaornis polaris
Pachydyptes ponderosus
Palaeeudyptes gunnari
Palaeeudyptes klekowskii
Palaeospheniscus bergi
Palaeospheniscus biloculata
Palaeospheniscus patagonicus
Paraptenodytes antarcticus
Perudyptes devriesi
Platydyptes marplesi
Platydyptes novaezealandiae
Waimanu
Archaeodyptes stilwelli

The heuristic search of the dataset modified from Ksepka et al. (2012), including both molecular and all morphological characters retained 312 MPTs, with a score of 5372. The matrix of Ksepka et al. (2012) where osteology-only characters were included in the dataset, and all other characters were omitted produced 496 trees, of 359 steps. Similar to the consensus trees produced through the application of the modified datasets of Ksepka and Clarke (2010) (Figure 4.1), the strict consensus trees of the modified Ksepka et al. (2012) datasets (Figure 4.2) also retrieved Procellariiformes and Sphenisciformes as distinct monophyletic clades. *Archaeodyptes stilwelli* was recovered as a basal stem penguin in both the molecular and morphology character, and osteology-only character matrixes analyses of the modified Ksepka et al. (2012) dataset. Specifically, in the analysis with all characters included, *Archaeodyptes stilwelli* occupied a position one node crownward relative to *Gavia stellata*, and was placed as a sister taxon to both recognised *Waimanu* species, *Marambiornis exilis*, *Mesetaorrnis polaris*, and all *Delphinornis* species, and one node basal relative to *Perudyptes devriesi*. *Archaeodyptes stilwelli*is placed in an identical position in the osteology-only character analysis relative to *Gavia stellata*, yet sister taxa pairings with all included extinct penguin taxa were supported, in contrast. Poorer resolution was recovered in the osteology-only strict consensus tree, and also resulted in different pairing relationships between crown taxa in both Sphenisciformes and Procellariiformes, however the position of *Archaeodyptes stilwelli* remained constant.

Figure 4.2 (next page): Comparison of strict consensus parsimony-based phylogenetic trees produced via heuristic search analyses, using PAUP*. A. shows the phylogenetic tree generated from the modified dataset of Ksepka et al., (2012) using both genetic and all morphological characters. B. is the result of the modified dataset from Ksepka et al., (2012) using only osteological morphological characters. Gaviiformes are presented in black; Procellariiformes are presented in blue; Sphenisciformes are presented in red; and the position of *Archaeodyptes stilwelli* is presented in green.

A.


Gavia immer
Gavia stellata
Daption capense
Macronectes giganteus
Procellaria cherea
Puffinus gravis
Pachyptila desolata
Pterodroma brevirostris
Pelecanoides urinatrix
Oceanites oceanicus
Oceanodroma leucorhoa
Diomedea exulans
Phoebastria immutabilis
Phoebetria palpebrata
Thalassarche melanophrys
Aptenodytes forsteri
Aptenodytes patagonicus
Pygoscelis antarctica
Pygoscelis papua
Pygoscelis adeliae
Megadyptes antipodes
Eudyptes chrysocome
Eudyptes filholi
Eudyptes moseleyi
Eudyptes chrysolophus
Eudyptes schlegeli
Eudyptes pachyrhynchus
Eudyptes robustus
Eudyptes sclateri
Madrynornis mirandus
Eudyptula minor
Spheniscus demersus
Spheniscus magellanicus
Spheniscus humboldti
Spheniscus mendiculus
Spheniscus muizoni
Spheniscus urbinai
Spheniscus megaramphus
Pygoscelis grandis
Marplesornis novaezealandiae
Palaeospheniscus biloculata
Palaeospheniscus bergi
Palaeospheniscus patagonicus
Eretiscus tonnii
Platydyptes novaezealandiae
Platydyptes marplesi
Paraptenodytes antarcticus
Archaeospheniscus lopdelli
Archaeospheniscus lowei
Duntroonornis parvus
Kairuku waitaki
Kairuku grebneffi
Pachydyptes ponderosus
Icadyptes salasi
Inkayacu paracasensis
Burnside ??Palaeeudyptes??
Palaeeudyptes klekowskii
Palaeeudyptes gunnari
Palaeeudyptes antarcticus
Anthropornis sp. UCMP 321023
Anthropornis nordenskjoeldi
Anthropornis grandis
Perudyptes devriesi
Delphinornis wimani
Delphinornis gracilis
Delphinornis arctowskii
Delphinornis larseni
Mesetaornis polaris
Marambiornis exilis
Waimanu tuatahi
Waimanu manneringi
Archaeodyptes stilwelli

B.

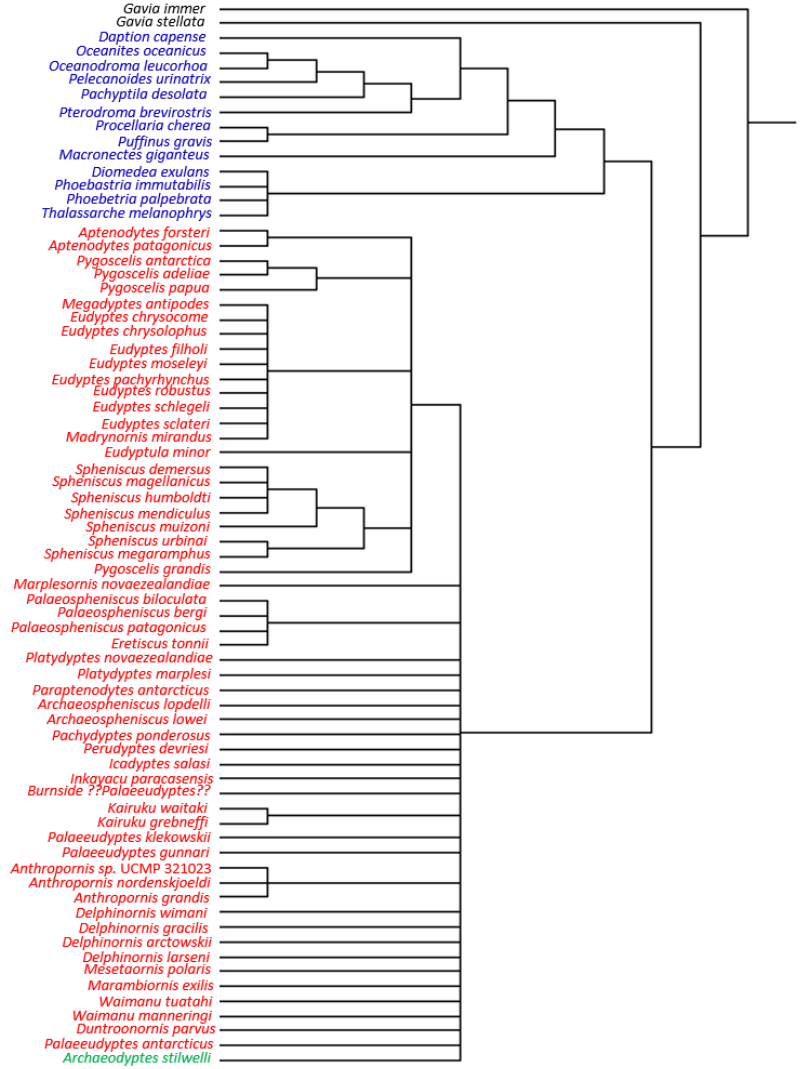
Gavia immer
Gavia stellata
Daption capense
Oceanites oceanicus
Oceanodroma leucorhoa
Pelecanoides urinatrix
Pachyptila desolata
Pterodroma brevirostris
Procellaria cherea
Puffinus gravis
Macronectes giganteus
Diomedea exulans
Phoebastria immutabilis
Phoebetria palpebrata
Thalassarche melanophrys
Aptenodytes forsteri
Aptenodytes patagonicus
Pygoscelis antarctica
Pygoscelis adeliae
Pygoscelis papua
Megadyptes antipodes
Eudyptes chrysocome
Eudyptes chrysolophus
Eudyptes filholi
Eudyptes moseleyi
Eudyptes pachyrhynchus
Eudyptes robustus
Eudyptes schlegeli
Eudyptes sclateri
Madrynornis mirandus
Eudyptula minor
Spheniscus demersus
Spheniscus magellanicus
Spheniscus humboldti
Spheniscus mendiculus
Spheniscus muizoni
Spheniscus urbinai
Spheniscus megaramphus
Pygoscelis grandis
Marplesornis novaezealandiae
Palaeospheniscus biloculata
Palaeospheniscus bergi
Palaeospheniscus patagonicus
Eretiscus tonnii
Platydyptes novaezealandiae
Platydyptes marplesi
Paraptenodytes antarcticus
Archaeospheniscus lopdelli
Archaeospheniscus lowei
Pachydyptes ponderosus
Perudyptes devriesi
Icadyptes salasi
Inkayacu paracasensis
Burnside ??Palaeeudyptes??
Kairuku waitaki
Kairuku grebneffi
Palaeeudyptes klekowskii
Palaeeudyptes gunnari
Anthropornis sp. UCMP 321023
Anthropornis nordenskjoeldi
Anthropornis grandis
Delphinornis wimani
Delphinornis gracilis
Delphinornis arctowskii
Delphinornis larseni
Mesetaornis polaris
Marambiornis exilis
Waimanu tuatahi
Waimanu manneringi
Duntroonornis parvus
Palaeeudyptes antarcticus
Archaeodyptes stilwelli

4.1.2 Bayesian Analyses

"

The two independent Bayesian analyses performed on the modified osteology-only dataset of Ksepka and Clarke (2010) achieved stationarity and convergence: log likelihood statistics (LnL) after Burnin = 4,001 for Run 1 (mean = 1,195.09, s.d. = 0.099, Effective Sample Size after Burnin = 20,002) and for Run 2 (1192.49, 0.113, 20,012), and after 5,000,000 generations each the average standard deviation of split frequencies were 0.008 and 0.044, well within the recommended cut-off value of < 0.1. In the tree produced (Figure 4.3), both Sphensiciformes and Procellariiformes are recovered as monophyletic clades, yet many of the clades within Spheniscifomes are collapsed, and thus a poor resolution is retrieved—particularly in more crownward species. Regardless, the general basal position of *Archaeodyptes stilwelli* relative to surrounding taxa is consistent with that of parsimony-based heuristic searches conducted. Specifically, *Archaeodyptes stilwelli* is recovered in a position one node basal to all currently known extinct and extant penguin taxa included in this analysis—one node basal relative to *Waimanu* genus, and as a sister taxon to *Pelecanoides urinatrix* within Procellariiformes.

The Bayesian analysis of the modified dataset of Ksepka et al. (2012) produced consensus tree derived from 15,002 sampled trees (of 20,002 trees produced, 25% of which were discarded as Burnin). All clades are shown regardless of posterior probabilities—the percentage of sampled generations that present that node. The two analyses (runs) achieved stationarity and convergence: LnL after Burnin=15,002 for Run 1 (mean= -1,528.46, s.d. = 9.16, Effective Sample Size after Burnin = 2,474) and Run 2 (-1,528.49, 0.113, 9.34, 7, 2,362). After 10,000,000 generations the average standard deviation of split frequencies was 0.011468, well less than the frequency cut off value of 0.1.

Figure 4.3 (next page): The Bayesian tree produced through the analysis of the modified osteology-only character dataset of Ksepka and Clarke (2010), using the program MrBayes (Ronquist & Huelsenbeck, 2003). Scale bar is shown at the bottom of the figure. Gaviiformes are presented in black, Procellariiformes are presented in blue, Sphenisciformes are shown in red, and the position of *Archaeodyptes stilwelli* is shown in green.

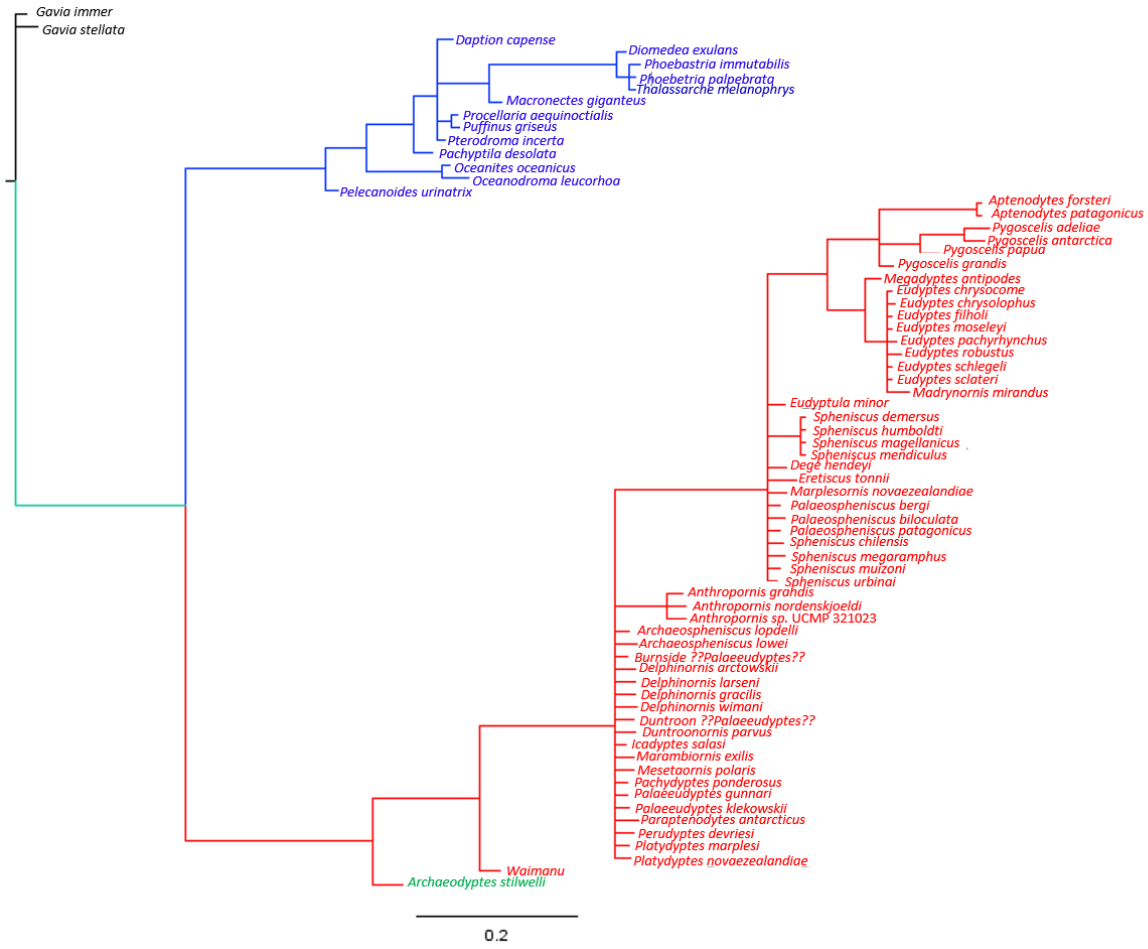

The Bayesian consensus tree produced a similar result to that of the parsimony-based heuristic searches and the Bayesian consensus tree produced by the utilization of the dataset modified from Ksepka and Clarke (2010). Monophyly is supported for Sphenisciformes and Procellariiformes, and *Archaeodyptes stilwelli* is recovered in an identical position to the previous Bayesian analysis; as one node basal relative to *Waimanu manneringi*, and effectively basal to all penguin taxa included. This analysis resulted in greater resolution of taxa within Sphenisciformes particularly, resulting in numerous different relationships and species pairings between extant and extinct penguin taxa. Different species pairings are also supported within crown Procellariiformes compared to the Bayesian analysis of the dataset modified from Ksepka and Clarke (2010).

Figure 4.4 (next page): The Bayesian tree produced through the analysis of the modified osteology-only character dataset of Ksepka et al., (2012), using the program MrBayes (Ronquist & Huelsenbeck, 2003). Scale bar is shown at the bottom of the figure. Gaviiformes are presented in black, Procellariiformes are presented in blue, Sphenisciformes are shown in red, and the position of *Archaeodyptes stilwelli* is shown in green.

That *Archaeodyptes stilwelli* is recovered in the same basal position across both Bayesian analyses, and also occupies a similar position in all other phylogenetic analyses provides evidence that the position presented may be considered robust.

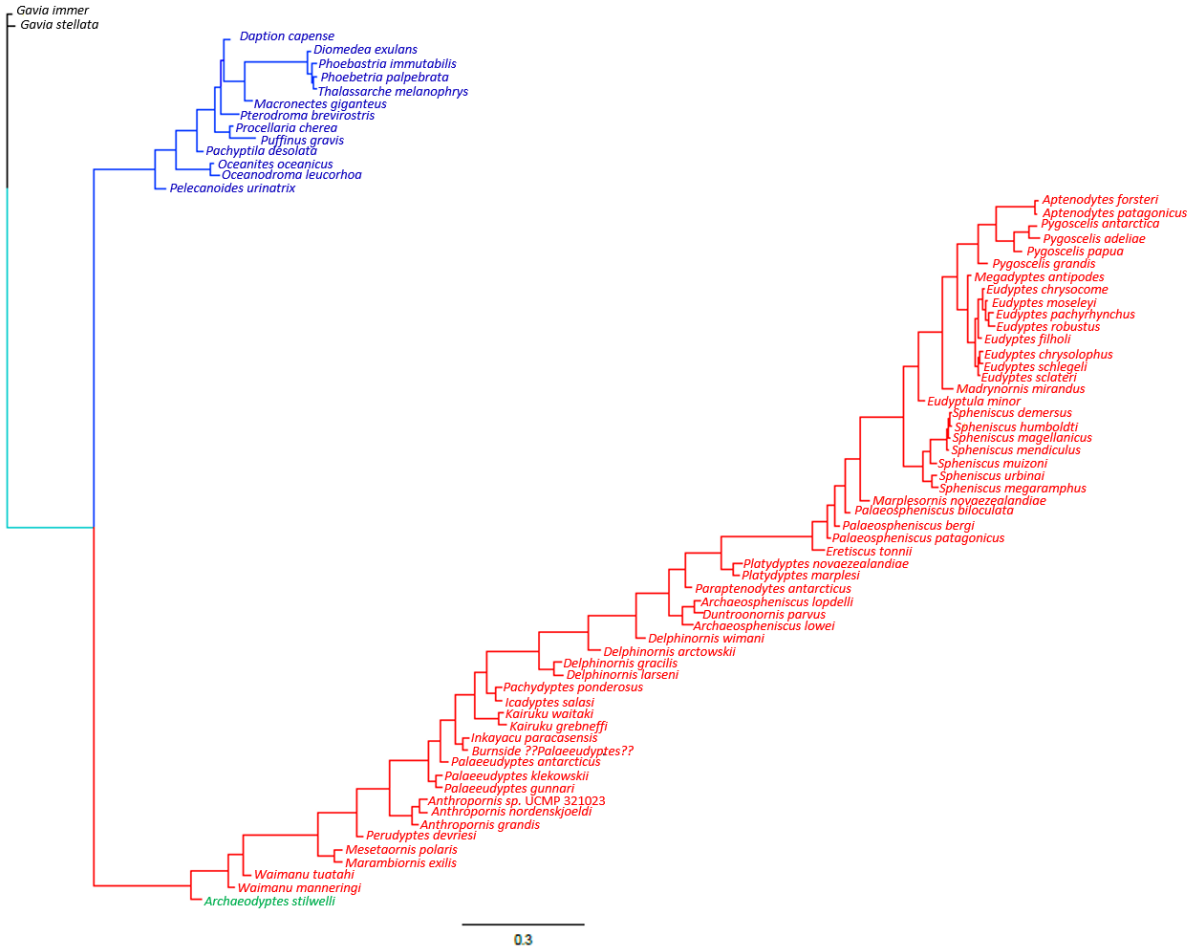

4.2 Comparative Palaeontology

4.2.1 Anatomical Comparison of JDS8341.b: Cervical Vertebrae IV

The comparative analysis of cervical vertebrae IV, compared samples of numerous species of Auquorlitornithes with that of cervical vertebra IV from JDS8341.b through a Principal Components Analysis (PCA). The PCA showed most distinctive separation correlating with each Auquorlitornithes clade using principal components 1 and 2 (PC1 and PC2) (Figure 4.5). On the scatterplot diagram Figure 4.5, JDS8341.b occupies a position between plots associated with *Diomedea exulans*, *Waimanu*, and *Aptenodytes patagonicus*.

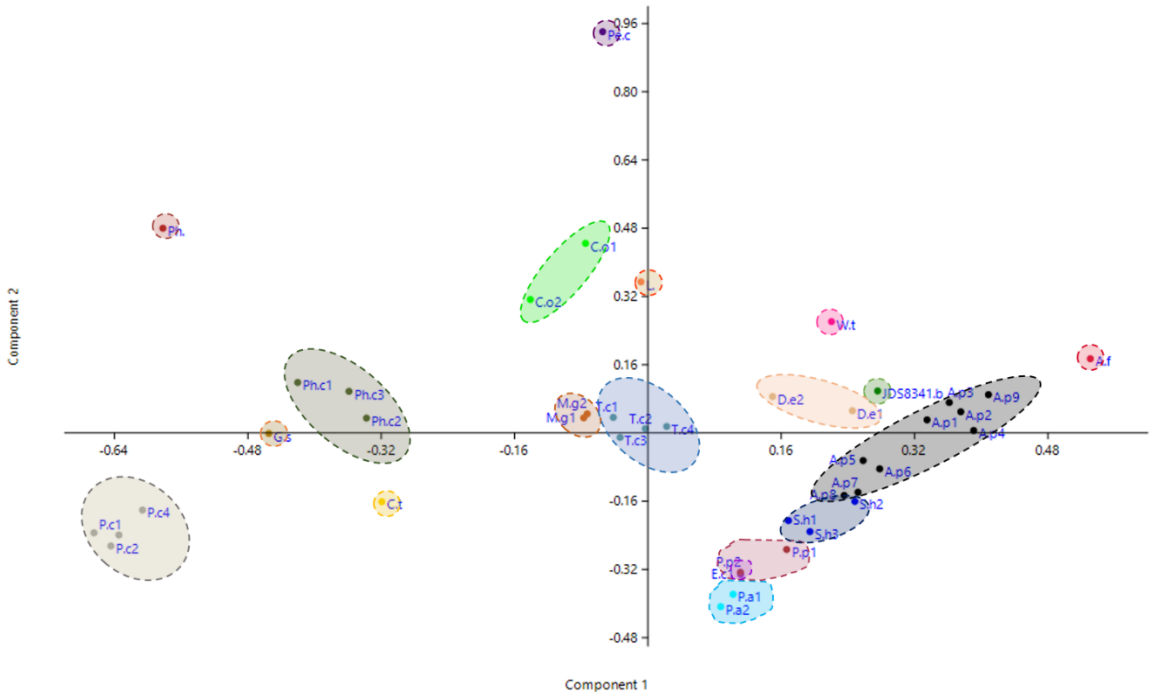

Figure 4.5: PCA scatterplot of cervical vertebra IV measurements, comparing PC1 and PC2. Dashed lines around plotted points indicate clusters relating to similar taxa. Initial component abbreviations describe taxa as follows: **A.f**—*Aptenodytes forsteri* (emperor penguin), **A.p**—*Aptenodytes patagonicus* (king penguin), **C.o**—*Cynus olor* (mute swan), **C.t**—*Chauna torquata* (southern screamer), **D.e**—*Diomedea exulans* (wandering albatross), **E.c**—*Eudyptes chrysolophus* (macaroni penguin), **G.s**—*Gavia stellata* (red-throated diver), **JDS8341.b**—*Archaeodyptes stilwelli*, **L.**—*Leptoptilos* sp. (adjutant stork), **M.g**—*Macronectes giganteus* (southern giant petrel), **P.a**—*Pygoscelis adeliae* (Adelie penguin), **P.c**—*Podiceps crisatus* (great crested grebe), **Pe.c**—*Pelecanus conspicilatus* (Australian pelican), **Ph.**—*Phoeicopterus* sp. (flamingo), **Ph.c**—*Phalacrocorax carbo* (black shag), **S.h**—*Spheniscus humboldti* (Humboldt penguin), **T.c**—*Thalassarche cauta* (shy mollymawk), **W.t**—*Waimanu tuatahi*. Clusters to show visual separation between datapoints are marked with coloured shapes and dashed lines.

PC1 describes 58.29% of the total variance, explaining the majority of the variance between these cervical vertebrae, compared to the other principal components. PC1 has relatively large positive loadings on variables Fw1, Bw1 and Bw2 (Figure 4.6A), variables that were associated with the measurement of the front width, and both back width measurements of the vertebrae respectively (see ***Chapter II: Methods***, Figure 2.3 for description of specific acronyms). Relatively smaller (but still positive) loadings were presented in association with the L1, L2, L3 and L4 (see Chapter IImeasurement variables (Figure 4.6A), and thus these length variables had less of a contribution to the variability of the dataset in PC1. PC2 explains 36.04% of the total variance, and thus contributes significantly to the variability presented in the PCA. Contrary to PC1, PC2 has relatively large

positive loadings related to the length measurement variables L1, L2, L3 and L4 (Figure 4.6B)—indicating that these length variables contributed most to the variance presented in PC2. Relatively smaller positive loadings are associated with the Fw1 and Bw2 (Figure 4.6B), representing the front and back total widths of the vertebrae. A negative loading of relatively moderate size is also presented in relation with Bw1 (Figure 4.6B). PC3 describes a further 4% of the total variance, while subsequent principal components that explain less than 1% and hence provide a minor contribution to the dataset's variability. PC3 presents positive loadings associated with Bw1, L1, L2, and L3 (Figure 4.6C). Bw1 is the largest of the loadings relative to the others, where L1 can be described as a moderately positive loading and L2 and L3 as smaller loadings. Negative loadings are shown for the other variables (Figure 4.6C), where Bw2 represents the largest negative loading, followed by Fw1 of moderate size, and L4 of relatively smaller size.

The majority of the variance describing the positions occupied by the different taxa in the scatterplot shown in Figure 4.5 can therefore be described predominately by the variance in the width of the front (cranial) and back (caudal) in cervical vertebra IV amongst species. The vertebrae medial length also significantly contributes to the differentiation of shapes and sizes between taxa.

Figure 4.6 (next page): The PCA loadings plots of multiple principal components from the comparison of cervical vertebra IV measurements across auquorlitornithes (performed in PAST). **A.** is the loadings plot of PC1, **B.** is the loadings plot of PC2, and **C.** is the loadings plot of PC3. Fwd1 IV is the forward width of the cervical vertebrae, Bw1 and Bw2 are the measurements of the back width of the vertebrae, and L1, L2, L3 and L4 represent the different measurements of the length of the cervical vertebrae (please refer to Chapter II: Methods, Figure 2.5, for more details).

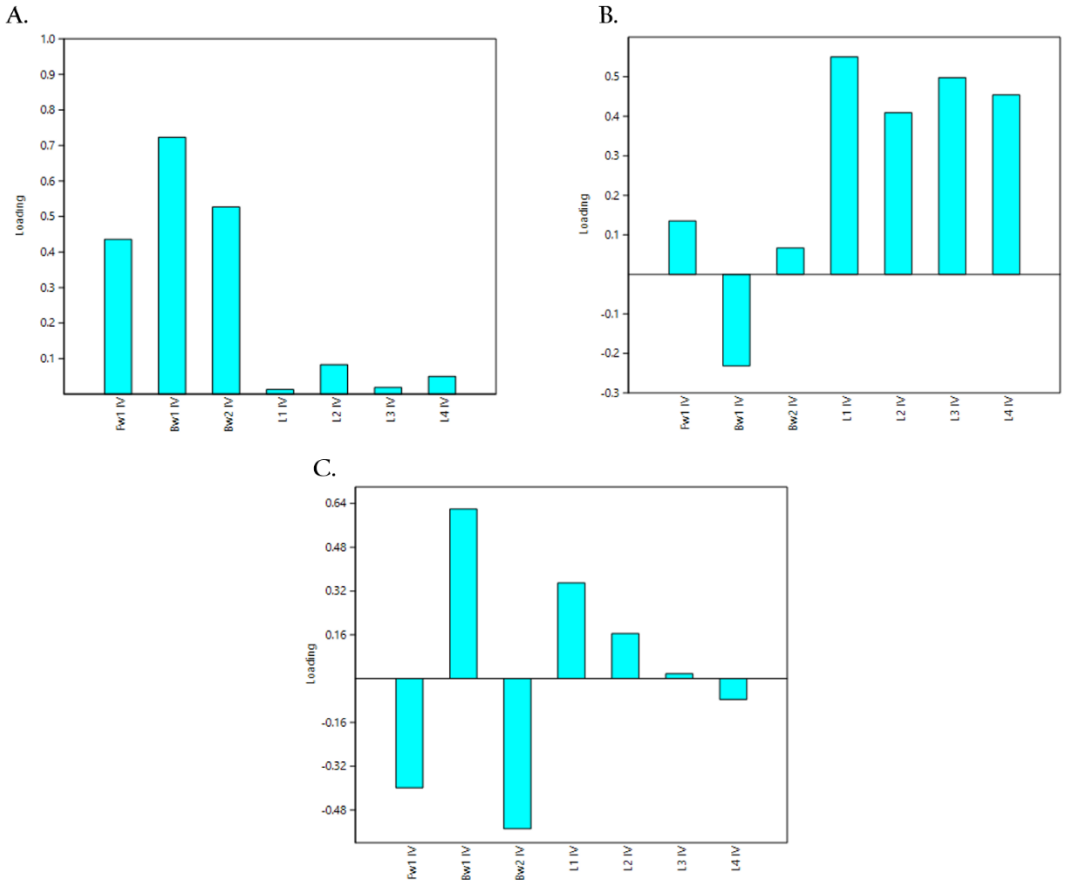

4.2.2 Anatomical Comparison of JDS8344: Ulna and Radius

Comparison of separation of radius and ulna measurements from various *Waimanu tuatahi* specimens and that of JDS8344 are presented through a multivariate PCA, as scatterplot diagrams (Figure 4.7). Most distinctive separation of data points in the PCA can be observed when comparing PC1 and PC2, and also PC1 with PC3. PC1 accounts for 85.07% of the total variance, while PC2 accounts for 7.97%, and PC3 4.49%. PC4 accounts for 1.60%, and subsequent principal components account for less than 1% of the total variance.

Figure 4.7 (next page): PCA scatterplots of comparing the visual separation of plots associated with radius and ulna measurements in *Waimanu tuatahi* and JDS8344. In **A.** PC1 is plotted against PC2, and in **B.** PC1 is plotted against PC3. Points labelled "JDS8344" correspond to datapoint measurements associated with the ulna or radius of JDS8344. Points labelled "Waimanu" correspond to datapoint measurements associated with measurements of the radius or ulna or *Waimanu tuatahi*, while digits/letters following refer to the exact specimen number associated. Clusters to show visual separation between datapoints are marked with coloured shapes with dashed lines.

A.

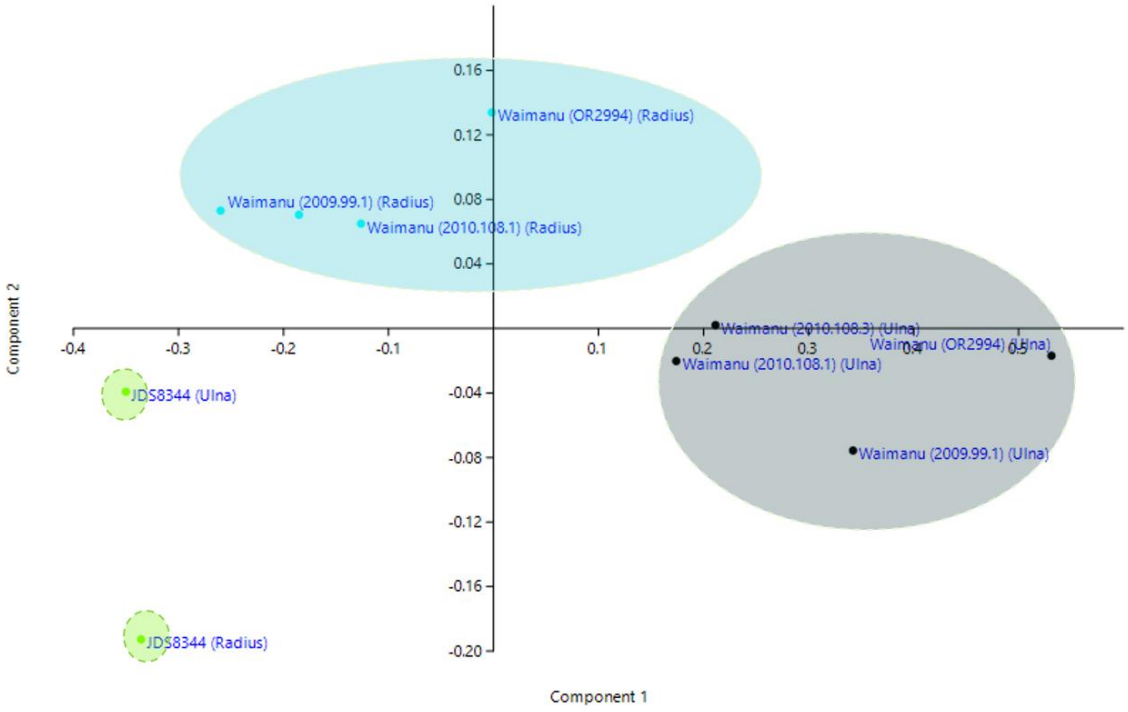

B.

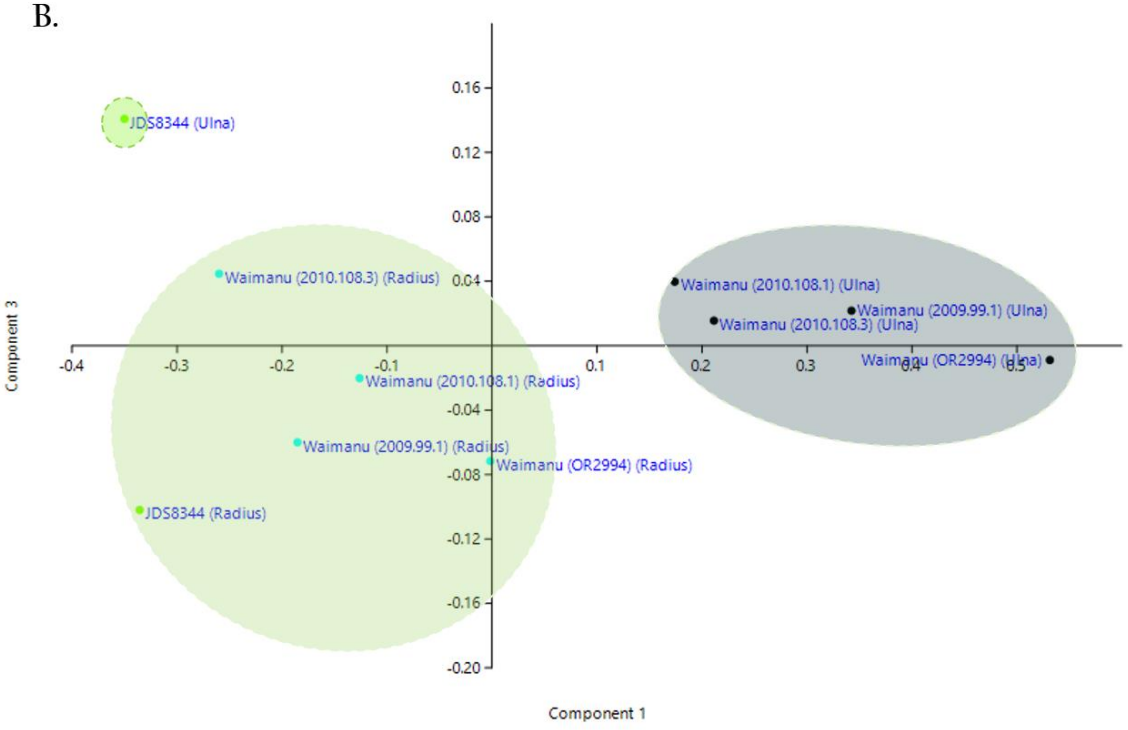

PC1 describes the vast majority of the variance in the dataset of ulna and radius measurements. In the loadings plot presented in Figure 4.8A, it can be observed that the most positive loadings relative to other loadings are associated with the proximal width, the proximal depth, and mid-shaft depth. These variables therefore have the most positive impact on variability within the dataset, explaining the majority of separation observed. Moderately positive loadings are

also shown for total element length and mid-shaft width. A relatively small negative loading is also retrieved for variance explained by the distance from the proximal facet to the bend in each element, and thus was a relatively minor contributing factor.

The loadings plot for PC2 (Figure 4.8B) shows that the majority of the variance explained predominately by PC2 is described by a relatively large positive loading associated with the overall length of each element. A moderate-size negative loading is also presented for the proximal width. All other loadings for PC2 are associated with relatively small positive loadings, while the distance to bend variable has a small negative loading, showing they had a minor impact on the variance compared to the overall length and proximal width.

The near 5% of total variance explained by PC3 (Figure 4.8C) is associated with relatively large positive loadings for variables relating to the distance to the bend, and the proximal width. A moderately positive loading is associated with the overall length, while a negatively moderate loading is related to the proximal depth variate. A large negative loading associated with the mid-shaft width contributes to the variance of PC3, in the overall variability of the dataset. A relatively small-moderate negative loading is described by the mid-shaft depth.

Figure 4.8 (next page): The PCA loadings plots of multiple principal components from the comparison of radius and ulna measurements of *Waimanu tuatahi* and JDS8344 (performed in PAST). **A.** is the loadings plot of PC1, **B.** is the loadings plot of PC2, and **C.** is the loadings plot of PC3. The Length variable describes the overall length measurement of the element, PW refers to the proximal width, MW refers to the mid-shaft width, PD refers to the proximal depth, MD refers to the mid-shaft depth, and DB is the abbreviation for distance to bend (please refer to Chapter II: Methods for further details).

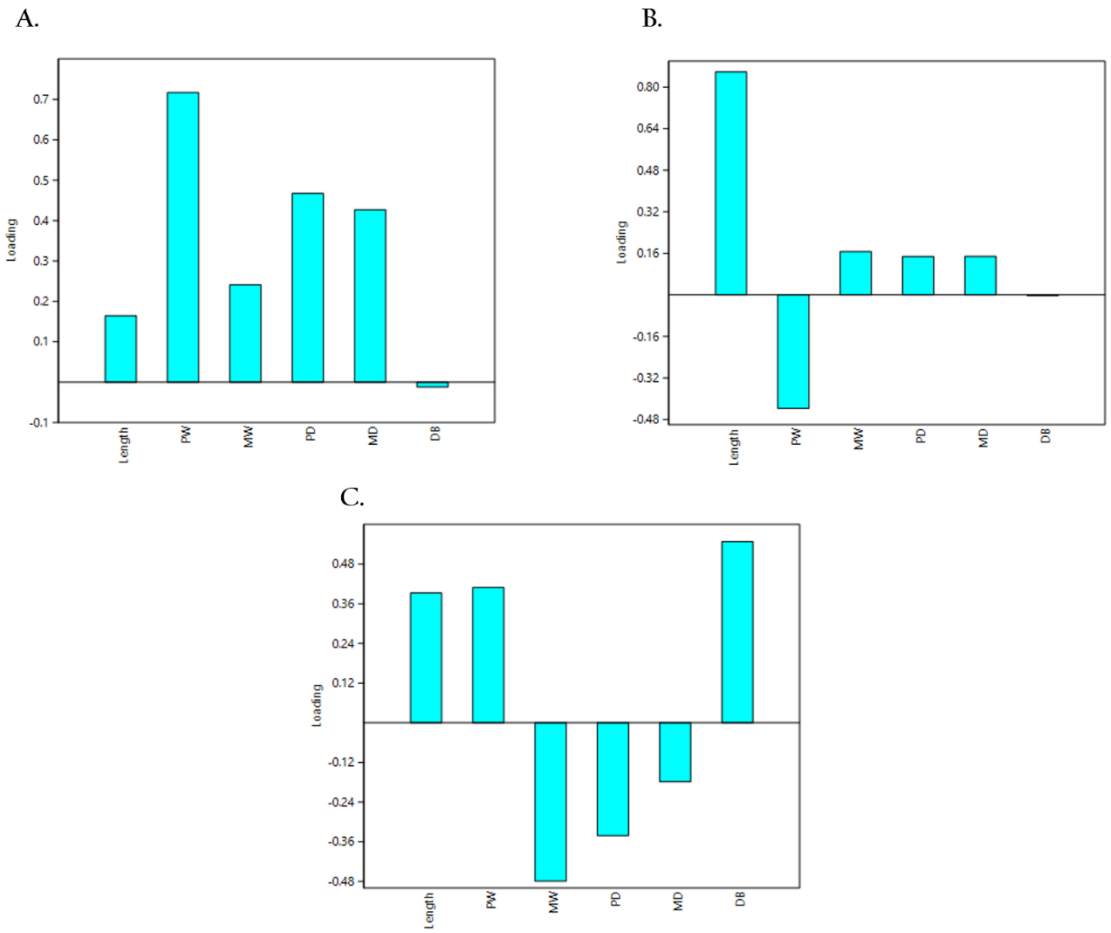

The most distinctive separation of the plots in the dataset is observed when comparing both PC1 with PC2 (Figure 4.7A), and also PC1 with PC3 (Figure 4.7B). The scatterplot of PC1 against PC2 gives distinctive separation without overlap, where separate clusters are observed for the radii of *W. tuatahi* specimens, and ulnae of *W. tuatahi* specimens. The ulna and radius of JDS8344 exist distinctly apart from each of these clusters, and are separate from each other (i.e. are not grouped together). Accordingly, both the ulna and radius are morphologically dissimilar from one another, and also distinct compared to the morphology of the same elements of *W. tuatahi*. In contrast, the scatterplot of PC1 and PC3 (Figure 4.7B) presents a cluster associated with all *W. tuatahi* radii plots, and also the radius of JDS8244. In comparison, *W. tuatahi* ulnae plot as a distinct cluster, but the ulna of JDS8344 does not and is visually separate to all other clusters. While the radii share similar morphology therefore, the ulna of JDS8344 is morphologically distinct compared to *W. tuatahi.*

CHAPTER V: DISCUSSION

This chapter aims to discuss the validity of the taxon *Archaeodyptes stilwelli*, its phylogenetic position, as well as interpret its palaeobiology, and address implications that this material has on the understanding of the current state of bird evolution. It will also attempt to put the fossil material in the context of the New Zealand palaeoenvironment at the time of deposition of the Takatika Grit.

5.1 Taxonomic Implications—the Validity of Archaeodyptes stilwelli

Archaeodyptes stilwelli is the single novel taxon recognised based on the study of the holotype specimen JDS8344, and also the referred material of JDS8341.b. The validity of this assignment however should be questioned; Are JDS8344 and JDS8341.b representative of the same, or separate species from a phylogenetic and morphometric perspective?

5.1.1 Are JDS8344 and JDS8341.b the Same Species?

The material available in this study comprises of two associated part skeletons, as referred specimens belonging to the taxon *Archaeodyptes stilwelli* (Figure 5.1). The holotype JDS8344, and JDS8341.b were both excavated from the same approximate location along Maunganui Beach on the Chatham Islands, corresponding to the same nodular-phosphate and bone horizon of the Takatika Grit rock unit. Previously published work suggests the Takatika Grit is of late early-middle Paleocene age, with a reworked Cretaceous component (Hollis, in press). Considering the Late Cretaceous-Paleocene age range (Consoli and Stilwell, 2009), and the variety of taxa recovered from the sequence, justification of both specimens belonging to the same taxon is required.

Considering that the Takatika Grit includes an allochthonous accumulation of reworked latest Cretaceous material, deposited in the Danian (Hollis, in press)—and is even associated with earliest Tertiary microfossils (Stilwell et al., 2006), reworking is known to have occurred in this sequence. However, elements of JDS8344 and JDS8341.b show no evidence of the elements being reworked, since partially exhumed and reburied elements are unlikely to be deposited as associated partial skeletons. Considering that Cretaceous elements of the Takatika Grit are inferred to have been reworked (Hollis, in press), in contrast, the lack of reworking in JDS8344 and JDS8341.b re-

affirms that both specimens are representative of partial skeletons deposited *in situ*, in the late early-middle Paleocene.

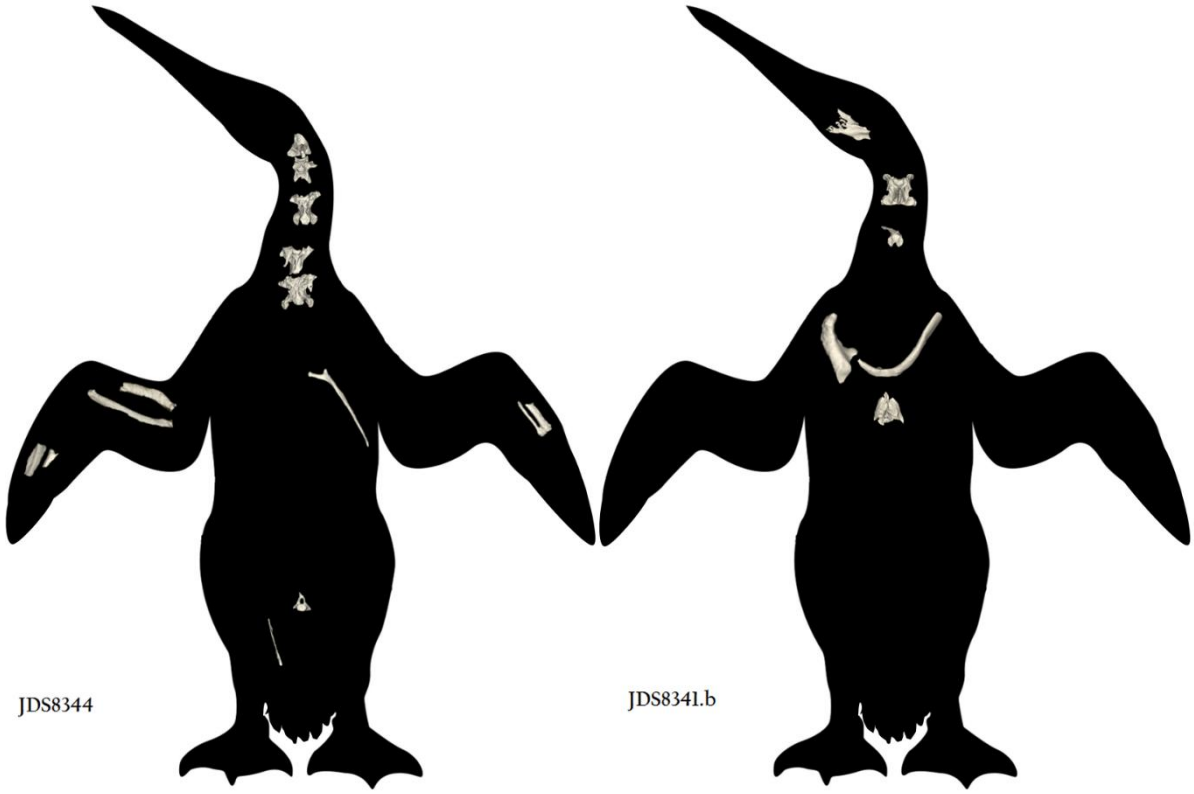

Figure 5.1: Reconstructions of *Archaeodyptes stilwelli*, showing the elements of specimens JDS8344 and JDS8341.b respectively. Images were based on and modified from silhouette image used in Slack et al. (2006), that was based on original art by Chris Gaskin © Geology Museum, University of Otago.

Phylogenetic analyses (see ***Chapter IV: Analyses***), testing the phylogenetic placement of each specimen separately, revealed that JDS8344 displayed morphological characters that placed it in a basal position to Sphenisciformes. In contrast, the same analysis performed on JDS8341.b suggested that JDS8341.b might occupy a more crownward position alongside modern penguins. There is no evidence, however, to suggest reworking in JDS8341.b consistent with reworked fossils and sediments associated with the much younger crown group penguin taxa (~12.7 Ma and younger) (Gavryushkina et al., 2016). The initial phylogenetic position occupied by JDS8341.b may be better explained therefore by an artefact produced from the relative lack of scores that could be performed on the elements available for study, as well as that the scored elements are similar in all crown penguins. Consequently, an exact phylogenetic position of JDS8341.b could not be recovered with confidence using the information available for that specimen alone, other than determining it had morphological character scores consistent with synapomorphies characteristic of the Spheniscifomes

clade. When coupled with JDS8344 however, subsequent phylogenetic analysis of JDS8344 and JDS8341.b combined occupied the same position that JDS8344 did during previous testing. This showed that the character scores of JDS8341.b did not affect phylogenetic placement of JDS8344, and were also compatible with that basal position. As such, JDS8344 and JDS8341.b were compatible as existing as the same taxon, based on their morphological characters.

Shared skeletal elements between specimens (i.e. a radius in each specimen) would be a significant aspect of identifying the more specific nature of each specimen compared to the other. However, since there is no overlap in skeletal material between JDS8344 and JDS8341.b, it cannot be said with certainty whether the specimens refer to different individuals of the same species, or separate ancient penguin taxa entirely. Using the elements available however, it is evident that as well as possessing elements synapopmorphic of Sphenisciformes, both specimens share anatomical measurements (see ***3.1.9 Table of Measurements (JDS8344)*** and ***3.1.11 Table of Measurements (JDS8341.b)***) consistent with both specimens being of a similar size. In particular, different components of the spinal column exist in both specimens, and can be comparatively examined.

When considering that the vertebrae present among the holotype specimen of *Archaeodyptes stilwelli* compared to JDS8341.b occupy different positions in the vertebral column, even considering the vertebrae in JDS8344 are in various broken and incomplete states, the overall general morphology of the vertebrae appears alike. Notably, the measurements of cervical vertebra IV of JDS8341.b are consistently similar with measurements of vertebra from JDS8344. In particular, the length of the neural canal in cervical vertebra IV of JDS8341.b was recorded as 19.28 mm, and is similar to the neural canal length in cervical (b) (19.07 mm), cervical (c) (17.45 mm), and cervical (d) (16.80 mm) of JDS8344. Similar measurements are also observed when comparing cervical IV of JDS8341.b in regards to the maximum width at cranial and caudal zygapophyses in cervical (d), the lateral diameter of the neural canal in cervical (a), (c) and (d), and the maximum cranial width in cervical (d) was also similar to the maximum caudal width of cervical vertebra IV of JDS8341.b. It is thus evident to a degree that the vertebrae possessed by JDS8344 and JDS8341.b were of a similar size.

Furthermore, shared morphological features observed among vertebrae across both specimens include the presence of a blade-like *processus spinosus*, and a *processus ventralis corporis*—both orientated posteriorly, as well as *tori dorsalis* (dorsal tubercle processes) on the caudal zygapophyses (see Figure 3.7, 3.9 and 3.18). All these features can be observed on cervical vertebra IV of JDS8341.b,

and the axis of JDS8344. While incomplete and broken, the *processes spinosus* on cervical (a) likewise appears to be directed posteriorly, and the incomplete ventral surface of the *corpus vertebrae* is also orientated in a posterior direction—perhaps indicative that the *processus ventralis corporis* was orientated in a similar way (Figure 3.9C and D). Additionally, the size of the *processes spinosus* and *processus ventralis corporis* also decreases relative to subsequent vertebra and their placement in the spinal column. This can be observed when comparing the axis of JDS8344, which has large sail-like *processus ventralis corporis* and *processes spinosus*, compared to the reduced (albeit incomplete) *processes spinosus* on cervical (a) of JDS8344, and further reduced on cervical IV of JDS8341.b. Effectively, this is consistent with a 2nd, 3rd and 4th vertebra placement respectively in the vertebral column. In modern Sphenisciformes, these features of the cervical vertebra, when linked as a cohesive structure, allow reduction in neck length through folding of the cervical system into a strong "S"-shape, allowing a more hydrodynamic morphology in penguin, and also aids in the capability of erect posture on land (Guinard et al., 2010). While all birds have a flexible "S"-shaped neck to a certain extent (Guinard et al., 2010), these posterior directed features of cervical vertebrae in extant penguins allow greater capacity of flexion (Watson, 1883), to bring the head back towards the body (Guinard et al., 2010). The vertebral column of early Sphenisciformes (66.0-39.9 Ma) is not well understood (Jadwiszczak, 2014), however based on these features, it would appear that JDS8344 and JDS8341.b exhibit morphological features consistent with neck flexion capabilities similar to modern penguins.

Consequently, phylogenetic analyses and locality support that both JDS8344 and JDS8341.b were both ancient Sphenisciformes that occupied the same region of the Chatham Islands in the late early-middle Paleocene. Furthermore, morphometric study suggests that the two penguins exhibited similar vertebrae anatomy and size measurements, consistent with animals of comparable size. While further evidence is needed to robustly assign JDS8341.b to *Archaeodyptes stilwelli*, for the purpose of this research thesis, JDS8341.b has tentatively been referred to as the same species as JDS8344 (*Archaeodyptes stilwelli*). In the circumstance that more definitive evidence should come to light, this placement may be more accurately revised.

5.2 Evaluation of Phylogenetic Placement

Phylogenetic analyses were performed using two recent phylogenetic matrices for Sphenisciformes, to evaluate the phylogenetic matrices in comparison with one another, and test the

phylogenetic placement of *Archaeodyptes stilwelli* in each. In effect, this was done not only determine the placement of *Archaeodyptes stilwelli* in multiple studies, but to also provide an indication of consistency and accuracy across the phylogenetic datasets. Overall, the placement of the taxa in phylogenetic analyses is consistent with previously published nuclear gene and whole genome sequence analyses that have supported Gaviiformes as the earliest branching aquatic taxa used in this analysis, with a crownwards sister-group relationship between the Procellariiformes and Sphenisciformes (Hackett et al., 2008; Jarvis et al., 2014; Prum et al., 2015). The placement of Gaviidae, Procellariiformes and Sphenisciformes from these analyses are also in agreement with the published results of Ksepka and Clarke (2010), and Ksepka et al. (2012), however the more specific placement of taxa within these clades is variable.

Within the Procellariiformes clade the storm petrels of the Hydrobatidae family are recovered by primary and Bayesian analysis of Ksepka and Clarke (2010) and Ksepka (2012) datasets, and are predominately in agreement with originally published material, where *Oceanites oceanicus* and *Oceanodroma leucohoa* are grouped similarly together. The Diomedeidae family of albatrosses is also recovered in Bayesian analyses of each respective dataset, yet in both Bayesian phylogenies *Diomedea exulans* is positioned in most basal position compared to other members of Diomedeidae, in contrast to the original published results in Ksepka and Clarke (2010) and Ksepka et al. (2012) where it occupies a relatively crownward position. All strict consensus trees from the primary analysis in both datasets also recovered all taxa of the Diomedeidae clade together, yet the resolution and exact placement of each taxon varies.

Considerably less resolution within the Sphenisciformes clade is recovered in primary and Bayesian analyses compared to the original phylogeny as per Ksepka and Clarke (2010). In particular, many of the clades recovered in the original analysis have been collapsed, meaning stem penguin taxa lack a large degree of differentiation in the analyses of this study. The Spheniscidae family as published in Ksepka and Clarke (2010) is recovered in both strict consensus trees produced from primary analyses of this dataset, with variable placement of the taxa within it. While Spheniscidae is also recovered in the Bayesian analysis of this research, taxa considered relatively more basal in the original phylogeny published by Ksepka and Clarke (2010) are also included within this family, including *Palaeospheniscus bergi*, *P. biloculata*, *P. patagonicus*, *Marplesornis novazealandiae*, *Eretiscus tonnii* and *Dege hendeyi*. Both *Waimanu manneringi* and *tuatahi* occupy a basal position to all Sphenisciformes in

Ksepka and Clarke (2010), as sister-taxa to the Procellariiformes clade. This result is similarly found in primary and Bayesian analyses of this study, where *Waimanu* is recovered as basal to all other Spheniscidae—with the exception of the novel taxon *A. stilwelli*.

Phylogenies published in Ksepka et al. (2012) are in general agreement with the strict consensus trees produced for this study, using the modified dataset of Ksepka et al. (2012). Overall, using the Ksepka et al. (2012) datasets appear to have allowed higher resolution of phylogenies in this study than compared to the phylogenies recovered using the Ksepka and Clarke (2010) datasets. In comparison to the published phylogenies in Ksepka et al. (2012), taxon grouping consistent with the Spheniscidae clade as published in Ksepka and Clarke (2010) is recorded, and are recovered similarly in both Bayesian and primary analyses of the Ksepka et al. (2012) datasets used for this study, with variable exact taxon placement within this clade. Less resolution is observed in the positioning of several fossil taxa recovered in strict consensus trees from the primary analysis compared to the published material, including the placement of *Waimanu manneringi*, *W. tuatahi*, *Marambiornis exilis*, *Mesetaornis polaris*, *Delphinornis larseni*, *D. arctowskii*, and *D. wimani*. Despite this, these fossil taxa are consistently basal relative to all other Spheniscidae throughout the published phylogenies in Ksepka et al. (2012), and also those of this study using the data from Ksepka et al. (2012). In contrast to the primary analysis, while fossil taxa occupy basal positions relative to those that are included within Spheniscidae (as per Ksepka and Clarke, 2010), the phylogeny from the Bayesian analysis of the modified Ksepka et al. (2012) dataset additionally recovers a similar placement and a greater resolution of fossil taxa compared to that of the published material, described as follows: Specifically, *Waimanu* is recovered as a paraphyletic group, where *Waimanu manneringi* is positioned ancestral to *W. tautahi*—which itself is basal to all other Spheniscidae. *Mesetaornis polaris* and *Marambiornis exilis* are recovered as a monophyletic clade immediately crownward of *Waimanu*. Similar to the published results of Ksepka et al. (2012), all three *Anthropornis* species are grouped monophyletically, however *Anthropornis grandis* is recovered in a more basal position than the two other species. Further resolution is displayed where *Palaeeudyptes* spp. occupy a paraphyletic position within the stem portion of this Bayesian tree, and Burnside "*Palaeeudyptes*" is nested with *Inkayacu paracasensis*, crownward relative to all other *Palaeuudyptes* taxa. Furthermore, crownward of the monophyletic *Kairuku* clade, *Pachydyptes ponderosus* and *Icadyptes salasi* are recovered together monophyletically, and

are positioned as the sister-taxon group to *Delphiornis*—which are presented paraphyletically. The Bayesian analysis of the modified Ksepka et al. (2012) dataset also describes *Archaeospheniscus lowei*, *Archaeospheniscus lowei* and *Duntroonornis parvis* as a monophyletic group, and as sister-taxon to *Paraptenodytes antarcticus*, crownward relative to *Delphiornis*. Like the published phylogeny of Ksepka et al. (2012), *Platydyptes* are recovered as a monophyletic clade, and is basal to *Eretiscus tonnii* and *Palaeospheniscus.* In contrast to published phylogeny however, the Bayesian analysis recovers *Palaeospheniscus* as a paraphyletic group, crownward of *Eretiscus tonnii*.

Despite the variance in crownward Sphenisciformes and fossil penguins, the basal positioning of *Waimanu* is constant in all primary and Bayesian analyses performed in this study, indicating that this consistently basal positioning recovered in the analyses of this study is well supported. Furthermore, all phylogenetic analyses performed in ***Chapter IV: Analyses*** support the placement of *Archaeodyptes stilwelli* within the Sphenisciformes clade, notably as a basal taxon, with either a basal or sister-taxon relationship to *Waimanu*. This is found in all primary and Bayesian analyses using the Ksepka and Clarke (2010) datasets, which specifically placed *Archaeodyptes stilwelli* in a basal position relative to *Waimanu* and all other penguin taxa, living and extinct. In comparison, using the datasets from Ksepka et al. (2012), *Archaeodyptes stilwelli* similarly occupied this same basal position in Sphenisciformes, and additionally existed as a sister-taxon to other contemporary stem penguin taxa including *Waimanu manneringi*, *Waimanu tuatahi*, *Marambiornis exilis*, *Mesetaorrnis polaris*, and all *Delphinornis* species; a single node basal relative to *Perudyptes devriesi.* Bayesian analysis, however, using the Ksepka et al. (2012) dataset yielded results which placed *Archaeodyptes stilwelli* as basal to all other known Sphenisciformes, including *Waimanu* and other stem penguin taxa—identical the position recovered using Ksepka and Clarke (2010) datasets.

An identical relationship was recovered between *Archaeodyptes stilwelli*, Procellariiformes and Gaviidae throughout all analyses performed over all datasets; where *Archaeodyptes stilwelli* was recovered a sister taxon to the Procellariiformes clade and crownward to Gaviidae. Therefore, in all analyses regardless of dataset and analysis used, *Archaeodyptes stilwelli* has been recovered as a basal taxon of the Sphenisciformes clade, immediately crownward of Gaviidae, and as a sister-taxon to the Procellariiformes clade. The predominately consistent placement of clades and inclusive taxa, over both Ksepka and Clarke (2010) and Ksepka et al. (2012) datasets, used in comparison with one

another, using the same methodology, thus gives an indication of general consistency and accuracy of the datasets. Furthermore, this consistency provides a more robust and effectively accurate phylogenetic placement of *Archaeodyptes stilwelli*.

5.2.1 Phylogenetic Placement Based on Comparative Study

The morphology of cervical system in the neck of seabirds is highly specialised, based on their specific interaction with the aquatic environment (Guinard et al., 2010). Thus the nature of the cervical vertebra between aquatic taxa in the Aequorlitornithes clade maybe indicative of species specialisation, and may correlate with evolutionary trends.

The PCA scatterplot (Figure 4.5) compares the measurements of cervical vertebra IV across taxa of different lineages within Auquorlitornithes to that of JDS8341.b. Based on PCA loadings (Figure 4.6), the inter- and intraspecific variation observed in the PCA is controlled by the front and back widths of cervical vertebra IV, and clusters specimens accordingly with vertebra of similar measurements in closer proximity. JDS8341.b is plotted between that of the procellariiform *Diomedea exulans* and various penguin taxa including *Aptenodytes patagonicus*, *Aptenodytes forsteri*, and *Waimanu tuatahi*. The plots associated with *Diomedea exulans* are in close proximity to those associated with penguins, distinctly separate from plots associated with other Procellariiformes. Visually, the shape of the vertebra from JDS8341.b is very similar to the same vertebra from the extant *Diomedea exulans*, which supports the close proximity between their plots, and indicates a close relationship in cervical IV vertebra shape. In addition, the plot of JDS8341.b is surrounded by plots from various Sphenisciformes, and gives evidence of placement within this clade. The plot associated with *Waimanu tuatahi* is most closely placed to plots of *Diomedea exulans* and JDS8341.b, rather than those from extant penguins. This similarity in vertebra measurements gives evidence of a close relationship between the Procellariiformes and basal penguin taxa—and given that *Archaeodyptes stilwelli* is found as a basal or sister-taxon to *Waimanu*, this plot placement further supports the sister-taxon phylogenetic relationship of *Archaeodyptes stilwelli* relative to Procellariiformes. Consequently, the variation in plots observed through the PCA correlate with the placement of *Archaeodyptes stilwelli* in phylogenetic analyses performed, and are consistent with a basal Sphenisciform placement of JDS8341.b.

While this result is based on the measurements of a single vertebra, in the event of further discoveries, similar analyses based on other cervical vertebra and other elements highly influenced by the aquatic environment may provide a more robust comparison. Furthermore, this analysis is subject to a small sample size and hence a lack of genetic variation. It should also be noted that due to diagenesis both fossil elements may have been susceptible to distortion. Considering that the plots of *Waimanu tuatahi* and JDS8341.b are each based on single specimens, subsequent discoveries and measurements may expand the range of plots observed, and give more robust evidence of relationships among taxa in this regard. However, using the information currently available, a relationship consistent with phylogenetic analyses is supported.

As per the phylogenetic results of this study, in conjunction with comparative analyses performed, it can be considered robust that *Archaeodyptes stilwelli* belongs to the Sphenisciformes clade, particularly crown + stem penguins sensu Clarke et al. (2003). A basal placement of *Archaeodyptes stilwelli* is well supported from all phylogenetic analyses, as basal to all currently known Sphenisciformes, and/or as a sister-taxon to Procellariiformes and *Waimanu*.

5.2.1.1 Genus Assignment of stilwelli

Throughout phylogenetic simulations, *Archaeodyptes stilwelli* is consistently found with a close relationship to *Waimanu*, which poses the question; is *Archaeodyptes stilwelli* better assigned as a previously described species of *Waimanu*, or more appropriately placed within the *Waimanu* genus? Indeed, visually the radii associated with *Waimanu* compared to the radius from JDS8344 are almost identical (Figure 5.2).

Comparison of the shape of the radius between *Waimanu tuatahi* and *Archaeodyptes stilwelli* was carried out through performing a multivariate PCA (Figure 4.7). The results from the PCA showed that the variation in shape observed between the radii was primarily controlled by the proximal width of the radii, and also the proximal depth and mid-shaft depth to a lesser extent. The PCA scatterplot diagram that compared the principal component associated with these variables (PC1) with the principal component predominately associated with radius length (PC2) showed a large separation in plots between *Waimanu* radii and that of JDS8344 (Figure 4.7A). This separation indicates that the based predominately on those variables, there is a large differentiation in radii shape between those belonging to *Waimanu tuatahi*, compared to that associated with *Archaeodyptes*

stilwelli. However, the radius preserved in JDS8344 was only partially preserved and the length could not be measured, meaning that the missing length measurement data was replaced with the average of observed values for the length variable, as a function of mean substitution in PAST (Hammer, 2001). Mean substitution may accurately replace the missing data, but at the cost of distorting estimated correlations and variances (Schafer and Graham, 2002). Furthermore, mean substitution means that the averaged value cannot be evaluated outside the analysis it is embedded in (Schafer and Graham, 2002). Even though radius length described less than 8% of total variation, considering that the only one radius was available for study associated with *Archaeodyptes stilwelli*, column average substitution may not accurately and reliably represent the actual length of the radius when it was complete. Hence, the scatterplot shown in Figure 4.7A can only give inference of separation when the length of the radius of JDS8344 is assumed to be similar to that of *Waimanu tuatahi*—which considering the visual similarities in shape, may not be unrealistic. Consequently, however, without assuming the length of the radius of JDS8344, separation and thus shape difference observed in Figure 4.7A alone cannot be confidently relied upon.

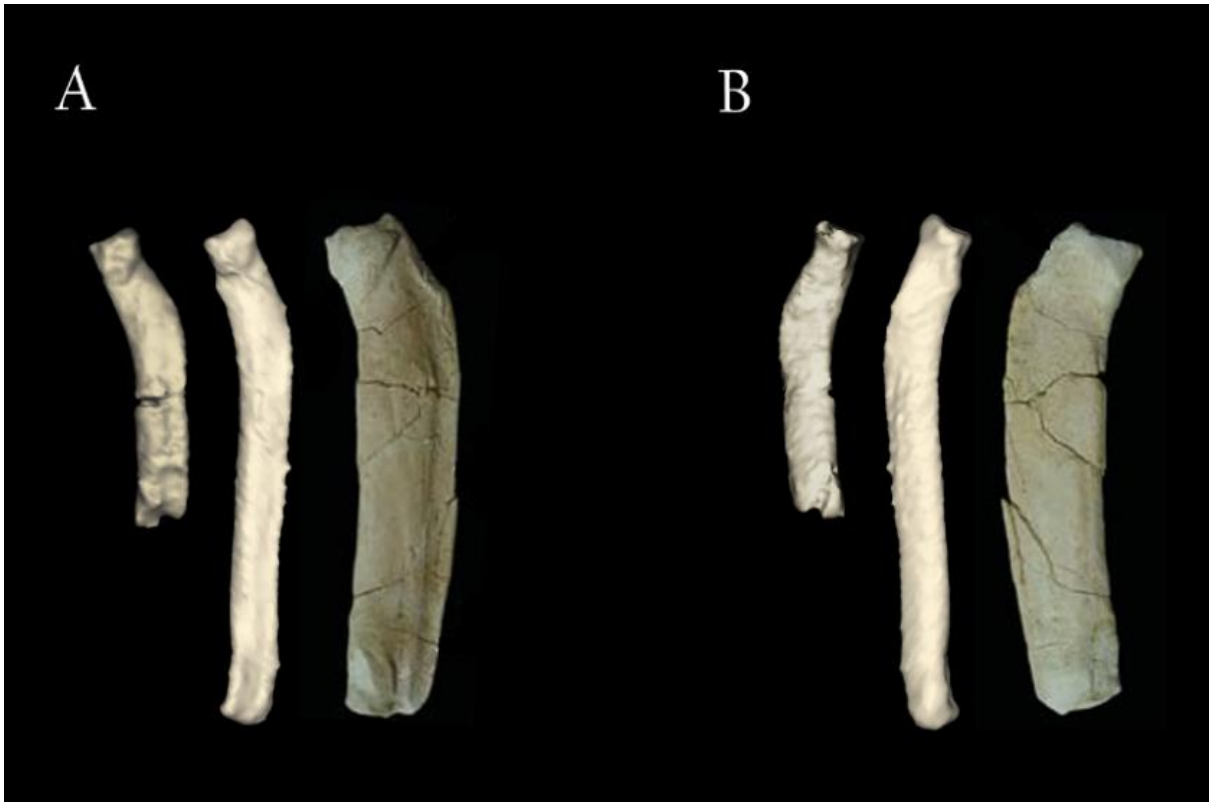

Figure 5.2: Comparison of radius shape in dorsal (A) and ventral (B) aspects. Left to right: *Archaeodyptes stilwelli* (JDS8344), *Waimanu tuatahi* (2009.99.1) and *Icadyptes salasi* (MUSM 897) (Ksepka et al., 2008). Not to scale.

PC3 describes almost 5% of total variance, and is predominately associated with distance from the proximal humeral facet to the bend in the radius, and mid-shaft width. In contrast to the results of PC1 and PC2, when PC1 was plotted against PC3, separation between the radii of *Waimanu* and that of JDS8344 is observed to a much lesser extent, to the degree where the radii irrespective of taxon are clustered together (Figure 4.7B). Since the distance to bend and mid-shaft depth were real measured values, this separation observed can be considered accurate and reliable, meaning a similarity in radii shape between *Waimanu* and *Archaeodyptes stilwelli* is supported.

As a result of these analyses, the shape of radii between *Waimanu tuatahi* and *Archaeodyptes stilwelli* can be considered as not dissimilar, and is further supported by their visual similarity (Figure 5.2).

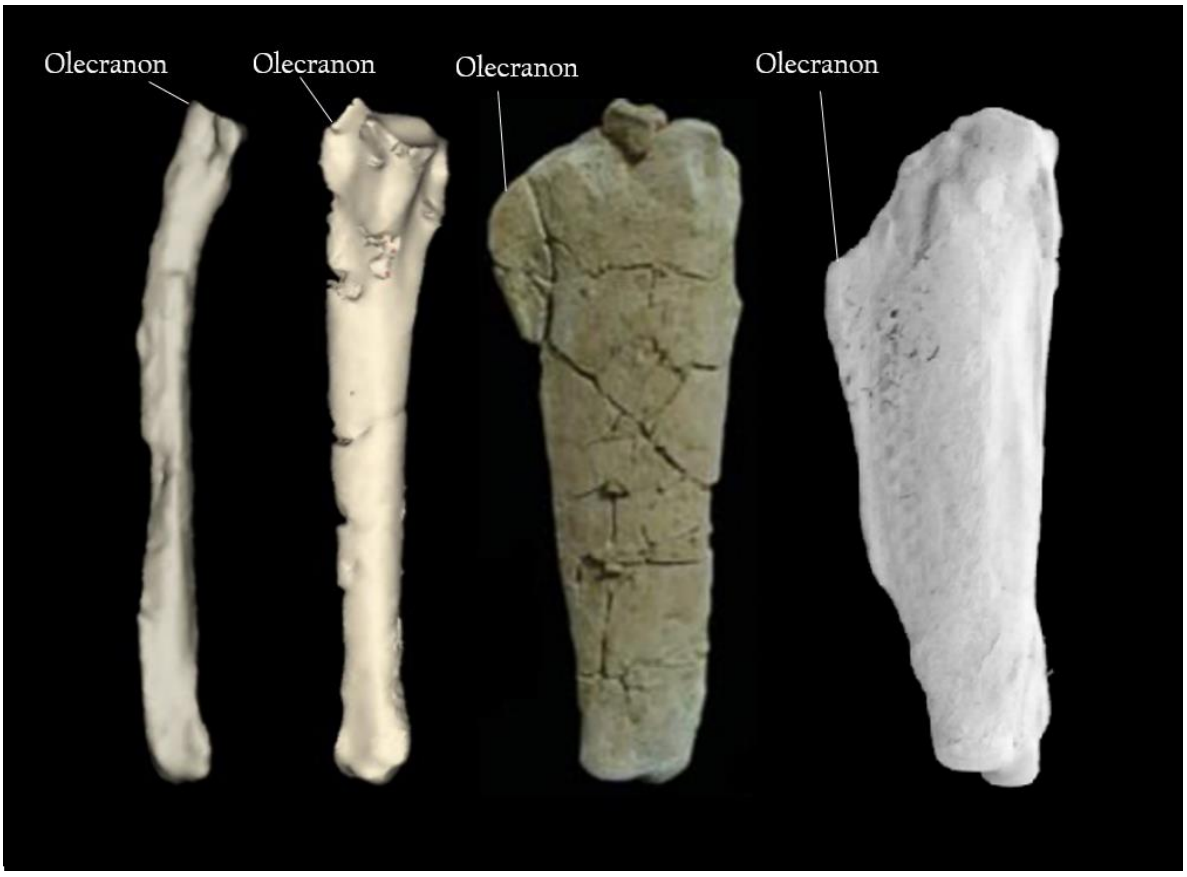

Figure 5.3: Comparison of ulna shape in dorsal aspect. Left to right: *Archaeodyptes stilwelli* (JDS8344), Palaeocene *Waimanu tuatahi* (2010.108.3), Eocene *Icadyptes salasi* (MUSM 897) (Ksepka et al., 2008), and extant *Spheniscus demersus* (NSM 6294). Not to scale.

In contrast, the comparison of ulnae between *Waimanu tuatahi* and *Archaeodyptes stilwelli* in the same PCA (Figure 4.7A and B) are not in correlation with the similarities between radii. Regardless of whether PC2 (Figure 4.7A) or PC3 (Figure 4.7B) was paired with PC1, the ulna of JDS8344 can be

observed as significantly separate from respective clusters associated with *Waimanu* ulnae. The PCA analyses therefore support a dissimilarity in shape between the ulnae of *Waimanu tuatahi* and *Archaeodyptes stilwelli*. A distinct difference in shape between the two taxa can also be observed when visually comparing the element from each respective taxon. In *Waimanu tuatahi*, the ulna is notably wider at the proximal facet and at the mid-shaft, when viewed in dorsal and ventral aspects, compared to the ulna associated with *Archaeodyptes stilwelli* (Figure 5.3). The olecranon is distinctly different between the two taxa; the apex of the olecranon in *Waimanu tuatahi* exists as a tab-like projection level with the proximal facet, while the olecranon in *Archaeodyptes stilwelli* is rises proximally as an acute projection from the proximal facet with the humerus. Additionally, the ulna in *Waimanu tuatahi* is straight and broad proximally, and has a ridged anterior proximal margin (Slack et al., 2006), whereas the ulna of *Archaeodyptes stilwelli* is proximally curved and is rounded along the anterior and posterior proximal margins. The ulna of both taxa are similar however in that neither are widened distally, and the size of the ulnae in both birds suggest that the wing was short relative to body size—unlike that of solely volant birds. Wide and flattened bones are often associated with penguins, and other wing-propelled divers; specialised morphology that can be observed at the proximal end of the ulnae of *Waimanu* (Slack et al., 2006), to a greater extent in the Eocene *Icadyptes salasi* (Ksepka et al., 2008), and are specialised even further in extant penguins (Figure 5.3). In contrast the ulna of *Archaeodyptes stilwelli*—while flattened to some extent—does not display widening morphologies that are diagnostic of the specialised wing-propelled nature of penguins. Hence, the ulna of *Archaeodyptes stilwelli* is characteristic of more primitive features than that of previously known penguins, and shares relatively greater similarity in shape with the ulna of volant birds in comparison.

The other forewing element of JDS8344 of particular interest that is available for comparison with *Waimanu tuatahi* is the carpometacapus. The proximal portion of the carpometacarpus was not preserved, and hence is not available for comparison, however, similar to the comparison between radii, the extent of carpometacarpus preserved in *Archaeodyptes stilwelli* shows almost identical visual similarities with the carpometacarpus of *Waimanu tuatahi*. Like in other forewing elements, extant penguin carpometacarpi exhibit a specialised flattened and widened morphology. In *Waimanu* and *Archaeodyptes stilwelli*, both taxa show subtle flattening on the dorsal and ventral surfaces of the

carpometacarpus, but the elements are relatively more ovoid in cross-section dorsoventrally compared to other penguins, and do not display such an extent specialised flattened and widened morphology (Figure 5.4). Like with the ulna and radius, the flattening and widening observed in extant and stem penguins is an adaption for propelling the penguin through the water in their diving habitat, characteristics that evolved gradually to the extent observed in crown group penguins (Mayr, 2016). Similarly, this can be further illustrated by the presence of a long and ovoid *spatium intermetacarpale* between metacarpals II and III in dorsal and ventral aspects, which in comparison to extant penguins, and even the Eocene *Icadyptes salasi*, is much reduced through widening of the metacarpals (Figure 5.4).

Figure 5.4 (left): Comparison of carpometacarpus shape in dorsal aspect. Top to bottom: *Archaeodyptes stilwelli* (JDS8344), Palaeocene *Waimanu tuatahi* (2009.99.1) Eocene *Icadyptes salasi* (MUSM 897) (Ksepka et al., 2008), and extant *Aptenodytes forsteri* (AMNH 8110). Not to scale.

Figure 5.5 (next page): Comparison of coracoid shapes in ventral aspect. Left to right: extant *Oceanodroma leucorhoa* (USNM 614217; Smithsonian Bird Collections), *Archaeodyptes stilwelli* (JDS8341.b), Palaeocene *Waimanu tuatahi* (CM zfa 34) Eocene *Palaeeudyptes klekowski* (MLP 12-1-20-289) (Hospitaleche, 2016), Oligocene *Archaeospheniscus lowei* (OM GL407), and extant *Aptenodytes forsteri* (AMNH 3767). Not to scale.

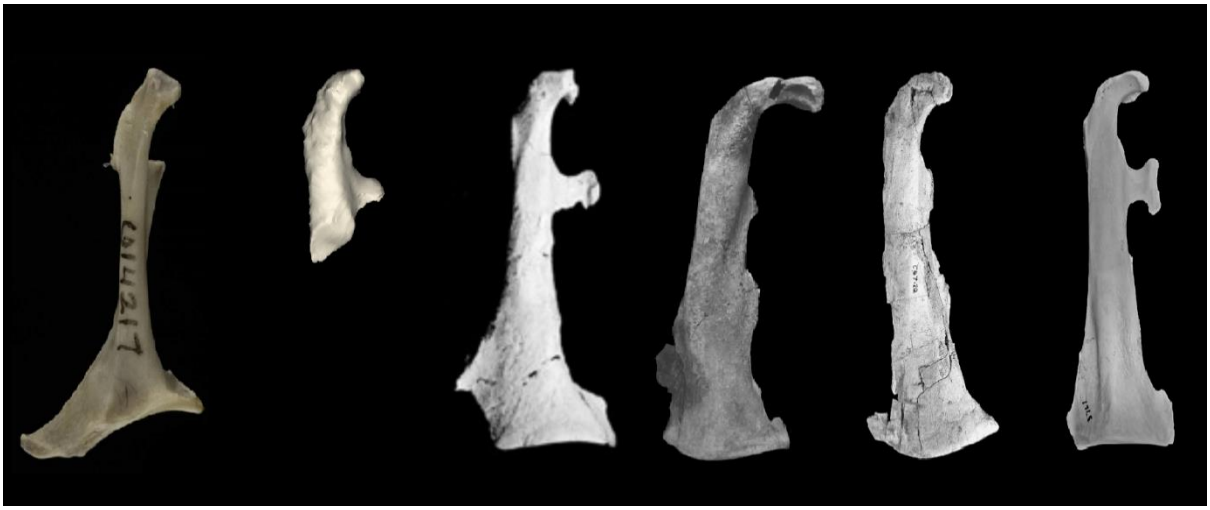

Coracoids are some of the most frequently discovered avian fossils, and thus are important for comparative relationships between fossil birds (Elzanowski et al., 2012). Visually, what is preserved of the coracoid in JDS8341.b is similar to the coracoid present in *Waimanu tuatahi* (Figure 5.5). Notably in ventral aspect, the omal portion of each element and the curvature of the coracoidal fenestra is alike, albeit more concave nearer the procoracoid process in *Waimanu tuatahi*. A difference can be observed in the concavity of the *facies articularis humeralis*, where more pronounced facet is present in *Waimanu tuatahi* compared to JDS8341.b.

A variable characteristic among Sphenisciformes is the degree of curvature in the omal end of the coracoid, particularly the region associated with the *facies articularis clavicularis* and *processus acrocoracoideus*. In JDS8341.b the omal portion of the coracoid including the *facies articularis clavicularis* and *processus acrocoracoideus* does not display "hooked" curvature, and shows a curvature in ventral and dorsal aspects more similar to Oligocene Procellariiformes (Elzanowski et al., 2012), and the extant *Oceanodroma leucorhoa* and *Thalassarche cauta*, rather than the majority of Sphenisciformes—including *Waimanu tuatahi*. Comparison of coracoids from both extant and Oligocene Procellariiformes indicated that the specific anatomy of the acrocoracoid process was variable to the degree of describing genus-level diversity among Procellariiformes, and that an allometric trend for deeper (more dorsoventrally elongate) coracoid heads displaying stronger curvature of the acrocoracoid process (and thus ventral head projection) correlated with larger species of petrels, but not albatrosses (Elzanowski et al., 2012). Thus, for some Procellariiformes, a dorsoventrally orientated "hooked" shape related to the acrocoracoid process may be related to larger body size. Similarly, the omal portion of the coracoid in the giant Eocene penguin *Palaeeudyptes klekowskii* is distinctly hook-like (Hospitaleche, 2016)

compared to other, smaller Sphenisciformes (Figure 5.5). The acrocoracoid process in *Waimanu tuatahi*, in contrast, shows more anatomical similarities with *Aptenodytes forsteri*. Apart from the apparent shape of the acrocoracoid process, the shape of the omal end in JDS8341.b is otherwise comparable to the shape of the omal portion of the coracoid in *Waimanu tuatahi*. Furthermore, the lack of hook-like acrocoracoid process in JDS8341.b may be explained as a product of erosion. The shape of the *facies articularis scapularis* in JDS8341.b is rounded in dorsal and ventral aspects, and the procoracoid process also shorter in medial extent compared to *Waimanu tuatahi*. However, similar to the acrocoracoid process, erosion may have obscured the true nature of the procoracoid process and its specific anatomy. Consequently, the coracoid of JDS8341.b, associated with *Archaeodyptes stilwelli*, displays notable differences in morphology to other Sphenisciformes, but also shares similarities with the coracoid anatomy of both *Waimanu tuatahi* and Procellariiformes. Further material is required however, in order to make a more conclusive statement.

Based on the PCA comparison between cervical vertebra IV among Auquorlitornithes (Figure 4.5) the cervical vertebra IV in JDS8341.b is distinctly different compared to *Waimanu tuatahi*. However, other studies using PCAs have found that when comparing common elements between and within taxa, size is a more accurate descriptor of plot placement than element shape. PCA and univariate analyses performed on numerous Procellariiform coracoids found that when comparing shape, measurements were heavily size dependent, meaning other shape characters and proportions had very little use as phylogenetic markers (Elzanowski et al., 2012). Similarly, Cracraft (1976), in the comparison of size-shape patterns within and between the hindlimbs of moa species, also showed in multivariate analyses that size was the major discriminator overall across and within species, more so than shape (Cracraft, 1976). Hence the difference in plot placement between *Waimanu* and JDS8341.b may largely be a result of vertebra size, rather than a distinct difference in shape between the two. This however, only provides evidence that *Archaeodyptes stilwelli* was smaller than *Waimanu tuatahi*. Regardless, it should be noted that the plots of both taxa in the scatterplot were each based on measurements of a single specimen, and a comparative analysis using a larger sample size may yield more accurate results.

Comparison between skeletal elements between associated material of *Waimanu tuatahi* and *Archaeodyptes stilwelli* reveals numerous similarities in skeletal anatomy, but also several key

differences that distinguish one from the other. Notably, the difference in ulna and perhaps coracoid morphology suggests that *Archaeodyptes stilwelli* differed from *Waimanu tuatahi* in numerous plesiomorphic features, and is characteristic of a more primitive penguin. Nevertheless, *Archaeodyptes stilwelli* possesses many apomorphic features shared with the known material of *Waimanu*, unique to other Sphenisciformes. Effectively, this comparison shows similarities and minor degrees in change among these early stem penguins, consistent with a gradual evolution of traits towards the skeletal characteristics of crown group Sphenisciformes. In conclusion, the assignment of *Archaeodyptes stilwelli* as a separate taxon from *Waimanu* is well justified.

5.3 What was Archaeodyptes stilwelli*? (Palaeobiology)*

While exhibiting the dorsoventrally flattened shape of forewing elements, a synapomorphy among Sphenisciformes, *Archaeodyptes stilwelli* is especially distinguished from other penguins by the presence several plesiomorphic features. Of particular note, *Archaeodyptes stilwelli* possesses a narrow radius and ulna shaft, and is further unique in that the olecranon and posterior border of the ulna arises as an acute rounded projection from the humeral facet. In addition, the morphology of the acrocoracoid neck of the omal coracoid displays a curvature more similar to Procellariiformes than other stem or crown Sphenisciformes. Based on the two associated partial skeletons of this taxon, an interpretation of its palaeobiology is discussed as follows.

The forewing elements preserved of *Archaeodyptes stilwelli* include (Figure 5.6) a left carpometacarpus, a right ulna, the proximal half of a right radius, a right proximal phalanx of the second digit, and a right phalanx of the third digit—skeletal elements that were integral to the function and behaviour of the animal in its ecological niche. Modern penguins are known for having a very specialised apparatus evolved for "underwater flight" (Bannasch, 1994; Ksepka and Ando, 2011); and the highly flattened and shortened morphology of their forewing is a notable example. Of note,

the dorsoventrally flattened nature of the forewing elements possessed by *Archaeodyptes stilwelli* is considered a synapomorphy shared with the rest of the Sphenisciformes clade.

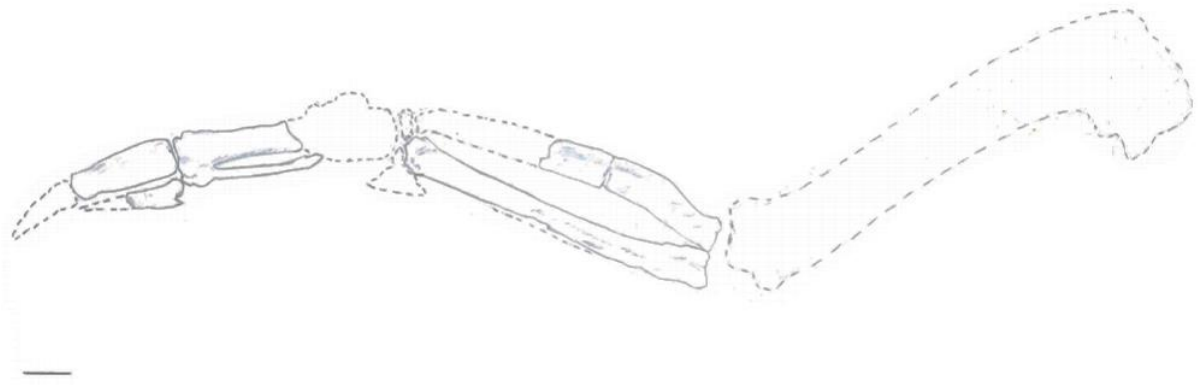

Figure 5.6: The forewing of *Archaeodyptes stilwelli*. Dotted lines represent elements or parts of elements not available for study. Humerus shape and proportion in relation to other elements is based on *Waimanu tuatahi.* Scale line is 1 cm. Original art by Jacob Blokland.

As modern penguins "fly" through the water—approximately 800 times greater density than air at sea level—the flipper remains stiff (Ksepka and Ando, 2011), to increase thrust generation efficiency in both upstroke and downstroke movements (Clark and Bemis, 1979; Ksepka and Ando, 2011). In contrast, volant birds typically fold their wings during the upstroke, and only produce thrust during the downstroke (Ksepka and Ando, 2011). The ulnar condyle in extant penguins exists as an almost flat articular surface, where the forewing elements are bound together by various ligaments, which results in a greatly reduced range of motion at the joints, incompatible with aerial flight, but greater efficiency for underwater flight (Ksepka and Ando, 2011). In contrast, basal penguins, including *Archaeodyptes stilwelli*, have a prominent subhemispherical ulnar condyle, to allow a greater range of motion between the humerus and the rest of the wing (Ksepka and Ando, 2011). Reduction of this ulnar condyle may have limited movement between the forewing and the humerus during the upstroke, producing greater underwater flight efficiency (Ksepka and Ando, 2011). Additionally, many fossil penguin taxa also have evolved a large shelf dorsal to the ulnar condyle, that may have further stiffened the joint movement during the downstroke—part of a gradual evolution to the morphology of modern penguins (Ksepka and Ando, 2011). Extensive flattening (and a more elliptical cross-section) in long bones such as the radius, ulna and humerus, has been hypothesised to

be associated with increased hydrodynamic efficiency, but less resistance to shear forces (Ksepka et al., 2006). However, while flattened, the forewing elements associated with *Archaeodyptes stilwelli* are neither as comparably wide in medial extent, nor as dorsoventrally flattened as those of extant penguins. Instead, while dorsoventrally flattened to a degree, a sub-ovoid shape in cross-section is also observed in the forewing elements of *Archaeodyptes stilwelli*—similar to modern auks (Alcidae). As wing-propelled diving seabirds, auks are not as adapted for swimming as penguins, but also use their wings in a flapping motion to propel themselves through the water (Pennycuick, 1987). However, where penguins use both upstroke and downstroke for thrust (Clark and Bemis, 1979), auks only use the downstroke for propulsion (Raikow et al., 1988), with wrist and elbow joints of the wing rigid (Pennycuick, 1987), and also partly folded (Raikow et al., 1988). Diving petrels (Procellariidae), also use their wings to swim in a similar motion to auks through pursuit diving, as an example of convergent behaviour (Pennycuick, 1987). The morphology of *Waimanu* is regarded as one of the earliest stages in the evolution of Sphenisciformes following the loss of aerial flight (Ksepka and Ando, 2011), and is closely related to *Archaeodyptes stilwelli* compared to other Sphenisciformes, as designated through phylogenetic analyses. In the skeletal elements of *Waimanu tuatahi*, shortened wing elements are observed compared to flying birds, indicating a high wing loading, yet the wing is proportionally longer than that of modern penguins (Ksepka and Ando, 2011; Slack et al., 2006). Particularly, the humerus is comparatively longer than the ulna and radius length, and is also more flattened in the dorsoventral dimension—but is not as flattened as the humerus of modern penguins (Ksepka and Ando, 2011; Slack et al., 2006). Flattened humeri in penguins may be an indication of being more resistant to torsion than the humeri in typical birds, where flattened morphology allows the capacity to twist to a certain degree without breaking (Kaiser, 2007; Ksepka and Ando, 2011). Unfortunately, since a humerus was not preserved in either specimen associated with *Archaeodyptes stilwelli*, the extent of flattening in the particular element is unknown, and thus a further detailed biological function of the animal's entire wing cannot be properly ascertained.

A free alular phalanx is assumed to have been present in basal Sphenisciformes, as based on the shape of the carpometacarpus in both *Waimanu* and *Icadyptes*, before gradually becoming assimilated into the widened and flattened carpometacarpus of crown penguin taxa (Ksepka and Ando, 2011). As previously mentioned, and shown in Figure 5.4, the extent of the carpometacarpus recovered of *Archaeodyptes stilwelli* is visually similar to that of *Waimanu tuatahi*, and while no proximal

portion of the carpometacarpus, nor a free alular phalanx was recovered of *Archaeodyptes stilwelli*, it is hypothesised this taxon also shared similar morphology to *Waimanu tuatahi* in this regard. While both *Waimanu* and *Icadyptes* both have an articular facet for the alular phalanx (Ksepka et al., 2008; Slack et al., 2006), because an alular phalanx has yet to be recovered from basal penguin taxa, the palaeobiological function of this element in such taxa is unknown (Ksepka and Ando, 2011). However, a rare circumstance amongst fossil penguins (Ksepka and Ando, 2011), the manus phalanx of the second (phalanx II-1) and third digit (phalanx III-1) of *Archaeodyptes stilwelli* have been recovered. While both of these digits are relatively unspecialised in modern birds (Ksepka and Ando, 2011; Ksepka et al., 2008), phalanx III-1 of *Archaeodyptes stilwelli* possesses a proximal tubercle similar to extant penguins. This is in contrast with the fossil penguin *Icadyptes salasi*, which does not possess a proximal tubercle in digit III-1, (Ksepka et al., 2008), correlating with the animal having a higher aspect ratio compared to modern penguins, which was thus assumed to be reflective of more primitive proportions (Ksepka and Ando, 2011). The mid-wing of *Archaeodyptes stilwelli* therefore may have had a lower aspect ratio in the mid-wing compared to *Icadyptes salasi.* Because the recovered material of digit III-1 is incomplete, it is not known if the element's length exceeded that of digit II-1, as it does in modern penguins, or if it was shorter, like in *Icadyptes salasi* and typical volant birds (Ksepka et al., 2008). It is therefore unknown whether the wing-tip of *Archaeodyptes stilwelli* had a more tapered shape like *Icadyptes* (Ksepka et al., 2008), or was more similar to extant penguins in this regard.

The coracoids are a key element in the locomotion of penguins in underwater flight (Hospitaleche, 2016). In general, acrocoracoid processes of the coracoid are longer in penguins compared to volant birds, and also display an increased ventromedial curvature that forms the *facies articularis clavicularis* (Hospitaleche and Di Carlo, 2010). The coracoid recovered of *Archaeodyptes stilwelli* shows reduced ventromedial and dorsoventral curvature associated with acrocoracoid head of the coracoid, and the *facies articularis clavicularis*, compared with the coracoid shape of other Spheniscifomes—baring closest resemblance to *Waimanu*, or Procellariiformes (see section ***5.2.1.1 Genus Assignment of* stilwelli**). A shallow curvature in the dorsoventral dimension of the acrocoracoid head, as possessed by *Archaeodyptes stilwelli*, is a feature correlated with smaller taxa in Procellariiformes (Elzanowski et al., 2012), a trend that may also be observed when comparing the

coracoids of larger Sphenisciformes (i.e. *Palaeeudyptes klekowskii*) to smaller forms (Figure 5.4). This may suggest that *Archaeodyptes stilwelli* had a flight locomotion and behaviour more similar to volant birds and/or *Waimanu* than other Sphenisciformes. However, because only the omal portion of a coracoid was recovered, a more detailed account of possible kinematics associated with *Archaeodyptes stilwelli* cannot be reliably made. *Waimanu*, which has a coracoid that is consistent with that of other wing-propelled divers (Slack et al., 2006), shares visual similarities with the coracoid portion preserved, is closely related cladistically, and possesses an elongate coracoid compared to volant taxa (Ksepka and Ando, 2011), but not as elongate as all other penguins (Ksepka, 2007). Increased elongation in the coracoids displaces the triosseal canal relative to the sternum, which in turn increases space for the pectoralis muscles, and leverage for the major muscle (*muscularis supracoracoideus*) for the upbeat of the wing (Bannasch, 1994). Additionally, *Waimanu* lacks the specialised hyper-elongate features, which are related with increased downstroke underwater flight efficiency displayed in other Sphenisciformes (Ksepka, 2007). It may be hypothesised therefore, that *Archaeodyptes stilwelli*, as basal to *Waimanu*, may have also been similar or even more primitive in this regard.

The furcula is also an important element related to locomotion of birds (Hospitaleche and Di Carlo, 2010), and varies significantly between different avian taxa. The shape of the furcula is characterised by two fused clavicles (Baumel and winter 1993), the extent of anterior curvature of which affects flight locomotion (Hui, 2002). As clavicles among taxa vary between straight and anteriorly curved, the force vector applied to the wing from the anterior sternobrachialis also varies; Specifically, in an anteroventrally curved furcula, outwards from the sagittal plane, the protraction force is increased, through where the anterior sternobrachialis pulls on the humerus (Hui, 2002). Conversely, a laterally or posteriorly curved furcula will either have no effect or decreases protraction force of the wing (Hui, 2002). Hui (2002), compared furcula over avian eight different orders, and found that furcular shape affected furcular function, where taxa with similar flight behaviours possessed a similar furcular morphology. The furcula in penguins was found to be distinctly "V"-shaped, a trait shared with other aquatic fliers such as the great auks, specific to birds incapable of aerial locomotion. This trend also can be observed in the "V" shape furcula of stem penguins like *Waimanu* (Slack et al., 2006). In contrast, aerial based birds were found to have a shallow "U" shaped furcula, while birds that used their wings for locomotion in both water and air such as alcids and

storm petrels had furcula shapes more "U" shaped than solely aquatic birds, but more "V" shaped than air-based avifauna. The greater density of water produces significantly more profile drag on the wing compared to moving at the same speed in an air medium, thus meaning a greater protraction force is required to actively move the wings through the aquatic environment (Hui, 2002). The pronounced "V" shape, greater anterior curving—and hence greater protraction force capable—displayed in aquatic birds such as penguins can be associated with accommodation for profile drag of the wing in the aquatic environment (Hui, 2002). Compared to modern penguins, the furcula shape of *Archaeodyptes stilwelli*, while incomplete, appears to be less "V" shaped, and rather "U" shaped (Figure 3.17), but not as shallow in anterior curvature compared to soaring birds such as albatrosses. Considering Hui (2002) found that less able aerial fliers appeared to have more anterior curvature of the furcula, this may suggest that the furcula of *Archaeodyptes stilwelli* was not well adapted for subaqueous flight, but also that it wasn't specialised for soaring either. The shape of the partial furcula of *Archaeodyptes stilwelli* is therefore consistent with birds that utilise both the aquatic and aerial environment, such as diving petrels (Procellariidae) which use their wings aerially, but also in submerged propulsion when diving (Navarro et al., 2014) and flying through waves (Hui, 2002).

In three-dimensional manipulation of the fossil specimens of *Archaeodyptes stilwelli*, resolution was not sufficient to determine whether the bones were largely pneumatic as they are in volant birds, an adaptation to reduce the metabolic cost of flight (Dumont, 2010), or dense as they are in modern penguins as an adaptation to counteract buoyancy (Meister, 1962). However, through three-dimensional manipulation, using *Materialise Mimics*, a reduced marrow cavity is observed (Figure 5.7). Compared to volant birds, penguins have a more robust bone structure due to reduction of the marrow cavity, which also results in bones that are more likely to withstand pre-burial damage through wave action or biotic influence (Ksepka and Ando, 2011). This, combined with a near-shore and aquatic habitat shared among penguin species, increases the preservation potential of such bones (Ksepka and Ando, 2011), and may also explain the preservation of the bones associated with *Archaeodyptes stilwelli*. The fossils exposed at the surface also appear to be porous or show pneumatic foramina (Figure 3.1), however further microscopic histological study may shed more light on whether these bones more resemble that of aquatic or volant birds. Additionally, the partial sternum preserved of *Archaeodyptes stilwelli* appears to have preserved a pneumatic foramen, typical of avifauna that utilize the aerial environment. However, because the sternum is incomplete, the true nature of

how pneumatic the sternum really was, whether it is extremely pneumatized as in albatrosses, or partially pneumatized as it is in gulls and related taxa (Soldaat, 2009), is unknown—if indeed the foramen was of a pneumatic nature. Because lack of pneumaticity and denser bones is correlated with an increase in diving ability (Schorger, 1947), the density of the bones is directly related to the lifestyle and behaviour of *Archaeodyptes stilwelli.*

Unfortunately, because no hind limb bones have been recovered, body mass estimates using methods such as those done for other penguin taxa (Jadwiszczak, 2001) cannot be performed accurately for *Archaeodyptes stilwelli*. Furthermore, it should be considered that there is limited practical use for accurate estimates of body size using the dimensions of isolated limb bones (Ksepka

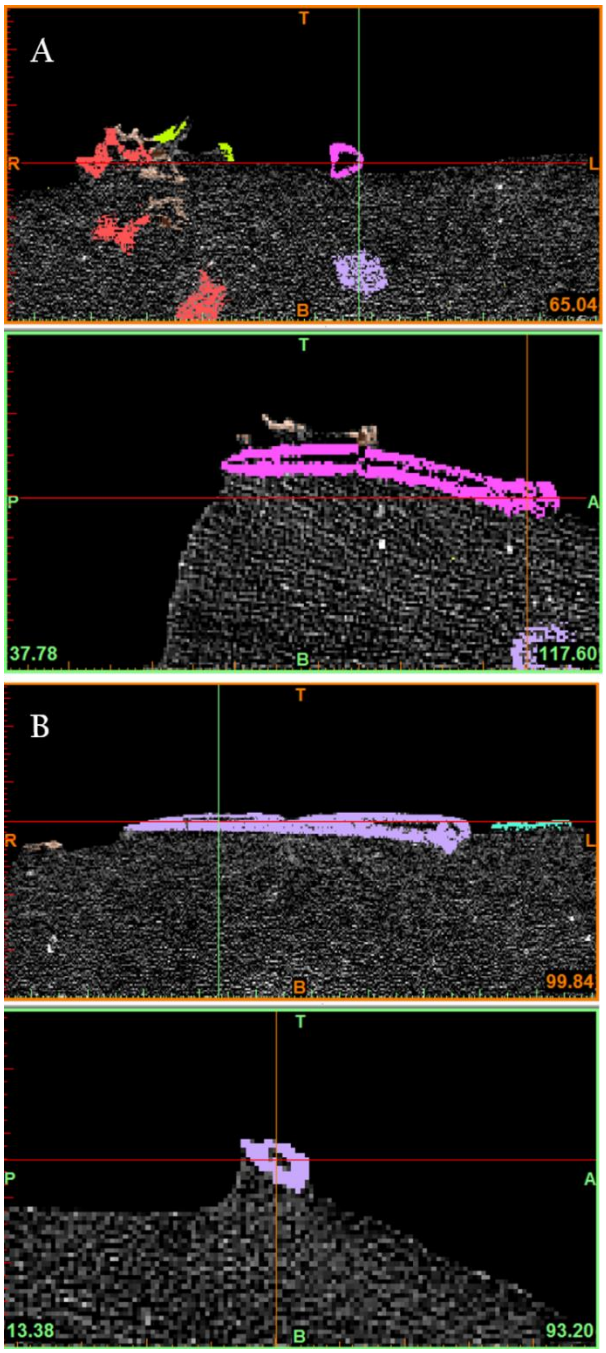

Figure 5.7: A cross-section of the long bones in *Archaeodyptes stilwelli* (JDS8344), as shown in Materialise *Mimics*, displaying a reduced marrow cavity. The radius (A) is shown in pink, while the ulna (B) is highlighted in a grey-purple colour.

et al., 2012). The dimensions of the elements reveal that *Archaeodyptes stilwelli* was certainly a smaller penguin compared to *Waimanu*. In order to provide a very broad estimate, the size of *Archaeodyptes stilwelli* was based on the proportionate dimensions of forewing elements in *Archaeodyptes stilwelli* to those of multiple *Waimanu tuatahi* specimens (see Appendix 4). Given the approximate height of *Waimanu tuatahi* as 80 cm (Slack et al., 2006), the approximate height of *Archaeodyptes stilwelli* may have ranged between 76 cm and 57 cm, a size range similar to the Gentoo penguin (*Pygoscelis papua*), and numerous other extant penguins. It should be noted though that because these estimates of height are based on forewing elements alone, these results should be taken tentatively.

Overall, the skeletal features present in *Archaeodyptes stilwelli* are reminiscent of a bird adapted for wing-propelled diving. Dorsoventrally flattened bones of the forewing, as well as further adaptations such as a proximal tubercle in phalanx III-1, and reduced marrow cavities in bones suggest that *Archaeodyptes stilwelli* had adaptations for an aquatic lifestyle, but not specialised to the extent of any other currently known Sphenisciformes. Conversely, the shape of the furcula in *Archaeodyptes stilwelli* appears to resemble an intermediate form between soaring birds such as albatrosses, and solely aquatic penguins, indicative of a bird that occupied both aerial and aquatic environments, such as auks and diving petrels. While it can be postulated that *Archaeodyptes stilwelli* was capable of utilising both aerial and aquatic environments, the true nature of this taxon is unknown due to lack of fossil material recovered., and thus subsequent discoveries may shed further light on the palaeobiology of *Archaeodyptes stilwelli*. A discovery of a humerus associated with *Archaeodyptes stilwelli* for example may give more proportionate data about the overall wing length, and whether the animal was capable of aerial flight. Recovery of further elements such as hind limbs may also be able to give a more accurate estimate of body size and mass, and thus whether a bird with such dimensions and weight was capable of volancy. Based on the material available however, it is evident that *Archaeodyptes stilwelli* possesses plesiomorphic anatomical features consistent with aerial birds, and synapomorphies shared with solely aquatic penguins, and is thus representative of the most primitive currently known diver amongst Sphenisciformes.

5.4 Evolutionary Context

Through the study of fossils associated with *Archaeodyptes stilwelli*, combined with temporal data and a phylogenetic framework, an improved understanding of the general pattern of evolution in the basal Sphenisciformes lineage becomes more apparent. Numerous authors (Ksepka and Ando, 2011; Ksepka et al., 2015; Raikow et al., 1988) cite the evolution of penguins progressing as a three-tiered stage theory, as hypothesised by George Gaylord Simpson. This involved an initial stage of volancy; a stage where smaller forms utilised both aerial flight and wing-propelled diving; before the eventual solely aquatic wing propelled stage—reminiscent of all currently known penguin taxa (Simpson, 1946). In this way, Simpson argued that in the evolution of Sphenisciformes, the penguins passed through a stage with morphologies similar to that of modern alcids and diving petrels, from flighted ancestors, rather than undergoing a flightless terrestrial interval (Ksepka and Ando, 2011; Simpson, 1946). Under current definitions proposed by Clarke et al. (2003), the phylogenetic placement of Sphenisciformes is applied to all penguins that share the apomorphic loss of volancy, while if a basal volant penguin was discovered that was more related to Spheniscidae than any other avian lineage, it would be placed in the clade of Pansphenisciformes, yet excluded from the Sphenisciformes clade (Clarke et al., 2003). While more evidence may be needed to place *Archaeodyptes stilwelli* in either Pansphenisciformes or Sphenisciformes specifically, morphology possessed by *Archaeodyptes stilwelli*, as the most basal fossil penguin, shows many features consistent with a recent divergence from volant ancestors, and also features synapomorphic with the solely aquatic penguins that all currently known penguin fossils belong to.

If modern aquatic penguins evolved from volant ancestors, then why did this apparent pattern in evolution occur? It has been suggested that in terrestrial habitats where there is especially low productivity, the high energy cost of flying may be disadvantageous, presenting a potential hypothesis for terrestrial flightlessness in some birds (Elliott et al., 2013). However, this reasoning is less plausible when applied to a shift from volant to aquatic forms of locomotion; as while solely aquatic seabirds may take advantage of highly productive waters, compared to low-productivity on land, they are also of greater risk of predation by aquatic predators (Elliott et al., 2013). Alternatively, the transition from aerial to subaqueous flight may have been a result of a biomechanical tradeoff. In this way, adaptations that lead to wings becoming more efficient for swimming would have become less efficient for aerial flight, until aerial flight costs were physiologically unsustainable (Elliott et al.,

2013). This can be observed in living birds today, where aerial plunge-diving boobies (Sulidae) represent a more primitive stage in underwater propulsion efficiency, using partially open wings to steer through the water medium, in contrast to the flapping motion observed in auks (Pennycuick, 1987). Compared to boobies or some Procellariiformes, for example, auks have a more efficient means of underwater propulsion, but at the sacrifice of wing span and wing area, with little change in aspect ratio (Pennycuick, 1987). Auks and other birds that utilise this form of underwater locomotion thus retain flight, but at a reduced efficiency compared to more predominately aerial forms (Pennycuick, 1987). Penguins however, represent a lineage through which loss of and reduced musculature related to aerial flight, and stiffening of the wing (Raikow et al., 1988), aerial flight with such adaptations would have been too physiologically costly (Elliott et al., 2013; Raikow et al., 1988). Aerial flight must have been abandoned in the penguin lineage in this sense therefore, previous to specialised adaptations for underwater propulsion efficiency (Elliott et al., 2013). The stage whereby ancient penguins were capable of both aerial and subaqueous locomotion, as represented by living alcids and diving petrels, has been suggested to signify a compromise between birds that are well adapted for each media (Storer, 1960).

As explored in ***Chapter I: Introduction***, the subject of the timing and radiation of the Neornithes, or crown group birds, is a subject of ongoing debate (Brocklehurst et al., 2012; Burleigh et al., 2015; Chiappe and Dyke, 2002; Clarke, 2004; Ericson et al., 2006; Hackett et al., 2008; Jarvis et al., 2014; Lee et al., 2014; Prum et al., 2015). The fossils of *Waimanu manneringi* represent the oldest known widely regarded definitive fossils of crown group birds, specifically Sphenisciformes (Slack et al., 2006), within the diverse Aequorlitornithes seabird clade (Prum et al., 2015), dated to around ~60.5-61.6 Ma (Ksepka and Ando, 2011; Slack et al., 2006). Some molecular estimates suggest that the divergence of the Pansphenisciformes clade from its sister taxon Procellariiformes occurred within the Late Cretaceous (Baker et al., 2006; Brown et al., 2008; Ksepka and Ando, 2011; Slack et al., 2006), whereas others suggest an early Paleocene split and origin of the Sphenisciformes clade (Prum et al., 2015). Either way, this divergence is likely to have occurred before the loss of aerial flight in the penguin lineage, consistent with the large morphological disparity between these two clades, considering the definitive loss of aerial flight observed in *Waimanu* (Ksepka and Ando, 2011). The length of time of which penguins were flightless following this divergence however, is still unknown (Ksepka and Ando, 2011).

The fossils of *Archaeodyptes stilwelli* come from the Takatika Grit rock unit, which has other fossil elements from the Campanian, in the late Cretaceous, based on the interpretation of dinoflagellate assemblages (Consoli and Stilwell, 2009; Consoli and Stilwell, 2011; Wilson et al., 2005), and the date of matrix samples from around fossils (Consoli and Stilwell, 2009). This unit was also cited to contain taxa characteristic of the K/Pg boundary (Consoli and Stilwell, 2009; Wilson, 1982), and the Lower Paleocene (Consoli and Stilwell, 2009), extending the range of this rock unit, and thus the potential age of *Archaeodyptes stilwelli*, between the mid-Campanian and mid-Danian. Recently however, evidence has come to light that argues the specific age of the Takatika Grit. A new study by Hollis et al. (in press) shows that that there is no biostratigraphic evidence of the K/Pg boundary succession associated with the Takatika Grit, and the rock unit was deposited during the late early-middle Paleocene (~62.5-60 Ma). Additionally, microfossils attributed to the early Campanian (Early Haumurian, ~82-80 Ma), as well as vertebrate fossils such as that of Creteceous theropod dinosaurs (Stilwell et al., 2006) and marine reptiles are explained as the result of partial exhumation and *in situ* reburial (Consoli and Stilwell, 2009). Thus the material of *Archaeodyptes stilwelli* almost certainly represents *in situ* early-middle Paleocene fossils, considering the unlikeliness that Campanian fossils in the form of partial skeletons would have endured exhumation and reburial.

The divergence from volant to wing-propelled aquatic flight may have been influenced by biotic factors such as competition. Considering a Late Cretaceous shift, Slack et al. (2006) addressed that competitive interaction between Neornithes, and other Cretaceous avians, may have led to ecological displacement, sparking this ecological transition, that may have eventually lead to taxa like *Archaeodyptes stilwelli*. Enantiornithines represent the most diverse group of birds during the Mesozoic (Chiappe and Dyke, 2002), and dominated Cretaceous ecosystems (Chiappe and Dyke, 2002; Zhou, 2004). Of the variety of habitats accommodated by enantiornithines, birds such as *Halimornis* have been recorded from littoral environments, occupying marine beds formed at least 50 m offshore (Chiappe and Walker, 2002), and may have had ecological overlap with archaic penguins (Slack et al., 2006). Considering the volant and possible diving palaeobiology of the recently described *Tingmiatornis artica* (Bono et al., 2016), and the inferred habits of the toothed seabird *Ichthyornis* (Clarke, 2004; Marsh, 1880; Porras-Muzquiz et al., 2014), it is possible that other ornithurine birds, separate from Neornithes, may have also played a role in competitive overlap, if they occupied similar littoral habitats. Pterosaurs are also known to have overlapped habitat with birds, as evidenced from

fossil footprints. Interestingly, Slack et al. (2006) postulated that the loss of pterosaurs with under 2 m wingspans from the Mid-Cretaceous onwards, combined with an observed increase of pterosaur wingspan to over 11 m by the end of the Cretaceous, may have correlated with the Neornithine radiation. Additionally, further drops in pterosaur diversity towards the end of the Cretaceous, and the consideration that larger animals are most at risk to extinction, strengthens this argument—and may partly explain why neornithine lineages survived the K/Pg mass extinction, where other clades such as pterosaurs did not (Slack et al., 2006).

It has also been hypothesised that the aerial flightlessness of penguins may have occurred immediately following the K/Pg mass extinction event, where the extinction of marine reptiles and large sharks provided a relatively predator-free niche that early penguins could exploit (Ando, 2007; Ksepka and Ando, 2011). In this sense, morphological adaptations leading to aerial flightlessness, consistent with the time frame of archaic penguin evolution, may have occurred in geographic areas largely free of predation pressures (Ksepka and Ando, 2011; Mayr, 2016). Furthermore, the extinction of aquatic foot-propelled Hesperornithiformes, and their subsequent absence following the K/Pg mass extinction (Bell, 2014) would have provided a competition free niche for archaic penguins of the earliest Cenozoic.

While present, and representative of stem lineages of modern birds (Mayr, 2016), neornithine lineages are badly represented in the Late Cretaceous (Fountaine et al., 2005). Following the K/Pg boundary however, rapid adaptive radiation of these groups is observed (Jarvis et al., 2014). The successive and numerous speciation events occurring near the K/Pg boundary has been associated with extreme levels of incomplete lineage sorting (Jarvis et al., 2014; Suh et al., 2015), suggesting simultaneous divergence of these groups into the readily available niches from the absence of pre-K/Pg boundary taxa (Suh et al., 2015). Additionally, it is also possible that hybridisation between early lineages may have occurred during this interval (Jarvis et al., 2014). Considering that *Archaeodyptes stilwelli* is likely a late early-middle Paleocene taxon (~62.5-60.0 Ma), and with an age of ~60.5-61.6 Ma for *Waimanu manneringi* (Ksepka and Clarke, 2010; Slack et al., 2006), the numerous similarities in morphological characters shared between these taxa may be explained by such a phenomenon as incomplete lineage sorting during this time-frame. Further material is thus required however to ascertain whether additional skeletal differences further significantly differentiate these taxa.

A distinct shift to a solely aquatic lifestyle in the Early Cenozoic, would have been coupled with early adaptations for improved diving ability (Hospitaleche, 2016), freed from the evolutionary constraints of aerial flight (Ksepka and Ando, 2011). The evolution of features related to functionality of penguin locomotion in water, such as stronger bones and musculature, would have improved diving capacity, and endurance of the denser medium (Hospitaleche, 2016; Ksepka and Ando, 2011). Correspondingly, the aquatic shift would have allowed Sphenisciformes to attain larger sizes, leading to increased diving efficiency (Ksepka and Ando, 2011). A progressive pattern of such is consistent with the tentatively inferred smaller body size (~ 65 cm) of *Archaeodyptes stilwelli* compared to *Waimanu* (80-100 cm) (Slack et al., 2006), before the emergence of penguins that attained truly giant forms such as the Late Paleocene *Crossvallia unienwillia* (~ 1.5 m) from Antarctica, and numerous Eocene taxa (Clarke et al., 2007; Jadwiszczak et al., 2013; Tambussi et al., 2005). Early penguin evolution in the Early Cenozoic is evidenced to have paralleled the evolution of modern circulation patterns in the Southern Ocean between Antarctica and other southern landmasses, related to cool, temperate waters (Fordyce and Jones, 1990). In turn, the evolution of the Southern Ocean also saw the paralleled evolution of other marine vertebrates such as seals and cetaceans (Fordyce and Jones, 1990).

5.5 The Palaeogeographical and Palaeoecological Setting

Due to the region bearing the oldest known penguin fossils to date, Zealandia—and by extension the exposed landmass of present day New Zealand—is currently recognised as the cradle where Sphenisciformes evolved in the latest Cretaceous or earliest Cenozoic, before spreading to Antarctica, Australia and South America by the Late Eocene (Ksepka and Thomas, 2012; Mayr, 2016). At the time of the K/Pg boundary, 66.03 Ma, Zealandia and the Chatham Rise had completely separated from the eastern Gondwana margin (but was still connected to Australia) (Bache et al., 2014), and had drifted north compared to its position in the Late Cretaceous (Stilwell, 2016; Stilwell and Consoli, 2012), which resulted in it becoming increasingly isolated in terms of geography and biology (Stilwell, 2016). Relatively stable and untroubled by plate boundary activity, Zealandia after its separation from Gondwana is described as subdued and flat, without mountain ranges, and a rolling topography similar to modern day Australia (Campbell and Hutching, 2007). Similarly, the Chatham Rise landmass, where *Archaeodyptes stilwelli* was recovered, has been described as a peneplained topography comprised of low hills and broad coastal flood-plains, surrounded by a deep

ocean to the north and south, around the K/Pg boundary (Stilwell and Consoli, 2012). Due to the rifting of Zealandia from the West Antarctic margin, and the concurrent opening of the Tasman Sea 82.5-83.0 Ma (Campbell and Hutching, 2007; Stilwell, 2016), subsequent post-rift tectonic activity in the Campanian to the Maastrichtian resulted in the progressive transgression of Zealandia (Consoli and Stilwell, 2009; Consoli and Stilwell, 2011; Stilwell, 2016), and oceanic inundation of the Chatham Rise region (Consoli and Stilwell, 2011)—which would eventually reach 200-500 m below sea level by current times (Wood and Herzer, 1993). Global cooling ensued at the K/Pg boundary, and sea levels were rising (Stilwell, 2016; Stilwell and Consoli, 2012), activity that is coupled with the establishment of subtropical and proto-Antarctic driven currents over the Chatham Rise (Stilwell and Consoli, 2012)—an oceanographic regime that still dominates the area (Campbell et al., 1993; Stilwell and Consoli, 2012). However, contrary to research that suggested that the Chatham Peninsula was submerged by the Late Cretaceous, the discovery of numerous avian fossils 64-65 Ma indicate that land was exposed to some extent in this region (Stilwell, 2016; Stilwell and Consoli, 2012). Therefore, while the Chatham region was almost completely submerged, terrigenous components likely existed in the form of ephemeral oceanic islands through the Early Cenozoic (Consoli and Stilwell, 2011).

The Takatika Grit is thought to record a prolonged period of erosion over the latest Cretaceous and early Paleocene, followed by marine sedimentation in the late early Paleocene (Hollis, in press). Sedimentation of the Takatika Grit was deposited within intervening grabens (Consoli and Stilwell, 2005; Stilwell et al., 2006), from uplift and block faulting related to the region's divergent tectonic activity (Consoli and Stilwell, 2005; Stilwell and Consoli, 2012). The exact depositional conditions of the Takatika Grit are complex, thought to represent a mid-outer shelf marine sequence through marine transgression (Consoli and Stilwell, 2005), and the diversity of radiolarian assemblages are typical of deep marine and pelagic settings (Hollis, in press). Contrary to this, some Paleocene sediments of the Takatika Grit are also understood to have been deposited in a nearshore environment, based on the presence of the fern *Azolla* massulae; which occupied fresh, still-water bodies (Consoli and Stilwell, 2011). Basement highs and volcanic islands supporting fresh-water lakes must have thus existed near to the depositional setting of the Takatika Grit, during this time (Consoli and Stilwell, 2011). A mixture of shallow and deep marine deposits may be reflective of mass movements of sediments from shallow environments into bathyal depths, thus preserving this

mixture (Consoli, 2008). Overall however, the processes and depositional setting of the Takatika Grit in the Paleocene is thought to be analogous of what is occurring on the submerged crest of the Chatham Rise today (Consoli and Stilwell, 2005). The environmental setting occupied by *Archaeodyptes stilwelli* must have been related such marine and/or near-shore environments therefore.

The terrigenous landscape that *Archaeodyptes stilwelli* occupied would have been similar to Holocene Australia, only more wet and lush (Campbell and Hutching, 2007). A mixed vegetation would have existed on this late early Paleocene landscape, where forests dominated by *Podocarpus*, and *Nothofagus* existed, with a fern understory—albeit smaller to the relative abundance during the Late Cretaceous (Consoli and Stilwell, 2011). Climatic conditions in New Zealand at this time are understood to be cooler than the preceding latest Cretaceous, and experienced cool-temperate conditions, with mean annual temperatures around 6-12°C (Vajda et al., 2004). In the marine setting, *Archaeodyptes stilwelli* would have been subject to a world in the aftermath of intense global change, during the early Cenozoic (Stilwell et al., 2006). This was reflected in the loss of large sharks and marine reptiles (Ando, 2007; Ksepka and Ando, 2011), as well as all hard shelled cephalopods (apart from nautiloids), from the K/Pg extinction event, which would have allowed a rise in dominance of soft-bodied taxa such as octopi and squid in these oceans (Consoli, 2008). During this time, *Archaeodyptes stilwelli* would have coexisted with frilled sharks such as *Chlamydoselachus tatere* that have also been recovered from the Takatika Grit during the Early Paleocene—and may have migrated from deeper marine environments in response to relatively devoid oceans (Consoli, 2008).

5.6 What Does This Mean for the Future of Palaeontology in New Zealand?

Archaeodyptes stilwelli is one of the earliest Neornithes discovered to date, exemplifying the earliest and most primitive of penguin taxa known. As such, this research not only adds to the already extensive fossil record of penguins (Mayr, 2016), as a basal fossil of an extant lineage of crown group birds, but also gives important information on the rapid radiation of Neornithes in the wake of the K/Pg mass extinction. Particularly, this basal penguin facilitates the understanding of the evolutionary processes that occurred during this 10-15 Ma to eventually produce all extant neoavian orders (Jarvis et al., 2014), and the extremely diverse range of characters that birds display today (Zhang et al., 2014).

New Zealand as we know it, dominated by active plate boundary tectonics, is unlike the Zealandia of 83-23 Mya (Campbell and Hutching, 2007). This discovery therefore, progresses our current knowledge of the region before such tectonic activity came into effect. Furthermore, separated from Gondwana in the Late Cretaceous, New Zealand represents an important sector of the southwest Pacific (Crampton and Cooper, 2010), as a unique, environmentally and biologically distinct entity (Stilwell, 2016). While the Chatham Rise and associated regions have not changed largely relative to New Zealand and the rest of the Pacific Plate since the Late Cretaceous divergence from Gondwana, gradual thermal subsidence (Consoli and Stilwell, 2009; Stilwell et al., 2006) has resulted in a comparatively small geographical extent of Zealandia's outcrop exposed (Consoli and Stilwell, 2011). Subsequently, a low representation of the original Zealandian flora and flora is currently understood through palaeobiogeographic analyses (Consoli and Stilwell, 2011). Therefore, even though the Chatham Islands preserve a range of flora and fauna from the Permian to the most recent Cenozoic, the palaeontological record of the area is limited (Consoli and Stilwell, 2011). While many studies have focused on the Chatham Islands geology, the palaeontology related to the area has been relatively neglected (Consoli and Stilwell, 2011). *Archaeodyptes stilwelli*, as a primitive bird from the Chatham Islands, represents an important fossil discovery for our understanding of endemism of Zealandia during the Early Cenozoic, and the ecosystems that were active after its split from Gondwana. As a result, *Archaeodyptes stilwelli* is a significant addition to the rich (Crampton and Cooper, 2010)—albeit patchy (Goldberg et al., 2008)—fossil record associated with New Zealand.

As a species of penguin, *Archaeodyptes stilwelli* also adds to our current state of knowledge of Zealandian seas. While we have "barely scratched the surface" of the terrestrial fossil record, much more is known about the marine record of Zealandia (Campbell and Hutching, 2007). Particularly, these Zealandian Late Cretaceous-Eocene marine sediments and fossils allow interpretations on life in the south-western Pacific before the separation of Antarctica and Australia, and before the development of the Circum-Antarctic Current (Campbell and Hutching, 2007), a greenhouse period with exceptionally warm poles (Zachos et al., 2008). Consequently, *Archaeodyptes stilwelli* gives information on life in this region, in a world before the southern polar ice cap; when ocean circulation and climate was drastically different as a result (Campbell and Hutching, 2007). This taxon adds to the unparalleled marine fossil record of life spanning 83 Ma, illustrating the history of Zealandia as it gradually sank, with increasingly deeper marine conditions (Campbell and Hutching, 2007).

Considering the modern relevance in examination of the response of climate to high values of atmospheric CO_2 during this early Cenozoic time-frame (Zachos et al., 2008), the study of taxa that lived in this time is of particular significance.

Future avenues of research from this discovery therefore promote New Zealand, building on its excellent Cenozoic Era fossil record (Crampton and Cooper, 2010), especially in regards to Zealandian seas (Campbell and Hutching, 2007). Considering that *Archaeodyptes stilwelli* and other fossils from this region are the only source of information of the biotic history of a large area of the south-west Pacific, they hold a global significance (Crampton and Cooper, 2010). Because of New Zealand's unique climatic, oceanographic and biogeographic setting, fossils like *Archaeodyptes stilwelli*, used in conjunction with other fossil fauna and flora, can therefore provide important information for testing and formulating palaeobiological, palaeoclimatic and palaeoceanographic hypotheses (Crampton and Cooper, 2010).

CHAPTER VI: CONCLUSIONS

This study investigated two fossil bird specimens recovered from the Takatika Grit, Chatham Island. This was conducted to formally identify and describe the specimens, interpret their palaeobiology, and consider them in an evolutionary phylogenetic framework, and in terms of their global significance. Manipulation of these specimens was performed virtually using CT scanned images and *Materialise Mimics* software. Subsequently, the specimens were examined through morphology-based comparative and phylogenetic analyses, and the results interpreted. By way of conclusion, the results of this study are summarised below.

The specimens investigated in this study are both associated partial skeletons that were deposited *in situ* during the late early-middle Paleocene. Significantly, the novel taxon *Archaeodyptes stilwelli* is recognised from the comparative and phylogenetic analyses of these fossils. There is no overlap in skeletal elements across the two specimens, however, locality, anatomical measurements, and phylogenetic analyses are compatible with both of these specimens sharing the same taxon. Hence, both specimens have been tentatively assigned here as referred specimens of *Archaeodyptes stilwelli*. While further evidence is needed to robustly support this assignment, in the circumstance that more definitive evidence should come to light, this placement may be more accurately revised.

Phylogenetic analyses using two different phylogenetic matrices recovered *Archaeodyptes stilwelli* in a basal position of the Sphenisciformes clade, as sister-taxon to Procellariiformes, and immediately crownwards relative to Gaviiformes. Morphological comparison by means of PCA, showed similarities in the morphology of cervical vertebra IV of *Archaeodyptes stilwelli* to extant and basal penguin taxa, as well as extant Procellariiformes. This morphometric comparison, in conjunction with the numerous phylogenetic analyses robustly supports the basal position in the Sphenisciformes clade for *Archaeodyptes stilwelli*. On the basis of these analyses, and the age of the fossils, this taxon is significant as it represents the most basal of Sphenisciformes currently known to science.

Archaeodyptes stilwelli was consistently found in close association with the early penguin *Waimanu* during phylogenetic analyses, and additionally displays numerous morphological similarities. Similarities are observed in the shape of the radius especially, and are supported by PCA. In contrast, the shape of the ulna is visually dissimilar, particularly regarding the shape of the olecranon, and distinctly different based on PCA. While the shape of the coracoid of *Archaeodyptes stilwelli* is most visually similar to *Waimanu* compared to other known penguin taxa, the shape of the acrocoracoid neck in *Archaeodyptes stilwelli* shows features more reminiscent of some Procellariiformes. *Archaeodyptes stilwelli* dsiplays plesiomorphic features representative of a more primitive penguin taxon, compared to *Waimanu*. In general, the similarities and differences between the elements of *Archaeodyptes stilwelli* and *Waimanu* are consistent with a gradual evolution of basal Sphenisciformes features towards the skeletal morphologies observed in crown group penguins. *Archaeodyptes stilwelli* is thus validated as a distinct genus from *Waimanu*.

The palaeobiology of *Archaeodyptes stilwelli*, interpreted from the two associated part skeletons, is reminiscent of a bird adapted for wing-propelled diving. Features observed in *Archaeodyptes stilwelli* such as dorsoventrally flattened forewing elements, the presence of proximal tubercle in phalanx III-1, and reduced marrow cavities are indicative of adaptations for an aquatic lifestyle and hydrodynamic efficiency. However, these elements are not as specialised for the aquatic environment relative to all other Sphenisciformes. The anterior curvature of the furcula in *Archaeodyptes stilwelli* resembles an intermediate shape between aerial birds such as albatrosses, and solely aquatic penguins, and is comparable to birds that utilise both aerial and aquatic environments, such diving petrels and auks. Further material and research may provide means of establishing an accurate body mass and proportions for *Archaeodyptes stilwelli*, and shed light on the extent to which it was able to exploit its environment. The material in this study shows that *Archaeodyptes stilwelli* possesses plesiomorphic anatomical features reminiscent of aerial birds, and synapomorphies shared with solely aquatic penguins, and thus has features representative of the most primitive currently known diver amongst Sphenisciformes.

The morphological features present in *Archaeodyptes stilwelli* are consistent with the model proposed by Simpson (1946), whereby archaic penguins passed through a stage with morphologies similar to modern auks, from volant ancestors. Specifically, *Archaeodyptes stilwelli* appears to be

representative of a form consistent with a recent divergence from ancestors capable of aerial flight, and specialisations to the aquatic environment. The aquatic transition may have occurred as a product of a biomechanical trade-off, where wings/flippers adapted for increased swimming efficiency were less efficient for aerial flight, and as this evolution progressed aerial flight costs eventually because physiologically unsustainable. It has been suggested that the divergence of Sphenisciformes from its sister-taxon clade Procellariiformes occurred in the Late Cretaceous or the early Paleocene, but regardless occurred before the loss of aerial flight in the penguin lineage. A transition from aerial flight to semi-aquatic wing-propelled diving may have been influenced by competitive interactions with other ornithurine and enantiornithine birds in the Late Cretaceous, and may also have paralleled the reduction in pterosaur diversity and decline of smaller pterosaur forms during this interval. Furthermore, aerial flightlessness and transition to the solely aquatic environment may have occurred in the vacuum immediately following the K/Pg mass extinction, in the absence of many large marine predators, and lack of competition from the extinction of the Hesperornithiformes. Exploitation of these niches in the relatively vacant marine environment may have allowed early Sphenisciformes to further specialise for more efficient diving abilities, and diversify into the Early Cenozoic.

Bearing the oldest known penguin fossils to date, Zealandia, and by extension New Zealand, represents a region where Sphenisciformes likely initially evolved before populating other regions of the Southern Hemisphere. In this setting, *Archaeodyptes stilwelli* would have experienced temperate climates cooler to the preceding Cretaceous, and occupied nearshore to deep marine environments, as well as ephemeral oceanic islands, on the Chatham Rise. In this earliest Cenozoic, Zealandia and the associated Chatham Rise had become increasingly isolated and biologically distinct as it drifted north from the eastern Gondwana margin.

Archaeodyptes stilwelli therefore not only holds global significance as the oldest currently known penguin taxon, and adds to our understanding of the early radiations of Neornithes, but also progresses of our current knowledge of the Zealandia region before modern plate boundary tectonic activity observed in New Zealand came into effect. Specifically, because a low representation of the original Zealandian fauna and flora is currently understood through palaeobiogeographic analyses, *Archaeodyptes stilwelli* represents an important fossil discovery for our understanding of endemism of Zealandia during the Early Cenozoic, and the ecosystems that were active after its split from

Gondwana. *Archaeodyptes stilwelli* adds to the unparalleled marine fossil record of Zealandia, as it gradually sank, with increasingly deeper marine conditions. Used in conjunction with other fossils and marine sediments, fossils such as *Archaeodyptes stilwelli* allow interpretations on life that existed in a relatively greenhouse world to today, before the development of the Circum-Antarctic Current. Considering the response of life to climate with high values of atmospheric CO_2 during this Early Cenozoic interval, the study of taxa that lived in this time is of particular modern global relevance.

REFERENCES

Adams, C., Campbell, H., Mortimer, N. and Griffin, W., 2016. Perspectives on Cretaceous Gondwana break-up from detrital zircon provenance of southern Zealandia sandstones. Geological Magazine: 1-22.

Adatte, T., Keller, G. and Stinnesbeck, W., 2002. Late Cretaceous to early Paleocene climate and sea-level fluctuations: the Tunisian record. Palaeogeography, Palaeoclimatology, Palaeoecology, 178(3): 165-196.

Ando, T., 2007. New Zealand fossil penguins: origin, pattern, and process. Unpublished Ph. D. dissertation, University of Otago, Dunedin, New Zealand.

Arostegi, J., Baceta, J., Pujalte, V. and Carracedo, M., 2011. Late Cretaceous–Palaeocene mid-latitude climates: inferences from clay mineralogy of continental-coastal sequences (Tremp-Graus area, southern Pyrenees, N Spain). Clay minerals, 46(1): 105-126.

Askin, R.A., 1990. Campanian to Paleocene spore and pollen assemblages of Seymour Island, Antarctica. Review of Palaeobotany and Palynology, 65(1-4): 105-113.

Bache, F., Mortimer, N., Sutherland, R., Collot, J., Rouillard, P., Stagpoole, V. and Nicol, A., 2014. Seismic stratigraphic record of transition from Mesozoic subduction to continental breakup in the Zealandia sector of eastern Gondwana. Gondwana Research, 26(3): 1060-1078.

Baker, A.J., Pereira, S.L., Haddrath, O.P. and Edge, K.-A., 2006. Multiple gene evidence for expansion of extant penguins out of Antarctica due to global cooling. Proceedings of the Royal Society of London B: Biological Sciences, 273(1582): 11-17.

Bannasch, R., 1994. Functional anatomy of the 'flight'apparatus in penguins. Mechanics and physiology of animal swimming: 163-192.

Barrera, E., 1994. Global Environmental Changes Preceding the Cretaceous-Tertiary Boundary: Early-Late Maastrichtian Transition. Geology, 22(10): 877-880.

Barron, E.J., Fawcett, P.J., Pollard, D., Thompson, S., Berger, A. and Valdes, P., 1993. Model simulations of Cretaceous climates: the role of geography and carbon dioxide [and Discussion]. Philosophical Transactions of the Royal Society of London B: Biological Sciences, 341(1297): 307-316.

Barron, E.J. and Peterson, W.H., 1989. Model simulation of the Cretaceous ocean circulation. Science, 244(4905): 684-686.

Baumel, J.J., and Witmer, L.M., 1993. Osteologia, p. 45-132. Handbook of Avian Anatomy Nomina Anatomica Avium, Cambridge University Press, Cambridge.

Bell, A. and Chiappe, L.M., 2015. A species-level phylogeny of the Cretaceous Hesperornithiformes (Aves: Ornithuromorpha): implications for body size evolution amongst the earliest diving birds. Journal of Systematic Palaeontology, 14(3): 239-251.

Bell, A.K.A., 2014. Evolution & ecology of Mesozoic birds: a case study of the derived Hesperornithiformes and the use of morphometric data in quantifying avian paleoecology. University of Southern California.

Benson, R.B.J., Mannion, P.D., Butler, R.J., Upchurch, P., Goswami, A. and Evans, S.E., 2013. Cretaceous tetrapod fossil record sampling and faunal turnover: Implications for biogeography and the rise of modern clades. Palaeogeography, Palaeoclimatology, Palaeoecology, 372: 88-107.

Benton, M.J., 1999. Early origins of modern birds and mammals: molecules vs. morphology. BioEssays, 21(12): 1043-1051.

Bertelli, S. and Giannini, N.P., 2005. A phylogeny of extant penguins (Aves: Sphenisciformes) combining morphology and mitochondrial sequences. Cladistics, 21(3): 209-239.

Bertelli, S., Giannini, N.P. and Ksepka, D.T., 2006. Redescription and phylogenetic position of the early Miocene penguin *Paraptenodytes antarcticus* from Patagonia. American Museum Novitates: 1-36.

Bono, R.K., Clarke, J., Tarduno, J.A. and Brinkman, D., 2016. A Large Ornithurine Bird (*Tingmiatornis arctica*) from the Turonian High Arctic: Climatic and Evolutionary Implications. Scientific Reports, 6.

Bourdon, E., Mourer-Chauvire, C., Amaghzaz, M. and Bouya, B., 2008. New specimens of *Lithoptila abdounensis* (Aves, Prophaethontidae) from the lower Paleogene of Morocco. Journal of Vertebrate Paleontology, 28(3): 751-761.

Bradshaw, J.D., 1989. Cretaceous Geotectonic Patterns in the New Zealand Region. Tectonics, 8(4): 803-820.

Brocklehurst, N., Upchurch, P., Mannion, P.D. and O'Connor, J., 2012. The Completeness of the Fossil Record of Mesozoic Birds: Implications for Early Avian Evolution. PLoS One, 7(6).

Brown, J.W., Rest, J.S., García-Moreno, J., Sorenson, M.D. and Mindell, D.P., 2008. Strong mitochondrial DNA support for a Cretaceous origin of modern avian lineages. BMC biology, 6(1): 1.

Brown, J.W. and Van Tuinen, M., 2011. Evolving Perceptions on the Antiquity of the Modern Avian Tree. Living Dinosaurs: The Evolutionary History of Modern Birds: 306.

Brugger, J., Feulner, G. and Petri, S., 2016. Baby, it's cold outside: Climate model simulations of the effects of the asteroid impact at the end of the Cretaceous. Geophysical Research Letters.

Brusatte, S.L., Butler, R.J., Barrett, P.M., Carrano, M.T., Evans, D.C., Lloyd, G.T., Mannion, P.D., Norell, M.A., Peppe, D.J., Upchurch, P. and Williamson, T.E., 2015. The extinction of the dinosaurs. Biological Reviews, 90(2): 628-642.
Burleigh, J.G., Kimball, R.T. and Braun, E.L., 2015. Building the avian tree of life using a large-scale, sparse supermatrix. Molecular Phylogenetics and Evolution, 84: 53-63.
Campbell, H. and Hutching, G., 2007. In search of ancient New Zealand.
Campbell, H.J., Andrews, P.B., Beu, A.G., Maxwell, P.A., Edwards, A.R., Laird, M.G., Hornibrook, N.d.B., Mildenhall, D.C., Watters, W.A., Buckeridge, J.S., Lee, D.E., Strong, C.P., Wilson, G.J. and Hayward, B.W., 1993. Cretaceous-Cenozoic geology and biostratigraphy of the Chatham Islands, New Zealand, 2. Institute of Geological & Nuclear Sciences, Lower Hutt, N.Z.
Cande, S.C. and Kent, D.V., 1995. Revised calibration of the geomagnetic polarity timescale for the Late Cretaceous and Cenozoic. Journal of Geophysical Research: Solid Earth, 100(B4): 6093-6095.
Carvalho, I.d.S., Brandoni de Gasparini, Z., Salgado, L., de Vasconcellos, F.M. and Marinho, T.d.S., 2010. Climate's role in the distribution of the Cretaceous terrestrial Crocodyliformes throughout Gondwana. Palaeogeography Palaeoclimatology Palaeoecology, 297(2): 252-262.
Case, J., Patrick, D., Nezat, C. and Clarke, J., 2011. Rare Earth Element Fingerprinting and 87Sr/86Sr Ratios Support a Latest Maastrichtian Age for Antarctica's First Discovered Cretaceous Bird, *Polarornis gregoryi*. Journal of Vertebrate Paleontology, 31: 86-86.
Chatterjee, S., 1989. The oldest Antarctic bird. Journal of Vertebrate Paleontology, 9(3): 16A.
Chatterjee, S., 2002. The morphology and systematics of *Polarornis*, a Cretaceous Loon (Aves: Gaviidae) from Antarctica. Proceedings of the 5th International Meeting of the Society of Avian Paleontology and Evolution (eds. Z. Zhou and F. Zhang), Science Press, Beijing,: 125-155.
Chiappe, L.M., 1996. Late Cretaceous birds of southern South America: anatomy and systematics of Enantiornithes and *Patagopteryx deferrariisi*. Münchner Geowissenschaftliche Abhandlungen, 30(A): 203-244.
Chiappe, L.M. and Dyke, G.J., 2002. The mesozoic radiation of birds. Annual Review of Ecology and Systematics, 33: 91-124.
Chiappe, L.M. and Walker, C.A., 2002. Skeletal morphology and systematics of the Cretaceous Euenantiornithes (Ornithothoraces: Enantiornithes). Mesozoic birds: above the heads of dinosaurs: 240-267.
Clark, B.D. and Bemis, W., 1979. Kinematics of swimming of penguins at the Detroit Zoo. Journal of Zoology, 188(3): 411-428.
Clarke, J.A., 2004. Morphology, Phylogenetic Taxonomy, and Systematics of Ichthyornis and Apatornis (Avialae : Ornithurae). Bulletin of the American Museum of Natural History(286): 1-+.
Clarke, J.A., Ksepka, D.T., Salas-Gismondi, R., Altamirano, A.J., Shawkey, M.D., D'Alba, L., Vinther, J., DeVries, T.J. and Baby, P., 2010. Fossil Evidence for Evolution of the Shape and Color of Penguin Feathers. Science, 330(6006): 954-957.
Clarke, J.A., Ksepka, D.T., Stucchie, M., Urbina, M., Giannini, N., Bertelli, S., Narvez, Y. and Boyd, C.A., 2007. Paleogene equatorial penguins challenge the proposed relationship between biogeography, diversity, and Cenozoic climate change. Proceedings of the National Academy of Sciences of the United States of America, 104(28): 11545-11550.
Clarke, J.A., Olivero, E.B. and Puerta, P., 2003. Description of the earliest fossil penguin from South America and first Paleogene vertebrate locality of Tierra del Fuego, Argentina. American Museum Novitates: 1-18.
Clarke, J.A., Tambussi, C.P., Noriega, J.I., Erickson, G.M. and Ketcham, R.A., 2005. Definitive fossil evidence for the extant avian radiation in the Cretaceous. Nature, 433(7023): 305-308.
Cnudde, V., Masschaele, B., Dierick, M., Vlassenbroeck, J., Van Hoorebeke, L. and Jacobs, P., 2006. Recent progress in X-ray CT as a geosciences tool. Applied Geochemistry, 21(5): 826-832.
Cohen, K., Finney, S. and Gibbard, P., 2015. International Commission of Stratigraphy (ICS) International Chronostratigraphic Chart 2015/01.
Conroy, G.C. and Vannier, M.W., 1984. Noninvasive three-dimensional computer imaging of matrix-filled fossil skulls by high-resolution computed tomography. Science, 226(4673): 456-458.
Consoli, C.P., 2006. *Edaphodon kawai*, sp. nov.(Chondrichthyes: Holocephali): a Late Cretaceous chimaeroid from the Chatham Islands, southwest Pacific. Journal of Vertebrate Paleontology, 26(4): 801-805.
Consoli, C.P., 2008. A rare Danian (early Paleocene) *Chlamydoselachus* (Chondrichthyes : Elasmobranchii) from the Takatika Grit, Chatham Islands, New Zealand. Journal of Vertebrate Paleontology, 28(2): 285-290.
Consoli, C.P., Pisera, A. and Stilwell, J.D., 2009. Siliceous Sponges of the Takatika Grit (Cretaceous-Paleogene), Chatham Islands, South Pacific. Journal of Paleontology, 83(5): 811-819.
Consoli, C.P. and Stilwell, J.D., 2009. Late Cretaceous marine reptiles (Elasmosauridae and Mosasauridae) of the Chatham Islands, New Zealand. Cretaceous Research, 30(4): 991-999.
Consoli, C.P. and Stilwell, J.D., 2011. Palaeontology of the Chatham Islands, SW Pacifica review. Alcheringa, 35(2): 285-301.
Consoli, C.P. and Stilwell, Y.D., 2005. Late Cretaceous Cephalopoda (Mollusca) from the Takatika Grit, Chatham Islands, Southwest Pacific. New Zealand Journal of Geology and Geophysics, 48(2): 389-393.
Corfield, R., 1994. Palaeocene oceans and climate: An isotopic perspective. Earth-Science Reviews, 37(3-4): 225-252.

Cracraft, J., 1976. Hindlimb Elements of Moas (Aves, Dinornithidae) - Multivariate Assessment of Size and Shape. Journal of Morphology, 150(2): 495-526.
Cracraft, J., 2001. Avian evolution, Gondwana biogeography and the Cretaceous–Tertiary mass extinction event. Proceedings of the Royal Society of London B: Biological Sciences, 268(1466): 459-469.
Crampton, J.S. and Cooper, R.A., 2010. The State of Paleontology in New Zealand. Palaeontologia Electronica, 13(2).
Crampton, J.S., Schiøler, P. and Roncaglia, L., 2006. Detection of Late Cretaceous eustatic signatures using quantitative biostratigraphy. Geological Society of America Bulletin, 118(7-8): 975-990.
Crouch, E.M., Willumsen, P.S., Kulhanek, D.K. and Gibbs, S.J., 2014. A revised Paleocene (Teurian) dinoflagellate cyst zonation from eastern New Zealand. Review of Palaeobotany and Palynology, 202: 47-79.
Davy, B., Hoernle, K. and Werner, R., 2008. Hikurangi Plateau: Crustal structure, rifted formation, and Gondwana subduction history. Geochemistry Geophysics Geosystems, 9.
Daza, J.D., Stanley, E.L., Wagner, P., Bauer, A.M. and Grimaldi, D.A., 2016. Mid-Cretaceous amber fossils illuminate the past diversity of tropical lizards. Science advances, 2(3): e1501080.
Dumont, E.R., 2010. Bone density and the lightweight skeletons of birds. Proceedings of the Royal Society of London B: Biological Sciences: rspb20100117.
Elliott, K.H., Ricklefs, R.E., Gaston, A.J., Hatch, S.A., Speakman, J.R. and Davoren, G.K., 2013. High flight costs, but low dive costs, in auks support the biomechanical hypothesis for flightlessness in penguins. Proceedings of the National Academy of Sciences, 110(23): 9380-9384.
Elzanowski, A., BIEŃKOWSKA-WASILUK, M., CHODYŃ, R. and BOGDANOWICZ, W., 2012. Anatomy of the coracoid and diversity of the Procellariiformes (Aves) in the Oligocene of Europe. Palaeontology, 55(6): 1199-1221.
Ericson, P.G.P., Anderson, C.L., Britton, T., Elzanowski, A., Johansson, U.S., Kallersjo, M., Ohlson, J.I., Parsons, T.J., Zuccon, D. and Mayr, G., 2006. Diversification of Neoaves: integration of molecular sequence data and fossils. Biology Letters, 2(4): 543-U1.
Falvey, D.A., 1974. The development of continental margins in plate tectonic theory. Australian Petroleum Exploration Association Journal, 14(1): 95-106.
Fara, E. and Benton, M.J., 2000. The fossil record of Cretaceous tetrapods. Palaios, 15(2): 161-165.
Feduccia, A., 1995. Explosive Evolution in Tertiary Birds and Mammals. Science, 267(5198): 637-638.
Feduccia, A., 1999. The Origin and Evolution of Birds. Yale University Press.
Feduccia, A., 2003. 'Big bang' for tertiary birds? Trends in Ecology & Evolution, 18(4): 172-176.
Feduccia, A., 2014. Avian extinction at the end of the Cretaceous: Assessing the magnitude and subsequent explosive radiation. Cretaceous Research, 50: 1-15.
Fordyce, R., 1991. A new look at the fossil vertebrate record of New Zealand. Vertebrate Paleontology of Australasia (Vickers-Rich, P.; Monaghan, JM: 1191-1316.
Fordyce, R.E. and Jones, C., 1990. Penguin History and New Fossil Material from New Zealand. In: L. Davis and J. Darby (Editors), Penguin Biology, pp. 419-446.
Fountaine, T.M.R., Benton, M.J., Dyke, G.J. and Nudds, R.L., 2005. The quality of the fossil record of Mesozoic birds. Proceedings of the Royal Society B-Biological Sciences, 272(1560): 289-294.
Fürbringer, M., 1888. Untersuchungen zur Morphologie und Systematik der Vögel: zugleich ein Beitrag zur Anatomie der Stütz-und Bewegungsorgane, 15. T. van Holkema.
Gauthier, J. and De Queiroz, K., 2001. Feathered dinosaurs, flying dinosaurs, crown dinosaurs, and the name" Aves. New Perspectives on the Origin and Early Evolution of Birds: 7-41.
Gavryushkina, A., Heath, T.A., Ksepka, D.T., Stadler, T., Welch, D. and Drummond, A.J., 2016. Bayesian total-evidence dating reveals the recent crown radiation of penguins. Systematic Biology: syw060.
Giannini, N.P. and Bertilli, S., 2004. Phylogeny of extant penguins based on integumentary and breeding characters. The Auk, 121(2): 422-434.
Goldberg, J., Trewick, S.A. and Paterson, A.M., 2008. Evolution of New Zealand's terrestrial fauna: a review of molecular evidence. Philosophical Transactions of the Royal Society B: Biological Sciences, 363(1508): 3319-3334.
Goloboff, P.A., Farris, J.S. and Nixon, K.C., 2008. TNT, a free program for phylogenetic analysis. Cladistics, 24(5): 774-786.
Guinard, G., Marchand, D., Courant, F., Gauthier-Clerc, M. and Le Bohec, C., 2010. Morphology, ontogenesis and mechanics of cervical vertebrae in four species of penguins (Aves: Spheniscidae). Polar biology, 33(6): 807-822.
Hackett, S.J., Kimball, R.T., Reddy, S., Bowie, R.C.K., Braun, E.L., Braun, M.J., Chojnowski, J.L., Cox, W.A., Han, K.-L., Harshman, J., Huddleston, C.J., Marks, B.D., Miglia, K.J., Moore, W.S., Sheldon, F.H., Steadman, D.W., Witt, C.C. and Yuri, T., 2008. A phylogenomic study of birds reveals their evolutionary history. Science, 320(5884): 1763-1768.
Haddrath, O. and Baker, A.J., 2012. Multiple nuclear genes and retroposons support vicariance and dispersal of the palaeognaths, and an Early Cretaceous origin of modern birds. Proc Biol Sci, 279(1747): 4617-25.
Haeckel, E.H., 1866. Generelle Morphologie der Organismen allgemeine Grundzuge der organischen Formen-Wissenschaft, mechanisch begrundet durch die von Charles Darwin reformirte Descendenz-Theorie von Ernst Haeckel: Allgemeine Entwickelungsgeschichte der Organismen kritische Grundzuge der

mechanischen Wissenschaft von den entstehenden Formen der Organismen, begrundet durch die Descendenz-Theorie, 2. Verlag von Georg Reimer.
Hammer, Ø., Harper D. A. T., and Ryan P. , 2001. PAST: Paleontological statistics software package for education and data analysis. Palaeontologia Electronica, 4(1).
Hansford, D., 2008. Dino-era seabird fossils found in New Zealand. National Geographic News. http://news.nationalgeographic.com/news/2008/02/080222-seabird-fossils.html. (Accessed 20/05/2016).
Hao, H., Ferguson, D.K., Feng, G.-P., Ablaev, A., Wang, Y.-F. and Li, C.-S., 2010. Early Paleocene vegetation and climate in Jiayin, NE China. Climatic Change, 99(3-4): 547-566.
Haubitz, B., Prokop, M., Döhring, W., Ostrom, J. and Wellnhofer, P., 1988. Computed tomography of Archaeopteryx. Paleobiology, 14(02): 206-213.
Hills, L., Nicholls, E., Núñez-Betelu, L.M. and McIntyre, D., 1999. Hesperornis (Aves) from Ellesmere Island and palynological correlation of known Canadian localities. Canadian Journal of Earth Sciences, 36(9): 1583-1588.
Hollis, C.J., Stickley, C.E., Bijl, P.K., Schiøler, P., Clowes, C.D., Li, X, Campbell, H., in press. The age of the Takatika Grit, Chatham Islands, New Zealand. Alcheringa.
Hope, S., 2002. The mesozoic radiation of Neornithes. Mesozoic birds: above the heads of dinosaurs: 339-388.
Hospitaleche, C.A., 2016. Paleobiological Remarks on a New Partial Skeleton of the Eocene Antarctic Penguin *Palaeeudyptes klekowskii*. Ameghiniana, 53(3): 269-281.
Hospitaleche, C.A. and Di Carlo, U., 2010. The coracoids in functional and morphological studies of penguins (Aves, Spheniscidae) of the Eocene of Antarctica. Rivista Italiana di Paleontologia e Stratigrafia (Research In Paleontology and Stratigraphy), 116(1).
Hospitaleche, C.A., Tambussi, C., Donato, M. and Cozzuol, M., 2007. A new Miocene penguin from Patagonia and its phylogenetic relationships. Acta Palaeontologica Polonica, 52(2): 299.
Hou, L., Chiappe, L.M., Zhang, F. and Chuong, C.-M., 2004. New Early Cretaceous fossil from China documents a novel trophic specialization for Mesozoic birds. Naturwissenschaften, 91(1): 22-25.
Hui, C.A., 2002. Avian furcula morphology may indicate relationships of flight requirements among birds. Journal of Morphology, 251(3): 284-293.
Hull, P., 2015. Life in the Aftermath of Mass Extinctions. Current Biology, 25(19): R941-R952.
Huxley, T.H., 1868. On the animals which are most nearly intermediate between birds and reptiles. Royal Institution of Great Britain.
Hwang, K.-G., Huh, M., Lockley, M.G., Unwin, D.M. and Wright, J.L., 2002. New pterosaur tracks (Pteraichnidae) from the Late Cretaceous Uhangri Formation, southwestern Korea. Geological Magazine, 139(04): 421-435.
Iurino, D.A., Danti, M., Della Sala, S.W. and Sardella, R., 2013. Modern techniques for ancient bones: vertebrate palaeontology and medical CT analysis. Boll. Soc. Paleontol. Ital, 52(3): 14.
Jadwiszczak, P., 2001. Body size of Eocene Antarctic penguins. Polish Polar Research, 22(2): 147-158.
Jadwiszczak, P., 2014. At the root of the early penguin neck: a study of the only two cervicodorsal spines recovered from the Eocene of Antarctica. Polar Research, 33.
Jadwiszczak, P., Hospitaleche, C.A. and Reguero, M., 2013. Redescription of *Crossvallia unienwillia*: the only Paleocene Antarctic penguin. Ameghiniana, 50(6): 545-553.
Jarvis, E.D., Mirarab, S., Aberer, A.J., Li, B., Houde, P., Li, C., Ho, S.Y.W., Faircloth, B.C., Nabholz, B., Howard, J.T., Suh, A., Weber, C.C., da Fonseca, R.R., Li, J., Zhang, F., Li, H., Zhou, L., Narula, N., Liu, L., Ganapathy, G., Boussau, B., Bayzid, M.S., Zavidovych, V., Subramanian, S., Gabaldon, T., Capella-Gutierrez, S., Huerta-Cepas, J., Rekepalli, B., Munch, K., Schierup, M., Lindow, B., Warren, W.C., Ray, D., Green, R.E., Bruford, M.W., Zhan, X., Dixon, A., Li, S., Li, N., Huang, Y., Derryberry, E.P., Bertelsen, M.F., Sheldon, F.H., Brumfield, R.T., Mello, C.V., Lovell, P.V., Wirthlin, M., Cruz Schneider, M.P., Prosdocimi, F., Samaniego, J.A., Vargas Velazquez, A.M., Alfaro-Nunez, A., Campos, P.F., Petersen, B., Sicheritz-Ponten, T., Pas, A., Bailey, T., Scofield, P., Bunce, M., Lambert, D.M., Zhou, Q., Perelman, P., Driskell, A.C., Shapiro, B., Xiong, Z., Zeng, Y., Liu, S., Li, Z., Liu, B., Wu, K., Xiao, J., Yinqi, X., Zheng, Q., Zhang, Y., Yang, H., Wang, J., Smeds, L., Rheindt, F.E., Braun, M., Fjeldsa, J., Orlando, L., Barker, F.K., Jonsson, K.A., Johnson, W., Koepfli, K.-P., O'Brien, S., Haussler, D., Ryder, O.A., Rahbek, C., Willerslev, E., Graves, G.R., Glenn, T.C., McCormack, J., Burt, D., Ellegren, H., Alstrom, P., Edwards, S.V., Stamatakis, A., Mindell, D.P., Cracraft, J., Braun, E.L., Warnow, T., Jun, W., Gilbert, M.T.P. and Zhang, G., 2014. Whole-genome analyses resolve early branches in the tree of life of modern birds. Science, 346(6215): 1320-1331.
Jetz, W., Thomas, G.H., Joy, J.B., Hartmann, K. and Mooers, A.O., 2012. The global diversity of birds in space and time. Nature, 491(7424): 444-448.
Johansson, L.C. and Norberg, U.L., 2001. Lift-based paddling in diving grebe. Journal of Experimental Biology, 204(10): 1687-1696.
Kaiser, G.W., 2007. The Inner Bird: Anatomy and Evolution. UBC Press, Vancouver.
Keller, G., 2008. Cretaceous climate, volcanism, impacts, and biotic effects. Cretaceous Research, 29(5-6): 754-771.
Keller, G., Punekar, J. and Mateo, P., 2016. Upheavals during the Late Maastrichtian: Volcanism, climate and faunal events preceding the end-Cretaceous mass extinction. Palaeogeography Palaeoclimatology Palaeoecology, 441: 137-151.

Kemp, T.S., 2005. The origin and evolution of mammals. Oxford University Press on Demand.
Ketcham, R.A. and Carlson, W.D., 2001. Acquisition, optimization and interpretation of X-ray computed tomographic imagery: applications to the geosciences. Computers & Geosciences, 27(4): 381-400.
Kim, C.B., Huh, M., Cheong, C.S., Lockley, M.G. and Chang, H.W., 2003. Age of the pterosaur and web-footed bird tracks associated with dinosaur footprints from South Korea. Island Arc, 12(2): 125-131.
Kimball, R.T., Wang, N., Heimer-McGinn, V., Ferguson, C. and Braun, E.L., 2013. Identifying localized biases in large datasets: a case study using the avian tree of life. Molecular phylogenetics and evolution, 69(3): 1021-1032.
Ksepka, D. and Clarke, J., 2015. Phylogenetically vetted and stratigraphically constrained fossil calibrations within Aves. Palaeontologia Electronica, 18(1).
Ksepka, D.T., 2007. Phylogeny, histology and functional morphology of fossil penguins (Sphenisciformes). Columbia University.
Ksepka, D.T. and Ando, T., 2011. Penguins past, present, and future: trends in the evolution of the Sphenisciformes. Living Dinosaurs: 155-186.
Ksepka, D.T. and Bertelli, S., 2006. Fossil penguin (Aves: Sphenisciformes) cranial material from the Eocene of Seymour Island (Antarctica). Historical Biology, 18(4): 389-395.
Ksepka, D.T., Bertelli, S. and Giannini, N.P., 2006. The phylogeny of the living and fossil Sphenisciformes (penguins). Cladistics, 22(5): 412-441.
Ksepka, D.T. and Clarke, J.A., 2010. The basal penguin (Aves: Sphenisciformes) Perudyptes devriesi and a phylogenetic evaluation of the penguin fossil record. Bulletin of the American Museum of Natural History, 337(1): 1-77.
Ksepka, D.T., Clarke, J.A., DeVries, T.J. and Urbina, M., 2008. Osteology of *Icadyptes salasi*, a giant penguin from the Eocene of Peru. Journal of Anatomy, 213(2): 131-147.
Ksepka, D.T. and Cracraft, J., 2008. An Avian Tarsometatarsus from Near the K-T Boundary of New Zealand. Journal of Vertebrate Paleontology, 28(4): 1224-1227.
Ksepka, D.T., Fordyce, R.E., Ando, T. and Jones, C.M., 2012. New Fossil Penguins (Aves, Sphenisciformes) from the Oligocene of New Zealand Reveal the Skeletal Plan of Stem Penguins. Journal of Vertebrate Paleontology, 32(2): 235-254.
Ksepka, D.T. and Thomas, D.B., 2012. Multiple Cenozoic Invasions of Africa by Penguins (Aves, Sphenisciformes), Proc. R. Soc. B. The Royal Society, pp. 1027-1032.
Ksepka, D.T., Werning, S., Sclafani, M. and Boles, Z.M., 2015. Bone histology in extant and fossil penguins (Aves: Sphenisciformes). Journal of Anatomy, 227(5): 611-630.
Laird, M.G. and Bradshaw, J.D., 2004. The break-up of a long-term relationship: the Cretaceous separation of New Zealand from Gondwana. Gondwana Research, 7(1): 273-286.
Lambrecht, K., 1929. *Neogaecornis wetzeli* ngn sp. der erste Kreidevogel der südlichen Hemisphäre. Palaeontologische Zeitschrift, 11(2): 121-129.
Lawver, L.A., Gahagan, L.M. and Coffin, M.F., 1992. The development of paleoseaways around Antarctica. The Antarctic Paleoenvironment: A Perspective on Global Change: Part One: 7-30.
Lee, M.S.Y., Cau, A., Naish, D. and Dyke, G.J., 2014. Morphological Clocks in Paleontology, and a Mid-Cretaceous Origin of Crown Aves. Systematic Biology, 63(3): 442-449.
Li, L.Q. and Keller, G., 1998. Maastrichtian climate, productivity and faunal turnovers in planktic foraminifera in south Atlantic DSDP sites 525A and 21. Marine Micropaleontology, 33(1-2): 55-86.
Linnaeus, C., 1758. Systema Naturæ per regna tria naturae, secundum classes, ordines, genera, species, cum characteribus, differentiis, synonymis, locis. Holmiae (Stockholm): Laurentii Salvii, 1 (10th ed.).
Livezey, B.C. and Zusi, R.L., 2007. Higher-order phylogeny of modern birds (Theropoda, Aves: Neornithes) based on comparative anatomy. II. Analysis and discussion. Zoological Journal of the Linnean Society, 149(1): 1-95.
Lockley, M.G., Li, R., Harris, J.D., Matsukawa, M. and Liu, M., 2007. Earliest zygodactyl bird feet: evidence from Early Cretaceous roadrunner-like tracks. Naturwissenschaften, 94(8): 657-665.
Longrich, N.R., Tokaryk, T. and Field, D.J., 2011. Mass extinction of birds at the Cretaceous-Paleogene (K-Pg) boundary. Proceedings of the National Academy of Sciences of the United States of America, 108(37): 15253-15257.
Luyendyk, B.P., 1995. Hypothesis for Cretaceous Rifting of East Gondwana Caused by Subducted Slab Capture. Geology, 23(4): 373-376.
Macleod, N., Rawson, P.F., Forey, P.L., Banner, F.T., BoudagherFadel, M.K., Bown, P.R., Burnett, J.A., Chambers, P., Culver, S., Evans, S.E., Jeffery, C., Kaminski, M.A., Lord, A.R., Milner, A.C., Milner, A.R., Morris, N., Owen, E., Rosen, B.R., Smith, A.B., Taylor, P.D., Urquhart, E. and Young, J.R., 1997. The Cretaceous-Tertiary biotic transition. Journal of the Geological Society, 154: 265-292.
Marsh, O.C., 1873. Notice of a new and remarkable fossil bird. Journal of Natural History, 11(61): 80-80.
Marsh, O.C., 1880. Odontornithes: A Monograph on the Extinct Toothed Birds of North America: with Thirty-four Plates and Forty Woodcuts, 18. US Government Printing Office.
Mayes, C.L., Lawver, L.A. and Sandwell, D.T., 1990. Tectonic history and new isochron chart of the South Pacific. Journal of Geophysical Research: Solid Earth, 95(B6): 8543-8567.
Mayr, G., 2004. A partial skeleton of a new fossil loon (Aves, Gaviiformes) from the early Oligocene of Germany with preserved stomach content. Journal of Ornithology, 145(4): 281-286.

Mayr, G., 2005. Tertiary plotopterids (Aves, Plotopteridae) and a novel hypothesis on the phylogenetic relationships of penguins (Spheniscidae). Journal of Zoological Systematics and Evolutionary Research, 43(1): 61-71.
Mayr, G., 2011. Metaves, Mirandornithes, Strisores and other novelties - a critical review of the higher-level phylogeny of neornithine birds. Journal of Zoological Systematics and Evolutionary Research, 49(1): 58-76.
Mayr, G., 2014. The origins of crown group birds: molecules and fossils. Palaeontology, 57(2): 231-242.
Mayr, G., 2016. Avian evolution: the fossil record of birds and its paleobiological significance. John Wiley & Sons.
Mayr, G. and Clarke, J., 2003. The deep divergences of neornithine birds: a phylogenetic analysis of morphological characters. Cladistics, 19(6): 527-553.
Mayr, G. and Scofield, R.P., 2014. First diagnosable non-sphenisciform bird from the early Paleocene of New Zealand. Journal of the Royal Society of New Zealand, 44(1): 48-56.
Mayr, G. and Wilde, V., 2014. Eocene fossil is earliest evidence of flower-visiting by birds. Biology letters, 10(5): 20140223.
McCormack, J.E., Harvey, M.G., Faircloth, B.C., Crawford, N.G., Glenn, T.C. and Brumfield, R.T., 2013. A Phylogeny of Birds Based on Over 1,500 Loci Collected by Target Enrichment and High-Throughput Sequencing. PLoS ONE, 8(1): e54848.
McCullough, E.C., 1975. Photon attenuation in computed tomography. Medical physics, 2(6): 307-20.
Meister, W., 1962. Histological structure of the long bones of penguins. The Anatomical Record, 143(4): 377-387.
Meredith, R.W., Janecka, J.E., Gatesy, J., Ryder, O.A., Fisher, C.A., Teeling, E.C., Goodbla, A., Eizirik, E., Simao, T.L.L., Stadler, T., Rabosky, D.L., Honeycutt, R.L., Flynn, J.J., Ingram, C.M., Steiner, C., Williams, T.L., Robinson, T.J., Burk-Herrick, A., Westerman, M., Ayoub, N.A., Springer, M.S. and Murphy, W.J., 2011. Impacts of the Cretaceous Terrestrial Revolution and KPg Extinction on Mammal Diversification. Science, 334(6055): 521-524.
Merrem, B., 1813. Tentamen systematis naturalis avium, Abh. Konigel. (Preussische) Akad. Wiss. Berlin 1812–1813(1816) (Physikal.):237–259.
Navarro, J., Votier, S.C. and Phillips, R.A., 2014. Diving capabilities of diving petrels. Polar Biology, 37(6): 897-901.
Norris, R.M., 1964. Sediments of Chatham Rise. Department of Scientific and Industrial Research, 59: 40.
O'Hara, R.J., 1989. Systematics and the study of natural history, with an estimate of the phylogeny of the living penguins(Aves: Spheniscidae), to: Dept. of Organismic and Evolutionary Biology.advisor: Peter Stevens.Harvard University.
Olson, S.L., 1992. *Neogaeornis wetzeli* Lambrecht, a Cretaceous loon from Chile (Aves: Gaviidae). Journal of Vertebrate Paleontology, 12(1): 122-124.
Olson, S.L. and Parris, D.C., 1987. The Cretaceous birds of New Jersey. Smithsonian Institution Press.
Ostrom, J.H., 1976. Archaeopteryx and the origin of birds. Biological Journal of the linnean Society, 8(2): 91-182.
Owen, R., 1863. On the *Archeopteryx* of von Meyer, with a description of the fossil remains of a long-tailed species, from the lithographic stone of Solenhofen. Philosophical Transactions of the Royal Society of London, 153: 33-47.
Pacheco, M.A., Battistuzzi, F.U., Lentino, M., Aguilar, R.F., Kumar, S. and Escalante, A.A., 2011. Evolution of Modern Birds Revealed by Mitogenomics: Timing the Radiation and Origin of Major Orders. Molecular Biology and Evolution, 28(6): 1927-1942.
Pansarin, E.R. and Pedro, S.R.d.M., 2016. Reproductive biology of a hummingbird-pollinated Billbergia: light influence on pollinator behaviour and specificity in a Brazilian semi-deciduous forest. Plant Biology, 18(6): 920-927.
Pennycuick, C., 1987. Flight of auks (Alcidae) and other northern seabirds compared with southern Procellariiformes: ornithodolite observations. Journal of Experimental Biology, 128(1): 335-347.
Pole, M. and Philippe, M., 2010. Cretaceous plant fossils of Pitt Island, the Chatham group, New Zealand. Alcheringa, 34(3): 231-263.
Porras-Muzquiz, H.G., Chatterjee, S. and Lehman, T.M., 2014. The carinate bird *Ichthyornis* from the Upper Cretaceous of Mexico. Cretaceous Research, 51: 148-152.
Prum, R.O., Berv, J.S., Dornburg, A., Field, D.J., Townsend, J.P., Lemmon, E.M. and Lemmon, A.R., 2015. A comprehensive phylogeny of birds (Aves) using targeted next-generation DNA sequencing. Nature, 526(7574): 569-U247.
Raikow, R.J., Bicanovsky, L. and Bledsoe, A.H., 1988. Forelimb joint mobility and the evolution of wing-propelled diving in birds. The Auk: 446-451.
Rambaut, A. and Drummond, A.J., 2004. TRACER. Version 1.3, MCMC. Trace Analysis Tool.
Ronquist, F. and Huelsenbeck, J.P., 2003. MrBayes 3: Bayesian phylogenetic inference under mixed models. Bioinformatics, 19(12): 1572-1574.
Rouillard, P., Collot, J., Sutherland, R., Bache, F., Patriat, M., Etienne, S. and Maurizot, P., 2015. Seismic stratigraphy and paleogeographic evolution of Fairway Basin, Northern Zealandia, Southwest Pacific: from Cretaceous Gondwana breakup to Cenozoic Tonga–Kermadec subduction. Basin Research.

Royer, J.-Y., Gahagan, L.M., Lawver, L.A., Mayes, C.L., Nürnberg, D., Sandwell, D.T. and Scotese, C.R., 1990. A tectonic chart for the Southern Ocean derived from Geosat altimetry data. Antarctica as an exploration frontier—hydrocarbon potential, geology, and hazards. AAPG Studies in Geology, 31: 89-99.
Schafer, J.L. and Graham, J.W., 2002. Missing data: our view of the state of the art. Psychological methods, 7(2): 147.
Schorger, A., 1947. The deep diving of the loon and old-squaw and its mechanism. The Wilson Bulletin, 59(3): 151-159.
Schreiweis, D.O., 1982. A comparative study of the appendicular musculature of penguins (Aves: Sphenisciformes). Smithsonian Institution Press.
Schulte, P., Alegret, L., Arenillas, I., Arz, J.A., Barton, P.J., Bown, P.R., Bralower, T.J., Christeson, G.L., Claeys, P. and Cockell, C.S., 2010. The Chicxulub asteroid impact and mass extinction at the Cretaceous-Paleogene boundary. Science, 327(5970): 1214-1218.
Sharpe, R. B., 1891. A review of recent attempts to classify birds: An address delivered before the Second International Ornithological Congress on the 18th of May, 1891. Pub. At the Office of the congress.
Seton, M., Müller, R., Zahirovic, S., Gaina, C., Torsvik, T., Shephard, G., Talsma, A., Gurnis, M., Turner, M. and Maus, S., 2012. Global continental and ocean basin reconstructions since 200Ma. Earth-Science Reviews, 113(3): 212-270.
Shimada, K. and Fernandes, M.V., 2006. *Ichthyornis* sp.(Aves: Ichthyornithiformes) from the lower Turonian (Upper Cretaceous) of western Kansas. Transactions of the Kansas Academy of Science, 109(1): 21-26.
Simpson, G.G., 1946. Fossil Penguins. Bulletin of the American Museum of Natural History, 87: 7-99.
Skelton, P.W., 2003. The Cretaceous world. Cambridge University Press, Cambridge.
Slack, K.E., Jones, C.M., Ando, T., Harrison, G.L., Fordyce, R.E., Arnason, U. and Penny, D., 2006. Early penguin fossils, plus mitochondrial genomes, calibrate avian evolution. Molecular Biology and Evolution, 23(6): 1144-1155.
Soldaat, E., 2009. Skeletonderdelen van zeevogels (1): Sternum. Sula, 22(3): 136-142.
Spicer, R.A. and Corfield, R.M., 1992. A review of terrestrial and marine climates in the Cretaceous with implications for modelling the 'Greenhouse Earth'. Geological Magazine, 129(02): 169-180.
Stilwell, J.D., 2007. First record of late cretaceous gastropoda (Mollusca) from the Takatika grit, Chatham Islands, Southwest Pacific. New Zealand Journal of Geology and Geophysics, 50(1): 21-25.
Stilwell, J.D., 2016. Zealandia's oldest volutes (Mollusca: Gastropoda: Volutidae) from the early Paleogene of South Island and Chatham Islands: post Gondwana break-up and evolutionary divergence. Journal of Paleontology, 90(1): 31-42.
Stilwell, J.D. and Consoli, C.P., 2012. Tectono-stratigraphic history of the Chatham Islands, SW Pacific—The emergence, flooding and reappearance of eastern 'Zealandia. Proceedings of the Geologists' Association, 123(1): 170-181.
Stilwell, J.D., Consoli, C.P., Sutherland, R., Salisbury, S., Rich, T.H., Vickers-Rich, P.A., Currie, P.J. and Wilson, G.J., 2006. Dinosaur sanctuary on the Chatham Islands, Southwest Pacific: First record of theropods from the K-T boundary Takatika Grit. Palaeogeography Palaeoclimatology Palaeoecology, 230(3-4): 243-250.
Storer, R.W., 1960. Evolution in the diving birds. Proceedings of the XII International Ornithological Congress. Tilgmannin Kirjapaino Helsinki, Finland, pp. 694-707.
Storey, B.C., Leat, P.T., Weaver, S.D., Pankhurst, R.J., Bradshaw, J.D. and Kelley, S., 1999. Mantle plumes and Antarctica-New Zealand rifting: evidence from mid-Cretaceous mafic dykes. Journal of the Geological Society, 156: 659-671.
Suh, A., Smeds, L. and Ellegren, H., 2015. The dynamics of incomplete lineage sorting across the ancient adaptive radiation of neoavian birds. PLoS Biol, 13(8): e1002224.
Swofford, D.L., 2003. PAUP*. Phylogenetic analysis using parsimony (* and other methods). Version 4. Sunderland, MA: Sinauer Associates.
Tajika, E., 1999. Carbon cycle and climate change during the Cretaceous inferred from a biogeochemical carbon cycle model. Island Arc, 8(2): 293-303.
Tambussi, C.P., de Mendoza, R., Degrange, F.J. and Picasso, M.B., 2012. Flexibility along the neck of the Neogene terror bird Andalgalornis steulleti (Aves Phorusrhacidae). PloS one, 7(5): e37701.
Tambussi, C.P., Reguero, M.A., Marenssi, S.A. and Santillana, S.N., 2005. *Crossvallia unienwillia*, a new Spheniscidae (Sphenisciformes, Aves) from the late Paleocene of Antarctica. Geobios, 38(5): 667-675.
Tappenden, V.E., 2003. Magmatic Response to the Evolving New Zealand Margin of Gondwana During the Mid-late Cretaceous: A Thesis Submitted in Partial Fulfilment of the Requirements for the Degree of Doctor of Philosophy in Geological Sciences at the University of Canterbury. University of Canterbury.
Thibault, N. and Husson, D., 2016. Climatic fluctuations and sea-surface water circulation patterns at the end of the Cretaceous era: Calcareous nannofossil evidence. Palaeogeography Palaeoclimatology Palaeoecology, 441: 152-164.
Thomas, G.H., 2015. Evolution: an avian explosion. Nature.
Upchurch, P., 2008. Gondwanan break-up: legacies of a lost world? Trends in Ecology & Evolution, 23(4): 229-236.

Vajda, V., Raine, J.I., Hollis, C.J. and Strong, C.P., 2004. Global effects of the Chicxulub impact on terrestrial vegetation—review of the palynological record from New Zealand Cretaceous/Tertiary boundary, Cratering in marine environments and on ice. Springer, pp. 57-74.
Vaughan, A.P.M. and Pankhurst, R.J., 2008. Tectonic overview of the West Gondwana margin. Gondwana Research, 13(2): 150-162.
Wang, M., Zhou, Z. and Xu, G., 2014a. The First Enantiornithine Bird from the Upper Cretaceous of China. Journal of Vertebrate Paleontology, 34(1): 135-145.
Wang, Y., Huang, C., Sun, B., Quan, C., Wu, J. and Lin, Z., 2014b. Paleo-CO2 variation trends and the Cretaceous greenhouse climate. Earth-Science Reviews, 129: 136-147.
Watson, M., 1883. Report on the anatomy of the Spheniscidae collected by HMS Challenger, during the years 1873–1876. Report on the Scientific Results of HMS Challenger During the Years 1873–1876 under the Command of Captain George S. Nares, RN, FRS. and Captain Frank Tourle Thomson, RN Zoology, 7: 1-243.
Wilson, G., 1982. Dinoflagellate assemblages from the Takatika Grit and Tutuiri Greensand (Tioriori Group), Chatham Islands, New Zealand. New Zealand Geological Survey Report PAL, 63: 1-12.
Wilson, G.J., 1984a. A new Paleocene dinoflagellate cyst from the Chatham Islands, New Zealand. New Zealand Journal of Botany, 22(4): 545-548.
Wilson, G.J., 1984b. Some new dinoflagellate species from the New Zealand Haumurian and Piripauan Stages (Santonian-Maastrichtian, Late Cretaceous). New Zealand Journal of Botany, 22(4): 549-556.
Wilson, G.J., Schiøler, P., Hiller, N. and Jones, C.M., 2005. Age and provenance of Cretaceous marine reptiles from the South Island and Chatham Islands, New Zealand. New Zealand Journal of Geology and Geophysics, 48(2): 377-387.
Wolfe, J.A. and Upchurch, G.R., 1987. North American nonmarine climates and vegetation during the Late Cretaceous. Palaeogeography, Palaeoclimatology, Palaeoecology, 61: 33-77.
Wood, R. and Herzer, R., 1993. The Chatham Rise, New Zealand. South Pacific Sedimentary Basins. Sedimentary basins of the world, 2: 329-349.
Wu, X. and Schepartz, L.A., 2009. Application of computed tomography in paleoanthropological research. Progress in Natural Science, 19(8): 913-921.
Xu, X., Zhou, Z.H., Dudley, R., Mackem, S., Chuong, C.M., Erickson, G.M. and Varricchio, D.J., 2014. An integrative approach to understanding bird origins. Science, 346(6215): 1341-+.
Yuri, T., Kimball, R.T., Harshman, J., Bowie, R.C., Braun, M.J., Chojnowski, J.L., Han, K.-L., Hackett, S.J., Huddleston, C.J. and Moore, W.S., 2013. Parsimony and model-based analyses of indels in avian nuclear genes reveal congruent and incongruent phylogenetic signals. Biology, 2(1): 419-444.
Zachos, J.C., Dickens, G.R. and Zeebe, R.E., 2008. An early Cenozoic perspective on greenhouse warming and carbon-cycle dynamics. Nature, 451(7176): 279-283.
Zhang, F., Zhou, Z., Hou, L. and Gu, G., 2001. Early diversification of birds: evidence from a new opposite bird. Chinese Science Bulletin, 46(11): 945-949.
Zhang, G., Li, C., Li, Q., Li, B., Larkin, D.M., Lee, C., Storz, J.F., Antunes, A., Greenwold, M.J., Meredith, R.W., Odeen, A., Cui, J., Zhou, Q., Xu, L., Pan, H., Wang, Z., Jin, L., Zhang, P., Hu, H., Yang, W., Hu, J., Xiao, J., Yang, Z., Liu, Y., Xie, Q., Yu, H., Lian, J., Wen, P., Zhang, F., Li, H., Zeng, Y., Xiong, Z., Liu, S., Zhou, L., Huang, Z., An, N., Wang, J., Zheng, Q., Xiong, Y., Wang, G., Wang, B., Wang, J., Fan, Y., da Fonseca, R.R., Alfaro-Nunez, A., Schubert, M., Orlando, L., Mourier, T., Howard, J.T., Ganapathy, G., Pfenning, A., Whitney, O., Rivas, M.V., Hara, E., Smith, J., Farre, M., Narayan, J., Slavov, G., Romanov, M.N., Borges, R., Machado, J.P., Khan, I., Springer, M.S., Gatesy, J., Hoffmann, F.G., Opazo, J.C., Hastad, O., Sawyer, R.H., Kim, H., Kim, K.-W., Kim, H.J., Cho, S., Li, N., Huang, Y., Bruford, M.W., Zhan, X., Dixon, A., Bertelsen, M.F., Derryberry, E., Warren, W., Wilson, R.K., Li, S., Ray, D.A., Green, R.E., O'Brien, S.J., Griffin, D., Johnson, W.E., Haussler, D., Ryder, O.A., Willerslev, E., Graves, G.R., Alstroem, P., Fjeldsa, J., Mindell, D.P., Edwards, S.V., Braun, E.L., Rahbek, C., Burt, D.W., Houde, P., Zhang, Y., Yang, H., Wang, J., Jarvis, E.D., Gilbert, M.T.P., Wang, J. and Avian Genome, C., 2014. Comparative genomics reveals insights into avian genome evolution and adaptation. Science, 346(6215): 1311-1320.
Zhou, Z., 2004. The origin and early evolution of birds: discoveries, disputes, and perspectives from fossil evidence. Naturwissenschaften, 91(10): 455-471.
Zhou, Z. and Zhang, F., 2001. Two new ornithurine birds from the Early Cretaceous of western Liaoning, China. Chinese Science Bulletin, 46(15): 1258-1264.
Zusi, R.L., 1975. An interpretation of skull structure in penguins. The biology of penguins: 59-84.

APPENDICES

Appendix 1 Unidentifiable Elements

Some elements contained within the scope of this research were unable to be accurately identified, and are shown here. STL files of each element are available upon request.

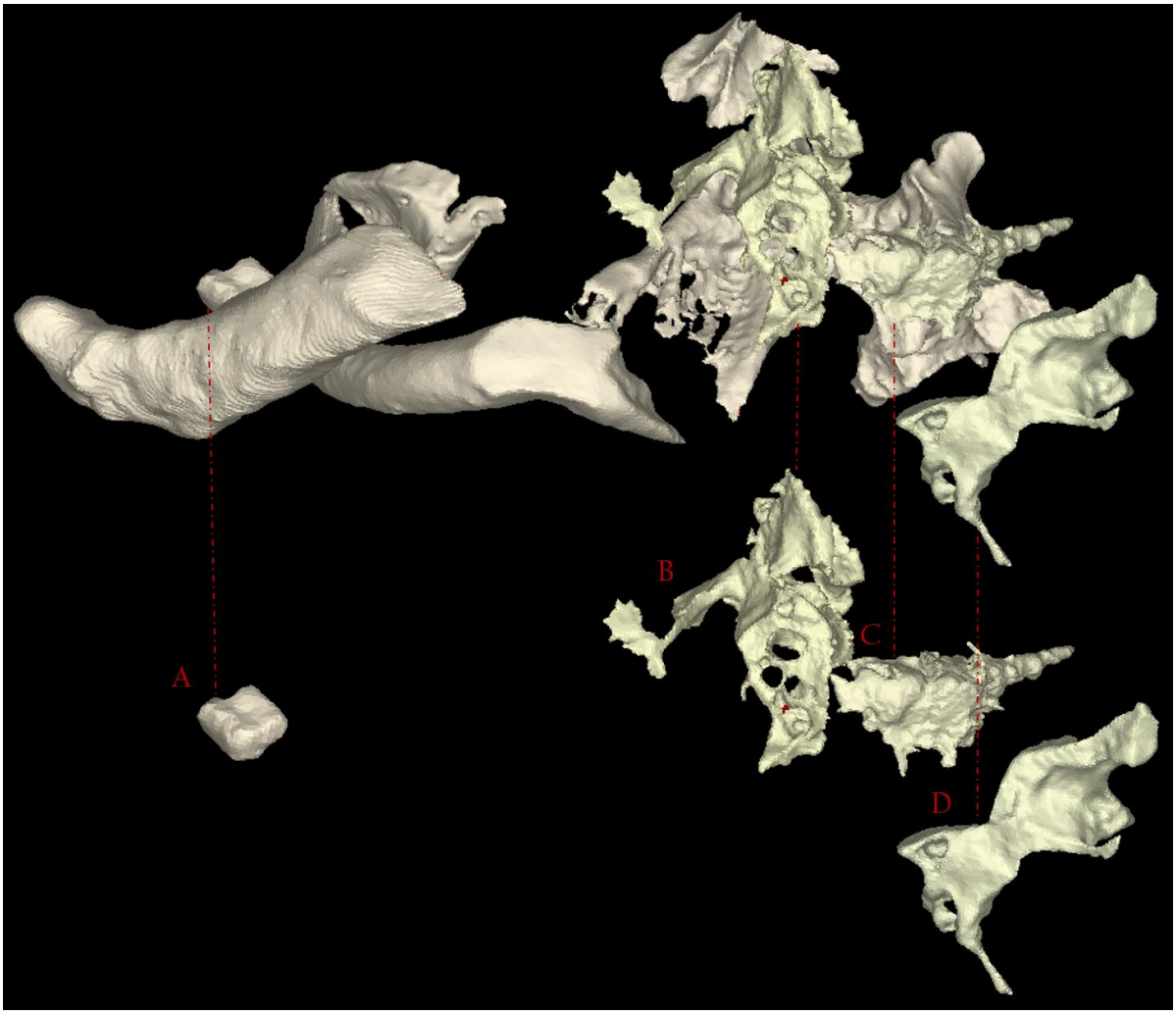

Figure A.1: The elements of JDS8341.b as they appear from the perspective as shown in **Figure 3.16**. Unidentified elements are shown in their positions among the other elements of JDS8341.b at the top of the image. Unidentified elements are focused on at the bottom of the image, where dashed red lines indicate their respective positions.

Appendix 1.1 JDS8341.b:

The elements labelled in Figure A.1 signify the elements in JDS8341.b that could not be accurately identified, and thus could not be properly described in this study. The element labelled A

in Figure A.1 appears to be a relatively small fossil fragment. In the case that A is representative of the entire element, it may be a radiale. Elements labelled B and D are hypothesised to be portions of a pelvis. However, exactly how the nature and anatomy of elements B and D fit within a pelvis structure have not been ascertained. It is also postulated that D may form part of a skull, specifically associated with an orbit. The element labelled C is suggested to be representative of a distal portion of a synsacrum within JDS8341.b. However, two-dimensional cross-sections and three dimensional models do not display adequate details to accurately support this assignment.

Appendix 2 Comparative Data

Data in the form of measurements were utilised in comparative analyses described in ***Chapter II: Methods***, from numerous sources. Exact measurements are given here.

Appendix 2.1 JDS8341.b: Cervical Vertebra IV

The comparative dataset here was used in comparative analyses of the morphology of cervical vertebrae IV of JDS8341.b to other Aequorlitornithes bird groups. Measurements were taken from specimens belonging to Canterbury Museum, New Zealand, and were also gratefully provided by Guinard et al. (2010). Please refer to ***Chapter II: Methods***, Figure 2.3, and/or Guinard et al. (2010) for descriptions of acronyms. Unavailable data is referred to in table format as "N/A". Specimens listed as "Not Registered" refer to specimens measured at Canterbury Museum, but did not have specimen identification numbers available.

Table 3: Table of Cervical Vertebra IV Measurements

Taxon/Specimen	Measurement (mm)						
	Fwl	Bwl	Bw2	L1	L2	L3	L4
Archaeodyptes stilwelli / JDS8341.b	25.471	22.103	29.416	17.583	23.71	21.331	16.476
Aptenodytes forsteri / AV17360	30.34	33.74	41.87	19.02	24.84	23.3	21.4
Aptenodytes patagonicus / 1229	23.153	31.21	25.51	16.217	24.077	18.437	18.7
Aptenodytes patagonicus / 1225	24.53	32.293	27.55	16.677	24.21	18.657	19.323
Aptenodytes patagonicus / 1241	24.59	31.797	26.287	18.037	25.37	18.857	18.557
Aptenodytes patagonicus / 1243	24.707	33.98	27.537	14.823	24.243	18.557	18.357
Aptenodytes patagonicus / Not Registered	20.833	27.433	24.323	13.033	23.867	16.943	16.157
Aptenodytes patagonicus / Not Registered	22.267	28.023	24.76	13.157	21.793	16.247	16.263
Aptenodytes patagonicus / Not Registered	21.65	26.967	24.313	12.043	20.547	15.43	15.15
Aptenodytes patagonicus / Not Registered	20.523	27.327	23.36	12.553	19.827	15.243	14.947
Aptenodytes patagonicus / Not Registered	26.28	29.24	35.05	18.16	20.71	20.55	19.88
Eudyptes chrysolophus / 1994-191	17.853	24.36	18.733	9.863	18.533	11.077	11.97
Pygoscelis papua / 1992-224	18.873	26.697	19.777	10.983	19.657	12.703	11.807
Pygoscelis papua / 1993-90	16.637	25.647	18.467	10.277	19.423	12.117	10.673
Pygoscelis adeliae / Not Registered	19.08	19.32	25.09	8.64	11.27	11.95	13.36
Pygoscelis adeliae / Not Registered	17.8	17.9	27.07	7.23	14.06	10.94	12.55
Spheniscus humboldti / 1993-91	18.267	25.497	21.4	11.15	19.443	14.177	14.26
Spheniscus humboldti / 1994-31	19.833	29.187	23.277	12.52	19.557	14.983	15.053
Spheniscus humboldti / 1997-113	18.267	27.833	21.49	11.193	18.323	13.943	13.99
Diomedea exulans / AV7000	23.68	24.04	24.16	14.68	23.94	19.53	19.45
Diomedea exulans / AV3351	22.36	20.12	21.22	16.09	24.18	19.7	19.15
Thalasscarche cauta / AV14476	20.27	11.72	21.51	13.3	22.96	17.67	17.32
Thalasscarche cauta / AV36796	20.24	13.22	21.76	12.66	21.78	18.06	17.5
Thalasscarche cauta / AV14738	19.43	12.56	21.35	12.59	21.45	17.39	16.59
Thalasscarche cauta / AV22627	20	14.51	21.55	13.72	22.71	17.8	16.81
Macronectes giganteus / AV20407	20.79	10.57	20.83	12.13	22.5	18.53	17.62
Macronectes giganteus / AV14405	20.77	10.68	20.87	12.35	22.64	18.73	17.88
Gavia stellata / AV10284	11.77	7.07	11.59	15.27	18.92	N/A	14.32
Podiceps cristatus / AV36812	8	7	7.83	10.73	15.38	13.11	13.01
Podiceps cristatus / AV38913	8.55	6.6	7.81	10.25	14.67	12.59	12.53
Podiceps cristatus / AV10285	7.98	6.53	7.64	11.11	14.81	13.54	12.39
Podiceps cristatus / AV36143	8.44	6.8	8.67	11.5	16.34	13.99	13.56
Phalacrocorax carbo / AV9775	9.61	9.11	10.65	18.94	22.11	21.28	17.58
Phalacrocorax carbo / AV19114	11.55	9.7	12.33	15.97	21.06	18.82	16.19
Phalacrocorax carbo / AV9774	11.57	8.98	12.26	17.36	22.5	20.26	16.8
Pelecanus conspicilatus / AV37035	21.93	9.1	19.94	46.23	56.4	50.66	45.79
Leptoptilos sp./ AV37491	19.72	13.94	17.96	23.62	30.72	24.96	25.82
Waimanu tuatahi / 2010.108.3	22.38	17.71	32.5	19.74	28.55	22.42	23.95
Cygnus olor / AV25436	18.65	11.65	17.65	24.9	30.56	29.91	29.32
Cygnus olor / AV23143	16.98	10.82	16.59	21.63	27.43	25.8	23.11
Phoeicopterus sp./ Not Registered	11.37	4.62	10.4	26.05	30.3	29.06	27.03
Chauna torquata / AV21208	13.53	9.02	13.94	12.06	16.39	13.32	13.9

Appendix 2.2 JDS8344: Ulna and Radius

The table of raw data here was used in the morphological comparison of JDS8344 to various *Waimanu tuatahi* specimens (see ***Chapter II: Methods, 2.5.2—JDS8344: Ulna and Radius***). Figure 2.4 should be referred to for more details on where measurements were taken from on each element. Measurement data that could not be obtained is referred to in table format as "N/A"

Table 4: Table of Ulna and Radius Measurements

Taxon (specimen) Ulna and Radius	Length (A) (mm)	Proximal width (B) (mm)	Mid-shaft width (C) (mm)	Proximal Depth (D) (mm)	Mid-shaft depth (E) (mm)	Distance to bend (F) (mm)
Waimanu tuatahi **(OR2994)**						
Ulna	89.57	27.2	12.44	13.46	8.2	N/A
Radius	91.05	8.92	10.82	8.58	5.3	19.57
Waimanu tuatahi **(2009.99.1)**						
Ulna	77.21	21.75	9.68	11.68	6.14	N/A
Radius	80.03	7.42	7.98	6.85	4.26	16.04
Waimanu tuatahi **(2010.108.1)**						
Ulna	82.04	15.73	8.42	9.63	5.57	N/A
Radius	79.92	8.07	8.04	7.99	4.31	19.83
Waimanu tuatahi **(2010.108.3)**						
Ulna	84.74	15.95	9.11	10.64	5.64	N/A
Radius	86.08	7.27	7.22	6.37	N/A	N/A
Archaeodyptes stilwelli **(JDS8344)**						
Ulna	69.16	7.33	6.38	4.61	3.35	24.82
Radius	41.91	7.06	7.58	5.75	3.3	17.5

Appendix 3 Morphological Character Datasets

Morphological datasets were used to determine phylogeny and evolutionary context of JDS8344 and JDS8341.b (*Archaeodyptes stilwelli*) among related taxa. ***Chapter II: Methods*** should be referred to for more information.

Appendix 3.1 Dataset Modified from Ksepka and Clarke (2010)

Three datasets modified from Ksepka and Clarke (2010), were used in this research. One dataset was used where JDS8344 and JDS8341.b were treated as separate taxa for phylogenetic analysis. Subsequent analyses were carried out with both JDS8344 and JDS8341.b merged into a single taxon (listed as *Archaeodyptes stilwelli*). For merged taxon analyses, two datasets were used: one with all characters scored across all taxa present (genetic and morphological), and another where

only osteological morphological characters were present (omitting all genetic and other morphological character scores). Character definitions used refer to those given in Ksepka and Clarke (2010). In these phylogenetic data matrices, A=0/1, B=1/2, C=3/4, D=0/1/2/3; Standard gap in data= - ; Missing data= ?.

Supporting nexus files of datasets are labelled as:

- Morphological character scoring, separate taxa, modified from Ksepka and Clarke (2010).nex
- Morphological character scoring, merged taxon, modified from Ksepka and Clarke (2010).nex
- Morphological character scoring, osteology only merged taxon, modified from Ksepka and Clarke (2010).nex

Appendix 3.2 Dataset Modified from Ksepka et al. (2012)

Two datasets modified from Ksepka et al. (2012) were used, both with *Archaeodyptes stilwelli* treated as a single merged taxon (listed as *Archaeodyptes stilwelli*). One dataset includes all characters scored across all taxa. The other phylogenetic dataset omits all genetic and non-osteological morphological character scores. Character definitions used, and character state labels/symbols are described in the original nexus file; provided as part of the Supplementary Information from Ksepka et al. (2012), and is also available from Dryad (dx.doi.org/10.5061/dryad.93j174jd).

Supporting nexus files of datasets are labelled as:

- Morphological character scoring, merged taxon, modified from Ksepka et al (2012).nex
- Morphological character scoring, osteology only, merged taxon, modified from Ksepka et al (2012).nex

Appendix 4 Estimation of Size for Archaeodyptes stilwelli

Broad estimation of the size of *Archaeodyptes stilwelli* was calculated based on the proportionate dimensions of forewing elements in JDS8341.b to those of multiple *Waimanu tuatahi* specimens. It should be noted that using isolated limb bones has limited use for body size and mass calculations, and thus the use of forewing elements alone here, in the calculation of body size, should

be used tentatively. Calculations are shown here in the table, using ulna, carpometacarpus (CMC), and radius measurements. Refer to Figure 2.6 for where specific measurements were taken from.

Table 5: Table for Estimation of Body Size

Taxon (specimen)	Ulna (mm)	CMC (B) (mm)	CMC (D) (mm)	CMC (E) (mm)	CMC (F) (mm)	Radius (B) (mm)	Radius (C) (mm)	Radius (D) (mm)	Radius (E) (mm)	Distance to Bend (F) (mm)	
Waimanu tuatahi (2009.99.1)	77.21	13.63	7.35	5.62	3.72	7.42	7.98	6.65	4.26	16.04	
Waimanu tuatahi (2010.108.1)	82.04					8.07	8.04	7.99	4.31	19.93	
Waimanu tuatahi (OR2994)	89.57	15.9	9.5	7.54	2.02	8.92	10.82	8.58	5.3	19.57	
Waimanu tuatahi (2010.108.3)	84.74					7.27	7.22	6.37			
Average	83.39	14.765	8.425	6.58	2.87	7.92	8.515	7.3975	4.6233	18.513	
Archaeodyptes stilwelli (JDS8344)	69.16	11.33	7.04	5.65	2.34	7.06	7.58	5.75	3.3	17.5	
											Average
% of Average *Waimanu tuatahi*	82.935604	76.73552	83.561	85.866	81.533	89.141	89.019	77.729	**71.3771**	**94.5265**	**83.2425**

Given that the approximate size of *Waimanu tuatahi* is 80 cm tall:

Minimum body size: 71.4% of *Waimanu tuatahi* = 57.1 cm tall

Maximum body size: 94.5% of *Waimanu tuatahi* = 75.6 cm tall

Average body size: 83.2% of *Waimanu tuatahi* = 66.6 cm tall